

Electronic Thesis and Dissertation Repository

---

7-23-2013 12:00 AM

## P2X7 Nucleotide Receptor Signaling in Osteoblasts

Matthew W. Grol, *The University of Western Ontario*

Supervisor: Dr. S. Jeffrey Dixon, *The University of Western Ontario*

A thesis submitted in partial fulfillment of the requirements for the Doctor of Philosophy degree  
in Anatomy and Cell Biology

© Matthew W. Grol 2013

Follow this and additional works at: <https://ir.lib.uwo.ca/etd>



Part of the [Cell Biology Commons](#)

---

### Recommended Citation

Grol, Matthew W., "P2X7 Nucleotide Receptor Signaling in Osteoblasts" (2013). *Electronic Thesis and Dissertation Repository*. 1470.

<https://ir.lib.uwo.ca/etd/1470>

This Dissertation/Thesis is brought to you for free and open access by Scholarship@Western. It has been accepted for inclusion in Electronic Thesis and Dissertation Repository by an authorized administrator of Scholarship@Western. For more information, please contact [wlsadmin@uwo.ca](mailto:wlsadmin@uwo.ca).

P2X7 NUCLEOTIDE RECEPTOR SIGNALING  
IN OSTEOBLASTS

(Thesis format: Integrated-Article)

by

Matthew William Grol

Graduate Program in  
Anatomy and Cell Biology

Submitted in partial fulfillment  
of the requirements for the degree of  
Doctor of Philosophy

School of Graduate and Postdoctoral Studies  
The University of Western Ontario  
London, Ontario, Canada

© Matthew William Grol 2013

## ABSTRACT

The structural integrity and functionality of the skeleton is maintained throughout life by remodeling, a process that involves the coordinated resorption of old bone by osteoclasts and formation of new bone by osteoblasts. Nucleotides are released from cells of the osteoblast lineage in response to mechanical stimulation and signal through two families of P2 nucleotide receptors – G protein-coupled P2Y receptors and ligand-gated P2X cation channels. Nearly every cell-type expresses multiple P2 receptor subtypes. However, the significance of these networks of receptors in any system remains unclear. In Chapter 2, we show that the endogenous network of P2 receptors expressed by osteoblasts permits graded increases in  $\text{Ca}^{2+}$  signaling over a million-fold range of ATP concentrations. P2Y receptors were found to mediate transient activation of the  $\text{Ca}^{2+}$ /NFATc1 pathway, whereas stimulation of P2X7 caused sustained  $\text{Ca}^{2+}$ /NFATc1 signaling. Systemic and local acidosis regulates the activity of both osteoblasts and osteoclasts. The P2X7 receptor promotes osteoblast differentiation, and has been shown to increase cellular metabolism in other cell-types. However, whether P2X7 increases metabolic acid production in osteoblasts or any other system is unclear. In Chapter 3, we show that activation of P2X7 elicits a  $\text{Ca}^{2+}$ -dependent increase in proton efflux from osteoblast-like cells. This increase in metabolic acid production is sustained, and dependent on glucose and PI3K activity. The P2X7 and Wnt/ $\beta$ -catenin pathways are both critical for the anabolic responses of bone to mechanical stimuli. However, whether these pathways interact to control osteoblast differentiation and function is unknown. In Chapter 4, we show that activation of P2X7 by exogenous nucleotides promotes inhibitory phosphorylation of GSK3 $\beta$  and transient  $\beta$ -catenin nuclear localization.

Stimulation of P2X7 also potentiates the  $\beta$ -catenin nuclear localization and transcriptional activation elicited by canonical Wnt signaling. In summary, we have shown that P2Y-P2X receptor networks allow cells to sense a wide range of ATP concentrations, and transduce this input into distinct cellular responses. Additionally, we have found that P2X7 couples through multiple anabolic pathways in osteoblasts, including  $\text{Ca}^{2+}$ /NFAT, PI3K/AKT and Wnt/ $\beta$ -catenin signaling. One or more of these pathways in turn may mediate the effects of P2X7 on osteoblast differentiation and mechanotransduction in bone.

**Keywords** – adenosine 5'-diphosphate (ADP), adenosine 5'-triphosphate (ATP), apoptosis,  $\beta$ -catenin, canonical, cellular mechanotransduction, cellular metabolism, confocal microscopy, cyclooxygenase-2 (COX-2), cytosolic calcium, dose-to-duration coupling, extracellular calcium, glycogen synthase kinase 3 $\beta$  (GSK3 $\beta$ ), immunofluorescence, knockout mice, lactic acid efflux, luciferase reporter, membrane blebbing, metabolic acid efflux, microphysiometer, nuclear factor of activated T cells (NFAT), osteoblasts, phosphatidylinositol 3-kinase (PI3K), phospholipase C (PLC), prostaglandin E2 (PGE<sub>2</sub>), proton efflux, purinergic P2 receptors, purinergic signaling, purinoceptor, P2X, P2X7, P2Y, real-time reverse transcription-polymerase chain reaction, spectrofluorimetry, terminal deoxynucleotidyl transferase dUTP nick end labeling, transcription factors, uridine 5'-triphosphate (UTP), Western blot, Wnt



## CO-AUTHORSHIP

Chapter 1 entitled “Introduction” was written by M.W. Grol with suggestions from Drs. S.J. Dixon and S.M. Sims. Certain sections were adapted from Grol et al., 2009. *Purinergic Signal.* 5:205-221, and reproduced here with permission from Springer Science + Business Media (see Appendix B).

Chapter 2 entitled “P2 Receptor Networks Regulate Signaling Duration over a Wide Dynamic Range of ATP Concentrations” was adapted from Grol et al., 2013. *J. Cell Sci.* 126:3615-3626, and reproduced here with permission from The Company of Biologists (see Appendix C). The publication was written by M.W. Grol and Dr. S.J. Dixon with suggestions from Drs. A. Pereverzev and S.M. Sims. Dr. A. Pereverzev grew up the NFAT luciferase reporter and NFATc1-EGFP fusion protein expression plasmids. All studies were performed by M.W. Grol. All experiments were carried out in the laboratories of Drs. S.J. Dixon and S.M. Sims.

Chapter 3 entitled “P2X7-mediated Calcium Influx Triggers a Sustained, PI3K-dependent Increase in Metabolic Acid Production by Osteoblast-like Cells” was adapted from Grol et al., 2012. *Am. J. Physiol. Endocrinol. Metab.* 302:E561-E575, and reproduced here with permission from The American Physiological Society (see Appendix D). The publication was written by M.W. Grol and Dr. S.J. Dixon with suggestions from I. Zelner. Fourth year thesis student I. Zelner assisted with some of the proton efflux experiments, data from which are a part of the means reported in Figures 3.2 B, 3.3 B, C and 3.4 B. All other studies were performed by M.W. Grol. All experiments were carried out in the laboratory of Dr. S.J. Dixon.

Chapter 4 entitled “P2X7 Nucleotide Receptor Signaling Potentiates the Wnt/ $\beta$ -

catenin Pathway in Osteoblasts” was written by M.W. Grol with suggestions from Drs. S.J. Dixon and S.M. Sims. Dr. A. Pereverzev performed the Western blot analyses shown in Figures 4.6 and 4.7. Dental summer student Dr. P.J. Brooks performed the immunofluorescence analyses shown in Figure 4.1 under the supervision of M.W. Grol. All other studies were performed by M.W. Grol. All experiments were carried out in the laboratories of Drs. S.J. Dixon and S.M. Sims.

## ACKNOWLEDGEMENTS

During my doctoral studies, I have been privileged to be a part of both the Skeletal Biology Group (formerly the Canadian Institutes of Health Research (CIHR) Group in Skeletal Development and Remodeling) and the Department of Anatomy and Cell Biology at The University of Western Ontario. I have met many wonderful people over the past six years who have contributed to my success.

First and foremost, I would like to thank my supervisor, Dr. S. Jeffrey Dixon, for allowing me the opportunity to pursue research in this fascinating area of cell biology. Words cannot express how important his positive mentorship, encouragement and support have been to my success. He is one of the most intelligent, kindest and humble people I have had the pleasure to meet in life. An example of excellence both professionally and personally, he has truly helped to improve me both as a scientist and a human being. I would also like to acknowledge Dr. Stephen M. Sims for being like a second supervisor to me. His personal and professional advice and insight have been invaluable to my achievements during my doctoral studies.

The members of the Dixon and Sims laboratories have been instrumental to my success during my PhD. Specifically, Tom Chrones and Dr. Souzan Armstrong were invaluable resources during my studies. I want to thank both of you not only for the technical assistance you provided me over the years, but also for being amazing friends and colleagues. I am also thankful for the assistance of my colleague Dr. Alexey Pereverzev, who contributed significantly to this body of work. I will miss our many conversations about science and culture. Additionally, I sincerely appreciate the friendship of both current and past students, including Dr. Nattapon Panupinthu, Irene

Zelner, Danielle Lapierre, Kim Beaucage, Ryan Shugg, Dr. Natsuko Tanabe, Jessica Jakob, Karen Ann Bridge, Benjamin Wheal, Dr. Patricia Brooks, Garth Brooks and Ryan Beach. Thank you all for the many laughs and support over the years. As my first fourth year thesis student, Irene contributed significantly to the studies examining P2X7 and cellular metabolism. Thank you for all of your hard work and determination. I also want to acknowledge Dr. Patricia Brooks for her tireless efforts and contributions over the past few summers to the studies on P2X7 and canonical Wnt signaling. Thank you for putting up with my very particular nature, and for being one of my closest and dearest friends. I am lucky to have met you. Finally, I am eternally thankful for my best friend and colleague Kim Beaucage. Thank you for your never ending understanding and support throughout my time in the Dixon and Sims laboratories. I really could not imagine this journey without our friendship to see me through.

I have also had the privilege to work with many amazing people as a member of the Skeletal Biology Group at The University of Western Ontario. I am grateful for the endless guidance and support provided by Erika Hegedues and Drs. Cheryle Séguin, Anita Woods and Veronica Ulici. Thank you for being people I could turn to and lean on in times of frustration, difficulty and need. I would also like to acknowledge the many friends who have gotten me to this point, including Drs. Ryan Gillespie and Rick Miron, Emily LeBlanc, Nicole Watts, Sadia Pabani, Chris Elliot, Shawna Kim and Matt McCann. I will always look back on our time together with fondness. Thank you for the laughs and support – I will miss you all greatly.

A number of staff and faculty in addition to those mentioned above have been instrumental in my success over the last six years. I greatly appreciate the positive advice

and guidance provided by past and present members of my committee, including Drs. Frank Beier, Paul Walton and Dan Belliveau. I am also grateful for the tireless efforts of the administrative staff in the Department of Anatomy and Cell Biology, especially Debra Grant. Thank you for always having an answer to my questions. You made my life during graduate school so much easier.

One of my closest and most important friendships during my doctoral studies has been with Dr. Shirine Usmani. Thank you for not only being a fantastic colleague but also a caring, dependable and supportive friend and roommate. I couldn't imagine this journey without our friendship to rely on. I am also grateful to the whole Usmani family, including Shirine's parents, Dr. Aman Usmani and Mrs. Geraldine Voros Usmani, and Shirine's sister, Dr. Yasmine Usmani. Thank you all for your encouragement and kind words over the years.

During my doctoral studies, I have been lucky to receive stipend support in the form of an Ontario Graduate Scholarship (OGS) as well as both a CIHR Fredrick Banting and Charles Best Canada Graduate Scholarship (CGS) Masters and Doctoral Awards. Moreover, my research in the Dixon laboratory was funded by the CIHR. Given that this money is a generous donation from the Canadian public, I hope that one day my work might lead to development of interventions for bone diseases such as osteoporosis.

Lastly, I would like to express eternal gratitude to my family, especially my parents, Casey and Barbara Grol, and my brothers, Michael and Christopher. Thank you all for your unconditional love, support, guidance and encouragement during this process. There is no way I could have completed my PhD without all of you. I am truly blessed!

# TABLE OF CONTENTS

	Page
ABSTRACT AND KEYWORDS .....	ii
CO-AUTHORSHIP .....	iv
ACKNOWLEDGEMENTS .....	vi
TABLE OF CONTENTS.....	ix
LIST OF FIGURES .....	xiv
LIST OF APPENDICES.....	xvi
LIST OF ABBREVIATIONS.....	xvii
CHAPTER ONE—INTRODUCTION .....	1
1.1 Chapter Summary.....	2
1.2 Bone Physiology.....	3
1.2.1 Structure, Components, and Functions of Bone .....	3
1.2.2 Skeletal Development .....	6
1.2.3 Bone Remodeling.....	9
1.3 Osteoblast Biology .....	18
1.3.1 Master Transcription Factors and Transcriptional Coactivators Regulating Osteoblast Differentiation and Function .....	18
1.3.2 Regulation of Bone Formation.....	26
1.4 Ion Transporters and Regulation of Cytosolic pH in Osteoblasts .....	41
1.4.1 Effects of Acid on Bone.....	41
1.4.2 Proton Production and Transport by Osteoblasts.....	42
1.5 P2 Nucleotide Receptors .....	47
1.5.1 Sources and Fates of Extracellular Nucleotides.....	47
1.5.2 Classification and Properties of P2 Nucleotide Receptors.....	51
1.5.3 P2 Nucleotide Receptors in Bone .....	53
1.6 P2X7 in Osteoblasts .....	58
1.6.1 Expression of P2X7 in Cells of the Osteoblast Lineage .....	58
1.6.2 P2X7 Receptor Signaling in Osteoblasts .....	59
1.6.3 Functions of P2X7 Receptors in Osteoblasts.....	62

1.6.4 Genetic Polymorphisms of the Human P2X7 Receptor .....	65
1.7 Rationale and Objectives of the Research.....	68
1.7.1 Role of P2 Receptor Networks in Osteoblasts.....	68
1.7.2 Regulation of Metabolic Acid Production in Osteoblasts by P2 Receptors.....	69
1.7.3 Cross-talk between P2X7 and Wnt/ $\beta$ -catenin Pathways in Osteoblasts .....	70
1.8 References .....	71

CHAPTER TWO—P2 RECEPTOR NETWORKS REGULATE SIGNALING  
DURATION OVER A WIDE DYNAMIC RANGE OF ATP  
CONCENTRATIONS .....

2.1 Chapter Summary.....	99
2.2 Introduction .....	100
2.3 Materials and Methods .....	103
2.3.1 Materials and Solutions.....	103
2.3.2 Animals and Cell Culture.....	104
2.3.3 Fluorescence Measurement of $[Ca^{2+}]_i$ .....	105
2.3.4 Expression and Localization of NFATc1-EGFP .....	106
2.3.5 Immunofluorescence Localization of Native NFATc1.....	107
2.3.6 Real-time RT-PCR Analyses .....	108
2.3.7 Luciferase Reporter Assay for NFATc1 .....	109
2.3.8 Statistical Analyses .....	110
2.4 Results .....	111
2.4.1 Effect of ATP Concentration on the Duration of Cytosolic $Ca^{2+}$ Signals .....	111
2.4.2 P2X7 is Essential for Sustained Cytosolic $Ca^{2+}$ Signaling Elicited by High Concentrations of ATP .....	118
2.4.3 Source of $Ca^{2+}$ Underlying the Transient and Sustained Elevations of $[Ca^{2+}]_i$ Elicited by ATP .....	123
2.4.4 Effect of ATP Concentration on the Duration of NFATc1 Nuclear Localization .....	129
2.4.5 P2X7 is Essential for Sustained NFATc1 Nuclear Localization Elicited by High Concentrations of ATP .....	134
2.4.6 Effects of Nucleotides on NFAT Transcriptional Activity.....	137

2.4.7 P2X7 is Essential for Mediating Effects of High Concentrations of ATP on NFAT Transcriptional Activity.....	143
2.5 Discussion .....	146
2.5.1 P2 Receptor Networks Impart Sensitivity over a Wide Dynamic Range of ATP Concentrations .....	146
2.5.2 P2 Receptor Networks Enable Dose-to-Duration Encoding of Ca <sup>2+</sup> /NFAT Signaling.....	150
2.5.3 Potential Physiological Roles of P2 Receptor Networks in Osteoblasts ..	152
2.6 References .....	154
CHAPTER THREE—P2X7-MEDIATED CALCIUM INFLUX TRIGGERS A SUSTAINED, PI3K-DEPENDENT INCREASE IN METABOLIC ACID PRODUCTION BY OSTEOBLAST-LIKE CELLS .....	160
3.1 Chapter Summary.....	161
3.2 Introduction .....	162
3.3 Materials and Methods .....	166
3.3.1 Materials and Solutions.....	166
3.3.2 Cells and Culture.....	167
3.3.3 Morphological Assessments .....	168
3.3.4 Measurement of Proton Efflux.....	169
3.3.5 Measurement of Lactate Efflux.....	170
3.3.6 Spectrofluorometric Measurement of [Ca <sup>2+</sup> ] <sub>i</sub> .....	171
3.3.7 Assessment of Apoptosis .....	172
3.3.8 Statistical Analyses .....	172
3.4 Results .....	174
3.4.1 The P2X7 Agonist BzATP Induces Dynamic Membrane Blebbing in MC3T3-E1 Osteoblast-like Cells .....	174
3.4.2 Effects of BzATP on Proton Efflux from MC3T3-E1 Cells.....	177
3.4.3 Role of P2X7 in Mediating Nucleotide-induced Increases in Proton Efflux.....	183
3.4.4 Effects of P2X7 Agonists on Survival and Apoptosis of MC3T3-E1 Cells.....	186
3.4.5 Role of Glucose Metabolism in Generating Sustained Nucleotide-induced Proton Efflux.....	194



3.4.6	Dependence of Nucleotide-induced Proton Efflux on $\text{Ca}^{2+}$ .....	199
3.4.7	Dependence of Nucleotide-induced Proton Efflux on PI3K Signaling ....	204
3.5	Discussion .....	211
3.5.1	BzATP Elicits Membrane Blebbing in Osteoblast-like Cells Expressing the P2X7 Receptor .....	211
3.5.2	P2X7 Receptors Stimulate Sustained Proton Efflux.....	214
3.5.3	Dependence of P2X7-induced Proton Efflux on $\text{Ca}^{2+}$ .....	216
3.5.4	Role of PI3K in Mediating P2X7-induced Proton Efflux.....	218
3.5.5	Potential Physiological Roles of P2X7-induced $\text{Ca}^{2+}$ Elevation, PI3K Signaling and Proton Efflux in Osteoblast Regulation and Function....	220
3.6	References .....	221

## CHAPTER FOUR—P2X7 NUCLEOTIDE RECEPTOR SIGNALING

	POTENTIATES THE WNT/ $\beta$ -CATENIN PATHWAY IN OSTEOBLASTS .....	227
4.1	Chapter Summary.....	228
4.2	Introduction .....	229
4.3	Materials and Methods .....	233
4.3.1	Materials and Solutions.....	233
4.3.2	Animals and Cell Culture.....	235
4.3.3	Immunofluorescence Localization of $\beta$ -catenin.....	236
4.3.4	Luciferase Reporter Assay for $\beta$ -catenin Transcriptional Activity.....	236
4.3.5	Western Blot Analysis of GSK3 $\alpha/\beta$ Phosphorylation.....	237
4.3.6	Statistical Analyses .....	239
4.4	Results .....	240
4.4.1	Effect of the P2X7 Agonist BzATP on Wnt-induced $\beta$ -catenin Nuclear Localization .....	240
4.4.2	Effect of BzATP on Wnt-induced $\beta$ -catenin Transcriptional Activity .....	243
4.4.3	P2X7 is Essential for Mediating Effects of Nucleotides on Wnt- induced $\beta$ -catenin Transcriptional Activity.....	243
4.4.4	Activation of P2X7 Increases Inhibitory Phosphorylation of GSK3 $\alpha/\beta$ ...	253
4.5	Discussion .....	258
4.5.1	P2X7 Potentiates the Wnt/ $\beta$ -catenin Pathway .....	258
4.5.2	P2X7 Promotes Inhibitory Phosphorylation of GSK3 $\beta$ .....	263

4.5.3 Potential Physiological Roles of P2X7-induced Potentiation of Canonical Wnt Signaling in Osteoblasts .....	264
4.6 References .....	266
 CHAPTER FIVE—GENERAL DISCUSSION .....	273
5.1 Summary and Conclusions .....	274
5.1.1 Role of P2 Receptor Networks in Osteoblasts: Objective, Summary and Conclusions.....	274
5.1.2 Regulation of Metabolic Acid Production in Osteoblasts by P2 Receptors: Objective, Summary and Conclusions.....	276
5.1.3 Cross-talk between P2X7 and Wnt/ $\beta$ -catenin Pathways in Osteoblasts: Objective, Summary and Conclusions .....	278
5.2 Limitations of the Research.....	280
5.3 Contributions of the Research to the Current State of Knowledge .....	283
5.4 References .....	290
 APPENDIX A.....	296
APPENDIX B .....	299
APPENDIX C .....	301
APPENDIX D.....	303
APPENDIX E .....	305
 CURRICULUM VITAE.....	307

## LIST OF FIGURES

FIGURE	Page
1.1 Bone Remodeling by Osteoblasts and Osteoclasts .....	12
1.2 Transcriptional Control of Osteoblast Differentiation.....	20
1.3 Schematic of the Canonical Wnt/ $\beta$ -catenin Signaling Pathway in Osteoblasts .....	29
1.4 Schematic of the $\text{Ca}^{2+}$ /NFAT Signaling Pathway in Osteoblasts .....	34
1.5 Schematic of the Class I PI3K/AKT Signaling Pathway in Osteoblasts .....	39
1.6 Regulation of Cytosolic pH by Transporters in Osteoblasts.....	45
1.7 Extracellular Nucleotides and P2 Nucleotide Receptors in Mammalian Cell-Types .....	50
1.8 P2 Nucleotide Receptors in Bone .....	56
2.1 P2 Nucleotide Receptor-induced Elevations in Cytosolic Free $\text{Ca}^{2+}$ are Dependent on ATP Concentration.....	113
2.2 Vehicle-induced Elevations in $[\text{Ca}^{2+}]_i$ are Suppressed by ATP.....	115
2.3 Vehicle-induced Elevations in $[\text{Ca}^{2+}]_i$ are Blocked by a P2 Nucleotide Receptor Antagonist .....	117
2.4 The Percentage of Cells Exhibiting P2 Nucleotide Receptor-induced Elevations in $[\text{Ca}^{2+}]_i$ is Dependent on ATP Concentration.....	120
2.5 The P2X7 Receptor is Required for Sustained Elevations in $[\text{Ca}^{2+}]_i$ .....	122
2.6 Distinct Sources of $\text{Ca}^{2+}$ Underlie Transient and Sustained Elevations in $[\text{Ca}^{2+}]_i$ ...	126
2.7 P2Y <sub>2</sub> and/or P2Y <sub>4</sub> Mediate Elevations in $[\text{Ca}^{2+}]_i$ Elicited by $\text{ATP}_{\text{low}}$ .....	128
2.8 Live-Cell Confocal Microscopy Reveals that Duration of NFATc1 Nuclear Localization is Dependent on ATP Concentration .....	131
2.9 Duration of NFATc1 Nuclear Localization is Dependent on ATP Concentration..	133
2.10 The P2X7 Receptor is Required for Sustained NFATc1 Nuclear Localization ....	136
2.11 P2 Nucleotide Receptor-induced Changes in NFAT Transcriptional Activity are Dependent on ATP Concentration .....	139
2.12 P2 Nucleotide Receptor-induced Changes in NFAT Transcriptional Activity are Mediated by $\text{Ca}^{2+}$ /Calcineurin Signaling .....	142
2.13 The P2X7 Receptor is Required for Changes in NFAT Transcriptional Activity Elicited by $\text{ATP}_{\text{high}}$ or BzATP.....	145
2.14 Proposed Role for P2 Nucleotide Receptor Network in ‘Dose-to-Duration’ Encoding of $\text{Ca}^{2+}$ /NFATc1 Signaling .....	148

3.1 The P2X7 Agonist BzATP Induces Membrane Blebbing in MC3T3-E1 Osteoblast-like, but not UMR-106 Osteosarcoma Cells.....	176
3.2 BzATP Causes a Sustained Increase in Proton Efflux from MC3T3-E1 Cells .....	179
3.3 Increases in Proton Efflux are Dependent on BzATP Concentration.....	182
3.4 P2X7 Receptor Agonists alone Induce Sustained Increases in Proton Efflux.....	185
3.5 BzATP Induces an Increase in Proton Efflux from MC3T3-E1 but not UMR-106 Cells.....	188
3.6 Blockade of P2X7 Receptors Suppresses the Increase in Proton Efflux Induced by BzATP.....	190
3.7 P2X7 Agonists do not Induce Death of MC3T3-E1 Cells.....	193
3.8 Sustained Increase in Proton Efflux Induced by BzATP is Dependent on Extracellular Glucose.....	196
3.9 BzATP Increases Lactate Production by MC3T3-E1 Cells.....	198
3.10 Patterns of $[Ca^{2+}]_i$ Elevations Elicited by P2 Receptor Agonists.....	201
3.11 Initiation of the BzATP-induced Increase in Proton Efflux is Dependent on Extracellular $Ca^{2+}$ .....	203
3.12 The Irreversible PI3K Inhibitor Wortmannin Inhibits the Sustained Increase in Proton Efflux Induced by BzATP.....	206
3.13 The Reversible PI3K Inhibitor LY 294002 Inhibits Maintenance of the Sustained Increase in Proton Efflux Induced by BzATP.....	209
3.14 Proposed Role for P2X7 Receptor Signaling in Regulation of the PI3K/AKT Pathway and Cellular Metabolism.....	213
4.1 The P2X7 Agonist BzATP Potentiates $\beta$ -catenin Nuclear Localization Elicited by Canonical Wnt3a.....	242
4.2 BzATP Potentiates $\beta$ -catenin Transcriptional Activity Elicited by Wnt3a .....	245
4.3 P2X7 Receptor Agonists Potentiate $\beta$ -catenin Transcriptional Activity Elicited by Wnt3a.....	248
4.4 P2X7 Receptor Antagonists Block the Effects of BzATP on Wnt3a-induced $\beta$ -catenin Transcriptional Activity .....	250
4.5 Functional P2X7 Receptors are Required for Complete Activation of Wnt3a-induced $\beta$ -catenin Transcriptional Activity .....	252
4.6 BzATP Induces Inhibitory Phosphorylation of GSK3 $\alpha/\beta$ .....	255
4.7 A P2X7 Antagonist Blocks BzATP-induced Inhibitory Phosphorylation of GSK3 $\alpha/\beta$ .....	257
4.8 Possible Mechanism for Cross-talk between P2X7 Nucleotide Receptor and Canonical Wnt Signaling Pathways in Cells of the Osteoblast Lineage .....	260

## LIST OF APPENDICES

APPENDIX	Page
A. Supplementary Video Legends .....	297
B. Permission for Reproduction from Springer Science + Business Media .....	300
C. Permission for Reproduction from The Company of Biologists.....	302
D. Permission for Reproduction from The American Physiological Society .....	304
E. Ethics Approval of Animal Use.....	306

## LIST OF ABBREVIATIONS

[Ca <sup>2+</sup> ] <sub>i</sub>	cytosolic free Ca <sup>2+</sup> concentration
1,25(OH) <sub>2</sub> D <sub>3</sub>	1,25 dihydroxyvitamin D <sub>3</sub>
α-MEM	α-minimum essential medium
A 438079	3-(5-(2,3-dichlorophenyl)-1 <i>H</i> -tetrazol-1-yl)methyl pyridine hydrochloride
A 740003	N-[1-[[[(cyanoamino)(5-quinolinylamino)methylene]amino]-2,2-dimethylpropyl]-3,4 dimethoxybenzene-acetamide
ADP	adenosine 5'-diphosphate
ALP	alkaline phosphatase
AMP	adenosine 5'-monophosphate
ANOVA	analysis of variance
AP-1	activator protein 1
APC	adenomatous polyposis coli
ATF4	activating transcription factor 4
ATP	adenosine 5'-triphosphate
BMD	bone mineral density
BMP	bone morphogenetic protein
BMU	basic multicellular unit
BSP	bone sialoprotein
BzATP	2',3'- <i>O</i> -(4-benzoylbenzoyl)ATP
C/EBP	CCAAT/enhancer binding protein
CaMKII	calmodulin-dependent protein kinase II
cAMP	adenosine 3',5'-cyclic monophosphate
CCL8	monocyte chemoattractant chemokine (C-C motif) ligand 8
CIHR	Canadian Institutes of Health Research
CK1	casein kinase 1
COL1	collagen type I
COX-2	cyclooxygenase-2
CTGF	connective tissue growth factor
DAPI	4,6-diamidino-2-phenylindole

DKK1	dickopff 1
DMEM	Dulbecco's Modified Eagle Medium
DMSO	dimethyl sulfoxide
Dvl	dishevelled
E-5'-NT	ecto-5'-nucleotidase
E-NPP	ecto-nucleotide pyrophosphatase/phosphodiesterase
E-NTPDase	ecto-nucleoside 5'-triphosphate diphosphohydrolases
EGFP	enhanced green fluorescent protein
EGR	early growth response protein
EGTA	ethylene glycol-bis( $\beta$ -aminoethylether)- <i>N,N,N',N'</i> -tetraacetic acid
ERK	extracellular signal-regulated kinase
FBS	fetal bovine serum
F <sub>C</sub>	average fluorescence intensity in the cytosol
FGF	fibroblast growth factor
F <sub>N</sub>	average fluorescence intensity in the nucleus
Foxp3	forkhead box protein 3
Fzd	frizzled receptors
GATA	GATA-binding protein
GSK3 $\beta$	glycogen synthase kinase 3 $\beta$
HEPES	4-(2-hydroxyethyl)-1-piperazineethanesulfonic acid
IGF	insulin-like growth factor
IHH	Indian hedgehog
IL	interleukin
IP <sub>3</sub>	inositol 1,4,5-trisphosphate
JNK	c-jun NH <sub>2</sub> -terminal protein kinase
LPA	lysophosphatidic acid
LRP	lipoprotein receptor-related protein
LY 294002	2-(4-morpholinyl)-8-phenyl-4 <i>H</i> -1-benzopyran-4-one
M-CSF	macrophage colony stimulating factor
MAPK	mitogen-activated protein kinase
MCT	monocarboxylate transporter

MEF-2	myocyte enhancer factor-2
mTORC	mammalian target of rapamycin complex
NF- $\kappa$ B	nuclear factor- $\kappa$ B
NFATc1-4	nuclear factor of activated T-cells, cytoplasmic 1-4
NHE	Na <sup>+</sup> /H <sup>+</sup> exchanger
OCN	osteocalcin
OGR	ovarian cancer G protein-coupled receptor
OPG	osteoprotegerin
OPN	osteopontin
OSX	osterix
PBS	phosphate-buffered saline
PDGF	platelet-derived growth factor
PGE <sub>2</sub>	prostaglandin E <sub>2</sub>
pH <sub>i</sub>	cytosolic pH
pH <sub>o</sub>	extracellular pH
P <sub>i</sub>	inorganic phosphate
PI3K	phosphatidylinositol 3-kinase
PIP <sub>2</sub>	phosphatidylinositol-4,5-bisphosphate
PIP <sub>3</sub>	phosphatidylinositol-3,4,5-trisphosphate
PKA	protein kinase A
PKC	protein kinase C
PLA <sub>2</sub>	phospholipase A <sub>2</sub>
PLC	phospholipase C
PLD	phospholipase D
PP <sub>i</sub>	pyrophosphate
PTEN	phosphatase and tensin homolog
PTH	parathyroid hormone
RANK	receptor activator of nuclear factor $\kappa$ B
ROCK	Rho-associated protein kinase
RT-PCR	reverse transcription-polymerase chain reaction
RUNX2	runt-related transcription factor 2



SEM	standard error of the mean
SOST	sclerostin
SOX9	sex-determining region Y (SRY)-box 9
TGF $\beta$	transforming growth factor $\beta$
TNAP	tissue non-specific alkaline phosphatase
TRAP	tartrate-resistant acid phosphatase
TUNEL	terminal deoxynucleotidyl transferase-mediated dUTP nick-end labeling
UDP	uridine 5'-diphosphate
UTP	uridine 5'-triphosphate
VEGF	vascular endothelial growth factor

## CHAPTER ONE

### INTRODUCTION<sup>1</sup>

---

<sup>1</sup> Certain sections of this Chapter has been reproduced with permission from:  
Grol, M.W., N. Panupinthu, J. Korcok, S. M. Sims, and S.J. Dixon. 2009. Expression, signaling, and function of P2X7 receptors in bone. *Purinergic Signal*. 5(2):205-221, with some modifications.

## 1.1 Chapter Summary

Bone consists of a mineralized extracellular matrix, composed largely of collagen type I and hydroxyapatite, and three major cell-types: the bone-resorbing osteoclast, the bone-forming osteoblast and the mechanosensitive osteocyte (terminally differentiated osteoblast). The structural integrity and functionality of bone are maintained throughout life by remodeling, a process that involves the coordinated resorption of old or damaged bone and its replacement with newly mineralized bone matrix. Osteoblast proliferation, differentiation, and function are regulated by the actions of key transcription factors including RUNX2, OSX and ATF4. Various autocrine, paracrine and endocrine mediators in turn modulate the activity of these and other transcription factors to control bone formation. Mechanical loading is an important anabolic stimulus in the vertebrate skeleton. In this regard, nucleotides such as ATP are released from osteoblast lineage cells in response to mechanical stimulation and signal through two families of cell surface P2 nucleotide receptors – the P2Y family of G protein-coupled receptors and the P2X family of ligand-gated cation channels. Nearly every cell-type including osteoblasts expresses multiple P2Y and P2X receptor subtypes, though the significance of these networks of P2 receptors is unclear. P2X7 loss-of-function mice exhibit decreased periosteal bone formation, increased trabecular bone resorption and impaired anabolic responses to mechanical loading. Activation of P2X7 receptors by exogenous nucleotides *in vitro* couples to production of LPA and PGE<sub>2</sub>, resulting in increased osteoblast differentiation and matrix mineralization. However, the underlying signaling events mediating the effects of P2X7 in osteoblasts remain largely undefined. In this chapter, the rationale and objectives of the research will be discussed.

## **1.2 Bone Physiology**

### **1.2.1 Structure, Components and Functions of Bone**

The skeleton is composed anatomically of flat bones, including the skull bones, mandible and scapulae, and long bones, such as the humeri, radii, ulnae, femurs, tibiae and fibulae (Baron, 2003; Clarke, 2008). Long bones consist of two rounded epiphyses separated by a hollow shaft, or diaphysis, with flared, cone-shaped metaphyses between them (Baron, 2003; Clarke, 2008). The exterior of both long and flat bones is formed by a dense layer of calcified tissue termed cortical (or compact) bone. In the diaphysis of long bones, the cortical bone is thick and encloses the hematopoietic bone marrow within the medullary cavity. Moving toward the metaphyses and epiphyses, cortical bone becomes progressively thinner and the marrow space fills with a honeycomb-like network of thin, calcified plates and rods termed trabecular (or cancellous) bone. The spaces between trabeculae in both long and flat bones are filled with hematopoietic bone marrow, which is continuous with the diaphyseal medullary cavity in long bones (Baron, 2003; Clarke, 2008). As a result of its organization, bone has two surfaces at which it is in contact with soft tissues: an external periosteal surface and an internal endosteal surface. The endosteal surface is further subdivided into trabecular, endocortical and intracortical (or Haversian) surfaces based on location. These four surfaces serve as sites for bone formation and resorption during growth and remodeling.

The extracellular matrix of bone consists of mineral and organic material. The organic matrix is composed largely of collagen type 1 (COL1) (Baron, 2003; Clarke, 2008). A number of noncollagenous proteins are also present, including osteopontin (OPN), bone sialoprotein (BSP) and osteocalcin (OCN), which are thought to regulate

bone cell activity and the process of mineralization. The mineral content of bone is mostly hydroxyapatite [ $\text{Ca}_{10}(\text{PO}_4)_6(\text{OH})_2$ ], with trace amounts of carbonate, magnesium, and acid phosphate. Following remodeling, collagen fibers are arranged in parallel layers at right angles to one another resulting in a lamellar structure. Spindle- or plate-shaped crystals of hydroxyapatite then form on and between collagen fibers in the same general orientation (Baron, 2003; Clarke, 2008). This organization of the collagenous matrix together with the mineral component provides the resistance of bone to mechanical strain. In some instances, when bone is formed rapidly, as observed during development and fracture healing, collagen fibers are first deposited loosely in randomly oriented bundles (termed woven bone) before subsequently being remodeled into lamellar bone.

In addition to its matrix, bone is composed of three major cell-types responsible for regulation of its synthesis and remodeling: the bone-forming osteoblast, the mechanosensitive osteocyte (terminally differentiated osteoblasts embedded within the bone matrix), and the bone-resorbing osteoclast (Baron, 2003; Clarke, 2008). Cells of the osteoblast lineage develop from mesenchymal progenitor cells that also give rise to other cell-types including chondrocytes, adipocytes, and fibroblasts (Minguell et al., 2001; Harada and Rodan, 2003). In contrast, osteoclasts form by the fusion of mononucleated precursors of the monocyte/macrophage lineage derived from hematopoietic origins (Boyle et al., 2003; Teitelbaum and Ross, 2003; Novack and Teitelbaum, 2008). The major function of mature osteoblasts is to synthesize and secrete osteoid, the organic phase of the bone matrix, and regulate its mineralization (Baron, 2003; Clarke, 2008). Ultrastructurally, osteoblasts exhibit a cuboidal morphology and are characterized by the presence of a well-developed rough endoplasmic reticulum and a large Golgi apparatus –

two structures that are essential for extensive matrix protein synthesis. Osteoblasts also exhibit numerous processes on their secreting (or apical) side that extend deep into the osteoid matrix forming contacts with osteocytes (Dudley and Spiro, 1961; Baron, 2003).

As mature osteoblasts secrete osteoid, a subset becomes embedded within the bone matrix and terminally differentiates to form osteocytes. The remaining osteoblasts either undergo apoptosis or become quiescent bone lining cells (Bonewald, 2011). Transition from osteoblasts to osteocytes leads to reductions in cytoplasmic volume and in the size of the rough endoplasmic reticulum and Golgi apparatus; changes that reflect an overall decrease in protein synthesis and secretion. In addition to these morphological changes, older osteocytes, embedded deeper within the mineralized bone, exhibit glycogen accumulations within the cytoplasm (Baron, 2003). During their maturation, osteocytes develop extensive cell processes housed within canaliculi in calcified bone. These processes metabolically and electrically link osteocytes, through gap junctions (composed primarily of connexin 43), to other osteocytes, bone lining cells, and mature osteoblasts. In fact, it is thought that mechanotransduction, the process through which mechanical stimuli are translated into cellular responses, is mediated primarily by this syncytial network of osteocytes in bone (Bonewald, 2011).

Mononucleated precursors of the monocyte/macrophage lineage proliferate and fuse to form mature, multinucleated osteoclasts at the bone surface (Novack and Teitelbaum, 2008). In contrast to the osteoblast, the major function of the osteoclast is bone resorption. At the ultrastructural level, osteoclasts are characterized by the presence of approximately 4-20 nuclei, abundant mitochondria, an extensive Golgi apparatus, and numerous vesicles filled with lysosomal enzymes and vacuoles containing acid

phosphatase. However, the most prominent feature of an actively resorbing osteoclast is its ruffled border – a region consisting of deep plasma membrane folds in contact with the bone matrix (Baron, 2003). To resorb mineralized bone, active osteoclasts create an acidic microenvironment to dissolve bone mineral, while secreting various proteases and other hydrolases to degrade the organic matrix (Novack and Teitelbaum, 2008).

Throughout life, bones of the skeleton impart mechanical stability for body posture, provide protection to vital organs, and serve as sites for muscle attachments to permit locomotion. Moreover, bone provides an environment for hematopoiesis and is a major repository for  $\text{Ca}^{2+}$  and inorganic phosphate ( $\text{P}_i$ ), thus contributing to systemic ion homeostasis (Baron, 2003; Clarke, 2008). To maintain its mass and functionality throughout life, bone undergoes remodeling, a dynamic process that involves its coordinated resorption and formation (*see below*). In adults under physiological conditions, resorption and formation are tightly coupled, and perturbations to this balance cause bone loss in metabolic diseases such as osteoporosis and inflammatory diseases including rheumatoid arthritis and periodontitis (Novack and Teitelbaum, 2008).

### **1.2.2 Skeletal Development**

The vertebrate skeleton is produced by cells from three distinct embryonic lineages. The craniofacial bones are derived from neural crest cells, whereas axial and appendicular bones arise from cells of the paraxial mesoderm (somites) and lateral plate mesoderm, respectively (Olsen et al., 2000). During embryonic development, cells of these lineages migrate to sites of future skeletal elements, adhere and proliferate to form highly cellular mesenchymal condensations, and undergo differentiation (Hall and

Miyake, 2000). Bone formation within these mesenchymal condensations occurs by one of two distinct processes: intramembranous ossification (flat bones) and endochondral ossification (long bones).

*Intramembranous ossification* – Mesenchymal condensations, which form in highly vascularized areas of the embryonic connective tissue, predetermine the site, size, and shape of future skeletal elements (Hall and Miyake, 2000). During intramembranous ossification, mesenchymal progenitor cells within these condensations proliferate and differentiate directly into osteoblasts, forming ossification centres (Karaplis, 2002; Baron, 2003). The osteoblasts within these centres produce osteoid consisting of irregular collagen fibre bundles interspersed between embryonic blood vessels. The resulting calcification of this matrix is delayed and disorganized, resulting in irregular mineralization that leads to the formation of woven bone. At the external face of woven bone, vascularized mesenchyme condenses to form the periosteum, and thickening of trabeculae deep to the periosteal surface leads to formation of the woven bone collar; a structure that is later replaced by mature lamellar bone (or cortical bone) through remodeling. The spongy (or trabecular) bone that persists internally is also remodeled into lamellar bone, and the embryonic vascular tissue between trabeculae becomes the hematopoietic bone marrow (Karaplis, 2002; Baron, 2003).

*Endochondral ossification* – The process by which a cartilage template (or cartilage anlagen) is deposited and subsequently replaced by bone is termed endochondral ossification (Karaplis, 2002; Baron, 2003; Kronenberg, 2003). In the vertebrate embryo, mesoderm-derived mesenchymal progenitor cells form condensations as described above (Hall and Miyake, 2000). However, unlike intramembranous ossification, cells at the



centre of these mesenchymal condensations undergo chondrocyte differentiation (Karaplis, 2002; Baron, 2003; Kronenberg, 2003). Chondrocytes emerge and secrete a cartilaginous extracellular matrix rich in collagen type II and the proteoglycan aggrecan, leading to formation of the cartilage anlagen. Mesenchymal cells surrounding the anlagen form a perichondrium, which consists of an outer fibrous layer and an inner chondrogenic layer.

Chondrocyte proliferation and matrix production contribute to enlargement of the cartilage anlagen. Division of chondrocytes within the cartilage anlagen drives interstitial (or longitudinal) growth, whereas appositional growth of the template is accomplished by perichondrial cells (Karaplis, 2002). Eventually, mature chondrocytes at the centre of the template become postmitotic and undergo hypertrophy. These hypertrophic (or enlarged) chondrocytes secrete a matrix rich in collagen type X and direct its calcification (Karaplis, 2002; Baron, 2003; Kronenberg, 2003). Hypertrophic chondrocytes also stimulate adjacent perichondrial cells to become osteoblasts, leading to the formation of a woven bone collar (future cortical bone), which encompasses the future mid-shaft (or diaphysis) (Kronenberg, 2003). Following mineralization of the bone collar, and in response to proangiogenic factors, such as vascular endothelial growth factor (VEGF), produced by hypertrophic chondrocytes, blood vessels invade the cartilage template. At the same time, hypertrophic chondrocytes undergo apoptosis, leaving behind an acellular scaffold to guide bone formation (Karaplis, 2002; Baron, 2003; Kronenberg, 2003).

Vascular invasion of the cartilage anlagen brings the blood supply that will form the future hematopoietic bone marrow. Moreover, the invading blood vessels provide a source of osteoblast progenitors for bone formation (Baron, 2003). Following resorption

of the calcified cartilage matrix by osteoclasts, osteoblasts differentiate and form a layer of woven bone guided by cartilaginous remnants (Karaplis, 2002; Baron, 2003). The resulting bony trabeculae are referred to as the primary spongiosa. During a second cycle of bone remodeling, this woven bone, as well as remnants of the cartilage matrix, are replaced by lamellar bone resulting in formation of mature trabecular bone called secondary spongiosa (Baron, 2003).

The growth plate is established shortly after formation of the primary ossification centre within the future diaphysis. Longitudinal bone growth during embryonic development and postnatally is driven by the growth plate, which provides a continuous source of cartilaginous matrix for conversion to bone (Karaplis, 2002). Chondrocytes within the growth plate are arranged into serial columns of resting, proliferating, prehypertrophic and hypertrophic chondrocytes (Stevens and Williams, 1999). In early childhood, secondary centres of ossification form within the cartilaginous epiphyses by a similar mechanism described above for the primary ossification centre. Cartilage is retained at the joint surface (articular cartilage) and at the growth plate, which extends the full width of the bone (within the metaphysis) separating the epiphysis and diaphysis on either end (Karaplis, 2002).

### **1.2.3 Bone Remodeling**

Bone remodeling occurs asynchronously at millions of sites throughout the skeleton, regulated by autocrine, paracrine, and endocrine mediators as well as mechanical stimuli (Harada and Rodan, 2003). This process provides a mechanism for preventative maintenance of the skeleton and the targeted replacement of fatigued or

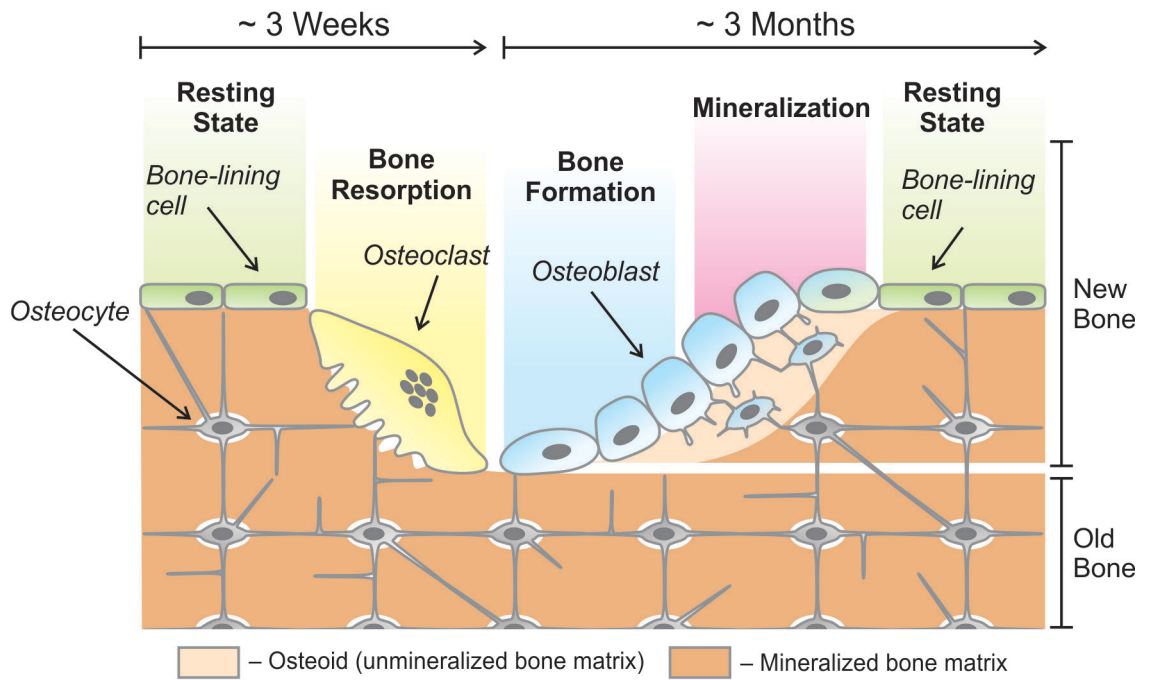
damaged bone. In addition, it allows prompt access to mineral stores in response to reduced serum  $\text{Ca}^{2+}$  and  $\text{P}_i$  levels (Parfitt, 1994). Bone remodeling is accomplished by the sequential actions of osteoclasts and osteoblasts, which form a transient structure at localized sites within the skeleton, termed the basic multicellular unit (BMU) (Frost, 1986). At intracortical surfaces, the BMU appears as a tunnel-shaped cavity consisting of osteoclasts at its leading edge and a trailing closing cone lined by osteoblasts, with connective tissue, blood vessels and nerves localized to its centre (the site of the future Haversian canal). In contrast, BMUs at trabecular and endocortical surfaces form trenches resulting in the replacement of packet-like regions of bone matrix (Parfitt, 1994). At all sites, bone remodeling involves the same four distinct phases: activation, resorption, reversal, and formation (Parfitt, 1994; Mundy et al., 2003; Sims and Gooi, 2008) (Figure 1.1).

*Activation Phase* – Localized damage to the bone matrix provides signals necessary to initiate remodeling, resulting in recruitment of osteoclast precursors to the bone surface (Parfitt, 1994; Sims and Gooi, 2008). Cells of the osteoblast lineage promote osteoclast precursor recruitment and differentiation through expression of two key signaling molecules: macrophage colony stimulating factor (M-CSF) and receptor activator of nuclear factor  $\kappa\text{B}$  ligand (RANKL) (Boyle et al., 2003; Teitelbaum and Ross, 2003). On the other hand, osteoprotegerin (OPG), a soluble decoy receptor also secreted by osteoblast lineage cells, can bind RANKL, thereby limiting signaling through receptor activator of nuclear factor  $\kappa\text{B}$  (RANK), the receptor for RANKL, and inhibiting osteoclast formation and function.

The osteocyte is a key sensor for microdamage within the skeleton

**Figure 1.1 Bone Remodeling by Osteoblasts and Osteoclasts.**

The structural integrity and functionality of the skeleton is maintained throughout life by bone remodeling; a process that involves the removal of old bone by osteoclasts and its replacement by osteoblasts. Bone remodeling at any one site within the skeleton takes up to four months and occurs in four phases: activation, resorption, reversal and formation. In response to localized damage to the bone matrix or the actions of systemic hormones, factors are released from osteoblast lineage cells resulting in recruitment of monocyte/macrophage precursors to the bone surface. Differentiation of these precursors leads to formation of a mature osteoclast characterized by its attachment to the bone surface (mediated by integrins such as  $\alpha_v\beta_3$ ) and formation of a specialized apical membrane structure termed the ruffled border. Transport of protons and secretion of hydrolytic enzymes across the ruffled-border membrane causes dissolution of bone mineral and degradation of the organic matrix. The activation and resorption phases take ~3 weeks to complete, and end with death of the osteoclast by apoptosis. During reversal, factors released either from the bone matrix or directly by the osteoclast lead to recruitment and proliferation of mesenchymal progenitor cells at the site of resorbed bone. These mesenchymal precursors then differentiate to form osteoblasts. Over the next 3 months, osteoblasts form bone through secretion of an organic matrix composed primarily of collagen type 1 (COL1), termed osteoid, and regulate its subsequent mineralization. During this process, a number of osteoblasts become embedded within the matrix and terminally differentiate into osteocytes, the most abundant cell-type in bone.



(Sims and Gooi, 2008; O'Brien et al., 2013). Studies have demonstrated that increased bone remodeling at sites of microdamage is preceded by osteocyte apoptosis (Verborgt et al., 2002; Noble et al., 2003; Mann et al., 2006; Cardoso et al., 2009). Deletion of osteocytes *in vivo* causes increased RANKL expression that is associated with increases in bone resorption (Tatsumi et al., 2007). In contrast, loss of RANKL specifically in osteocytes leads to increased cancellous bone mass associated with decreases in osteoclast numbers and resorption markers (Xiong et al., 2011). In this same study, osteocyte-specific deletion of RANKL was shown to protect against bone loss caused by skeletal unloading. Anatomically, osteocyte apoptosis appears to localize to areas of fatigue damage, whereas expression of factors that promote bone remodeling, including RANKL and VEGF, are elevated in osteocytes surrounding these apoptotic cells (Kennedy et al., 2012). In addition to mechanical stimuli, many local and systemic factors, including prostaglandin E<sub>2</sub> (PGE<sub>2</sub>), interleukins (ILs), parathyroid hormone (PTH), 1,25 dihydroxyvitamin D<sub>3</sub> (1,25(OH)<sub>2</sub>D<sub>3</sub>), and corticosteroids, mediate their effects on osteoclast differentiation and activity by signaling through osteoblasts, bone lining cells and/or osteocytes to modulate expression of RANKL and OPG (Martin, 2004).

In the early stages of osteoclast differentiation, M-CSF acts on its receptor c-Fms to stimulate proliferation and expression of RANK in cells of the monocyte/macrophage lineage. Through its interactions with RANK, RANKL, in concert with M-CSF, drives overt osteoclastogenesis in precursor cells resulting in formation of mature, multinucleated osteoclasts at the bone surface (Boyle et al., 2003; Teitelbaum and Ross, 2003). In addition to their unique morphology, mature osteoclasts are characterized by

expression of a variety of genes, including tartrate-resistant acid phosphatase (TRAP), cathepsin K, calcitonin receptor and  $\beta_3$ -integrin (Lacey et al., 1998). *Rank*<sup>-/-</sup> and *Rankl*<sup>-/-</sup> mice exhibit severe osteopetrosis (increased bone mass) due to a complete lack of mature osteoclasts and osteoclast-mediated bone resorption (Dougall et al., 1999; Kong et al., 1999; Li et al., 2000). Similarly, *op/op* mice, which possess an inactivating mutation in the gene encoding M-CSF, present with a high bone mass phenotype at birth (Begg et al., 1993). However, bone mass progressively normalizes to control levels as *op/op* mice age concomitant with the delayed appearance of TRAP-positive osteoclasts. Taken together, these data demonstrate that while RANKL-RANK signaling is absolutely required for osteoclast differentiation *in vivo*, other factors, such as VEGF, may be able to substitute for M-CSF to promote osteoclastogenesis (Niida et al., 1999).

In both precursors and mature osteoclasts, binding of RANKL to RANK activates multiple signaling pathways, including mitogen-activated protein kinases (MAPKs), phosphatidylinositol 3-kinase (PI3K), and  $\text{Ca}^{2+}$ /calcineurin. In turn, these pathways activate several transcription factors such as activator protein-1 (AP-1) family members (e.g., c-fos), nuclear factor- $\kappa$ B (NF- $\kappa$ B), and nuclear factor of activated T cells, cytoplasmic 1-4 (NFATc1-4) (Boyle et al., 2003; Teitelbaum and Ross, 2003). Of these, NFATc1 is believed to be one of the master transcriptional regulators of osteoclast differentiation downstream of RANKL signaling. *Nfatc1*<sup>-/-</sup> embryonic stem cells fail to form osteoclasts in response to RANKL, and ectopic NFATc1 expression in precursor cells is sufficient to drive osteoclastogenesis in the absence of RANKL stimulation (Takayanagi et al., 2002). Impaired osteoclast differentiation and NFATc1 expression is also observed following inhibition of calcineurin *in vitro* (Ishida et al., 2002). In addition

to NFATc1, c-fos and NF- $\kappa$ B have been shown to play critical roles at various stages of osteoclastogenesis (Grigoriadis et al., 1994; Iotsova et al., 1997).

*Resorption Phase* – Bone resorption begins with attachment of mature, multinucleated osteoclasts to the bone surface (Parfitt, 1994; Sims and Gooi, 2008). Osteoclast attachment to the extracellular matrix is mediated by a family of heterodimeric transmembrane receptors called integrins. At least four integrin receptors are expressed by mature osteoclasts: the classical vitronectin receptor  $\alpha_v\beta_3$  (predominant integrin receptor in osteoclasts); the collagen receptors  $\alpha_v\beta_5$  and  $\alpha_2\beta_1$ ; and  $\alpha_v\beta_1$ , which bind a variety of extracellular matrix proteins through an Arg-Gly-Asp (RGD) motif, including vitronectin, collagen, OPN and BSP (Nesbitt et al., 1993). In addition to vitronectin,  $\alpha_v\beta_3$  also interacts with other RGD-containing bone matrix proteins such as OPN (Miyachi et al., 1991). The importance of integrin receptor signaling in osteoclast biology is emphasized by the ability of  $\alpha_v\beta_3$  antibodies, RGD mimetics, and RGD peptides to inhibit bone resorption *in vitro* (Sato et al., 1990; Horton et al., 1991; Lakkakorpi et al., 1991) and *in vivo* (Fisher et al., 1993). Moreover, deletion of the gene encoding  $\beta_3$  integrin in mice leads to an osteosclerotic phenotype (increased bone mass) resulting from deficits in osteoclast-mediated bone resorption and spreading (McHugh et al., 2000). Integrin-mediated attachment of the osteoclast to the bone surface results in its polarized morphology, consisting of a ruffled border at the osteoclast-bone interface, surrounded by an annular sealing zone – a ring of actin localized within podosomes at the site of osteoclast adhesion (Baron, 2003; Novack and Teitelbaum, 2008). The primary function of the sealing zone is to isolate the resorption site and restrict lacunar acid leakage.

During bone resorption, vacuolar  $H^+$ -ATPases within the ruffled-border



membrane of the osteoclast acidify an extracellular compartment termed the resorption lacuna, leading to dissolution of bone mineral and exposure of the organic matrix (Baron, 2003; Novack and Teitelbaum, 2008). Bicarbonate, which is generated during this process, leaves the cell in exchange for chloride at the basolateral membrane. To maintain electroneutrality within the resorbing osteoclast, chloride channels, localized within the ruffled-border membrane, permit passive movement of chloride into the resorption compartment. Next, collagenous and non-collagenous matrix proteins exposed by the process of demineralization are degraded by a variety of hydrolytic enzymes, such as cathepsin K, matrix metalloproteinase 9 and TRAP, released from the osteoclast by exocytosis (Baron, 2003; Novack and Teitelbaum, 2008). Fragments of these matrix proteins are then endocytosed and released from the cell at its basolateral membrane. The importance of osteoclast-mediated resorption during bone remodeling is highlighted by the osteopetrotic phenotypes observed in mice and humans carrying loss-of-function mutations in various osteoclast channel proteins and enzymes, such as the CIC-7 chloride exchanger and cathepsin K, associated with lacunar acidification and protein digestion (Gelb et al., 1996; Kornak et al., 2001).

*Reversal Phase* – Following osteoclast-mediated bone resorption, mononuclear cells of unknown lineage modify the resorbed surface in preparation for bone formation, and deposit a substance referred to as the cement (or reversal) line (Parfitt, 1994; Baron, 2003). The cement line is a thin, mineral-deficient, sulfur-rich layer of matrix that separates new bone from the old bone matrix (Schaffler et al., 1987).

The coupling signals that direct bone formation to sites of bone resorption remain unclear. Older theories postulated that proteins present within the cement line, such as

OPN, could serve as signals to initiate bone formation (McKee and Nanci, 1996). Others suggest that growth factors, including insulin-like growth factors (IGFs), transforming growth factor  $\beta$  (TGF $\beta$ ), and bone morphogenetic proteins (BMPs), are released from bone matrix during the resorption phase, and function to recruit osteoblast precursors to resorbed surfaces and promote osteoblastogenesis (Mundy et al., 2003; Sims and Gooi, 2008). More recently, a number of studies have demonstrated that osteoclasts can serve as a direct source of both soluble and membrane-bound factors that stimulate osteoblast proliferation and differentiation (Zhao et al., 2006; Pederson et al., 2008; Walker et al., 2008), findings that implicate the osteoclast itself in the coupling of bone resorption to formation.

*Bone Formation Phase* – The formation phase of the remodeling cycle begins when cells of osteoblast lineage, recruited to the resorbed surface following the reversal phase, proliferate and differentiate into mature osteoblasts (*regulation of osteoblast differentiation is described below*) (Parfitt, 1994; Sims and Gooi, 2008). Following secretion and subsequent mineralization of the osteoid, some osteoblasts die by apoptosis or become quiescent and line the inactive bone surface (bone lining cells). Still other osteoblasts, which were embedded within the bone matrix during its formation, terminally differentiate into osteocytes (Baron, 2003; Clarke, 2008; Sims and Gooi, 2008; Bonewald, 2011).

## **1.3 Osteoblast Biology**

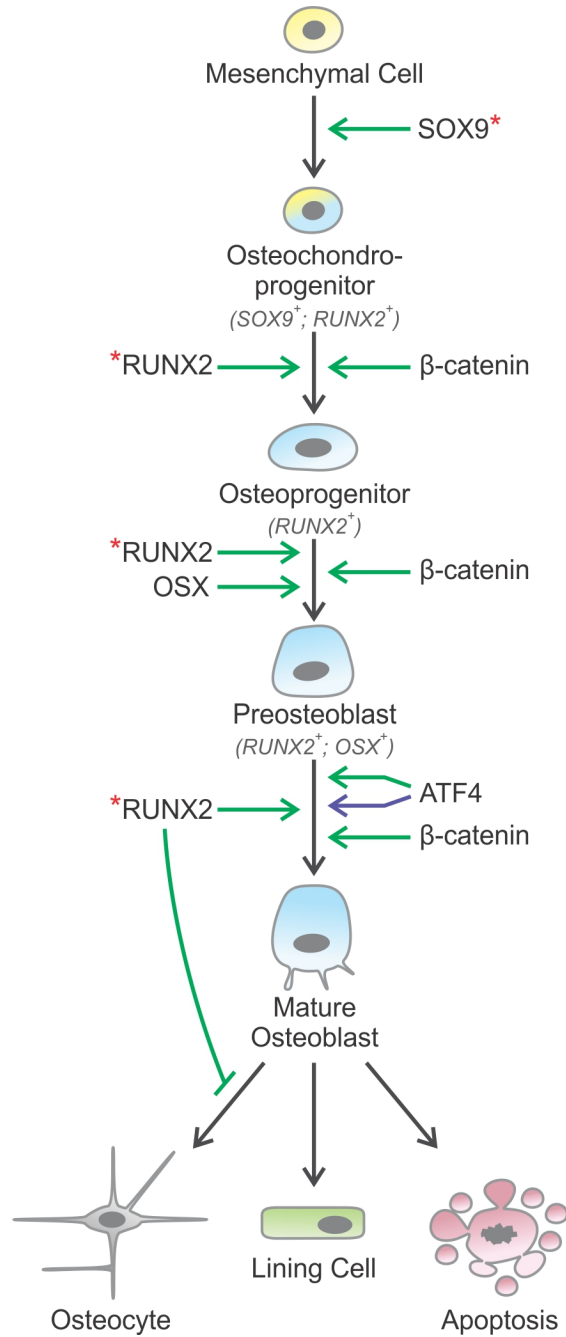
### **1.3.1 Master Transcription Factors and Transcriptional Coactivators Regulating Osteoblast Differentiation and Function**

As the cells responsible for bone formation and regulation of osteoclast differentiation and function, osteoblasts are essential for normal skeletal development and remodeling. Extensive analyses of human genetic bone disorders and mouse models of skeletal disease have revealed a number of key transcription factors as well as transcriptional coactivators required for differentiation of osteoblasts from mesenchymal progenitors (Figure 1.2). As these factors function only at specific times during osteoblastogenesis, their expression defines the various developmental stages within the osteoblast lineage.

*SOX9* – Sex-determining region Y (SRY)-box 9 (*SOX9*), a transcription factor containing a SRY-related high-mobility-group-box DNA binding domain, is expressed in all non-hypertrophic chondrocytes including articular chondrocytes (Wright et al., 1995; Ng et al., 1997; Zhao et al., 1997; Davies et al., 2002). The importance of *SOX9* in skeletal biology was first established when an inactivating mutation in the human gene was shown to cause campomelic dysplasia, a disease characterized by severe cartilage abnormalities (Foster et al., 1994; Wagner et al., 1994). Subsequent studies using a variety of animal models provided the conclusive evidence that *SOX9* is the key transcription factor for chondrocyte differentiation (Bi et al., 1999; Bi et al., 2001; Akiyama et al., 2002; Kist et al., 2002). In addition to its role during chondrogenesis, *SOX9* marks the mesenchymal progenitor cells that give rise to cells of the osteoblast lineage (Akiyama et al., 2005). Though the exact function of *SOX9* in osteoblast

**Figure 1.2 Transcriptional Control of Osteoblast Differentiation.**

Commitment of mesenchymal progenitor cells to the osteoblast lineage is controlled by a number of key transcriptional events during osteoblastogenesis. The chondrocyte master transcription factor sex-determining region Y (SRY)-box 9 (SOX9) is first upregulated in mesenchymal progenitors that give rise to either chondrocytes or osteoblasts. The osteoblast master transcription factor runt-related transcription factor 2 (RUNX2) is then expressed resulting in formation osteochondroprogenitors. Subsequent downregulation of SOX9 gives rise to RUNX2-positive osteoprogenitors. The actions of RUNX2 at this stage of osteoblastogenesis result in expression of osteoblast-specific genes, including collagen type I (COL1) and alkaline phosphatase (ALP), and the upregulation of Osterix (OSX), a second osteoblast master transcription factor. In turn, OSX regulates expression of COL1 and bone sialoprotein (BSP) and, together with RUNX2, promotes formation of the pre- (or immature) osteoblast. The transcription factor ATF-4 accumulates specifically within later stage osteoblasts, and functions downstream of, but in concert, with RUNX2 and OSX to activate expression of mature osteoblast markers such as osteocalcin (OCN). In addition, ATF-4 post-transcriptionally modulates cellular amino acid uptake to control COL1 synthesis. Taken together, the actions of ATF-4, OSX, and RUNX2 are necessary to promote acquisition of the mature osteoblast phenotype. At the same time, the canonical Wnt transcriptional coactivator  $\beta$ -catenin is also required at all stages of the osteoblast differentiation cascade. In this regard, loss of  $\beta$ -catenin in osteochondroprogenitors, osteoprogenitors or preosteoblasts results in chondrogenic differentiation of these cells. At the terminal stages, mature osteoblasts either differentiate to form osteocytes or bone lining cells, or undergo apoptosis. Transcriptional regulation is shown in **green**; posttranscriptional regulation is shown in **blue**. **Red** asterisks indicate the existence of a disease-causing mutation in humans.



differentiation is unclear, it is known to be absent from mature osteoblasts (Long, 2012).

*RUNX2* – Runt-related transcription factor 2 (*RUNX2*), a member of the Runt domain family of transcription factors, is a master regulator of osteoblast differentiation (Long, 2012). During limb development, *RUNX2* is first expressed in osteochondroprogenitors of the chondrogenic mesenchyme following and dependent upon *SOX9* expression (Akiyama et al., 2005). Subsequent to formation of the cartilage anlagen, *RUNX2* localizes more specifically to cells of the osteoblast lineage and perichondrium (Ducy et al., 1997; Otto et al., 1997). Though *RUNX2* expression is slowly lost in differentiating chondrocytes (Ducy et al., 1997; Bialek et al., 2004; Hinoi et al., 2006a), it is upregulated during hypertrophy where it controls expression of collagen type X  $\alpha 1$  (Enomoto et al., 2000; Zheng et al., 2003).

Studies in mice and humans have demonstrated unequivocally that *RUNX2* is required for osteoblast differentiation during both endochondral and intramembranous ossification. In humans, heterozygous inactivating mutations in the *RUNX2* gene cause cleidocranial dysplasia, a disease characterized by hypoplastic or absent clavicles, delayed closure of the fontanelles, dental abnormalities, and delayed skeletal development (Lee et al., 1997; Mundlos et al., 1997; Zhou et al., 1999). Genetically modified mice with *RUNX2* haploinsufficiency phenotypically copy human patients with cleidocranial dysplasia (Lee et al., 1997; Otto et al., 1997); whereas, homozygous deletion of this transcription factor results in a cartilaginous skeleton completely devoid of osteoblasts (Komori et al., 1997; Otto et al., 1997). Consistent with evidence that human mutations in *RUNX2* abolish its DNA-binding ability, deletion of the *RUNX2* nuclear localization signal, located at its COOH-terminus, recapitulates the phenotype of *Runx2*<sup>-/-</sup> mice (Choi

et al., 2001). Ducky and colleagues further solidified the importance of RUNX2 in osteoblast differentiation by demonstrating that its forced expression in nonosteoblastic cells could upregulate a variety of osteoblast-specific genes (Ducky et al., 1997). RUNX2 has since been shown to directly regulate many genes critical to the osteoblast phenotype, including COL1, alkaline phosphatase (ALP), OPN, osteonectin, and OCN (Harada et al., 1999; Kern et al., 2001; Otto et al., 2003; Lian et al., 2004; Schroeder et al., 2005). In addition to its roles during embryogenesis, RUNX2 regulates a variety of functions in mature osteoblasts, including the synthesis of bone matrix proteins (Ducky et al., 1999).

During limb development, RUNX2 expression is regulated by a number of important growth factors. Prehypertrophic and early hypertrophic chondrocytes within the endochondral cartilage anlagen express Indian hedgehog (IHH), which promotes osteoblast differentiation of adjacent perichondrial cells (St-Jacques et al., 1999). Perichondrial progenitor cells in *Ihh*<sup>-/-</sup> mice fail to express RUNX2 resulting in an endochondral skeleton lacking osteoblasts (St-Jacques et al., 1999; Long et al., 2004). At the same time, osteoblasts derived via intramembranous ossification still form in IHH-deficient mice (St-Jacques et al., 1999), indicating that IHH signaling is not required for intramembranous osteoblast differentiation. In addition to IHH, BMP-2 has been shown to induce Smad-dependent expression of RUNX2 in a mesenchymal progenitor cell line (Lee et al., 2000; Lee et al., 2003). Moreover, Smad proteins are known to physically interact with RUNX2 to cooperatively regulate osteoblast-specific gene expression downstream of BMP signaling (Zhang et al., 2000; Ito and Miyazono, 2003; Miyazono et al., 2004).

*OSX* – A transcription factor belonging to the Sp-family of Krüppel-like zinc

finger proteins, Osterix (OSX) is essential for osteoblast differentiation and function. Homozygous deletion of OSX in mice results in the complete absence of osteoblasts and associated bone formation (Nakashima et al., 2002). Though bones formed by intramembranous ossification in OSX-deficient mice fail to calcify, endochondral skeletal elements do contain some mineralized matrix; however, this matrix resembles calcified cartilage as opposed to bone (Nakashima et al., 2002). Given that the skeleton of RUNX2-deficient mice is completely nonmineralized (Komori et al., 1997; Otto et al., 1997), these data suggest that RUNX2 and OSX together regulate osteoblast differentiation, whereas RUNX2 alone controls chondrocyte hypertrophy. Detailed analyses of *Runx2*<sup>-/-</sup> and *Osx*<sup>-/-</sup> mice further revealed that while RUNX2 is expressed in *Osx*<sup>-/-</sup> embryos, expression of OSX is absent in *Runx2*<sup>-/-</sup> embryos (Nakashima et al., 2002). Taken together, these data demonstrate that OSX functions downstream of RUNX2 in the control of osteoblastogenesis (Nakashima et al., 2002). In addition to its roles during skeletal development, OSX regulates differentiation and function of osteoblasts and osteocytes in postnatal life (Zhou et al., 2010).

OSX controls the expression of a variety of matrix proteins, such as COL1, BSP, and OCN, in cells of the osteoblast lineage (Nakashima et al., 2002). The expression of OSX is in turn regulated by a number of transcription factors and signaling pathways (*see detailed discussion below*). Consistent with OSX functioning downstream of RUNX2 during osteoblastogenesis, RUNX2 directly interacts with the OSX promoter (Nishio et al., 2006), and regulation of OSX expression has been shown to be mediated by both RUNX2-dependent and -independent mechanisms (Celil and Campbell, 2005; Matsubara et al., 2008). BMP-2 also induces expression of OSX during osteoblast differentiation of



mesenchymal progenitors *in vitro* through Smad-dependent and -independent signaling (Celil and Campbell, 2005; Celil et al., 2005; Matsubara et al., 2008).

*ATF4* – Activating transcription factor 4 (ATF4), a member of the basic Leu zipper family of transcription factors, is ubiquitously expressed, but selectively accumulates in osteoblasts due to lack of proteasomal degradation (Yang and Karsenty, 2004). In humans, misregulation of ATF4 activity, caused by loss-of-function mutations in genes encoding neurofibromatosis 1 and ribosomal S6 kinase 2, is associated with the skeletal phenotypes observed in neurofibromatosis type I and Coffin-Lowry syndrome, respectively (Yang et al., 2004; Elefteriou et al., 2006). Consistent with these findings, *Atf4*<sup>-/-</sup> mice exhibit delays in skeletal development and a low bone mass phenotype throughout postnatal life (Yang et al., 2004). Molecular markers of differentiated osteoblasts, including BSP and OCN, are decreased in ATF4-deficient mice; whereas, genes associated with earlier stages, such as RUNX2, OSX and COL1 $\alpha$ 1, remain unchanged (Yang et al., 2004). These data suggest that ATF4 functions downstream of RUNX2 and OSX to regulate terminal osteoblast differentiation. In addition to its effects on osteoblastogenesis, absence of ATF4 in mice leads to severe impairments in bone formation owing to decreased COL1 $\alpha$ 1 synthesis by mature osteoblasts (Yang et al., 2004).

Unlike other transcription factors, ATF4 promotes osteoblast differentiation and function through both transcriptional and post-transcriptional mechanisms. ATF4 binds the promoters of OCN and RANKL, thereby directly activating transcription of these genes (Yang and Karsenty, 2004; Yang et al., 2004; Elefteriou et al., 2005; Elefteriou et al., 2006). In addition, ATF4 regulates amino acid import independent of its

transcriptional activity to ensure proper synthesis of bone matrix proteins, such as COL1, by mature osteoblasts (Yang et al., 2004; Elefteriou et al., 2006).

*β-catenin* – Though not specifically expressed in cells of the osteoblast lineage, *β-catenin*, the transcriptional coactivator of canonical Wnt signaling (*discussed in detail below*), plays a critical role in the regulation of osteoblast differentiation and bone formation during development. Homozygous deletion of *β-catenin* in mesenchymal progenitor cells results in a lack of mineralized bone matrix within both intramembranous and endochondral skeletal elements of the murine embryo (Day et al., 2005; Hill et al., 2005; Hu et al., 2005). Though perichondrial and periosteal cells in these *β-catenin*<sup>-/-</sup> mice express a number of early osteoblast markers, including ALP, COL1 $\alpha$ 1 and RUNX2, at similar or reduced levels compared to controls, they fail to form mature osteoblasts as evidenced by the complete absence of OSX and OCN expression (Hill et al., 2005; Hu et al., 2005). Loss of *β-catenin* in more differentiated osteoblasts (RUNX2<sup>+</sup>;OSX<sup>+</sup>) results in a similar absence of both OCN-positive osteoblasts and mineralized bone matrix (Rodda and McMahon, 2006). The requirement for *β-catenin* during osteoblastogenesis seems to be associated with Wnt signaling, as phenotypic characteristics of mice lacking lipoprotein receptor-related protein (LRP) 5 and LRP6 in mesenchymal progenitors closely resemble those observed in *β-catenin*-deficient embryos (Joeng et al., 2011). Taken together, these data show that *β-catenin* functions downstream of RUNX2 but upstream of OSX to regulate osteoblast maturation and function at multiple stages of differentiation in a Wnt-dependent manner. In this regard, *β-catenin* directly regulates expression of COL1 $\alpha$ 1 and COL1 $\alpha$ 2 (Glass et al., 2005), and enhances RUNX2 expression and transcriptional activity (Gaur et al., 2005). Since RUNX2 can directly

regulate transcription of the *Osx* gene (Celil and Campbell, 2005; Nishio et al., 2006; Matsubara et al., 2008),  $\beta$ -catenin may indirectly regulate OSX expression through its interactions with RUNX2. Another mechanism by which  $\beta$ -catenin promotes osteoblast differentiation is through suppression of other mesenchymal cell fates. In this regard, loss of  $\beta$ -catenin in mesenchymal progenitor cells causes ectopic chondrocyte differentiation at sites of osteoblastogenesis, such as the perichondrium and periosteum (Day et al., 2005; Hill et al., 2005). Moreover, Wnt/ $\beta$ -catenin signaling has been reported to promote osteoblast differentiation in mesenchymal precursor cells and mouse embryonic fibroblasts in part by suppressing expression of key adipogenic transcription factors (Kang et al., 2007).

### **1.3.2 Regulation of Bone Formation**

Bone formation is regulated during skeletal development and remodeling by a number of local and systemic factors including Wnts, BMPs, TGF- $\beta$ , fibroblast growth factors (FGFs), platelet-derived growth factors (PDGFs), PTH, glucocorticoids and mechanical loading (Harada and Rodan, 2003; Long, 2012). Each of these stimuli in turn activates an array of intracellular signaling pathways that have been implicated in the regulation of osteoblast differentiation, survival and function. In this section, signaling pathways pertinent to this thesis, including Wnt, Ca<sup>2+</sup>/NFAT and PI3K/AKT signaling, will be discussed. The importance of adenosine 3',5'-cyclic monophosphate (cAMP)/protein kinase A (PKA) and MAPK signaling in bone formation has been reviewed by others (Swarthout et al., 2002; Soltanoff et al., 2009; Marie, 2012; Greenblatt et al., 2013) and will not be mentioned below.

*Wnt signaling* – Canonical and noncanonical signaling mediated by the Wnt family of cysteine-rich secreted glycoproteins is essential for the regulation of cell proliferation and differentiation during skeletal development and bone remodeling (Westendorf et al., 2004; Bodine and Komm, 2006; Hartmann, 2006; Krishnan et al., 2006; Long, 2012; Baron and Kneissel, 2013). Moreover, canonical Wnt signaling is a critical mediator of anabolic responses of the skeleton to mechanical loading (Bonewald and Johnson, 2008; Bonewald, 2011; Baron and Kneissel, 2013).

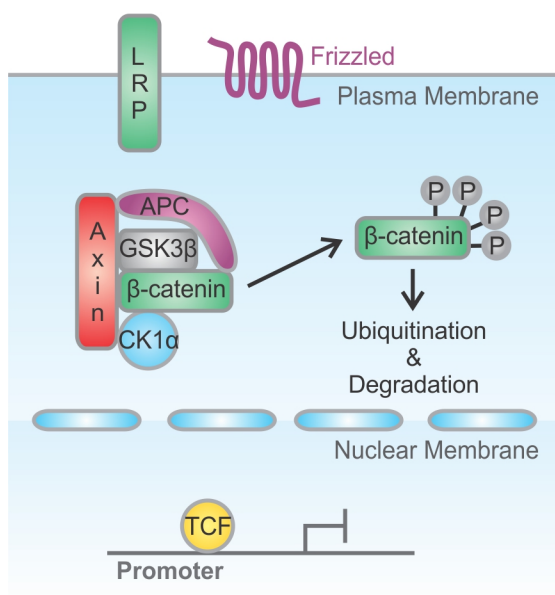
Canonical Wnt signaling is initiated when Wnt ligands bind Frizzled receptors (Fzd) and their co-receptors low density LRP5 or LRP6 leading to stabilization and subsequent accumulation of  $\beta$ -catenin within the cytosol. As a result,  $\beta$ -catenin translocates to the nucleus where it activates transcription of Wnt target genes (MacDonald et al., 2009) (*for more detailed information, see Figure 1.3*). Alternatively, non-canonical Wnt ligands act through Fzd receptors independent of LRP5/6 and  $\beta$ -catenin to stimulate signaling pathways involving  $\text{Ca}^{2+}$  and  $\text{Ca}^{2+}$ -sensitive effectors (including protein kinase C (PKC),  $\text{Ca}^{2+}$ /calmodulin-dependent protein kinase II (CaMKII) and NFAT), the small GTPases Rho and Rac, Rho-associated protein kinase (ROCK) and c-Jun NH<sub>2</sub>-terminal kinase (JNK) (Veeman et al., 2003; Seifert and Mlodzik, 2007; Wang and Nathans, 2007; Angers and Moon, 2009). Though both canonical and noncanonical pathways regulate osteoblastogenesis and bone formation in mice, known mutations associated with human skeletal disease appear to target canonical Wnt signaling alone in postnatal life (Baron and Kneissel, 2013).

As opposed to skeletal development, the role of Wnt/ $\beta$ -catenin signaling in postnatal bone homeostasis is less clear. In humans, loss-of-function mutations in the

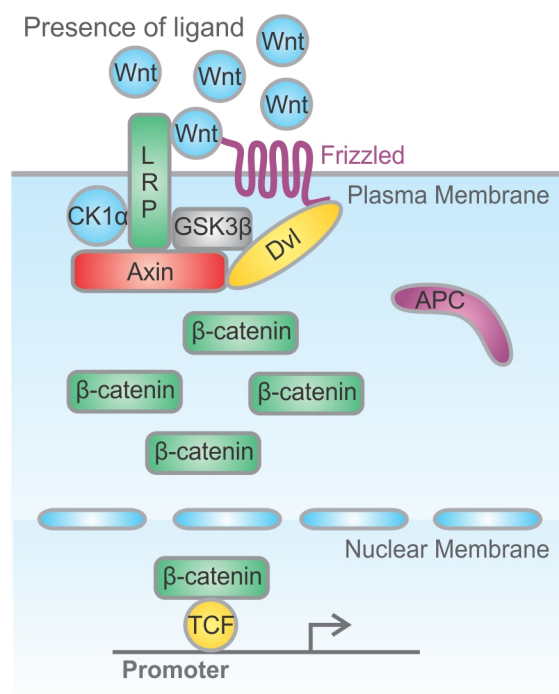
**Figure 1.3 Schematic of the Canonical Wnt/ $\beta$ -catenin Signaling Pathway in Osteoblasts.**

In the absence of Wnt,  $\beta$ -catenin is targeted to a multiprotein destruction complex within the cytosol consisting of the scaffolding protein axin, the tumor suppressor adenomatous polyposis coli (APC), glycogen synthase kinase 3 $\beta$  (GSK3 $\beta$ ), and casein kinase 1 (CK1). GSK3 $\beta$  and CK1 phosphorylate  $\beta$ -catenin at specific serine/threonine residues within its NH<sub>2</sub>-terminal, resulting in its polyubiquitination and proteasomal degradation. Canonical Wnt ligands bind to a dual receptor complex, consisting of the Wnt co-receptors low-density lipoprotein receptor-related protein (LRP) 5 or LRP6 and one of 10 known seven-pass transmembrane Frizzled receptors (Fzd). Upon activation of the receptor complex, the scaffolding protein dishevelled (Dvl) binds Fzd and recruits the destruction complex to the plasma membrane. Actions of GSK3 $\beta$  and CK1 at the membrane lead to phosphorylation of LRP5/6, which further enhances destruction complex recruitment. As a result, the destruction complex is inhibited and phosphorylation of  $\beta$ -catenin is suppressed, thereby allowing it to accumulate within the cytosol and translocate to the nucleus to activate Wnt target gene expression.

Absence of ligand



Presence of ligand



*LRP5* gene cause osteoporosis-pseudoglioma syndrome, an autosomal recessive disease of juvenile-onset characterized by low bone mass and increased skeletal fragility (Gong et al., 2001). Conversely, gain-of-function mutations in the same gene cause high bone mass syndrome by lowering LRP5's affinity for extracellular Wnt inhibitors, such as dickkopf 1 (DKK1) and sclerostin (SOST) (Boyden et al., 2002; Little et al., 2002; Ai et al., 2005; Ellies et al., 2006; Semenov and He, 2006). In addition, a number of polymorphisms in the *LRP5* gene have been associated with differences in human bone mineral density and fracture risk (Urano et al., 2004; Ferrari et al., 2005; Hartikka et al., 2005; Koller et al., 2005; Kiel et al., 2007). Similar to findings in humans, homozygous deletion of LRP5 in mice leads to reduced postnatal bone mass caused by impaired osteoblast proliferation and function with little-to-no alteration in osteoclastogenesis and bone resorption (Kato et al., 2002). Loss of a single LRP6 allele further exacerbates the phenotype seen in *Lrp5*<sup>-/-</sup> mice (Holmen et al., 2004), demonstrating that both LRP5 and LRP6 influence postnatal bone remodeling. Alternatively, mice overexpressing a human gain-of-function LRP5 mutation exhibit high bone mass resulting from increased osteoblast activity and reduced apoptosis (Babij et al., 2003). As opposed to findings during embryogenesis (*described above*), deletion of  $\beta$ -catenin in more mature osteoblasts (either COL1<sup>+</sup> or COL1<sup>+</sup>;OCN<sup>+</sup>) causes osteopenia of the postnatal skeleton due to decreased osteoblast-mediated OPG expression, which results in non-cell-autonomous increases in osteoclast differentiation and bone resorption (Glass et al., 2005; Holmen et al., 2005). However, unlike the LRP5-deficient mouse models, osteoblastogenesis and bone formation are unaffected in these  *$\beta$ -catenin*<sup>-/-</sup> mice (Glass et al., 2005; Holmen et al., 2005).

Differences in the postnatal phenotypes of LRP5- and  $\beta$ -catenin-deficient mouse

models suggest that LRP5/6 may activate other pathways independent of Wnt/ $\beta$ -catenin signaling. In this regard, non-canonical Wnt signaling via CaMKII has been shown to transcriptionally repress adipogenesis, while inducing RUNX2 expression to promote osteoblast differentiation (Takada et al., 2007). Wnt3a and Wnt7b both signal in part via PKC $\delta$  to stimulate osteoblastogenesis from mesenchymal progenitor cells *in vitro* (Tu et al., 2007). In this regard, PKC $\delta$ <sup>-/-</sup> mice exhibit deficits in bone formation during embryogenesis resulting from impaired osteoblast differentiation (Tu et al., 2007).

Canonical Wnt signaling within osteocytes is essential for the sensing of and anabolic responses to mechanical stimuli in bone (Bonewald and Johnson, 2008; Bonewald, 2011; Baron and Kneissel, 2013). Mature osteocytes are known to selectively secrete SOST (van Bezooijen et al., 2004; Poole et al., 2005), a glycoprotein that antagonizes LRP5/6 to inhibit Wnt/ $\beta$ -catenin signaling (MacDonald et al., 2009). In the absence of mechanical stimuli, SOST diffuses to the bone surface through the canalicular system where it inhibits osteoblast-mediated bone formation (van Bezooijen et al., 2004; Poole et al., 2005). In mice, skeletal loading or unloading leads to corresponding decreases or increases in SOST expression, respectively (Robling et al., 2008; Tu et al., 2012b). Elevations in serum SOST levels are also observed in human patients subjected to periods of prolonged immobilization (Gaudio et al., 2010). In agreement with these findings, genetic deletion of SOST or treatment with a SOST antibody protects against bone loss after unloading in mice (Lin et al., 2009; Tian et al., 2011); whereas, forced overexpression of SOST in osteocytes reduces load-induced bone formation (Tu et al., 2012b). Moreover, both whole-body and osteocyte-specific homozygous deletion of LRP5 almost completely abolishes the anabolic response of the murine ulna to



mechanical loading (Sawakami et al., 2006; Zhao et al., 2013).

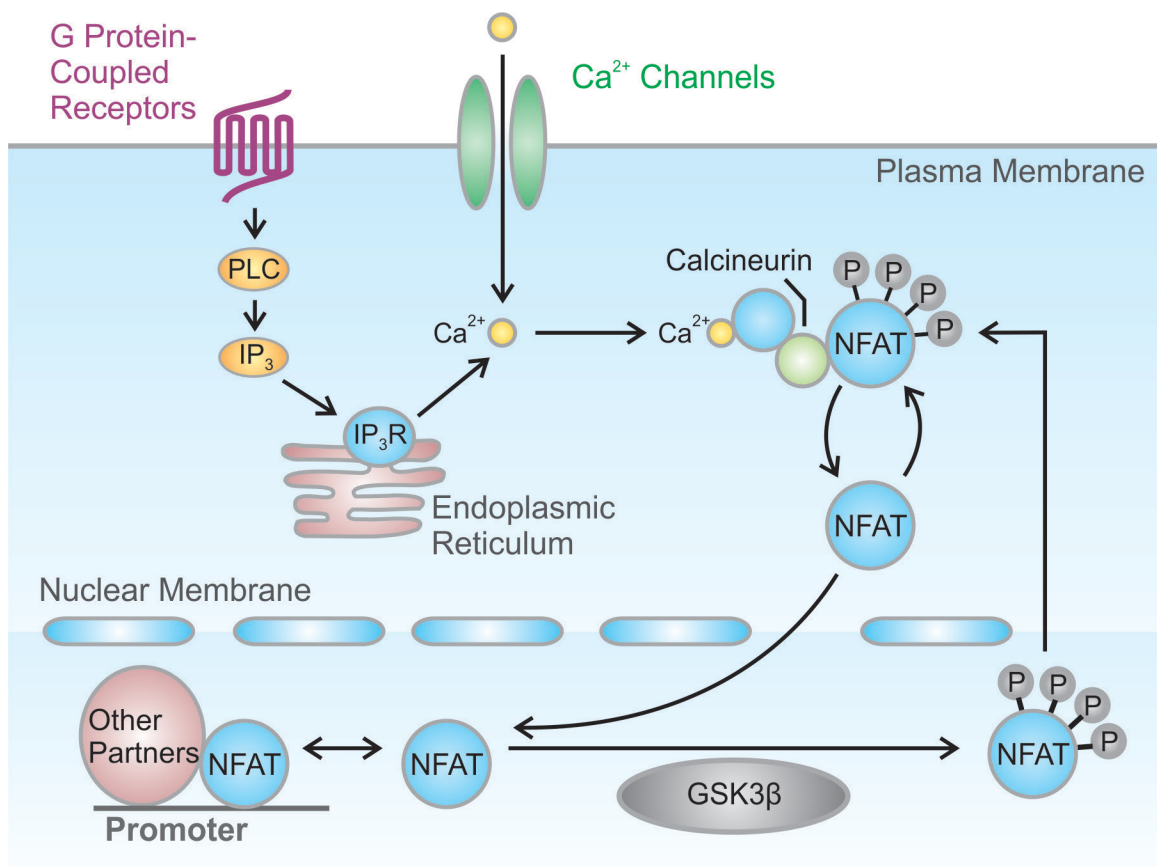
*Ca<sup>2+</sup>/NFAT signaling* – In general, stimulation of specific receptors that couple to elevations of cytosolic free Ca<sup>2+</sup> concentration ([Ca<sup>2+</sup>]<sub>i</sub>) result in activation of calcineurin, a serine/threonine phosphatase that dephosphorylates NFATc1-4 transcription factors within the cytosol leading to their nuclear translocation and transcriptional activation (Rao et al., 1997; Hogan et al., 2003; Macian, 2005) (*for more detailed information, see Figure 1.4*). Though classically described as a master regulator of osteoclastogenesis (Boyle et al., 2003; Teitelbaum and Ross, 2003; Novack and Teitelbaum, 2008), the Ca<sup>2+</sup>/NFAT pathway has since been shown to play important roles in regulation of osteoblast proliferation, differentiation, and function.

Bone marrow-derived mesenchymal precursors and MC3T3-E1 osteoblast-like cells express all isoforms of calcineurin A and B. Overexpression of calcineurin A $\alpha$  in differentiating cultures of MC3T3-E1 cells enhances osteoblastogenesis as evidenced by increases in expression of RUNX2, ALP, BSP and OCN (Sun et al., 2005). Moreover, calvarial bones transduced with calcineurin A $\alpha$  *in situ* exhibit marked increases in BMP-2-induced bone formation (Sun et al., 2005). In contrast, homozygous deletion of calcineurin A $\alpha$  in mice causes decreased bone formation within the postnatal skeleton and attenuated osteoblast differentiation of mesenchymal precursor cells *in vitro* (Sun et al., 2005). Pharmacological inhibition of calcineurin using FK506 phenotypically copies both the *in vivo* and *in vitro* effects seen in calcineurin A $\alpha$ -deficient mice (Koga et al., 2005; Sun et al., 2005), further demonstrating the importance of the Ca<sup>2+</sup>/calcineurin pathway in osteoblast biology.

In addition to calcineurin, embryonic fibroblasts from *Nfatc1*<sup>-/-</sup> mice exhibit

**Figure 1.4 Schematic of the Ca<sup>2+</sup>/NFAT Signaling Pathway in Osteoblasts.**

In resting cells, nuclear factor of activated T-cells, cytoplasmic 1-4 (NFATc1-4) proteins are phosphorylated and localized to the cytosol. Activation of receptors coupled to specific Ca<sup>2+</sup> signaling pathways trigger elevations of cytosolic Ca<sup>2+</sup> concentration ([Ca<sup>2+</sup>]<sub>i</sub>) that lead to calmodulin-dependent activation of the serine/threonine phosphatase calcineurin. Dephosphorylation of NFATc1-4 by calcineurin causes a conformational change that exposes their nuclear localization signal resulting in their nuclear translocation and transcriptional activation. These events are opposed by kinases, including casein kinase 1 (CK1) and glycogen synthase kinase 3β (GSK3β), which help to maintain NFATc1-4 in a phosphorylated state within the cytosol (maintenance kinase) and/or induce rephosphorylation of nuclear NFATc1-4 proteins to expose a nuclear export signal and promote export of NFATc1-4 from the nucleus (export kinases). Within the nucleus, NFATc1-4 interact with a number of transcriptional binding partners, such as activator protein-1 (AP-1) family members (e.g., c-fos), transcription factor GATA-binding protein 3 (GATA3), CCAAT/enhancer binding protein (C/EBP), early growth response protein (EGR) 1/4, myocyte enhancer factor-2 (MEF-2), forkhead box protein 3 (Foxp3) and Osx, allowing for integration of Ca<sup>2+</sup> signaling with many other signaling pathways.



decreased osteoblast differentiation in response to BMP-2 treatment *in vitro* (Koga et al., 2005). Moreover, loss of NFATc2 in mice leads to reduced embryonic bone formation and trabecular bone volume with no observed changes in osteoclast numbers or bone resorption (Koga et al., 2005). Conversely, mice expressing a constitutively active variant of NFATc1 (NFATc1<sup>nuc</sup>) in osteoblasts display increased bone formation owing to enhanced proliferation *in vivo* and *in vitro* (Winslow et al., 2006). A more recent study demonstrates that canonical Notch signaling inhibits embryonic bone formation and osteoblast differentiation *in vivo* through suppression of NFATc1 transcriptional activity in osteoblasts (Tu et al., 2012a), thereby confirming an important role for NFATc1 in osteoblast proliferation and differentiation. NFATc1 may regulate osteoblastogenesis through its interactions with OSX, which lead to enhanced OSX-dependent transcriptional activity at the COL1 $\alpha$ 1 promoter (Koga et al., 2005). At the same time, NFATc1<sup>nuc</sup> mice exhibit increased osteoclastogenesis associated with osteoblast-mediated expression of the monocyte chemoattractant chemokine (C-C motif) ligand 8 (CCL8) (Winslow et al., 2006), thereby implicating osteoblast-specific NFATc1 activity in the regulation of osteoclast differentiation and bone resorption.

Despite numerous genetic and pharmacological investigations into its role in bone formation, little-to-nothing is known regarding the physiological ligands that activate Ca<sup>2+</sup>-sensitive NFAT transcription factors in osteoblasts. In this regard, PTH and connective tissue growth factor (CTGF) activate Ca<sup>2+</sup>-sensitive NFAT transcription factors in osteoblast-like and stromal cell lines (Huang et al., 2010; Smerdel-Ramoya et al., 2010). The Ca<sup>2+</sup>/NFAT pathway has also emerged as a key regulator of mechanotransduction in cells of the osteoblast lineage. Specifically, C3H10T1/2 or

marrow-derived mesenchymal progenitor cells subjected to mechanical strain exhibit Wnt-independent inhibition of glycogen synthase kinase 3 $\beta$  (GSK3 $\beta$ ), resulting in activation of  $\beta$ -catenin and NFATc1 (Sen et al., 2009). Whereas strain-induced activation of  $\beta$ -catenin inhibited adipogenesis in these cells, NFATc1 promoted osteoblast differentiation through transcriptional activation of the cyclooxygenase-2 (COX-2) gene (Sen et al., 2009). Fluid shear stress also activates the Ca<sup>2+</sup>/NFATc1 pathway in human mesenchymal precursors and MC3T3-E1 osteoblast-like cells resulting in increased COX-2 expression (Celil Aydemir et al., 2007). Interestingly, exposure of osteoblasts to fluid shear stress *in vitro* triggers NFATc1 activation in a manner dependent upon release of ATP into the extracellular milieu and subsequent P2 nucleotide receptor signaling (Riddle et al., 2007). However, the specific P2 receptors that couple to the Ca<sup>2+</sup>/NFATc1 pathway in cells of the osteoblast lineage remain unknown.

*PI3K/AKT signaling* – Class IA and IB PI3Ks are heterodimeric lipid kinases composed of a regulatory and catalytic subunit that act via AKT-dependent and -independent mechanisms to regulate various cellular processes, including proliferation, metabolism, survival, differentiation, and cytoskeletal organization (Vivanco and Sawyers, 2002; Engelman et al., 2006; Manning and Cantley, 2007). In brief, activation of class I PI3Ks causes phosphorylation of phosphatidylinositol-4,5-bisphosphate (PIP<sub>2</sub>) leading to formation of the potent second messenger phosphatidylinositol-3,4,5-trisphosphate (PIP<sub>3</sub>); a reaction that is reversed by phosphatase and tensin homolog (PTEN). The serine/threonine protein kinase AKT is recruited to the plasma membrane through direct binding of its pleckstrin-homology domain to PIP<sub>3</sub> and subsequently activated through phosphorylation by PDK1 and mTORC2 (Vivanco and Sawyers, 2002;

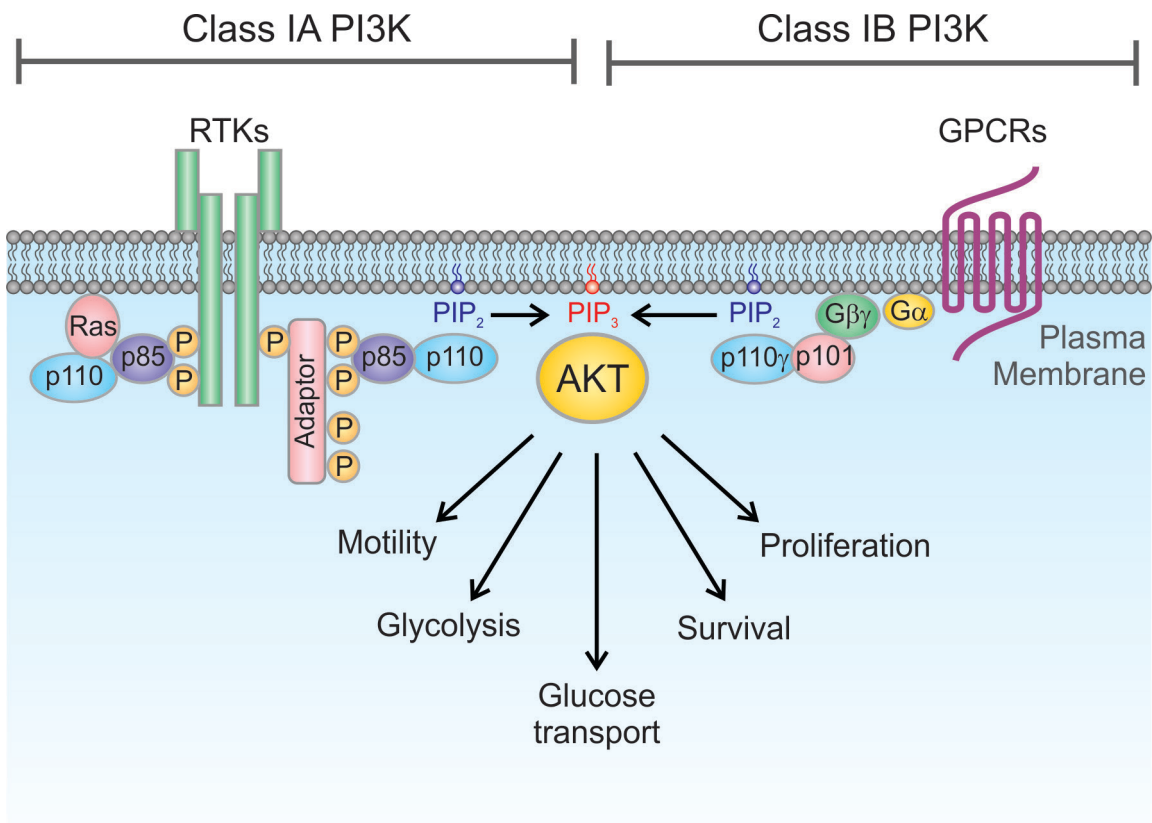
Engelman et al., 2006; Manning and Cantley, 2007) (*for more detailed information, see Figure 1.5*).

A number of important roles for PI3K/AKT signaling in skeletal biology have emerged in recent years (Guntur and Rosen, 2011). Whole-body deletion of AKT1 or AKT1/AKT2 causes reductions in longitudinal bone growth and mineralization in murine embryos resulting from decreased proliferation, increased apoptosis and delayed chondrocyte hypertrophy (Peng et al., 2003; Ulici et al., 2009). Pharmacological inhibition of PI3K in tibial organ cultures also leads to reduced endochondral ossification and bone length *in vitro* (Ulici et al., 2008). Conversely, chondrocyte-specific loss of PTEN causes constitutive PI3K signaling within growth plate chondrocytes resulting in greater skeletal size, premature chondrocyte differentiation and increased postnatal bone mass (Ford-Hutchinson et al., 2007). Studies using cell culture models have demonstrated that PI3K/AKT signaling also functions in mesenchymal progenitor cells to promote osteoblast differentiation downstream of BMP-2 (Ghosh-Choudhury et al., 2002; Fujita et al., 2004). In this regard, RUNX2 overexpression *in vitro* upregulates components of the PI3K/AKT pathway and pharmacological inhibition of PI3K or introduction of dominant-negative AKT diminishes DNA-binding of RUNX2 and RUNX2-dependent transcription (Fujita et al., 2004).

Like canonical Wnt and Ca<sup>2+</sup>/NFAT signaling, the PI3K/AKT pathway also mediates mechanotransduction in cells of the osteoblast lineage. Mechanical loading by fluid shear stress enhances PGE<sub>2</sub> release in MC3T3-E1 osteoblast-like, MLO-Y4 osteocyte-like and primary calvarial cells *in vitro* (Li et al., 2005). In this regard, fluid shear stress and PGE<sub>2</sub> both activate PI3K/AKT signaling in MLO-Y4 cells, leading to

**Figure 1.5 Schematic of the Class I PI3K/AKT Signaling Pathway in Osteoblasts.**

Class IA phosphatidylinositol 3-kinases (PI3Ks) are heterodimers consisting of a p85 regulatory subunit (p85 $\alpha$ , p85 $\beta$ , p55 $\gamma$ , p55 $\alpha$ , or p50 $\alpha$ ) and a p110 catalytic subunit (p110 $\alpha$ , p110 $\beta$ , or p110 $\delta$ ) that are activated by growth factor receptor tyrosine kinases (RTKs). Recruitment and activation of class IA PI3Ks at the plasma membrane is mediated by binding to phosphorylated RTKs or phosphorylated RTK-bound adaptor molecules (depending on the receptor). Class IB PI3Ks are also heterodimers that consist of a p101 regulatory subunit and a p110 $\gamma$  catalytic subunit. In contrast to class IA PI3Ks, class IB PI3Ks are activated by G protein-coupled receptors via interactions with G $\beta\gamma$  subunits of heterotrimeric G proteins. Activation of both class IA and class IB PI3Ks results in phosphorylation of phosphatidylinositol-4,5-bisphosphate (PIP<sub>2</sub>, **blue**) leading to formation of the potent second messenger phosphatidylinositol-3,4,5-trisphosphate (PIP<sub>3</sub>, **red**). PI3K signaling is attenuated by phosphatase and tensin homologue (PTEN)-dependent dephosphorylation of PIP<sub>3</sub> (*not shown*). The serine/threonine protein kinase AKT is then recruited to the plasma membrane through direct binding to PIP<sub>3</sub> and subsequently activated through phosphorylation by PDK1 and mTORC2 (*PDK1 and mTORC2 are not shown on diagram*).





inactivation of GSK3 $\beta$  and subsequent nuclear localization of  $\beta$ -catenin independent of canonical Wnt ligands (Xia et al., 2010). In turn,  $\beta$ -catenin binds the connexin 43 promoter and activates its transcription to presumably increase osteocyte intercellular communication (Xia et al., 2010). Further studies have also demonstrated that fluid shear stress in primary human and mouse osteoblasts as well as MC3T3-E1 osteoblast-like cells can activate AKT through Ca<sup>2+</sup>-dependent stimulation of focal adhesion kinase and Src, resulting in  $\beta$ -catenin nuclear translocation, activation of c-fos and COX-2 gene expression, and increased osteoblast proliferation (Rangaswami et al., 2012). Interestingly, the P2X7 nucleotide receptor couples to production of PGE<sub>2</sub> in cells of the osteoblast lineage (Panupinthu et al., 2008), and P2X7 signaling is required to mediate the effects of fluid shear stress in osteoblast-like and osteocyte-like cells *in vitro* (Li et al., 2005).

## 1.4 Ion Transporters and Regulation of Cytosolic pH in Osteoblasts

### 1.4.1 Effects of Acid on Bone

The vertebrate skeleton contains a large quantity of the alkaline mineral hydroxyapatite, which can be utilized to buffer systemic acid if acid-base balance falls outside the appropriate physiological limits (Arnett, 2008). In addition to passive, physiochemical dissolution of bone mineral, the negative effects of systemic and local acidosis on the skeleton (depletion of bone mineral) have been attributed to alterations in the activities of osteoclasts and osteoblasts (Bushinsky, 2001; Arnett, 2003; Arnett, 2008). Acidification of culture medium increases resorption pit formation in cultures of rat, avian and human osteoclasts (Arnett and Dempster, 1986; Arnett and Dempster, 1987; Arnett, 2008; Arnett and Spowage, 1996). At pH 7.4 or above, rat osteoclasts exhibit almost no resorptive activity, and are insensitive to RANKL and other proresorptive agents. Conversely, reductions of as little as 0.1 pH units are sufficient to double osteoclast-mediated pit formation, with a maximum response observed at pH 6.8 *in vitro* (Arnett and Spowage, 1996). Acid activation of osteoclasts increases expression or function of a number of enzymes required for bone resorption, including carbonic anhydrase II, vacuolar-type H<sup>+</sup>-ATPase, cathepsin K, and TRAP (Nordstrom et al., 1997; Biskobing and Fan, 2000; Arnett, 2008). Moreover, extracellular acidification acts through the proton-sensing receptor ovarian cancer G protein-coupled receptor 1 (OGR1) to promote osteoclast survival and resorption pit formation downstream of Ca<sup>2+</sup>/NFATc1 signaling (Komarova et al., 2005; Pereverzev et al., 2008).

In contrast to its effects on bone resorption, acidosis causes decreased bone formation *in vitro* (Bushinsky, 2001; Arnett, 2003; Arnett, 2008); however, the precise

effects of extracellular acidification on osteoblast function are somewhat unclear (Arnett, 2008). Bushinsky and colleagues demonstrated that acidification of osteoblast culture medium during *in vitro* differentiation inhibits bone nodule formation and mineralization as well as decreases expression of extracellular matrix genes including OPN, COL1 $\alpha$ 1 and matrix gla protein (Sprague et al., 1994; Frick et al., 1997; Frick and Bushinsky, 1998). A second group has since reported decreased alkaline phosphatase activity (a marker of early osteoblasts) and reduced mineralization of bone nodules in cultures of differentiating osteoblasts with no observed changes in COL1 $\alpha$ 1 expression or osteoblast proliferation (Brandao-Burch et al., 2005). In any event, it is of great interest to understand the regulation of extracellular pH (pH<sub>o</sub>) given its dramatic effects on osteoblast and osteoclast function as well as its greater role in controlling systemic acidosis.

#### **1.4.2 Proton Production and Transport by Osteoblasts**

Acute alterations to cellular physiology, as occurs during activation of receptor-mediated signaling, lead to increased rates of metabolism that culminate in formation of acid metabolites such as carbonic, lactic, and pyruvic acids. Changes to cytosolic pH (pH<sub>i</sub>) associated with this increased metabolic flux in turn influence a number of cellular processes, including vesicular trafficking, cellular metabolism, cytoskeletal remodeling, and signaling mediated by Ca<sup>2+</sup> and cAMP (Puceat, 1999; Loiselle and Casey, 2010). To this end, every cell expresses ion transporters that function to take-up or expel protons (H<sup>+</sup>) or H<sup>+</sup> equivalents to maintain an appropriate pH<sub>i</sub>. However, H<sup>+</sup> extrusion can also affect pH<sub>o</sub> in the bone microenvironment, which, as discussed in section **1.4.1**, may lead

to changes in osteoblast and osteoclast function.

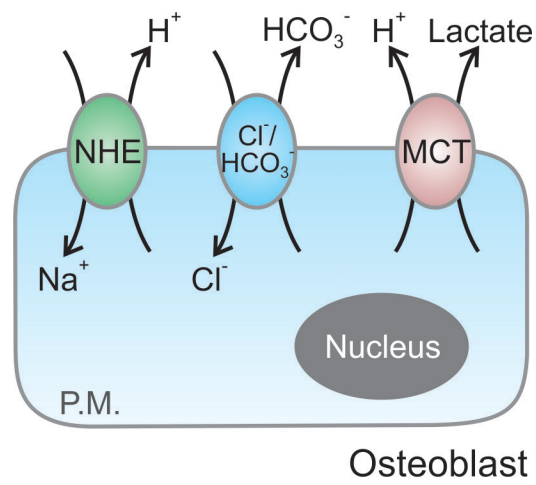
In cells of the osteoblast lineage,  $H^+$  transport mechanisms maintain  $pH_i$  homeostasis and may regulate local interstitial fluid  $pH_o$  to control bone remodeling (Figure 1.6). The ubiquitous  $Na^+/H^+$  exchanger (NHE) and the  $Na^+$ -independent  $Cl^-/HCO_3^-$  exchanger are thought to be two of the main transport mechanisms through which  $pH_i$  is maintained in osteoblasts (Green, 1994). In addition to regulation of  $pH_i$ , these transport proteins may also control cell volume (Green, 1994) and polarity during migration (Frantz et al., 2007).

Of the 6 isoforms that have been identified and sequenced in mammalian cells (Orlowski and Grinstein, 1997), cells of the osteoblast lineage express NHE-1, -3, -4 and -6 (Green, 1994; Mobasher et al., 1998; Liu et al., 2011). Activation of NHE is achieved through acidification of  $pH_i$ ,  $[Ca^{2+}]_i$ , osmotic stress and cell spreading (Orlowski and Grinstein, 1997). In turn, NHE functions to export a  $H^+$  in exchange for a  $Na^+$  to increase  $pH_i$  (Green, 1994; Orlowski and Grinstein, 1997). Recent evidence demonstrates that both NHE-1 and -6 localize to the basolateral surface of human osteoblasts and are upregulated during *in vitro* matrix mineralization (Liu et al., 2011), suggesting that NHE isoforms may play a role in the process of mineralization.

Expression and functional analyses have demonstrated that osteoblasts express  $Na^+$ -independent  $Cl^-/HCO_3^-$  exchangers such as anion exchanger 2 (Redhead, 1988; Green, 1994; Liu et al., 2011), which, like NHE-1 and -6, localize to the basolateral surface of differentiating human osteoblasts *in vitro* (Liu et al., 2011). The exchanger is activated by alkaline  $pH_i$ , and allows the transport of  $Cl^-$ ,  $HCO_3^-$  or  $OH^-$  in opposite directions via a single anion translocation site (Green, 1994). Under physiological

**Figure 1.6 Regulation of Cytosolic pH by Transporters in Osteoblasts.**

Proton ( $H^+$ ) and  $HCO_3^-$  transport mechanisms maintain cytosolic pH ( $pH_i$ ) in cells of the osteoblast lineage. Modulation of  $pH_i$  influences a variety of cellular functions such as metabolism and signaling, whereas changes to extracellular pH ( $pH_o$ ) alter osteoblast and osteoclast activity. In cells of the osteoblast lineage, increased cytosolic acidity activates  $Na^+/H^+$  exchangers (NHEs; osteoblasts express NHE-1,-3,-4 and -6) to promote  $H^+$  efflux in exchange for influx of  $Na^+$  across the plasma membrane. On the other hand, alkalisation of the cytosol stimulates efflux of  $HCO_3^-$  or  $OH^-$  through  $Na^+$ -independent  $Cl^-/HCO_3^-$  exchangers such as anion exchanger 2. Osteoblasts also express proton-linked monocarboxylate transporters (MCTs) such as MCT2 and MCT8, which in most cell-types mediate lactic acid extrusion into the extracellular space. However, in cells of the osteoblast lineage, the role of MCTs in lactic acid transport remains unclear.



conditions, the  $\text{Na}^+$ -independent  $\text{Cl}^-/\text{HCO}_3^-$  exchanger will acidify the cell given that direction of transport is determined solely by anion distribution across the plasma membrane (Green, 1994). Though one study has reported activation of this exchanger by PTH in calvarial cell cultures (Redhead, 1988), little-to-nothing is known regarding their significance in osteoblast biology.

During glycolysis, two molecules of lactic acid are produced for every molecule of glucose consumed. To maintain proper rates of glycolytic flux, lactic acid is extruded from the cell by  $\text{H}^+$ -linked monocarboxylate transporters (MCTs) (Juel and Halestrap, 1999). Eight MCTs have been identified in mammals, and the distribution of each varies significantly from tissue-to-tissue (Juel and Halestrap, 1999). Recent studies have demonstrated expression of MCT2 and MCT8 in postnatal long bones as well as in cultures of calvarial and osteoblast-like cells (Hinoi et al., 2006b; Williams et al., 2008; Capelo et al., 2009). Though their exact functions in bone remain unclear, MCT2 may mediate the cytoprotective effects of pyruvate against hydrogen peroxide-induced cell death in osteoblasts (Hinoi et al., 2006b). On the other hand, expression patterns of MCT8 *in vitro* and *in vivo* suggest a potential role for this transporter in modulation of thyroid hormone effects on osteoblastogenesis and bone development (Williams et al., 2008; Capelo et al., 2009). However, to date, no one MCT transporter has been directly associated with lactic acid efflux in cells of the osteoblast lineage.

## **1.5 P2 Nucleotide Receptors**

### **1.5.1 Sources and Fates of Extracellular Nucleotides**

In both the peripheral and central nervous system, nucleotides such as ATP serve as transmitters or co-transmitters that act on pre- or postjunctional synaptic membranes to elicit a variety of neuronal responses (referred to as purinergic neurotransmission) (Burnstock, 2007). Nucleotides are also released physiologically from nearly every cell-type in response to mechanical stimulation, including shear stress and osmotic swelling, hypoxia and activation of receptor-mediated signaling (Bodin and Burnstock, 2001; Lazarowski et al., 2011). Although the exact mechanisms remain widely debated, growing evidence suggests that nucleotide release may be mediated by either vesicular exocytosis or transporter and channel proteins such as ATP-binding cassette transporters, volume-regulated anion channels, and connexin or pannexin hemichannels, depending on the cell-type (Bodin and Burnstock, 2001; Lazarowski et al., 2011). In cells of the osteoblast lineage, ATP release in response to hypoxia, fluid shear stress and hypotonic shock is thought to be mediated by vesicular exocytosis (Genetos et al., 2005; Romanello et al., 2005; Riddle et al., 2007; Orriss et al., 2009; Brandao-Burch et al., 2012). Constitutive vesicular release of ATP is also observed in primary cultures of rat osteoblasts and murine osteoclasts, and is dependent on P2X7 nucleotide receptor signaling (Brandao-Burch et al., 2012).

The levels of extracellular nucleotides and nucleosides are controlled by a number of membrane-bound ecto-nucleotidases, including ecto-nucleoside 5'-triphosphate diphosphohydrolases (E-NTPDase), ecto-nucleotide pyrophosphatase/ phosphodiesterases (E-NPP), ALPs and ecto-5'-nucleotidases (E-5'-NT) (Zimmermann et al., 2012). E-



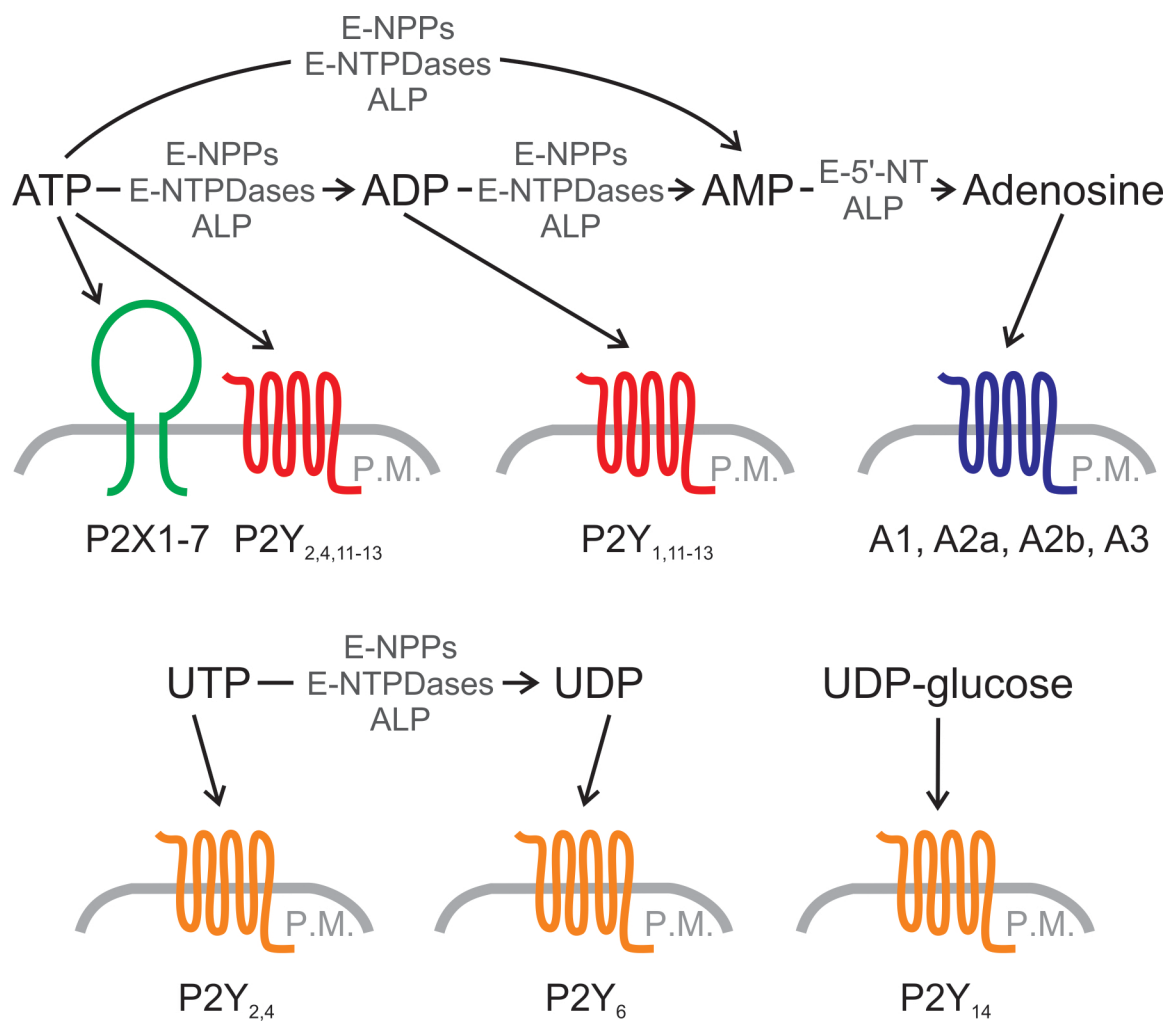
NTPDase1-3 and -8 as well as E-NPP1-3 and ALPs catalyze the conversion of nucleoside 5'-tri- and diphosphates to nucleoside 5'-monophosphates. Adenosine 5'-monophosphate (AMP) is in turn hydrolyzed by both ALPs and E-5'-NTs to produce adenosine (Zimmermann et al., 2012). The products of ATP and UTP hydrolysis then act through distinct cell-surface nucleotide and nucleoside receptors to exert their physiological effects (*described below*) (Figure 1.7).

In addition to their roles in purinergic signaling, E-NPP1 and ALPs regulate the respective production and hydrolysis of the biological calcification inhibitor inorganic pyrophosphate (PP<sub>i</sub>) (Zimmermann et al., 2012). Global disruption of the *E-npp1* gene in mice causes periosteal hyperostosis (excessive bone growth and mineralization) and trabecular osteopenia at certain sites (i.e., calvaria and spine) within the skeleton that is associated with decreased levels of PP<sub>i</sub> and ectopic calcification of arteries, joints and tendons (Sakamoto et al., 1994; Okawa et al., 1998; Rutsch et al., 2001). Conversely, homozygous deletion of tissue nonspecific alkaline phosphatase (TNAP) results in osteomalacia (hypomineralized skeleton) and increased PP<sub>i</sub> levels (Narisawa et al., 1997; Fedde et al., 1999). The abnormal PP<sub>i</sub> levels and some (but not all) mineralization defects observed in *Tnap*<sup>-/-</sup> or *E-npp1*<sup>-/-</sup> mice are normalized and reversed in mice lacking both enzymes (Hessle et al., 2002), emphasizing the importance of PP<sub>i</sub> homeostasis in regulation of bone matrix mineralization.

Finally, the actions of many ecto-nucleotidases generate P<sub>i</sub> (Zimmermann et al., 2012), which is required for formation of hydroxyapatite, and may even serve as a signaling molecule to regulate osteoblast differentiation (Hansen et al., 1976; Khoshniat et al., 2011).

**Figure 1.7 Extracellular Nucleotides and P2 Nucleotide Receptors in Mammalian Cell-Types.**

Most mammalian cell-types synthesize and release nucleotides either constitutively or in response to various stimuli. Once in the extracellular space, levels of nucleotides are controlled by the actions of several families of ecto-nucleotidases, including ecto-nucleoside 5'-triphosphate diphosphohydrolases (E-NTPDase), ecto-nucleotide pyrophosphatase/phosphodiesterases (E-NPP), alkaline phosphatases (ALPs) and ecto-5'-nucleotidases (E-5'-NT). ATP, UTP and their breakdown products bind to distinct P2 nucleotide receptors present on the cell surface. Additionally, adenosine binds to P1 receptors, whereas UDP-glucose, which is synthesized intracellularly and released, signals through P2Y<sub>14</sub>.



### 1.5.2 Classification and Properties of P2 Nucleotide Receptors

Extracellular nucleotides bind to cell surface P2 nucleotide receptors expressed in a virtually every cell-type and tissue. These receptors are divided into two families: the P2Y family of G protein-coupled receptors and the P2X family of ligand-gated cation channels. Multiple subtypes of P2Y and P2X receptors have been identified in mammals, including eight P2Y subtypes (P2Y<sub>1</sub>, P2Y<sub>2</sub>, P2Y<sub>4</sub>, P2Y<sub>6</sub>, P2Y<sub>11-14</sub>) and seven subtypes of P2X (P2X<sub>1-7</sub>) (Abbracchio et al., 2006; Khakh and North, 2006).

*Metabotropic P2Y receptors* – P2Y receptors are members of the rhodopsin family of G protein-coupled receptors characterized by the presence of an extracellular NH<sub>2</sub> terminus, an intracellular COOH-terminus, and seven transmembrane domains (Abbracchio et al., 2006; Burnstock, 2007). The transmembrane-spanning regions of P2Y receptors contribute to formation of the ligand binding pocket, whereas both the intracellular loops and COOH-termini regulate downstream intracellular signaling and receptor activity (Abbracchio et al., 2006; Burnstock, 2007). Sequence variability amongst P2Y receptors results in differences in their selectivity for endogenous purine and pyrimidine nucleotides. In this regard, ADP is more potent than ATP at P2Y<sub>1</sub> receptors, whereas uridine nucleotides have no effect. In contrast, ATP and ADP bind P2Y<sub>11</sub>, P2Y<sub>12</sub> and P2Y<sub>13</sub> with equal potency. UTP and ATP are strong agonists for P2Y<sub>2</sub> and P2Y<sub>4</sub>, but UDP and ADP display only weak receptor binding. On the other hand, UDP and UDP-glucose are the only purinergic agonists known to activate P2Y<sub>6</sub> and P2Y<sub>14</sub>, respectively (Abbracchio et al., 2006; Burnstock, 2007).

Intracellular signaling downstream of P2Y receptors involves activation of one of four heterotrimeric G protein isoforms (G<sub>s</sub>, G<sub>q/11</sub>, G<sub>i</sub> or G<sub>o</sub>) and its associated effectors

(Abbracchio et al., 2006; Burnstock, 2007). P2Y<sub>1</sub>, P2Y<sub>2</sub>, P2Y<sub>4</sub>, P2Y<sub>6</sub> and P2Y<sub>11</sub> typically couple through G<sub>q/11</sub> to activation of phospholipase C (PLC) culminating in the formation of inositol 1,4,5-trisphosphate (IP<sub>3</sub>) and subsequent release of Ca<sup>2+</sup> from intracellular stores (Abbracchio et al., 2006; Burnstock, 2007). Additionally, evidence suggests that P2Y<sub>2</sub>, P2Y<sub>4</sub> and P2Y<sub>6</sub> can interact with G<sub>i/o</sub>, G<sub>i</sub> and G<sub>s</sub>, respectively. In contrast, P2Y<sub>12</sub>, P2Y<sub>13</sub> and P2Y<sub>14</sub> couple to G<sub>i</sub> and in turn inhibit adenylyl cyclase to lower cAMP production within the cell (Abbracchio et al., 2006; Burnstock, 2007).

*Ionotropic P2X receptors* – A single P2X subunit consists of two transmembrane domains, a large N-glycosylated, disulfide-rich extracellular loop, and intracellular NH<sub>2</sub>- and COOH-termini, the latter of which possess consensus binding motifs for various protein kinases (Khakh and North, 2006; Browne et al., 2010). Functional channels are either homo- or heteromultimers composed of three P2X subunits. The extracellular domain of a multimeric P2X receptor harbors the inter-subunit binding site for ATP as well as binding sites for competitive antagonists and modulatory metal ions (Browne et al., 2010; Hattori and Gouaux, 2012). In contrast, transmembrane domains 1 and 2 function in channel gating and formation of the ion pore, respectively (Khakh and North, 2006; Browne et al., 2010). Given that most P2X channels are permeable to Na<sup>+</sup>, K<sup>+</sup> and Ca<sup>2+</sup>, receptor activation results in depolarization and Ca<sup>2+</sup> influx across the plasma membrane (Khakh and North, 2006; Browne et al., 2010), thereby contributing to downstream signaling (Surprenant and North, 2009).

Unlike P2Y family members, which interact with various combinations of adenine and uridine nucleotides, P2X receptors are activated physiologically by ATP. At the same time, channel gating varies greatly amongst the different P2X subtypes with respect to

kinetics of activation, desensitization, and recovery (North, 2002). For instance, P2X1 and P2X3 exhibit rapid desensitization of inward currents in the continued presence of agonist. On the other hand, currents elicited by P2X2 and P2X4 exhibit slow rates of decay (North, 2002). Interestingly, prolonged stimulation of P2X7 receptors with 2',3'-O-(4-benzoylbenzoyl)ATP (BzATP, a relatively potent P2X7 agonist) or high concentrations of ATP (in the millimolar range) elicit sustained inward currents that deactivate slowly relative to all other P2X receptors, even following removal of agonists (Surprenant et al., 1996; Naemsch et al., 2001; North, 2002).

### **1.5.3 P2 Nucleotide Receptors in Bone**

Cells of the osteoblast lineage possess a variety of P2 receptors, including P2Y<sub>1</sub>, P2Y<sub>2</sub>, P2Y<sub>6</sub>, P2Y<sub>12-14</sub> and P2X1-7 (Orriss et al., 2010; Orriss et al., 2012), many of which are expressed in a differentiation-dependent manner (Orriss et al., 2006; Orriss et al., 2012). In this regard, transcript and protein for the P2Y<sub>2</sub> receptor increases in cultures of differentiating rat osteoblasts. In contrast, P2Y<sub>4</sub> and P2Y<sub>6</sub> transcripts are present only at more intermediate stages of osteoblastogenesis. Levels of P2X2, P2X5, P2X6 and P2X7 receptor protein, which are largely expressed in differentiating osteoblasts, are decreased to various degrees in more mature cells. Conversely, transcript and protein for the P2X4 receptor are most highly expressed in terminally differentiated osteoblasts. On the other hand, levels of P2X1 and P2X3 receptor protein remain constant at all stages of *in vitro* osteoblastogenesis (Orriss et al., 2006; Orriss et al., 2012).

Nucleotides elicit a number of diverse responses in cultures of primary osteoblasts and osteoblast-like cells. Stimulation of P2Y<sub>1</sub> or P2Y<sub>2</sub> in human SaOS-2 osteosarcoma

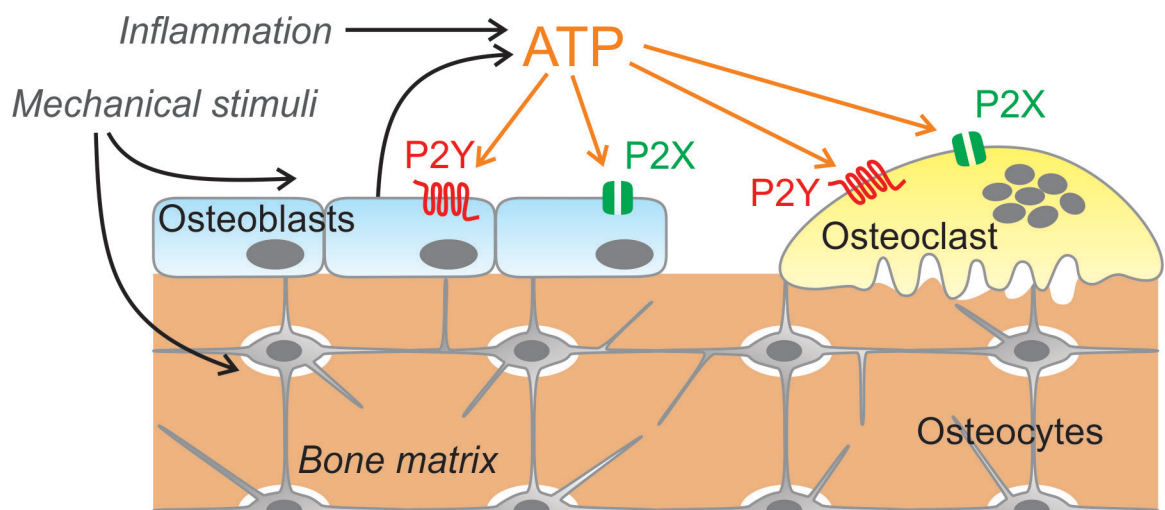
cells and primary osteoblasts induces elevations of  $[Ca^{2+}]_i$  and potentiates c-fos expression elicited by PTH/cAMP signaling (Bowler et al., 1999; Bowler et al., 2001). ATP in the micromolar range synergistically enhances PDGF- and IGF-1-induced proliferation of human MG-63 osteoblast-like cells via an unidentified P2 receptor (Nakamura et al., 2000). Increases in proliferation of both human and rat osteoblast-like cell lines can also be elicited by micromolar concentrations of ATP or UTP alone through a variety of potential downstream effectors, including PKC, PI3K, p38 MAPK, extracellular signal-regulated kinase (ERK) 1/2 and JNK1 (Nakamura et al., 2000; Katz et al., 2008; Katz et al., 2011). In addition to their effects on proliferation, stimulation of P2Y<sub>2</sub> with either ATP or UTP inhibits matrix mineralization in cultures of differentiating osteoblasts (Hoebertz et al., 2002; Orriss et al., 2007); however, lack of mineralization in these cultures is due at least in part to production of PP<sub>i</sub> (Orriss et al., 2007). At the same time, similar concentrations of these same nucleotides activate RUNX2 in the osteoblast-like HOBIT cell line (Costessi et al., 2005). It has also been suggested that skeletal mechanotransduction is mediated by nucleotide release and subsequent P2 receptor activation in osteoblasts and osteoclasts (Dixon and Sims, 2000) (Figure 1.8).

Generation of whole-body knockout mouse strains for various P2Y and P2X receptor subtypes has confirmed a number of important roles for purinergic signaling in postnatal skeletal homeostasis *in vivo*. Particularly important roles for ADP in bone remodeling have been demonstrated from analyses of P2Y<sub>12</sub>- and P2Y<sub>13</sub>-deficient mice (Su et al., 2012; Wang et al., 2012). In this regard, homozygous deletion of P2Y<sub>12</sub> causes increased bone mass and decreased osteoclast numbers with no effect on osteoblast numbers or bone formation parameters *in vivo* (Su et al., 2012). Studies of *P2y12*<sup>-/-</sup>

**Figure 1.8 P2 Nucleotide Receptors in Bone.**

Schematic diagram illustrating the potential roles for nucleotide signaling in bone. ATP and other nucleotides are released from cells of the osteoblast lineage in response to mechanical stimuli and accumulate at sites of inflammation or injury within the skeleton. Extracellular nucleotides signal through networks of cell-surface P2 nucleotide receptors expressed by osteoblasts and osteoclasts to modulate bone remodeling.





osteoclasts *in vitro* revealed that these cells do have the capacity to differentiate but fail to adhere and resorb mineralized substrates in response to ADP treatment (Su et al., 2012). On the other hand, loss of P2Y<sub>13</sub> results in a low bone mass phenotype characterized by reduced bone formation rates and decreased osteoblast and osteoclast numbers; changes that are associated with impaired osteoblast and osteoclast differentiation *in vitro* (Wang et al., 2012). However, osteoblasts from *P2y13<sup>-/-</sup>* mice also exhibit a reduced ratio of RANKL/OPG (Wang et al., 2012), which suggests that the osteoclast effects in this model may be non-cell autonomous. In addition to P2Y receptors, genetically modified mice carrying a non-functional P2X7 receptor have been shown to exhibit diminished periosteal bone formation, excessive trabecular bone resorption, and impaired skeletal responses to mechanical loading (Ke et al., 2003; Li et al., 2005). With the discovery of loss-of-function polymorphisms in P2X7 that associate with accelerated bone loss and vertebral fracture risk in postmenopausal women (Gartland et al., 2012; Jorgensen et al., 2012), this ATP-selective P2 receptor has been brought to the forefront in musculoskeletal research.

## 1.6 P2X7 in Osteoblasts

### 1.6.1 Expression of P2X7 in Cells of the Osteoblast Lineage

Over 15 years ago, Collo and coworkers noted expression of P2X7 in the developing vertebrae and mandible of E19 rat embryos by *in situ* hybridization (Collo et al., 1997). However, there have since been conflicting reports regarding expression of P2X7 receptors in cells of the osteoblast lineage. Expression of *P2x7* transcripts was initially demonstrated in the MG-63 human osteoblast-like cell line (Nakamura et al., 2000). On the other hand, specific immunostaining for the receptor could not be detected in osteoblast-enriched cultures of rat calvarial cells (Hoebertz et al., 2000). A subsequent study conducted by Gartland and colleagues localized the P2X7 receptor to a subpopulation of human bone-derived cells *in vitro* using immunocytochemical analyses and pore-formation assays (Gartland et al., 2001). However, others reported that the P2X7 agonist BzATP failed to elicit elevations of  $[Ca^{2+}]_i$  or to induce pore formation in osteoblasts from cultures of adherent human bone marrow cells (Jorgensen et al., 2002), leading these authors to conclude that functional P2X7 receptors are not expressed by osteoblasts.

More recent investigations have provided consistent evidence for the expression of P2X7 receptors in cells of the osteoblast lineage. In 2003, the presence of *P2x7* transcripts was demonstrated in cultures of mouse calvarial cells (Ke et al., 2003). Moreover, BzATP induced pore formation in approximately 30% of calvarial osteoblasts from wild-type but not *P2x7*<sup>-/-</sup> mice, indicating that functional P2X7 receptors are expressed by only a subpopulation of calvarial cells. P2X7 protein expression was later confirmed in mouse calvarial cultures and MC3T3-E1 osteoblast-like cells by

immunoblot analysis (Li et al., 2005). More recently, the expression of P2 receptors and nucleotide responses were examined during the differentiation of rat calvarial cells *in vitro* (Orriss et al., 2006). Using conventional RT-PCR, *P2r7* transcripts were found to be present at all time points examined in culture (from days 6 to 15).

Membrane blebbing is a unique response exhibited by some cell-types following activation of P2X7 receptors (North, 2002). Panupinthu and coworkers characterized blebbing in cultured calvarial cells to verify expression of functional P2X7 receptors *in vitro* (Panupinthu et al., 2007). In these experiments, live cells were loaded with the fluorescent dye FM4-64 to label membranes and morphology was monitored by confocal microscopy. BzATP induced formation of multiple dynamic blebs, which enlarged and shrunk in an asynchronous manner, and did not contain FM4-64-stained intracellular membranes. Approximately 40% of cultured rat and murine calvarial cells exhibited dynamic membrane blebbing in response to BzATP or high concentrations of ATP. In contrast, BzATP did not induce blebbing of calvarial cells from *P2x7<sup>-/-</sup>* mice (Panupinthu et al., 2007). These findings provide further evidence for heterogeneous expression of functional P2X7 receptors in calvarial cells. At the same time, calvarial cultures contain cells at various stages of osteoblast differentiation, a fact that could explain the heterogeneous pattern of P2X7 expression.

### **1.6.2 P2X7 Receptor Signaling in Osteoblasts**

ATP and BzATP induce opening of the P2X7 nonselective cation channel, which is permeable to Na<sup>+</sup>, K<sup>+</sup> and Ca<sup>2+</sup>. This event leads to elevation of [Ca<sup>2+</sup>]<sub>i</sub> and depolarization of the membrane potential. However, expression of multiple subtypes of

P2X and Ca<sup>2+</sup>-mobilizing P2Y receptors on cells of the osteoblast lineage (Orriss et al., 2006) make it difficult to attribute responses to specific P2 receptors. Moreover, heterogeneity within calvarial cell cultures and other *in vitro* osteoblast models adds to the complexity of interpreting data from single-cell electrophysiology or Ca<sup>2+</sup> fluorescence studies. Thus, future work comparing responses of osteoblasts isolated from *P2x7*<sup>-/-</sup> mice and wild-type controls should prove informative.

In many cell-types, decreasing divalent cation concentrations in the extracellular fluid potentiates the effects of P2X7 agonists, leading to formation of aqueous pores within the plasma membrane permeable to molecules as large as 900 Da (Pelegrin and Surprenant, 2006). Though its physiological relevance remains to be determined, this phenomenon has proven useful in characterizing P2X7 receptor expression. In this regard, high concentrations of ATP or BzATP induced uptake of ethidium bromide (394 Da) by cultured osteoblasts in divalent cation-free buffer (Gartland et al., 2001). In a separate study, cells on the ectocranial surfaces of calvariae, a site of active osteogenesis, exhibited pore formation in response to BzATP, thereby establishing that osteogenic cells express functional P2X7 receptors *in situ* (Panupinthu et al., 2008). This finding also confirmed that P2X7 expression in bone cells is not an artifact of *in vitro* culture, as has been found for some P2 receptors in other systems (Turner et al., 1997). Moreover, P2X7 receptors mediated dye uptake by mouse calvarial cells in response to fluid shear stress (Li et al., 2005), suggesting that pore formation may play a role in mechanotransduction.

In other cell-types, P2X7 receptor activation leads to stimulation of phospholipase D (PLD) and A<sub>2</sub> (PLA<sub>2</sub>) activity (Humphreys and Dubyak, 1996; Alzola et al., 1998), suggesting that P2X7 may couple to the production of bioactive lipids. In this regard,

fluid shear stress stimulates production of PGE<sub>2</sub> by osteoblasts in a manner dependent on P2X7 receptor signaling (Li et al., 2005). Panupinthu and coworkers have since identified a role for lipid signaling pathways in mediating P2X7-induced blebbing in osteoblasts (Panupinthu et al., 2007). Specifically, activation of P2X7 receptors leads to stimulation of PLD and PLA<sub>2</sub>, resulting in production of the potent lipid mediator lysophosphatidic acid (LPA). LPA then acts through its G protein-coupled receptor to induce membrane blebbing via a pathway dependent on ROCK. Thus, a number of the effects of P2X7 receptor activation in osteoblasts may be mediated by PGE<sub>2</sub> and LPA.

Ca<sup>2+</sup> influx through the P2X7 channel could couple to a number of intracellular signaling pathways activated by elevated [Ca<sup>2+</sup>]<sub>i</sub>. In this regard, Ca<sup>2+</sup> entry mediated by the P2X7 receptor leads to NFAT activation in microglial-like cells (Ferrari et al., 1999) and enhances IL-1β secretion from monocyte and macrophage cell lines (Gudipaty et al., 2003). However, the role of P2X7-mediated Ca<sup>2+</sup> influx in cells of the osteoblast lineage remains to be elucidated.

Most recently, P2X7 receptors have been shown to mediate ERK1/2 activation by fluid shear stress in an osteoblast-like cell line (Liu et al., 2008; Okumura et al., 2008). The phosphorylation of ERK1/2 required ATP release, and appeared to be dependent on both elevation of [Ca<sup>2+</sup>]<sub>i</sub> and activation of PKC (Liu et al., 2008). In summary, P2X7 receptors in cells of the osteoblast lineage couple to multiple signaling pathways. It will be of considerable interest to examine cross-talk among P2X7 receptor signaling and pathways that function downstream of other P2 receptors, as well as those activated by osteotropic hormones, growth factors and cytokines.

### 1.6.3 Functions of P2X7 Receptors in Osteoblasts

Overall,  $P2x7^{-/-}$  mice are viable and fertile and cannot be distinguished from wild-type littermates by gross observation alone (Solle et al., 2001). Nevertheless, defects have been described including impaired IL-1 release from  $P2x7^{-/-}$  macrophages challenged with ATP (Solle et al., 2001). Moreover, when arthritis is induced using a monoclonal anti-collagen antibody,  $P2x7^{-/-}$  mice exhibit an attenuated inflammatory response compared to wild-type controls (Solle et al., 2001; Labasi et al., 2002). In 2003, Ke and coworkers characterized the effects of targeted disruption of  $P2x7$  on bone formation and remodeling (Ke et al., 2003). Unexpectedly, this study identified a skeletal phenotype for the  $P2x7^{-/-}$  mouse consistent with a role for this receptor in osteogenesis. Specifically, when compared to wild-type littermates, adult  $P2x7^{-/-}$  mice displayed significant reduction in total and cortical bone content. Moreover, radiographs and peripheral quantitative computed tomography analyses demonstrated that femoral bone diameters were smaller in  $P2x7^{-/-}$  mice compared with wild-type controls, consistent with impaired periosteal bone formation. In contrast, femur length did not differ, indicating that P2X7 receptors do not regulate the longitudinal growth of bones. Since longitudinal growth is mediated primarily by the cartilaginous growth plate, this finding is in keeping with the absence of P2X7 in cells of the chondrocyte lineage (unpublished observations).

When double calcein labeling was used to reveal sites of active osteogenesis, reduced rates of bone formation were observed in  $P2x7^{-/-}$  mice, as revealed by the shorter interlabeling distance at periosteal surfaces of the tibial shafts (Ke et al., 2003). The unique phenotype of the  $P2x7^{-/-}$  mouse prompted Ke and colleagues to speculate that these mice may possess decreased sensitivity to mechanical loading (Ke et al., 2003).

This hypothesis was tested directly by Li and coworkers, who used an *in vivo* ulnar loading system to compare the anabolic effects of mechanical stimulation in  $P2x7^{-/-}$  and control mice (Li et al., 2005). Interestingly, the sensitivity to mechanical loading was reduced by up to 73% in  $P2x7^{-/-}$  mice as demonstrated by dual-fluorochrome labeling, establishing that the effects of mechanical stimulation on periosteal bone formation are dependent on the P2X7 receptor.

The skeletal phenotype of a second  $P2x7^{-/-}$  mouse has been described by Gartland and coworkers (Gartland et al., 2003). In contrast to the observations made by Ke et al. (2003), these mice showed no overt skeletal phenotype with the exception of thicker cortical bones than their wild-type controls. This discrepancy could be due to the different strategies used to generate the mice or their different genetic backgrounds. In this regard, the  $P2x7^{-/-}$  mice characterized by Gartland and coworkers were constructed by insertion of a *lacZ* gene at the beginning of exon 1 of  $P2x7$  (Sim et al., 2004). Due to the existence of an endogenously expressed P2X7 splice variant, this strategy created an inadvertent tissue-specific knockout (Nicke et al., 2009; Taylor et al., 2009) in which the presence or absence of P2X7 in osteoblasts has yet to be examined. In contrast, the  $P2x7^{-/-}$  mice described by Ke and colleagues carried a deletion within the region encoding C-terminal amino acids 506-532 (Solle et al., 2001). Though P2X7 is present in this mouse model, the protein is truncated at its COOH-terminus causing inefficient trafficking to the cell membrane and greatly diminished receptor function (Masin et al., 2012). It is also noteworthy that the decrease in bone density observed by Ke and colleagues was more pronounced in adult male mice, whereas Gartland and coworkers analyzed the bones of a relatively small number of animals, the gender of which was not specified.



Since a number of cell-types express P2X7 receptors, it was not known until recently whether the phenotype of the *P2x7<sup>-/-</sup>* mouse was due to an intrinsic defect in osteoblast function or to an indirect effect mediated by other cell-types. To address this question, Panupinthu and colleagues employed a well-characterized bone formation assay in which rat and murine calvarial osteoblasts differentiate and form bone-like nodules *in vitro* (Panupinthu et al., 2008). BzATP induced pore formation in cells within these nodules, indicating that the calvarial cells responsible for osteogenesis *in vitro* express functional P2X7 receptors. Moreover, activation of P2X7 receptors by exogenous nucleotides stimulated osteoblast differentiation and enhanced mineralization. On the other hand, the expression of osteoblast markers was suppressed in calvarial cells from *P2x7<sup>-/-</sup>* mice compared to wild-type controls. Interestingly, the stimulatory effects of P2X7 activation on bone formation *in vitro* were dependent on both LPA signaling and cyclooxygenase activity. Thus, P2X7 receptors enhance bone formation through an osteoblast-autonomous mechanism. Moreover, this study identified a novel signaling axis that links P2X7 receptors to production of LPA and cyclooxygenase metabolites, which in turn stimulate osteogenesis. The involvement of LPA, which signals in part through Rho, is consistent with the role of RhoA and ROCK in driving the differentiation of osteoblasts from mesenchymal stem cells (McBeath et al., 2004). Moreover, the dependence of osteogenesis on cyclooxygenase activity is in keeping with the well-established role of prostaglandins in stimulating bone formation (Ma et al., 1995) and in mediating skeletal mechanotransduction *in vivo* (Ehrlich and Lanyon, 2002).

It is possible that P2X7 may have other important functions in cells of the osteoblast lineage. For example, it has been suggested that ATP and other organic

phosphates provide a source of  $P_i$ , which is required for the formation of bone mineral crystals (Nakano et al., 2007). In this regard, P2X7 receptor activation triggers ATP efflux (Pellegatti et al., 2005), providing a possible source of  $P_i$  to support mineralization. It is also possible that P2X7 receptors on osteoblasts are involved in the processing and secretion of cytokines, as is well-established in leukocytes (Gabel, 2007). Lastly, activation of P2X7 receptors promotes apoptosis in a number of cell systems (Adinolfi et al., 2005b). In fact, Gartland and coworkers interpreted P2X7-induced membrane blebbing of human bone-derived cells as reflecting apoptosis (Gartland et al., 2001). In addition, ATP and BzATP induced delayed release of lactate dehydrogenase from osteoblastic cells, indicating cell death. However, Panupinthu and coworkers found BzATP-induced membrane blebbing of murine calvarial cells was reversible upon removal of agonist, indicating that P2X7 receptors do not induce acute cell death (Panupinthu et al., 2007). Moreover, stimulation of P2X7 receptors in MC3T3-E1 osteoblastic cells does not activate caspase 3, a key mediator of apoptosis (Li et al., 2005), arguing against a proapoptotic effect. Future studies are needed to clarify the roles of P2X7 receptors in regulating survival and other functions of osteoblasts.

#### **1.6.4 Genetic Polymorphisms of the Human P2X7 Receptor**

P2X7 is among the most polymorphic of P2 receptors (Di Virgilio and Wiley, 2002), with 40 nonsynonymous, amino-acid altering SNPs currently identified (Wesselius et al., 2011; Wesselius et al., 2012; Husted et al., 2013). When J.S. Wiley and co-workers examined 712 subjects (554 Caucasian) for the presence of 5 loss-of-function polymorphisms, 51% of Caucasian subjects were found to be wild-type at the five alleles,

40% were heterozygous and 9% carried at least two loss-of-function alleles (Shemon et al., 2006).

Polymorphisms identified within the coding region of the human P2X7 receptor have a wide range of outcomes, such as gain-of-function (Cabrini et al., 2005), loss-of-function (Gu et al., 2001; Wiley et al., 2002), impairment of cytokine release (Sluyter et al., 2004a; Sluyter et al., 2004b), and altered cell death (Le Stunff et al., 2004). The Thr357>Ser variant is present in ~11% of the population and Glu496>Ala occurs in over 25% of Caucasian subjects (Dao-Ung et al., 2004). Loss-of-function SNPs Glu496>Ala and Ile568>Asn are both associated with increased 10-year fracture risk in postmenopausal women (Ohlendorff et al., 2007). In this regard, the Glu496Ala variant results in reduced pore-forming ability (Gu et al., 2001) without altering channel function (Boldt et al., 2003), whereas the Ile568Asn variant prevents normal channel trafficking and function (Wiley et al., 2003). Loss-of-function SNP Arg307>Gln has also been linked to lower lumbar spine bone mineral density (Gartland et al., 2012) and an increased rate of bone loss (Jorgensen et al., 2012). Conversely, the gain-of-function SNP Ala348>Thr is associated with lower vertebral fracture incidence during the 10 years after menopause (Jorgensen et al., 2012).

Increased skeletal fragility in patients with loss-of-function polymorphisms in the P2X7 receptor is consistent with decreased susceptibility of osteoclasts to apoptosis (Ohlendorff et al., 2007). As well, impaired osteoblast differentiation and bone formation may contribute to increased fracture risk. It is worth noting that the skeletal changes observed in postmenopausal women with loss-of-function polymorphisms of the P2X7 receptor (Ohlendorff et al., 2007) correspond to the phenotypic changes in the *P2x7<sup>-/-</sup>*

mouse described by Ke and coworkers (Ke et al., 2003).

## 1.7 Rationale and Objectives of the Research

Given the importance of purinergic signaling in osteoblast biology, the overall objective of this thesis was to identify and characterize the signal transduction pathways that function downstream of P2X7 and other P2 receptors in cells of the osteoblast lineage. The following three specific objectives were proposed:

### 1.7.1 Role of P2 Receptor Networks in Osteoblasts

*Rationale* – All mammalian cell-types including osteoblasts express multiple P2Y and P2X receptor subtypes, each with varying affinities for purine and pyrimidine nucleotides (Volonte et al., 2006; Burnstock and Verkhratsky, 2009). Though functions have been attributed to individual subtypes of P2Y and P2X receptors in cells of the osteoblast lineage (Orriss et al., 2010; Orriss et al., 2011), the mechanisms by which they interact to regulate osteoblast differentiation and function remain unclear. More importantly, the overall significance of such an extensive network of distinct P2 nucleotide receptors remains a mystery in the field of purinergic signaling (Volonte et al., 2006; Burnstock, 2008).

In response to extracellular nucleotides, many P2Y and P2X receptors including P2X7 signal through elevations in  $[Ca^{2+}]_i$  to elicit changes in cell behaviour (Abbracchio et al., 2006; Khakh and North, 2006; Burnstock, 2007; Browne et al., 2010). The  $Ca^{2+}$ -regulated transcription factor NFATc1 plays an essential role in the differentiation of osteoblasts (Koga et al., 2005; Winslow et al., 2006); however, mechanisms leading to activation of NFATc1 in osteoblasts are unknown.

*Specific Objective 1* – To characterize the P2 network expressed by cells of the

osteoblast lineage and elucidate the role of P2Y and P2X receptor subtypes in regulation of  $\text{Ca}^{2+}$ /NFATc1 signaling in these cells.

### **1.7.2 Regulation of Metabolic Acid Production in Osteoblasts by P2 Receptors**

*Rationale* – Many metabolic demands are placed on osteoblasts during their differentiation and in the production and mineralization of the bone extracellular matrix. Given that the P2X7 receptor promotes osteoblastogenesis and bone formation both *in vitro* and *in vivo* (Ke et al., 2003; Li et al., 2005; Panupinthu et al., 2008), it is possible that it also regulates metabolism in cells of the osteoblast lineage. In this regard, exogenous expression of P2X7 receptors has been shown to elicit elevations in resting mitochondrial  $\Delta\psi$ , basal mitochondrial  $\text{Ca}^{2+}$  and intracellular ATP content (Adinolfi et al., 2005a). These changes are dependent both on P2X7-mediated pore-formation and autocrine/paracrine stimulation by endogenously released ATP. However, whether P2 receptors such as P2X7 couple to changes in cellular metabolism in osteoblast lineage cells remains unexplored.

Changes in  $\text{pH}_o$  regulate the activities of both osteoblasts and osteoclasts (Bushinsky, 2001; Arnett, 2003; Arnett, 2008). Receptor-mediated increases in cellular metabolism cause corresponding elevations in metabolic acid production (McConnell et al., 1992). Efflux of these acid metabolites from the cell in turn acidifies  $\text{pH}_o$  in the bone microenvironment. Though evidence suggests that P2X7 can increase cellular metabolism (Adinolfi et al., 2005a), its ability to regulate metabolic acid production in osteoblasts or other cell-types remains unexplored.

*Specific Objective 2* – To determine the effects of signaling through P2X7 as well

as other P2 receptor subtypes on energy metabolism in cells of the osteoblast lineage.

### **1.7.3 Cross-talk between P2X7 and Wnt/ $\beta$ -catenin Pathways in Osteoblasts**

*Rationale* – In bone, the process through which mechanical stimuli are translated into cellular responses, known as mechanotransduction, has been proposed to be mediated by nucleotide release and subsequent P2 receptor activation in osteoblasts and osteoclasts (Dixon and Sims, 2000). The P2X7 nucleotide receptor and Wnt/ $\beta$ -catenin pathway both promote osteoblast differentiation (Westendorf et al., 2004; Bodine and Komm, 2006; Hartmann, 2006; Krishnan et al., 2006; Panupinthu et al., 2008; Long, 2012; Baron and Kneissel, 2013) and are critical for anabolic responses of bone to mechanical loading (Li et al., 2005; Bonewald and Johnson, 2008; Bonewald, 2011; Baron and Kneissel, 2013). Activation of P2X7 in cerebellar granule neurons leads to inhibition of GSK3 $\beta$ , a negative regulator of canonical Wnt signaling, through mechanisms dependent on PI3K/AKT, PKC, and CaMKII (Leon et al., 2006; Ortega et al., 2009; Ortega et al., 2010). However, the ability of P2X7 to couple to GSK3 $\beta$  in cells of the osteoblast lineage remains unknown. Moreover, whether the P2X7 and Wnt pathways interact to modulate activation of  $\beta$ -catenin remains unexplored in any system.

*Specific Objective 3* – To investigate whether P2X7 and canonical Wnt signaling pathways interact to regulate  $\beta$ -catenin-mediated gene expression.

## 1.8 References

- Abbracchio, M.P., G. Burnstock, J.M. Boeynaems, E.A. Barnard, J.L. Boyer, C. Kennedy, G.E. Knight, M. Fumagalli, C. Gachet, K.A. Jacobson, and G.A. Weisman. 2006. International Union of Pharmacology LVIII: update on the P2Y G protein-coupled nucleotide receptors: from molecular mechanisms and pathophysiology to therapy. *Pharmacol Rev.* 58:281-341.
- Adinolfi, E., M.G. Callegari, D. Ferrari, C. Bolognesi, M. Minelli, M.R. Wieckowski, P. Pinton, R. Rizzuto, and F. Di Virgilio. 2005a. Basal activation of the P2X7 ATP receptor elevates mitochondrial calcium and potential, increases cellular ATP levels, and promotes serum-independent growth. *Mol Biol Cell.* 16:3260-3272.
- Adinolfi, E., C. Pizzirani, M. Idzko, E. Panther, J. Norgauer, F. Di Virgilio, and D. Ferrari. 2005b. P2X(7) receptor: Death or life? *Purinergic Signal.* 1:219-227.
- Ai, M., S.L. Holmen, W. Van Hul, B.O. Williams, and M.L. Warman. 2005. Reduced affinity to and inhibition by DKK1 form a common mechanism by which high bone mass-associated missense mutations in LRP5 affect canonical Wnt signaling. *Mol Cell Biol.* 25:4946-4955.
- Akiyama, H., M.C. Chaboissier, J.F. Martin, A. Schedl, and B. de Crombrughe. 2002. The transcription factor Sox9 has essential roles in successive steps of the chondrocyte differentiation pathway and is required for expression of Sox5 and Sox6. *Genes Dev.* 16:2813-2828.
- Akiyama, H., J.E. Kim, K. Nakashima, G. Balmes, N. Iwai, J.M. Deng, Z. Zhang, J.F. Martin, R.R. Behringer, T. Nakamura, and B. de Crombrughe. 2005. Osteochondroprogenitor cells are derived from Sox9 expressing precursors. *Proc Natl Acad Sci U S A.* 102:14665-14670.
- Alzola, E., A. Perez-Etxebarria, E. Kabre, D.J. Fogarty, M. Metioui, N. Chaib, J.M. Macarulla, C. Matute, J.P. Dehaye, and A. Marino. 1998. Activation by P2X<sub>7</sub> agonists of two phospholipases A<sub>2</sub> (PLA<sub>2</sub>) in ductal cells of rat submandibular gland. Coupling of the calcium-independent PLA<sub>2</sub> with kallikrein secretion. *J Biol Chem.* 273:30208-30217.
- Angers, S., and R.T. Moon. 2009. Proximal events in Wnt signal transduction. *Nat Rev Mol Cell Biol.* 10:468-477.
- Arnett, T. 2003. Regulation of bone cell function by acid-base balance. *Proc Nutr Soc.* 62:511-520.
- Arnett, T.R. 2008. Extracellular pH regulates bone cell function. *J Nutr.* 138:415S-418S.
- Arnett, T.R., and D.W. Dempster. 1986. Effect of pH on bone resorption by rat



- osteoclasts in vitro. *Endocrinology*. 119:119-124.
- Arnett, T.R., and D.W. Dempster. 1987. A comparative study of disaggregated chick and rat osteoclasts in vitro: effects of calcitonin and prostaglandins. *Endocrinology*. 120:602-608.
- Arnett, T.R., and M. Spowage. 1996. Modulation of the resorptive activity of rat osteoclasts by small changes in extracellular pH near the physiological range. *Bone*. 18:277-279.
- Babij, P., W. Zhao, C. Small, Y. Kharode, P.J. Yaworsky, M.L. Bouxsein, P.S. Reddy, P.V. Bodine, J.A. Robinson, B. Bhat, J. Marzolf, R.A. Moran, and F. Bex. 2003. High bone mass in mice expressing a mutant LRP5 gene. *J Bone Miner Res*. 18:960-974.
- Baron, R. 2003. General Principles of Bone Biology. In *Primer on the Metabolic Bone Diseases and Disorders of Mineral Metabolism*. M.J. Favus, editor. American Society for Bone and Mineral Research, Washington, DC. 1-8.
- Baron, R., and M. Kneissel. 2013. WNT signaling in bone homeostasis and disease: from human mutations to treatments. *Nat Med*. 19:179-192.
- Begg, S.K., J.M. Radley, J.W. Pollard, O.T. Chisholm, E.R. Stanley, and I. Bertoncello. 1993. Delayed hematopoietic development in osteopetrotic (op/op) mice. *J Exp Med*. 177:237-242.
- Bi, W., J.M. Deng, Z. Zhang, R.R. Behringer, and B. de Crombrughe. 1999. Sox9 is required for cartilage formation. *Nat Genet*. 22:85-89.
- Bi, W., W. Huang, D.J. Whitworth, J.M. Deng, Z. Zhang, R.R. Behringer, and B. de Crombrughe. 2001. Haploinsufficiency of Sox9 results in defective cartilage primordia and premature skeletal mineralization. *Proc Natl Acad Sci U S A*. 98:6698-6703.
- Bialek, P., B. Kern, X. Yang, M. Schrock, D. Susic, N. Hong, H. Wu, K. Yu, D.M. Ornitz, E.N. Olson, M.J. Justice, and G. Karsenty. 2004. A twist code determines the onset of osteoblast differentiation. *Dev Cell*. 6:423-435.
- Biskobing, D.M., and D. Fan. 2000. Acid pH increases carbonic anhydrase II and calcitonin receptor mRNA expression in mature osteoclasts. *Calcif Tissue Int*. 67:178-183.
- Bodin, P., and G. Burnstock. 2001. Purinergic signalling: ATP release. *Neurochem Res*. 26:959-969.
- Bodine, P.V., and B.S. Komm. 2006. Wnt signaling and osteoblastogenesis. *Rev Endocr*

Metab Disord. 7:33-39.

Boldt, W., M. Klapperstuck, C. Buttner, S. Sadtler, G. Schmalzing, and F. Markwardt. 2003. Glu496Ala polymorphism of human P2X<sub>7</sub> receptor does not affect its electrophysiological phenotype. *Am J Physiol Cell Physiol*. 284:C749-756.

Bonewald, L.F. 2011. The amazing osteocyte. *J Bone Miner Res*. 26:229-238.

Bonewald, L.F., and M.L. Johnson. 2008. Osteocytes, mechanosensing and Wnt signaling. *Bone*. 42:606-615.

Bowler, W.B., K.A. Buckley, A. Gartland, R.A. Hipskind, G. Bilbe, and J.A. Gallagher. 2001. Extracellular nucleotide signaling: a mechanism for integrating local and systemic responses in the activation of bone remodeling. *Bone*. 28:507-512.

Bowler, W.B., C.J. Dixon, C. Halleux, R. Maier, G. Bilbe, W.D. Fraser, J.A. Gallagher, and R.A. Hipskind. 1999. Signaling in human osteoblasts by extracellular nucleotides. Their weak induction of the c-fos proto-oncogene via Ca<sup>2+</sup> mobilization is strongly potentiated by a parathyroid hormone/cAMP-dependent protein kinase pathway independently of mitogen-activated protein kinase. *J Biol Chem*. 274:14315-14324.

Boyden, L.M., J. Mao, J. Belsky, L. Mitzner, A. Farhi, M.A. Mitnick, D. Wu, K. Insogna, and R.P. Lifton. 2002. High bone density due to a mutation in LDL-receptor-related protein 5. *N Engl J Med*. 346:1513-1521.

Boyle, W.J., W.S. Simonet, and D.L. Lacey. 2003. Osteoclast differentiation and activation. *Nature*. 423:337-342.

Brandao-Burch, A., M.L. Key, J.J. Patel, T.R. Arnett, and I.R. Orriss. 2012. The P2X<sub>7</sub> Receptor is an Important Regulator of Extracellular ATP Levels. *Front Endocrinol (Lausanne)*. 3:41.

Brandao-Burch, A., J.C. Utting, I.R. Orriss, and T.R. Arnett. 2005. Acidosis inhibits bone formation by osteoblasts in vitro by preventing mineralization. *Calcif Tissue Int*. 77:167-174.

Browne, L.E., L.H. Jiang, and R.A. North. 2010. New structure enlivens interest in P2X receptors. *Trends Pharmacol Sci*. 31:229-237.

Burnstock, G. 2007. Physiology and pathophysiology of purinergic neurotransmission. *Physiol Rev*. 87:659-797.

Burnstock, G. 2008. Unresolved issues and controversies in purinergic signalling. *J Physiol*. 586:3307-3312.

- Burnstock, G., and A. Verkhratsky. 2009. Evolutionary origins of the purinergic signalling system. *Acta Physiol (Oxf)*. 195:415-447.
- Bushinsky, D.A. 2001. Acid-base imbalance and the skeleton. *Eur J Nutr*. 40:238-244.
- Cabrini, G., S. Falzoni, S.L. Forchap, P. Pellegatti, A. Balboni, P. Agostini, A. Cuneo, G. Castoldi, O.R. Baricordi, and F. Di Virgilio. 2005. A His-155 to Tyr polymorphism confers gain-of-function to the human P2X<sub>7</sub> receptor of human leukemic lymphocytes. *J Immunol*. 175:82-89.
- Capelo, L.P., E.H. Beber, T.L. Fonseca, and C.H. Gouveia. 2009. The monocarboxylate transporter 8 and L-type amino acid transporters 1 and 2 are expressed in mouse skeletons and in osteoblastic MC3T3-E1 cells. *Thyroid*. 19:171-180.
- Cardoso, L., B.C. Herman, O. Verborgt, D. Laudier, R.J. Majeska, and M.B. Schaffler. 2009. Osteocyte apoptosis controls activation of intracortical resorption in response to bone fatigue. *J Bone Miner Res*. 24:597-605.
- Celil, A.B., and P.G. Campbell. 2005. BMP-2 and insulin-like growth factor-I mediate Osterix (Osx) expression in human mesenchymal stem cells via the MAPK and protein kinase D signaling pathways. *J Biol Chem*. 280:31353-31359.
- Celil, A.B., J.O. Hollinger, and P.G. Campbell. 2005. Osx transcriptional regulation is mediated by additional pathways to BMP2/Smad signaling. *J Cell Biochem*. 95:518-528.
- Celil Aydemir, A.B., S. Lee, D. Won Kim, T.R. Gardner, D. Prince, J. Mok Ahn, and F.Y. Lee. 2007. Nuclear factor of activated T cell mediates proinflammatory gene expression in response to mechanotransduction. *Ann N Y Acad Sci*. 1117:138-142.
- Choi, J.Y., J. Pratap, A. Javed, S.K. Zaidi, L. Xing, E. Balint, S. Dalamangas, B. Boyce, A.J. van Wijnen, J.B. Lian, J.L. Stein, S.N. Jones, and G.S. Stein. 2001. Subnuclear targeting of Runx/Cbfa/AML factors is essential for tissue-specific differentiation during embryonic development. *Proc Natl Acad Sci U S A*. 98:8650-8655.
- Clarke, B. 2008. Normal bone anatomy and physiology. *Clin J Am Soc Nephrol*. 3 Suppl 3:S131-139.
- Collo, G., S. Neidhart, E. Kawashima, M. Kosco-Vilbois, R.A. North, and G. Buell. 1997. Tissue distribution of the P2X<sub>7</sub> receptor. *Neuropharmacology*. 36:1277-1283.
- Costessi, A., A. Pines, P. D'Andrea, M. Romanello, G. Damante, L. Cesaratto, F. Quadrifoglio, L. Moro, and G. Tell. 2005. Extracellular nucleotides activate Runx2 in the osteoblast-like HOBIT cell line: a possible molecular link between

mechanical stress and osteoblasts' response. *Bone*. 36:418-432.

- Dao-Ung, L.P., S.J. Fuller, R. Sluyter, K.K. SkarRatt, U. Thunberg, G. Tobin, K. Byth, M. Ban, R. Rosenquist, G.J. Stewart, and J.S. Wiley. 2004. Association of the 1513C polymorphism in the P2X7 gene with familial forms of chronic lymphocytic leukaemia. *Br J Haematol*. 125:815-817.
- Davies, S.R., S. Sakano, Y. Zhu, and L.J. Sandell. 2002. Distribution of the transcription factors Sox9, AP-2, and [delta]EF1 in adult murine articular and meniscal cartilage and growth plate. *J Histochem Cytochem*. 50:1059-1065.
- Day, T.F., X. Guo, L. Garrett-Beal, and Y. Yang. 2005. Wnt/beta-catenin signaling in mesenchymal progenitors controls osteoblast and chondrocyte differentiation during vertebrate skeletogenesis. *Dev Cell*. 8:739-750.
- Di Virgilio, F., and J.S. Wiley. 2002. The P2X7 receptor of CLL lymphocytes-a molecule with a split personality. *Lancet*. 360:1898-1899.
- Dixon, S.J., and S.M. Sims. 2000. P2 purinergic receptors on osteoblasts and osteoclasts: Potential targets for drug development. *Drug Dev Res*. 49:187-200.
- Dougall, W.C., M. Glaccum, K. Charrier, K. Rohrbach, K. Brasel, T. De Smedt, E. Daro, J. Smith, M.E. Tometsko, C.R. Maliszewski, A. Armstrong, V. Shen, S. Bain, D. Cosman, D. Anderson, P.J. Morrissey, J.J. Peschon, and J. Schuh. 1999. RANK is essential for osteoclast and lymph node development. *Genes Dev*. 13:2412-2424.
- Ducy, P., M. Starbuck, M. Priemel, J. Shen, G. Pinero, V. Geoffroy, M. Amling, and G. Karsenty. 1999. A Cbfa1-dependent genetic pathway controls bone formation beyond embryonic development. *Genes Dev*. 13:1025-1036.
- Ducy, P., R. Zhang, V. Geoffroy, A.L. Ridall, and G. Karsenty. 1997. *Osf2/Cbfa1*: a transcriptional activator of osteoblast differentiation. *Cell*. 89:747-754.
- Dudley, H.R., and D. Spiro. 1961. The Fine Structure of Bone Cells. *J Biophys Biochem Cytol*. 11:627-649.
- Ehrlich, P.J., and L.E. Lanyon. 2002. Mechanical strain and bone cell function: a review. *Osteoporos Int*. 13:688-700.
- Eleftheriou, F., J.D. Ahn, S. Takeda, M. Starbuck, X. Yang, X. Liu, H. Kondo, W.G. Richards, T.W. Bannan, M. Noda, K. Clement, C. Vaisse, and G. Karsenty. 2005. Leptin regulation of bone resorption by the sympathetic nervous system and CART. *Nature*. 434:514-520.
- Eleftheriou, F., M.D. Benson, H. Sowa, M. Starbuck, X. Liu, D. Ron, L.F. Parada, and G. Karsenty. 2006. ATF4 mediation of NF1 functions in osteoblast reveals a

- nutritional basis for congenital skeletal dysplasiae. *Cell Metab.* 4:441-451.
- Ellies, D.L., B. Viviano, J. McCarthy, J.P. Rey, N. Itasaki, S. Saunders, and R. Krumlauf. 2006. Bone density ligand, Sclerostin, directly interacts with LRP5 but not LRP5G171V to modulate Wnt activity. *J Bone Miner Res.* 21:1738-1749.
- Engelman, J.A., J. Luo, and L.C. Cantley. 2006. The evolution of phosphatidylinositol 3-kinases as regulators of growth and metabolism. *Nat Rev Genet.* 7:606-619.
- Enomoto, H., M. Enomoto-Iwamoto, M. Iwamoto, S. Nomura, M. Himeno, Y. Kitamura, T. Kishimoto, and T. Komori. 2000. *Cbfa1* is a positive regulatory factor in chondrocyte maturation. *J Biol Chem.* 275:8695-8702.
- Fedde, K.N., L. Blair, J. Silverstein, S.P. Coburn, L.M. Ryan, R.S. Weinstein, K. Waymire, S. Narisawa, J.L. Millan, G.R. MacGregor, and M.P. Whyte. 1999. Alkaline phosphatase knock-out mice recapitulate the metabolic and skeletal defects of infantile hypophosphatasia. *J Bone Miner Res.* 14:2015-2026.
- Ferrari, D., C. Stroh, and K. Schulze-Osthoff. 1999. P2X7/P2Z purinoreceptor-mediated activation of transcription factor NFAT in microglial cells. *J Biol Chem.* 274:13205-13210.
- Ferrari, S.L., S. Deutsch, and S.E. Antonarakis. 2005. Pathogenic mutations and polymorphisms in the lipoprotein receptor-related protein 5 reveal a new biological pathway for the control of bone mass. *Curr Opin Lipidol.* 16:207-214.
- Fisher, J.E., M.P. Caulfield, M. Sato, H.A. Quartuccio, R.J. Gould, V.M. Garsky, G.A. Rodan, and M. Rosenblatt. 1993. Inhibition of osteoclastic bone resorption in vivo by echistatin, an "arginyl-glycyl-aspartyl" (RGD)-containing protein. *Endocrinology.* 132:1411-1413.
- Ford-Hutchinson, A.F., Z. Ali, S.E. Lines, B. Hallgrimsson, S.K. Boyd, and F.R. Jirik. 2007. Inactivation of *Pten* in osteo-chondroprogenitor cells leads to epiphyseal growth plate abnormalities and skeletal overgrowth. *J Bone Miner Res.* 22:1245-1259.
- Foster, J.W., M.A. Dominguez-Steglich, S. Guioli, C. Kwok, P.A. Weller, M. Stevanovic, J. Weissenbach, S. Mansour, I.D. Young, P.N. Goodfellow, and et al. 1994. Campomelic dysplasia and autosomal sex reversal caused by mutations in an *SRY*-related gene. *Nature.* 372:525-530.
- Frantz, C., A. Karydis, P. Nalbant, K.M. Hahn, and D.L. Barber. 2007. Positive feedback between *Cdc42* activity and H<sup>+</sup> efflux by the Na-H exchanger NHE1 for polarity of migrating cells. *J Cell Biol.* 179:403-410.
- Frick, K.K., and D.A. Bushinsky. 1998. Chronic metabolic acidosis reversibly inhibits

- extracellular matrix gene expression in mouse osteoblasts. *Am J Physiol.* 275:F840-847.
- Frick, K.K., L. Jiang, and D.A. Bushinsky. 1997. Acute metabolic acidosis inhibits the induction of osteoblastic egr-1 and type 1 collagen. *Am J Physiol.* 272:C1450-1456.
- Frost, H.M. 1986. *Intermediary organization of the skeleton.* CRC Press, Boca Raton, FL.
- Fujita, T., Y. Azuma, R. Fukuyama, Y. Hattori, C. Yoshida, M. Koida, K. Ogita, and T. Komori. 2004. Runx2 induces osteoblast and chondrocyte differentiation and enhances their migration by coupling with PI3K-Akt signaling. *J Cell Biol.* 166:85-95.
- Gabel, C.A. 2007. P2 purinergic receptor modulation of cytokine production. *Purinergic Signal.* 3:27-38.
- Gartland, A., K.A. Buckley, R.A. Hipskind, M.J. Perry, J.H. Tobias, G. Buell, I. Chessell, W.B. Bowler, and J.A. Gallagher. 2003. Multinucleated osteoclast formation in vivo and in vitro by P2X7 receptor-deficient mice. *Crit Rev Eukaryot Gene Expr.* 13:243-253.
- Gartland, A., R.A. Hipskind, J.A. Gallagher, and W.B. Bowler. 2001. Expression of a P2X7 receptor by a subpopulation of human osteoblasts. *J Bone Miner Res.* 16:846-856.
- Gartland, A., K.K. Skarratt, L.J. Hocking, C. Parsons, L. Stokes, N.R. Jorgensen, W.D. Fraser, D.M. Reid, J.A. Gallagher, and J.S. Wiley. 2012. Polymorphisms in the P2X7 receptor gene are associated with low lumbar spine bone mineral density and accelerated bone loss in post-menopausal women. *Eur J Hum Genet.* 20:559-564.
- Gaudio, A., P. Pennisi, C. Bratengeier, V. Torrisi, B. Lindner, R.A. Mangiafico, I. Pulvirenti, G. Hawa, G. Tringali, and C.E. Fiore. 2010. Increased sclerostin serum levels associated with bone formation and resorption markers in patients with immobilization-induced bone loss. *J Clin Endocrinol Metab.* 95:2248-2253.
- Gaur, T., C.J. Lengner, H. Hovhannisyanyan, R.A. Bhat, P.V. Bodine, B.S. Komm, A. Javed, A.J. van Wijnen, J.L. Stein, G.S. Stein, and J.B. Lian. 2005. Canonical WNT signaling promotes osteogenesis by directly stimulating Runx2 gene expression. *J Biol Chem.* 280:33132-33140.
- Gelb, B.D., G.P. Shi, H.A. Chapman, and R.J. Desnick. 1996. Pycnodysostosis, a lysosomal disease caused by cathepsin K deficiency. *Science.* 273:1236-1238.
- Genetos, D.C., D.J. Geist, D. Liu, H.J. Donahue, and R.L. Duncan. 2005. Fluid shear-

- induced ATP secretion mediates prostaglandin release in MC3T3-E1 osteoblasts. *J Bone Miner Res.* 20:41-49.
- Ghosh-Choudhury, N., S.L. Abboud, R. Nishimura, A. Celeste, L. Mahimainathan, and G.G. Choudhury. 2002. Requirement of BMP-2-induced phosphatidylinositol 3-kinase and Akt serine/threonine kinase in osteoblast differentiation and Smad-dependent BMP-2 gene transcription. *J Biol Chem.* 277:33361-33368.
- Glass, D.A., 2nd, P. Bialek, J.D. Ahn, M. Starbuck, M.S. Patel, H. Clevers, M.M. Taketo, F. Long, A.P. McMahon, R.A. Lang, and G. Karsenty. 2005. Canonical Wnt signaling in differentiated osteoblasts controls osteoclast differentiation. *Dev Cell.* 8:751-764.
- Gong, Y., R.B. Slee, N. Fukai, G. Rawadi, S. Roman-Roman, A.M. Reginato, H. Wang, T. Cundy, F.H. Glorieux, D. Lev, M. Zacharin, K. Oexle, J. Marcelino, W. Suwairi, S. Heeger, G. Sabatakos, S. Apte, W.N. Adkins, J. Allgrove, M. Arslan-Kirchner, J.A. Batch, P. Beighton, G.C. Black, R.G. Boles, L.M. Boon, C. Borrone, H.G. Brunner, G.F. Carle, B. Dallapiccola, A. De Paepe, B. Floege, M.L. Halfhide, B. Hall, R.C. Hennekam, T. Hirose, A. Jans, H. Juppner, C.A. Kim, K. Keppler-Noreuil, A. Kohlschuetter, D. LaCombe, M. Lambert, E. Lemyre, T. Letteboer, L. Peltonen, R.S. Ramesar, M. Romanengo, H. Somer, E. Steichen-Gersdorf, B. Steinmann, B. Sullivan, A. Superti-Furga, W. Swoboda, M.J. van den Boogaard, W. Van Hul, M. Vikkula, M. Votruba, B. Zabel, T. Garcia, R. Baron, B.R. Olsen, and M.L. Warman. 2001. LDL receptor-related protein 5 (LRP5) affects bone accrual and eye development. *Cell.* 107:513-523.
- Green, J. 1994. Cytosolic pH regulation in osteoblasts. *Miner Electrolyte Metab.* 20:16-30.
- Greenblatt, M.B., J.H. Shim, and L.H. Glimcher. 2013. Mitogen-Activated Protein Kinase Pathways in Osteoblasts. *Annu Rev Cell Dev Biol.*
- Grigoriadis, A.E., Z.Q. Wang, M.G. Cecchini, W. Hofstetter, R. Felix, H.A. Fleisch, and E.F. Wagner. 1994. c-Fos: a key regulator of osteoclast-macrophage lineage determination and bone remodeling. *Science.* 266:443-448.
- Gu, B.J., W. Zhang, R.A. Worthington, R. Sluyter, P. Dao-Ung, S. Petrou, J.A. Barden, and J.S. Wiley. 2001. A Glu-496 to Ala polymorphism leads to loss of function of the human P2X<sub>7</sub> receptor. *J Biol Chem.* 276:11135-11142.
- Gudipaty, L., J. Munetz, P.A. Verhoef, and G.R. Dubyak. 2003. Essential role for Ca<sup>2+</sup> in regulation of IL-1 $\beta$  secretion by P2X<sub>7</sub> nucleotide receptor in monocytes, macrophages, and HEK-293 cells. *Am J Physiol Cell Physiol.* 285:C286-299.
- Guntur, A.R., and C.J. Rosen. 2011. The skeleton: a multi-functional complex organ: new insights into osteoblasts and their role in bone formation: the central role of

- PI3Kinase. *J Endocrinol.* 211:123-130.
- Hall, B.K., and T. Miyake. 2000. All for one and one for all: condensations and the initiation of skeletal development. *Bioessays.* 22:138-147.
- Hansen, N.M., R. Felix, S. Bisaz, and H. Fleisch. 1976. Aggregation of hydroxyapatite crystals. *Biochim Biophys Acta.* 451:549-559.
- Harada, H., S. Tagashira, M. Fujiwara, S. Ogawa, T. Katsumata, A. Yamaguchi, T. Komori, and M. Nakatsuka. 1999. Cbfa1 isoforms exert functional differences in osteoblast differentiation. *J Biol Chem.* 274:6972-6978.
- Harada, S., and G.A. Rodan. 2003. Control of osteoblast function and regulation of bone mass. *Nature.* 423:349-355.
- Hartikka, H., O. Makitie, M. Mannikko, A.S. Doria, A. Daneman, W.G. Cole, L. Ala-Kokko, and E.B. Sochett. 2005. Heterozygous mutations in the LDL receptor-related protein 5 (LRP5) gene are associated with primary osteoporosis in children. *J Bone Miner Res.* 20:783-789.
- Hartmann, C. 2006. A Wnt canon orchestrating osteoblastogenesis. *Trends Cell Biol.* 16:151-158.
- Hattori, M., and E. Gouaux. 2012. Molecular mechanism of ATP binding and ion channel activation in P2X receptors. *Nature.* 485:207-212.
- Hessle, L., K.A. Johnson, H.C. Anderson, S. Narisawa, A. Sali, J.W. Goding, R. Terkeltaub, and J.L. Millan. 2002. Tissue-nonspecific alkaline phosphatase and plasma cell membrane glycoprotein-1 are central antagonistic regulators of bone mineralization. *Proc Natl Acad Sci U S A.* 99:9445-9449.
- Hill, T.P., D. Spater, M.M. Taketo, W. Birchmeier, and C. Hartmann. 2005. Canonical Wnt/beta-catenin signaling prevents osteoblasts from differentiating into chondrocytes. *Dev Cell.* 8:727-738.
- Hinoi, E., P. Bialek, Y.T. Chen, M.T. Rached, Y. Groner, R.R. Behringer, D.M. Ornitz, and G. Karsenty. 2006a. Runx2 inhibits chondrocyte proliferation and hypertrophy through its expression in the perichondrium. *Genes Dev.* 20:2937-2942.
- Hinoi, E., T. Takarada, Y. Tsuchihashi, S. Fujimori, N. Moriguchi, L. Wang, K. Uno, and Y. Yoneda. 2006b. A molecular mechanism of pyruvate protection against cytotoxicity of reactive oxygen species in osteoblasts. *Mol Pharmacol.* 70:925-935.
- Hoebertz, A., S. Mahendran, G. Burnstock, and T.R. Arnett. 2002. ATP and UTP at low



- concentrations strongly inhibit bone formation by osteoblasts: a novel role for the P2Y2 receptor in bone remodeling. *J Cell Biochem.* 86:413-419.
- Hoebertz, A., A. Townsend-Nicholson, R. Glass, G. Burnstock, and T.R. Arnett. 2000. Expression of P2 receptors in bone and cultured bone cells. *Bone.* 27:503-510.
- Hogan, P.G., L. Chen, J. Nardone, and A. Rao. 2003. Transcriptional regulation by calcium, calcineurin, and NFAT. *Genes Dev.* 17:2205-2232.
- Holmen, S.L., T.A. Giambernardi, C.R. Zylstra, B.D. Buckner-Berghuis, J.H. Resau, J.F. Hess, V. Glatt, M.L. Bouxsein, M. Ai, M.L. Warman, and B.O. Williams. 2004. Decreased BMD and limb deformities in mice carrying mutations in both *Lrp5* and *Lrp6*. *J Bone Miner Res.* 19:2033-2040.
- Holmen, S.L., C.R. Zylstra, A. Mukherjee, R.E. Sigler, M.C. Faugere, M.L. Bouxsein, L. Deng, T.L. Clemens, and B.O. Williams. 2005. Essential role of beta-catenin in postnatal bone acquisition. *J Biol Chem.* 280:21162-21168.
- Horton, M.A., M.L. Taylor, T.R. Arnett, and M.H. Helfrich. 1991. Arg-Gly-Asp (RGD) peptides and the anti-vitronectin receptor antibody 23C6 inhibit dentine resorption and cell spreading by osteoclasts. *Exp Cell Res.* 195:368-375.
- Hu, H., M.J. Hilton, X. Tu, K. Yu, D.M. Ornitz, and F. Long. 2005. Sequential roles of Hedgehog and Wnt signaling in osteoblast development. *Development.* 132:49-60.
- Huang, H., D. Chikazu, O.S. Voznesensky, H.R. Herschman, B.E. Kream, H. Drissi, and C.C. Pilbeam. 2010. Parathyroid hormone induction of cyclooxygenase-2 in murine osteoblasts: role of the calcium-calcineurin-NFAT pathway. *J Bone Miner Res.* 25:819-829.
- Humphreys, B.D., and G.R. Dubyak. 1996. Induction of the P2z/P2X<sub>7</sub> nucleotide receptor and associated phospholipase D activity by lipopolysaccharide and IFN- $\gamma$  in the human THP-1 monocytic cell line. *J Immunol.* 157:5627-5637.
- Husted, L.B., T. Harslof, L. Stenkjaer, M. Carstens, N.R. Jorgensen, and B.L. Langdahl. 2013. Functional polymorphisms in the P2X7 receptor gene are associated with osteoporosis. *Osteoporos Int.* 24:949-959.
- Iotsova, V., J. Caamano, J. Loy, Y. Yang, A. Lewin, and R. Bravo. 1997. Osteopetrosis in mice lacking NF- $\kappa$ B1 and NF- $\kappa$ B2. *Nat Med.* 3:1285-1289.
- Ishida, N., K. Hayashi, M. Hoshijima, T. Ogawa, S. Koga, Y. Miyatake, M. Kumegawa, T. Kimura, and T. Takeya. 2002. Large scale gene expression analysis of osteoclastogenesis in vitro and elucidation of NFAT2 as a key regulator. *J Biol Chem.* 277:41147-41156.

- Ito, Y., and K. Miyazono. 2003. RUNX transcription factors as key targets of TGF-beta superfamily signaling. *Curr Opin Genet Dev.* 13:43-47.
- Joeng, K.S., C.A. Schumacher, C.R. Zylstra-Diegel, F. Long, and B.O. Williams. 2011. Lrp5 and Lrp6 redundantly control skeletal development in the mouse embryo. *Dev Biol.* 359:222-229.
- Jorgensen, N.R., Z. Henriksen, O.H. Sorensen, E.F. Eriksen, R. Civitelli, and T.H. Steinberg. 2002. Intercellular calcium signaling occurs between human osteoblasts and osteoclasts and requires activation of osteoclast P2X7 receptors. *J Biol Chem.* 277:7574-7580.
- Jorgensen, N.R., L.B. Husted, K.K. Skarratt, L. Stokes, C.L. Tofteng, T. Kvist, J.E. Jensen, P. Eiken, K. Brixen, S. Fuller, R. Clifton-Bligh, A. Gartland, P. Schwarz, B.L. Langdahl, and J.S. Wiley. 2012. Single-nucleotide polymorphisms in the P2X7 receptor gene are associated with post-menopausal bone loss and vertebral fractures. *Eur J Hum Genet.* 20:675-681.
- Juel, C., and A.P. Halestrap. 1999. Lactate transport in skeletal muscle - role and regulation of the monocarboxylate transporter. *J Physiol.* 517 ( Pt 3):633-642.
- Kang, S., C.N. Bennett, I. Gerin, L.A. Rapp, K.D. Hankenson, and O.A. Macdougald. 2007. Wnt signaling stimulates osteoblastogenesis of mesenchymal precursors by suppressing CCAAT/enhancer-binding protein alpha and peroxisome proliferator-activated receptor gamma. *J Biol Chem.* 282:14515-14524.
- Karaplis, A.C. 2002. Embryonic development of bone and the molecular regulation of intramembranous and endochondral bone formation. In *Principles of Bone Biology*. Vol. 1. J.P. Bilezikian, L.G. Raisz, and G.A. Rodan, editors. Academic Press, San Diego, CA. 33-58.
- Kato, M., M.S. Patel, R. Levasseur, I. Lobov, B.H. Chang, D.A. Glass, 2nd, C. Hartmann, L. Li, T.H. Hwang, C.F. Brayton, R.A. Lang, G. Karsenty, and L. Chan. 2002. Cbfa1-independent decrease in osteoblast proliferation, osteopenia, and persistent embryonic eye vascularization in mice deficient in Lrp5, a Wnt coreceptor. *J Cell Biol.* 157:303-314.
- Katz, S., V. Ayala, G. Santillan, and R. Boland. 2011. Activation of the PI3K/Akt signaling pathway through P2Y(2) receptors by extracellular ATP is involved in osteoblastic cell proliferation. *Arch Biochem Biophys.* 513:144-152.
- Katz, S., R. Boland, and G. Santillan. 2008. Purinergic (ATP) signaling stimulates JNK1 but not JNK2 MAPK in osteoblast-like cells: contribution of intracellular Ca<sup>2+</sup> release, stress activated and L-voltage-dependent calcium influx, PKC and Src kinases. *Arch Biochem Biophys.* 477:244-252.

- Ke, H.Z., H. Qi, A.F. Weidema, Q. Zhang, N. Panupinthu, D.T. Crawford, W.A. Grasser, V.M. Paralkar, M. Li, L.P. Audoly, C.A. Gabel, W.S. Jee, S.J. Dixon, S.M. Sims, and D.D. Thompson. 2003. Deletion of the P2X<sub>7</sub> nucleotide receptor reveals its regulatory roles in bone formation and resorption. *Mol Endocrinol.* 17:1356-1367.
- Kennedy, O.D., B.C. Herman, D.M. Laudier, R.J. Majeska, H.B. Sun, and M.B. Schaffler. 2012. Activation of resorption in fatigue-loaded bone involves both apoptosis and active pro-osteoclastogenic signaling by distinct osteocyte populations. *Bone.* 50:1115-1122.
- Kern, B., J. Shen, M. Starbuck, and G. Karsenty. 2001. *Cbfa1* contributes to the osteoblast-specific expression of type I collagen genes. *J Biol Chem.* 276:7101-7107.
- Khakh, B.S., and R.A. North. 2006. P2X receptors as cell-surface ATP sensors in health and disease. *Nature.* 442:527-532.
- Khoshniat, S., A. Bourguine, M. Julien, P. Weiss, J. Guicheux, and L. Beck. 2011. The emergence of phosphate as a specific signaling molecule in bone and other cell types in mammals. *Cell Mol Life Sci.* 68:205-218.
- Kiel, D.P., S.L. Ferrari, L.A. Cupples, D. Karasik, D. Manen, A. Imamovic, A.G. Herbert, and J. Dupuis. 2007. Genetic variation at the low-density lipoprotein receptor-related protein 5 (LRP5) locus modulates Wnt signaling and the relationship of physical activity with bone mineral density in men. *Bone.* 40:587-596.
- Kist, R., H. Schrewe, R. Balling, and G. Scherer. 2002. Conditional inactivation of *Sox9*: a mouse model for campomelic dysplasia. *Genesis.* 32:121-123.
- Koga, T., Y. Matsui, M. Asagiri, T. Kodama, B. de Crombrughe, K. Nakashima, and H. Takayanagi. 2005. NFAT and Osterix cooperatively regulate bone formation. *Nat Med.* 11:880-885.
- Koller, D.L., S. Ichikawa, M.L. Johnson, D. Lai, X. Xuei, H.J. Edenberg, P.M. Conneally, S.L. Hui, C.C. Johnston, M. Peacock, T. Foroud, and M.J. Econs. 2005. Contribution of the LRP5 gene to normal variation in peak BMD in women. *J Bone Miner Res.* 20:75-80.
- Komarova, S.V., A. Pereverzev, J.W. Shum, S.M. Sims, and S.J. Dixon. 2005. Convergent signaling by acidosis and receptor activator of NF- $\kappa$ B ligand (RANKL) on the calcium/calcieneurin/NFAT pathway in osteoclasts. *Proc Natl Acad Sci U S A.* 102:2643-2648.
- Komori, T., H. Yagi, S. Nomura, A. Yamaguchi, K. Sasaki, K. Deguchi, Y. Shimizu, R.T. Bronson, Y.H. Gao, M. Inada, M. Sato, R. Okamoto, Y. Kitamura, S. Yoshiki, and T. Kishimoto. 1997. Targeted disruption of *Cbfa1* results in a complete lack of

bone formation owing to maturational arrest of osteoblasts. *Cell*. 89:755-764.

- Kong, Y.Y., H. Yoshida, I. Sarosi, H.L. Tan, E. Timms, C. Capparelli, S. Morony, A.J. Oliveira-dos-Santos, G. Van, A. Itie, W. Khoo, A. Wakeham, C.R. Dunstan, D.L. Lacey, T.W. Mak, W.J. Boyle, and J.M. Penninger. 1999. OPG is a key regulator of osteoclastogenesis, lymphocyte development and lymph-node organogenesis. *Nature*. 397:315-323.
- Kornak, U., D. Kasper, M.R. Bosl, E. Kaiser, M. Schweizer, A. Schulz, W. Friedrich, G. Delling, and T.J. Jentsch. 2001. Loss of the ClC-7 chloride channel leads to osteopetrosis in mice and man. *Cell*. 104:205-215.
- Krishnan, V., H.U. Bryant, and O.A. Macdougald. 2006. Regulation of bone mass by Wnt signaling. *J Clin Invest*. 116:1202-1209.
- Kronenberg, H.M. 2003. Developmental regulation of the growth plate. *Nature*. 423:332-336.
- Labasi, J.M., N. Petrushova, C. Donovan, S. McCurdy, P. Lira, M.M. Payette, W. Brissette, J.R. Wicks, L. Audoly, and C.A. Gabel. 2002. Absence of the P2X<sub>7</sub> receptor alters leukocyte function and attenuates an inflammatory response. *J Immunol*. 168:6436-6445.
- Lacey, D.L., E. Timms, H.L. Tan, M.J. Kelley, C.R. Dunstan, T. Burgess, R. Elliott, A. Colombero, G. Elliott, S. Scully, H. Hsu, J. Sullivan, N. Hawkins, E. Davy, C. Capparelli, A. Eli, Y.X. Qian, S. Kaufman, I. Sarosi, V. Shalhoub, G. Senaldi, J. Guo, J. Delaney, and W.J. Boyle. 1998. Osteoprotegerin ligand is a cytokine that regulates osteoclast differentiation and activation. *Cell*. 93:165-176.
- Lakkakorpi, P.T., M.A. Horton, M.H. Helfrich, E.K. Karhukorpi, and H.K. Vaananen. 1991. Vitronectin receptor has a role in bone resorption but does not mediate tight sealing zone attachment of osteoclasts to the bone surface. *J Cell Biol*. 115:1179-1186.
- Lazarowski, E.R., J.I. Sesma, L. Seminario-Vidal, and S.M. Kreda. 2011. Molecular mechanisms of purine and pyrimidine nucleotide release. *Adv Pharmacol*. 61:221-261.
- Le Stunff, H., R. Auger, J. Kanellopoulos, and M.N. Raymond. 2004. The Pro-451 to Leu polymorphism within the C-terminal tail of P2X<sub>7</sub> receptor impairs cell death but not phospholipase D activation in murine thymocytes. *J Biol Chem*. 279:16918-16926.
- Lee, B., K. Thirunavukkarasu, L. Zhou, L. Pastore, A. Baldini, J. Hecht, V. Geoffroy, P. Ducy, and G. Karsenty. 1997. Missense mutations abolishing DNA binding of the osteoblast-specific transcription factor OSF2/CBFA1 in cleidocranial dysplasia.

Nat Genet. 16:307-310.

- Lee, K.S., H.J. Kim, Q.L. Li, X.Z. Chi, C. Ueta, T. Komori, J.M. Wozney, E.G. Kim, J.Y. Choi, H.M. Ryoo, and S.C. Bae. 2000. Runx2 is a common target of transforming growth factor beta1 and bone morphogenetic protein 2, and cooperation between Runx2 and Smad5 induces osteoblast-specific gene expression in the pluripotent mesenchymal precursor cell line C2C12. *Mol Cell Biol.* 20:8783-8792.
- Lee, M.H., Y.J. Kim, H.J. Kim, H.D. Park, A.R. Kang, H.M. Kyung, J.H. Sung, J.M. Wozney, and H.M. Ryoo. 2003. BMP-2-induced Runx2 expression is mediated by Dlx5, and TGF-beta 1 opposes the BMP-2-induced osteoblast differentiation by suppression of Dlx5 expression. *J Biol Chem.* 278:34387-34394.
- Leon, D., C. Hervas, and M.T. Miras-Portugal. 2006. P2Y1 and P2X7 receptors induce calcium/calmodulin-dependent protein kinase II phosphorylation in cerebellar granule neurons. *Eur J Neurosci.* 23:2999-3013.
- Li, J., D. Liu, H.Z. Ke, R.L. Duncan, and C.H. Turner. 2005. The P2X<sub>7</sub> nucleotide receptor mediates skeletal mechanotransduction. *J Biol Chem.* 280:42952-42959.
- Li, J., I. Sarosi, X.Q. Yan, S. Morony, C. Capparelli, H.L. Tan, S. McCabe, R. Elliott, S. Scully, G. Van, S. Kaufman, S.C. Juan, Y. Sun, J. Tarpley, L. Martin, K. Christensen, J. McCabe, P. Kostenuik, H. Hsu, F. Fletcher, C.R. Dunstan, D.L. Lacey, and W.J. Boyle. 2000. RANK is the intrinsic hematopoietic cell surface receptor that controls osteoclastogenesis and regulation of bone mass and calcium metabolism. *Proc Natl Acad Sci U S A.* 97:1566-1571.
- Lian, J.B., A. Javed, S.K. Zaidi, C. Lengner, M. Montecino, A.J. van Wijnen, J.L. Stein, and G.S. Stein. 2004. Regulatory controls for osteoblast growth and differentiation: role of Runx/Cbfa/AML factors. *Crit Rev Eukaryot Gene Expr.* 14:1-41.
- Lin, C., X. Jiang, Z. Dai, X. Guo, T. Weng, J. Wang, Y. Li, G. Feng, X. Gao, and L. He. 2009. Sclerostin mediates bone response to mechanical unloading through antagonizing Wnt/beta-catenin signaling. *J Bone Miner Res.* 24:1651-1661.
- Little, R.D., J.P. Carulli, R.G. Del Mastro, J. Dupuis, M. Osborne, C. Folz, S.P. Manning, P.M. Swain, S.C. Zhao, B. Eustace, M.M. Lappe, L. Spitzer, S. Zweier, K. Braunschweiger, Y. Benchekroun, X. Hu, R. Adair, L. Chee, M.G. FitzGerald, C. Tulig, A. Caruso, N. Tzellas, A. Bawa, B. Franklin, S. McGuire, X. Nogues, G. Gong, K.M. Allen, A. Anisowicz, A.J. Morales, P.T. Lomedico, S.M. Recker, P. Van Eerdewegh, R.R. Recker, and M.L. Johnson. 2002. A mutation in the LDL receptor-related protein 5 gene results in the autosomal dominant high-bone-mass trait. *Am J Hum Genet.* 70:11-19.
- Liu, D., D.C. Genetos, Y. Shao, D.J. Geist, J. Li, H.Z. Ke, C.H. Turner, and R.L. Duncan.

2008. Activation of extracellular-signal regulated kinase (ERK1/2) by fluid shear is  $\text{Ca}^{2+}$ - and ATP-dependent in MC3T3-E1 osteoblasts. *Bone*. 42:644-652.
- Liu, L., P.H. Schlesinger, N.M. Slack, P.A. Friedman, and H.C. Blair. 2011. High capacity  $\text{Na}^+/\text{H}^+$  exchange activity in mineralizing osteoblasts. *J Cell Physiol*. 226:1702-1712.
- Loiselle, F.B., and J.R. Casey. 2010. Measurement of Intracellular pH. *Methods Mol Biol*. 637:311-331.
- Long, F. 2012. Building strong bones: molecular regulation of the osteoblast lineage. *Nat Rev Mol Cell Biol*. 13:27-38.
- Long, F., U.I. Chung, S. Ohba, J. McMahon, H.M. Kronenberg, and A.P. McMahon. 2004. Ihh signaling is directly required for the osteoblast lineage in the endochondral skeleton. *Development*. 131:1309-1318.
- Ma, Y.F., X.J. Li, W.S. Jee, J. McOsker, X.G. Liang, R. Setterberg, and S.Y. Chow. 1995. Effects of prostaglandin  $\text{E}_2$  and  $\text{F}_{2\alpha}$  on the skeleton of osteopenic ovariectomized rats. *Bone*. 17:549-554.
- MacDonald, B.T., K. Tamai, and X. He. 2009. Wnt/beta-catenin signaling: components, mechanisms, and diseases. *Dev Cell*. 17:9-26.
- Macian, F. 2005. NFAT proteins: key regulators of T-cell development and function. *Nat Rev Immunol*. 5:472-484.
- Mann, V., C. Huber, G. Kogianni, D. Jones, and B. Noble. 2006. The influence of mechanical stimulation on osteocyte apoptosis and bone viability in human trabecular bone. *J Musculoskelet Neuronal Interact*. 6:408-417.
- Manning, B.D., and L.C. Cantley. 2007. AKT/PKB signaling: navigating downstream. *Cell*. 129:1261-1274.
- Marie, P.J. 2012. Signaling pathways affecting skeletal health. *Curr Osteoporos Rep*. 10:190-198.
- Martin, T.J. 2004. Paracrine regulation of osteoclast formation and activity: milestones in discovery. *J Musculoskelet Neuronal Interact*. 4:243-253.
- Masin, M., C. Young, K. Lim, S.J. Barnes, X.J. Xu, V. Marschall, W. Brutkowski, E.R. Mooney, D.C. Gorecki, and R. Murrell-Lagnado. 2012. Expression, assembly and function of novel C-terminal truncated variants of the mouse P2X7 receptor: re-evaluation of P2X7 knockouts. *Br J Pharmacol*. 165:978-993.
- Matsubara, T., K. Kida, A. Yamaguchi, K. Hata, F. Ichida, H. Meguro, H. Aburatani, R.

- Nishimura, and T. Yoneda. 2008. BMP2 regulates Osterix through Msx2 and Runx2 during osteoblast differentiation. *J Biol Chem.* 283:29119-29125.
- McBeath, R., D.M. Pirone, C.M. Nelson, K. Bhadriraju, and C.S. Chen. 2004. Cell shape, cytoskeletal tension, and RhoA regulate stem cell lineage commitment. *Dev Cell.* 6:483-495.
- McConnell, H.M., J.C. Owicki, J.W. Parce, D.L. Miller, G.T. Baxter, H.G. Wada, and S. Pitchford. 1992. The cytosensor microphysiometer: biological applications of silicon technology. *Science.* 257:1906-1912.
- McHugh, K.P., K. Hodivala-Dilke, M.H. Zheng, N. Namba, J. Lam, D. Novack, X. Feng, F.P. Ross, R.O. Hynes, and S.L. Teitelbaum. 2000. Mice lacking beta3 integrins are osteosclerotic because of dysfunctional osteoclasts. *J Clin Invest.* 105:433-440.
- McKee, M.D., and A. Nanci. 1996. Osteopontin at mineralized tissue interfaces in bone, teeth, and osseointegrated implants: ultrastructural distribution and implications for mineralized tissue formation, turnover, and repair. *Microsc Res Tech.* 33:141-164.
- Minguell, J.J., A. Erices, and P. Conget. 2001. Mesenchymal stem cells. *Exp Biol Med.* 226:507-520.
- Miyauchi, A., J. Alvarez, E.M. Greenfield, A. Teti, M. Grano, S. Colucci, A. Zambonin-Zallone, F.P. Ross, S.L. Teitelbaum, D. Cheresch, and et al. 1991. Recognition of osteopontin and related peptides by an alpha v beta 3 integrin stimulates immediate cell signals in osteoclasts. *J Biol Chem.* 266:20369-20374.
- Miyazono, K., S. Maeda, and T. Imamura. 2004. Coordinate regulation of cell growth and differentiation by TGF-beta superfamily and Runx proteins. *Oncogene.* 23:4232-4237.
- Mobasheri, A., S. Golding, S.N. Pagakis, K. Corkey, A.E. Pocock, B. Fermor, M.J. O'Brien, R.J. Wilkins, J.C. Ellory, and M.J. Francis. 1998. Expression of cation exchanger NHE and anion exchanger AE isoforms in primary human bone-derived osteoblasts. *Cell Biol Int.* 22:551-562.
- Mundlos, S., F. Otto, C. Mundlos, J.B. Mulliken, A.S. Aylsworth, S. Albright, D. Lindhout, W.G. Cole, W. Henn, J.H. Knoll, M.J. Owen, R. Mertelsmann, B.U. Zabel, and B.R. Olsen. 1997. Mutations involving the transcription factor CBFA1 cause cleidocranial dysplasia. *Cell.* 89:773-779.
- Mundy, G.R., D. Chen, and B.O. Oyajobi. 2003. Bone Remodeling. In *Primer on the Metabolic Bone Diseases and Disorders of Mineral Metabolism.* M.J. Favus, editor. American Society for Bone and Mineral Research, Washinton, DC. 46-58.

- Naemsch, L.N., S.J. Dixon, and S.M. Sims. 2001. Activity-dependent development of P2X7 current and Ca<sup>2+</sup> entry in rabbit osteoclasts. *J Biol Chem.* 276:39107-39114.
- Nakamura, E., Y. Uezono, K. Narusawa, I. Shibuya, Y. Oishi, M. Tanaka, N. Yanagihara, T. Nakamura, and F. Izumi. 2000. ATP activates DNA synthesis by acting on P2X receptors in human osteoblast-like MG-63 cells. *Am J Physiol Cell Physiol.* 279:C510-519.
- Nakano, Y., W.N. Addison, and M.T. Kaartinen. 2007. ATP-mediated mineralization of MC3T3-E1 osteoblast cultures. *Bone.* 41:549-561.
- Nakashima, K., X. Zhou, G. Kunkel, Z. Zhang, J.M. Deng, R.R. Behringer, and B. de Crombrughe. 2002. The novel zinc finger-containing transcription factor osterix is required for osteoblast differentiation and bone formation. *Cell.* 108:17-29.
- Narisawa, S., N. Frohlander, and J.L. Millan. 1997. Inactivation of two mouse alkaline phosphatase genes and establishment of a model of infantile hypophosphatasia. *Dev Dyn.* 208:432-446.
- Nesbitt, S., A. Nesbit, M. Helfrich, and M. Horton. 1993. Biochemical characterization of human osteoclast integrins. Osteoclasts express alpha v beta 3, alpha 2 beta 1, and alpha v beta 1 integrins. *J Biol Chem.* 268:16737-16745.
- Ng, L.J., S. Wheatley, G.E. Muscat, J. Conway-Campbell, J. Bowles, E. Wright, D.M. Bell, P.P. Tam, K.S. Cheah, and P. Koopman. 1997. SOX9 binds DNA, activates transcription, and coexpresses with type II collagen during chondrogenesis in the mouse. *Dev Biol.* 183:108-121.
- Nicke, A., Y.H. Kuan, M. Masin, J. Rettinger, B. Marquez-Klaka, O. Bender, D.C. Gorecki, R.D. Murrell-Lagnado, and F. Soto. 2009. A functional P2X7 splice variant with an alternative transmembrane domain 1 escapes gene inactivation in P2X7 knock-out mice. *J Biol Chem.* 284:25813-25822.
- Niida, S., M. Kaku, H. Amano, H. Yoshida, H. Kataoka, S. Nishikawa, K. Tanne, N. Maeda, and H. Kodama. 1999. Vascular endothelial growth factor can substitute for macrophage colony-stimulating factor in the support of osteoclastic bone resorption. *J Exp Med.* 190:293-298.
- Nishio, Y., Y. Dong, M. Paris, R.J. O'Keefe, E.M. Schwarz, and H. Drissi. 2006. Runx2-mediated regulation of the zinc finger Osterix/Sp7 gene. *Gene.* 372:62-70.
- Noble, B.S., N. Peet, H.Y. Stevens, A. Brabbs, J.R. Mosley, G.C. Reilly, J. Reeve, T.M. Skerry, and L.E. Lanyon. 2003. Mechanical loading: biphasic osteocyte survival and targeting of osteoclasts for bone destruction in rat cortical bone. *Am J Physiol Cell Physiol.* 284:C934-943.



- Nordstrom, T., L.D. Shrode, O.D. Rotstein, R. Romanek, T. Goto, J.N. Heersche, M.F. Manolson, G.F. Brisseau, and S. Grinstein. 1997. Chronic extracellular acidosis induces plasmalemmal vacuolar type H<sup>+</sup> ATPase activity in osteoclasts. *J Biol Chem.* 272:6354-6360.
- North, R.A. 2002. Molecular physiology of P2X receptors. *Physiol Rev.* 82:1013-1067.
- Novack, D.V., and S.L. Teitelbaum. 2008. The osteoclast: friend or foe? *Annu Rev Pathol.* 3:457-484.
- O'Brien, C.A., T. Nakashima, and H. Takayanagi. 2013. Osteocyte control of osteoclastogenesis. *Bone.* 54:258-263.
- Ohlendorff, S.D., C.L. Tofteng, J.E. Jensen, S. Petersen, R. Civitelli, M. Fenger, B. Abrahamsen, A.P. Hermann, P. Eiken, and N.R. Jorgensen. 2007. Single nucleotide polymorphisms in the P2X<sub>7</sub> gene are associated to fracture risk and to effect of estrogen treatment. *Pharmacogenet Genomics.* 17:555-567.
- Okawa, A., I. Nakamura, S. Goto, H. Moriya, Y. Nakamura, and S. Ikegawa. 1998. Mutation in Npps in a mouse model of ossification of the posterior longitudinal ligament of the spine. *Nat Genet.* 19:271-273.
- Okumura, H., D. Shiba, T. Kubo, and T. Yokoyama. 2008. P2X<sub>7</sub> receptor as sensitive flow sensor for ERK activation in osteoblasts. *Biochem Biophys Res Commun.* 372:486-490.
- Olsen, B.R., A.M. Reginato, and W. Wang. 2000. Bone development. *Annu Rev Cell Dev Biol.* 16:191-220.
- Orlowski, J., and S. Grinstein. 1997. Na<sup>+</sup>/H<sup>+</sup> exchangers of mammalian cells. *J Biol Chem.* 272:22373-22376.
- Orriss, I., S. Syberg, N. Wang, B. Robaye, A. Gartland, N. Jorgensen, T. Arnett, and J.M. Boeynaems. 2011. Bone phenotypes of P2 receptor knockout mice. *Front Biosci (Schol Ed).* 3:1038-1046.
- Orriss, I.R., G. Burnstock, and T.R. Arnett. 2010. Purinergic signalling and bone remodelling. *Curr Opin Pharmacol.* 10:322-330.
- Orriss, I.R., M.L. Key, A. Brandao-Burch, J.J. Patel, G. Burnstock, and T.R. Arnett. 2012. The regulation of osteoblast function and bone mineralisation by extracellular nucleotides: The role of p2x receptors. *Bone.*
- Orriss, I.R., G.E. Knight, S. Ranasinghe, G. Burnstock, and T.R. Arnett. 2006. Osteoblast responses to nucleotides increase during differentiation. *Bone.* 39:300-309.

- Orriss, I.R., G.E. Knight, J.C. Utting, S.E. Taylor, G. Burnstock, and T.R. Arnett. 2009. Hypoxia stimulates vesicular ATP release from rat osteoblasts. *J Cell Physiol.* 220:155-162.
- Orriss, I.R., J.C. Utting, A. Brandao-Burch, K. Colston, B.R. Grubb, G. Burnstock, and T.R. Arnett. 2007. Extracellular nucleotides block bone mineralization in vitro: evidence for dual inhibitory mechanisms involving both P2Y2 receptors and pyrophosphate. *Endocrinology.* 148:4208-4216.
- Ortega, F., R. Perez-Sen, E.G. Delicado, and M.T. Miras-Portugal. 2009. P2X7 nucleotide receptor is coupled to GSK-3 inhibition and neuroprotection in cerebellar granule neurons. *Neurotox Res.* 15:193-204.
- Ortega, F., R. Perez-Sen, V. Morente, E.G. Delicado, and M.T. Miras-Portugal. 2010. P2X7, NMDA and BDNF receptors converge on GSK3 phosphorylation and cooperate to promote survival in cerebellar granule neurons. *Cell Mol Life Sci.* 67:1723-1733.
- Otto, F., M. Lubbert, and M. Stock. 2003. Upstream and downstream targets of RUNX proteins. *J Cell Biochem.* 89:9-18.
- Otto, F., A.P. Thornell, T. Crompton, A. Denzel, K.C. Gilmour, I.R. Rosewell, G.W. Stamp, R.S. Beddington, S. Mundlos, B.R. Olsen, P.B. Selby, and M.J. Owen. 1997. *Cbfa1*, a candidate gene for cleidocranial dysplasia syndrome, is essential for osteoblast differentiation and bone development. *Cell.* 89:765-771.
- Panupinthu, N., J.T. Rogers, L. Zhao, L.P. Solano-Flores, F. Possmayer, S.M. Sims, and S.J. Dixon. 2008. P2X7 receptors on osteoblasts couple to production of lysophosphatidic acid: a signaling axis promoting osteogenesis. *J Cell Biol.* 181:859-871.
- Panupinthu, N., L. Zhao, F. Possmayer, H.Z. Ke, S.M. Sims, and S.J. Dixon. 2007. P2X7 nucleotide receptors mediate blebbing in osteoblasts through a pathway involving lysophosphatidic acid. *J Biol Chem.* 282:3403-3412.
- Parfitt, A.M. 1994. Osteonal and hemi-osteonal remodeling: the spatial and temporal framework for signal traffic in adult human bone. *J Cell Biochem.* 55:273-286.
- Pederson, L., M. Ruan, J.J. Westendorf, S. Khosla, and M.J. Oursler. 2008. Regulation of bone formation by osteoclasts involves Wnt/BMP signaling and the chemokine sphingosine-1-phosphate. *Proc Natl Acad Sci U S A.* 105:20764-20769.
- Pelegrin, P., and A. Surprenant. 2006. Pannexin-1 mediates large pore formation and interleukin-1 $\beta$  release by the ATP-gated P2X<sub>7</sub> receptor. *EMBO J.* 25:5071-5082.
- Pellegatti, P., S. Falzoni, P. Pinton, R. Rizzuto, and F. Di Virgilio. 2005. A novel

- recombinant plasma membrane-targeted luciferase reveals a new pathway for ATP secretion. *Mol Biol Cell*. 16:3659-3665.
- Peng, X.D., P.Z. Xu, M.L. Chen, A. Hahn-Windgassen, J. Skeen, J. Jacobs, D. Sundararajan, W.S. Chen, S.E. Crawford, K.G. Coleman, and N. Hay. 2003. Dwarfism, impaired skin development, skeletal muscle atrophy, delayed bone development, and impeded adipogenesis in mice lacking Akt1 and Akt2. *Genes Dev*. 17:1352-1365.
- Pereverzev, A., S.V. Komarova, J. Korcok, S. Armstrong, G.B. Tremblay, S.J. Dixon, and S.M. Sims. 2008. Extracellular acidification enhances osteoclast survival through an NFAT-independent, protein kinase C-dependent pathway. *Bone*. 42:150-161.
- Poole, K.E., R.L. van Bezooijen, N. Loveridge, H. Hamersma, S.E. Papapoulos, C.W. Lowik, and J. Reeve. 2005. Sclerostin is a delayed secreted product of osteocytes that inhibits bone formation. *FASEB J*. 19:1842-1844.
- Puceat, M. 1999. pHi regulatory ion transporters: an update on structure, regulation and cell function. *Cell Mol Life Sci*. 55:1216-1229.
- Rangaswami, H., R. Schwappacher, T. Tran, G.C. Chan, S. Zhuang, G.R. Boss, and R.B. Pilz. 2012. Protein kinase G and focal adhesion kinase converge on Src/Akt/beta-catenin signaling module in osteoblast mechanotransduction. *J Biol Chem*. 287:21509-21519.
- Rao, A., C. Luo, and P.G. Hogan. 1997. Transcription factors of the NFAT family: regulation and function. *Annu Rev Immunol*. 15:707-747.
- Redhead, C.R. 1988. Ionic regulation of intracellular pH in rat calvarial osteoblasts. *J Physiol*. 401:455-468.
- Riddle, R.C., A.F. Taylor, J.R. Rogers, and H.J. Donahue. 2007. ATP release mediates fluid flow-induced proliferation of human bone marrow stromal cells. *J Bone Miner Res*. 22:589-600.
- Robling, A.G., P.J. Niziolek, L.A. Baldrige, K.W. Condon, M.R. Allen, I. Alam, S.M. Mantila, J. Gluhak-Heinrich, T.M. Bellido, S.E. Harris, and C.H. Turner. 2008. Mechanical stimulation of bone in vivo reduces osteocyte expression of Sost/sclerostin. *J Biol Chem*. 283:5866-5875.
- Rodda, S.J., and A.P. McMahon. 2006. Distinct roles for Hedgehog and canonical Wnt signaling in specification, differentiation and maintenance of osteoblast progenitors. *Development*. 133:3231-3244.
- Romanello, M., A. Codognotto, M. Bicego, A. Pines, G. Tell, and P. D'Andrea. 2005. Autocrine/paracrine stimulation of purinergic receptors in osteoblasts:

- contribution of vesicular ATP release. *Biochem Biophys Res Commun.* 331:1429-1438.
- Rutsch, F., S. Vaingankar, K. Johnson, I. Goldfine, B. Maddux, P. Schauerte, H. Kalhoff, K. Sano, W.A. Boisvert, A. Superti-Furga, and R. Terkeltaub. 2001. PC-1 nucleoside triphosphate pyrophosphohydrolase deficiency in idiopathic infantile arterial calcification. *Am J Pathol.* 158:543-554.
- Sakamoto, M., Y. Hosoda, K. Kojimahara, T. Yamazaki, and Y. Yoshimura. 1994. Arthritis and ankylosis in twy mice with hereditary multiple osteochondral lesions: with special reference to calcium deposition. *Pathol Int.* 44:420-427.
- Sato, M., M.K. Sardana, W.A. Grasser, V.M. Garsky, J.M. Murray, and R.J. Gould. 1990. Echistatin is a potent inhibitor of bone resorption in culture. *J Cell Biol.* 111:1713-1723.
- Sawakami, K., A.G. Robling, M. Ai, N.D. Pitner, D. Liu, S.J. Warden, J. Li, P. Maye, D.W. Rowe, R.L. Duncan, M.L. Warman, and C.H. Turner. 2006. The Wnt co-receptor LRP5 is essential for skeletal mechanotransduction but not for the anabolic bone response to parathyroid hormone treatment. *J Biol Chem.* 281:23698-23711.
- Schaffler, M.B., D.B. Burr, and R.G. Frederickson. 1987. Morphology of the osteonal cement line in human bone. *Anat Rec.* 217:223-228.
- Schroeder, T.M., E.D. Jensen, and J.J. Westendorf. 2005. Runx2: a master organizer of gene transcription in developing and maturing osteoblasts. *Birth Defects Res C Embryo Today.* 75:213-225.
- Seifert, J.R., and M. Mlodzik. 2007. Frizzled/PCP signalling: a conserved mechanism regulating cell polarity and directed motility. *Nat Rev Genet.* 8:126-138.
- Semenov, M.V., and X. He. 2006. LRP5 mutations linked to high bone mass diseases cause reduced LRP5 binding and inhibition by SOST. *J Biol Chem.* 281:38276-38284.
- Sen, B., M. Styner, Z. Xie, N. Case, C.T. Rubin, and J. Rubin. 2009. Mechanical loading regulates NFATc1 and beta-catenin signaling through a GSK3beta control node. *J Biol Chem.* 284:34607-34617.
- Shemon, A.N., R. Sluyter, S.L. Fernando, A.L. Clarke, L.P. Dao-Ung, K.K. Skarratt, B.M. Saunders, K.S. Tan, B.J. Gu, S.J. Fuller, W.J. Britton, S. Petrou, and J.S. Wiley. 2006. A Thr357 to Ser polymorphism in homozygous and compound heterozygous subjects causes absent or reduced P2X7 function and impairs ATP-induced mycobacterial killing by macrophages. *J Biol Chem.* 281:2079-2086.

- Sim, J.A., M.T. Young, H.Y. Sung, R.A. North, and A. Surprenant. 2004. Reanalysis of P2X<sub>7</sub> receptor expression in rodent brain. *J Neurosci.* 24:6307-6314.
- Sims, N.A., and J.H. Gooi. 2008. Bone remodeling: Multiple cellular interactions required for coupling of bone formation and resorption. *Semin Cell Dev Biol.* 19:444-451.
- Sluyter, R., J.G. Dalitz, and J.S. Wiley. 2004a. P2X<sub>7</sub> receptor polymorphism impairs extracellular adenosine 5'-triphosphate-induced interleukin-18 release from human monocytes. *Genes Immun.* 5:588-591.
- Sluyter, R., A.N. Shemon, and J.S. Wiley. 2004b. Glu496 to Ala polymorphism in the P2X<sub>7</sub> receptor impairs ATP-induced IL-1 $\beta$  release from human monocytes. *J Immunol.* 172:3399-3405.
- Smerdel-Ramoya, A., S. Zanotti, and E. Canalis. 2010. Connective tissue growth factor (CTGF) transactivates nuclear factor of activated T-cells (NFAT) in cells of the osteoblastic lineage. *J Cell Biochem.* 110:477-483.
- Solle, M., J. Labasi, D.G. Perregaux, E. Stam, N. Petrushova, B.H. Koller, R.J. Griffiths, and C.A. Gabel. 2001. Altered cytokine production in mice lacking P2X<sub>7</sub> receptors. *J Biol Chem.* 276:125-132.
- Soltanoff, C.S., S. Yang, W. Chen, and Y.P. Li. 2009. Signaling networks that control the lineage commitment and differentiation of bone cells. *Crit Rev Eukaryot Gene Expr.* 19:1-46.
- Sprague, S.M., N.S. Krieger, and D.A. Bushinsky. 1994. Greater inhibition of in vitro bone mineralization with metabolic than respiratory acidosis. *Kidney Int.* 46:1199-1206.
- St-Jacques, B., M. Hammerschmidt, and A.P. McMahon. 1999. Indian hedgehog signaling regulates proliferation and differentiation of chondrocytes and is essential for bone formation. *Genes Dev.* 13:2072-2086.
- Stevens, D.A., and G.R. Williams. 1999. Hormone regulation of chondrocyte differentiation and endochondral bone formation. *Mol Cell Endocrinol.* 151:195-204.
- Su, X., D.H. Floyd, A. Hughes, J. Xiang, J.G. Schneider, O. Uluckan, E. Heller, H. Deng, W. Zou, C.S. Craft, K. Wu, A.C. Hirbe, D. Grabowska, M.C. Eagleton, S. Townsley, L. Collins, D. Piwnica-Worms, T.H. Steinberg, D.V. Novack, P.B. Conley, M.A. Hurchla, M. Rogers, and K.N. Weilbaecher. 2012. The ADP receptor P2RY12 regulates osteoclast function and pathologic bone remodeling. *J Clin Invest.*

- Sun, L., H.C. Blair, Y. Peng, N. Zaidi, O.A. Adebajo, X.B. Wu, X.Y. Wu, J. Iqbal, S. Epstein, E. Abe, B.S. Moonga, and M. Zaidi. 2005. Calcineurin regulates bone formation by the osteoblast. *Proc Natl Acad Sci U S A*. 102:17130-17135.
- Surprenant, A., and R.A. North. 2009. Signaling at purinergic P2X receptors. *Annu Rev Physiol*. 71:333-359.
- Surprenant, A., F. Rassendren, E. Kawashima, R.A. North, and G. Buell. 1996. The cytolytic P2Z receptor for extracellular ATP identified as a P2X receptor (P2X7). *Science*. 272:735-738.
- Swarthout, J.T., R.C. D'Alonzo, N. Selvamurugan, and N.C. Partridge. 2002. Parathyroid hormone-dependent signaling pathways regulating genes in bone cells. *Gene*. 282:1-17.
- Takada, I., M. Mihara, M. Suzawa, F. Ohtake, S. Kobayashi, M. Igarashi, M.Y. Youn, K. Takeyama, T. Nakamura, Y. Mezaki, S. Takezawa, Y. Yogiashi, H. Kitagawa, G. Yamada, S. Takada, Y. Minami, H. Shibuya, K. Matsumoto, and S. Kato. 2007. A histone lysine methyltransferase activated by non-canonical Wnt signalling suppresses PPAR-gamma transactivation. *Nat Cell Biol*. 9:1273-1285.
- Takayanagi, H., S. Kim, T. Koga, H. Nishina, M. Isshiki, H. Yoshida, A. Saiura, M. Isobe, T. Yokochi, J. Inoue, E.F. Wagner, T.W. Mak, T. Kodama, and T. Taniguchi. 2002. Induction and activation of the transcription factor NFATc1 (NFAT2) integrate RANKL signaling in terminal differentiation of osteoclasts. *Dev Cell*. 3:889-901.
- Tatsumi, S., K. Ishii, N. Amizuka, M. Li, T. Kobayashi, K. Kohno, M. Ito, S. Takeshita, and K. Ikeda. 2007. Targeted ablation of osteocytes induces osteoporosis with defective mechanotransduction. *Cell Metab*. 5:464-475.
- Taylor, S.R., M. Gonzalez-Begne, D.K. Sojka, J.C. Richardson, S.A. Sheardown, S.M. Harrison, C.D. Pusey, F.W. Tam, and J.I. Elliott. 2009. Lymphocytes from P2X7-deficient mice exhibit enhanced P2X7 responses. *J Leukoc Biol*. 85:978-986.
- Teitelbaum, S.L., and F.P. Ross. 2003. Genetic regulation of osteoclast development and function. *Nat Rev Genet*. 4:638-649.
- Tian, X., W.S. Jee, X. Li, C. Paszty, and H.Z. Ke. 2011. Sclerostin antibody increases bone mass by stimulating bone formation and inhibiting bone resorption in a hindlimb-immobilization rat model. *Bone*. 48:197-201.
- Tu, X., J. Chen, J. Lim, C.M. Karner, S.Y. Lee, J. Heisig, C. Wiese, K. Surendran, R. Kopan, M. Gessler, and F. Long. 2012a. Physiological notch signaling maintains bone homeostasis via RBPjk and Hey upstream of NFATc1. *PLoS Genet*. 8:e1002577.

- Tu, X., K.S. Joeng, K.I. Nakayama, K. Nakayama, J. Rajagopal, T.J. Carroll, A.P. McMahon, and F. Long. 2007. Noncanonical Wnt signaling through G protein-linked PKCdelta activation promotes bone formation. *Dev Cell*. 12:113-127.
- Tu, X., Y. Rhee, K.W. Condon, N. Bivi, M.R. Allen, D. Dwyer, M. Stolina, C.H. Turner, A.G. Robling, L.I. Plotkin, and T. Bellido. 2012b. Sost downregulation and local Wnt signaling are required for the osteogenic response to mechanical loading. *Bone*. 50:209-217.
- Turner, J.T., G.A. Weisman, and J.M. Camden. 1997. Upregulation of P2Y<sub>2</sub> nucleotide receptors in rat salivary gland cells during short-term culture. *Am J Physiol*. 273:C1100-1107.
- Ulici, V., K.D. Hoenselaar, H. Agoston, D.D. McErlain, J. Umoh, S. Chakrabarti, D.W. Holdsworth, and F. Beier. 2009. The role of Akt1 in terminal stages of endochondral bone formation: angiogenesis and ossification. *Bone*. 45:1133-1145.
- Ulici, V., K.D. Hoenselaar, J.R. Gillespie, and F. Beier. 2008. The PI3K pathway regulates endochondral bone growth through control of hypertrophic chondrocyte differentiation. *BMC Dev Biol*. 8:40.
- Urano, T., M. Shiraki, Y. Ezura, M. Fujita, E. Sekine, S. Hoshino, T. Hosoi, H. Orimo, M. Emi, Y. Ouchi, and S. Inoue. 2004. Association of a single-nucleotide polymorphism in low-density lipoprotein receptor-related protein 5 gene with bone mineral density. *J Bone Miner Metab*. 22:341-345.
- van Bezooijen, R.L., B.A. Roelen, A. Visser, L. van der Wee-Pals, E. de Wilt, M. Karperien, H. Hamersma, S.E. Papapoulos, P. ten Dijke, and C.W. Lowik. 2004. Sclerostin is an osteocyte-expressed negative regulator of bone formation, but not a classical BMP antagonist. *J Exp Med*. 199:805-814.
- Veeman, M.T., J.D. Axelrod, and R.T. Moon. 2003. A second canon. Functions and mechanisms of beta-catenin-independent Wnt signaling. *Dev Cell*. 5:367-377.
- Verborgt, O., N.A. Tatton, R.J. Majeska, and M.B. Schaffler. 2002. Spatial distribution of Bax and Bcl-2 in osteocytes after bone fatigue: complementary roles in bone remodeling regulation? *J Bone Miner Res*. 17:907-914.
- Vivanco, I., and C.L. Sawyers. 2002. The phosphatidylinositol 3-Kinase AKT pathway in human cancer. *Nat Rev Cancer*. 2:489-501.
- Volonte, C., S. Amadio, N. D'Ambrosi, M. Colpi, and G. Burnstock. 2006. P2 receptor web: complexity and fine-tuning. *Pharmacol Ther*. 112:264-280.
- Wagner, T., J. Wirth, J. Meyer, B. Zabel, M. Held, J. Zimmer, J. Pasantes, F.D. Bricarelli, J. Keutel, E. Hustert, U. Wolf, N. Tommerup, W. Schempp, and G. Scherer. 1994.

Autosomal sex reversal and campomelic dysplasia are caused by mutations in and around the SRY-related gene SOX9. *Cell*. 79:1111-1120.

- Walker, E.C., N.E. McGregor, I.J. Poulton, S. Pompolo, E.H. Allan, J.M. Quinn, M.T. Gillespie, T.J. Martin, and N.A. Sims. 2008. Cardiotrophin-1 is an osteoclast-derived stimulus of bone formation required for normal bone remodeling. *J Bone Miner Res*. 23:2025-2032.
- Wang, N., B. Robaye, A. Agrawal, T.M. Skerry, J.M. Boeynaems, and A. Gartland. 2012. Reduced bone turnover in mice lacking the P2Y(13) receptor of ADP. *Mol Endocrinol*. 26:142-152.
- Wang, Y., and J. Nathans. 2007. Tissue/planar cell polarity in vertebrates: new insights and new questions. *Development*. 134:647-658.
- Wesselius, A., M.J. Bours, A. Agrawal, A. Gartland, P.C. Dagnelie, P. Schwarz, and N.R. Jorgensen. 2011. Role of purinergic receptor polymorphisms in human bone. *Front Biosci*. 16:2572-2585.
- Wesselius, A., M.J. Bours, I.C. Arts, E.H. Theunisz, P. Geusens, and P.C. Dagnelie. 2012. The P2X(7) loss-of-function Glu496Ala polymorphism affects ex vivo cytokine release and protects against the cytotoxic effects of high ATP-levels. *BMC Immunol*. 13:64.
- Westendorf, J.J., R.A. Kahler, and T.M. Schroeder. 2004. Wnt signaling in osteoblasts and bone diseases. *Gene*. 341:19-39.
- Wiley, J.S., L.P. Dao-Ung, B.J. Gu, R. Sluyter, A.N. Shemon, C. Li, J. Taper, J. Gallo, and A. Manoharan. 2002. A loss-of-function polymorphic mutation in the cytolytic P2X7 receptor gene and chronic lymphocytic leukaemia: a molecular study. *Lancet*. 359:1114-1119.
- Wiley, J.S., L.P. Dao-Ung, C. Li, A.N. Shemon, B.J. Gu, M.L. Smart, S.J. Fuller, J.A. Barden, S. Petrou, and R. Sluyter. 2003. An Ile-568 to Asn polymorphism prevents normal trafficking and function of the human P2X<sub>7</sub> receptor. *J Biol Chem*. 278:17108-17113.
- Williams, A.J., H. Robson, M.H. Kester, J.P. van Leeuwen, S.M. Shalet, T.J. Visser, and G.R. Williams. 2008. Iodothyronine deiodinase enzyme activities in bone. *Bone*. 43:126-134.
- Winslow, M.M., M. Pan, M. Starbuck, E.M. Gallo, L. Deng, G. Karsenty, and G.R. Crabtree. 2006. Calcineurin/NFAT signaling in osteoblasts regulates bone mass. *Dev Cell*. 10:771-782.
- Wright, E., M.R. Hargrave, J. Christiansen, L. Cooper, J. Kun, T. Evans, U.



- Gangadharan, A. Greenfield, and P. Koopman. 1995. The Sry-related gene Sox9 is expressed during chondrogenesis in mouse embryos. *Nat Genet.* 9:15-20.
- Xia, X., N. Batra, Q. Shi, L.F. Bonewald, E. Sprague, and J.X. Jiang. 2010. Prostaglandin promotion of osteocyte gap junction function through transcriptional regulation of connexin 43 by glycogen synthase kinase 3/beta-catenin signaling. *Mol Cell Biol.* 30:206-219.
- Xiong, J., M. Onal, R.L. Jilka, R.S. Weinstein, S.C. Manolagas, and C.A. O'Brien. 2011. Matrix-embedded cells control osteoclast formation. *Nat Med.* 17:1235-1241.
- Yang, X., and G. Karsenty. 2004. ATF4, the osteoblast accumulation of which is determined post-translationally, can induce osteoblast-specific gene expression in non-osteoblastic cells. *J Biol Chem.* 279:47109-47114.
- Yang, X., K. Matsuda, P. Bialek, S. Jacquot, H.C. Masuoka, T. Schinke, L. Li, S. Brancorsini, P. Sassone-Corsi, T.M. Townes, A. Hanauer, and G. Karsenty. 2004. ATF4 is a substrate of RSK2 and an essential regulator of osteoblast biology; implication for Coffin-Lowry Syndrome. *Cell.* 117:387-398.
- Zhang, Y.W., N. Yasui, K. Ito, G. Huang, M. Fujii, J. Hanai, H. Nogami, T. Ochi, K. Miyazono, and Y. Ito. 2000. A RUNX2/PEBP2alpha A/CBFA1 mutation displaying impaired transactivation and Smad interaction in cleidocranial dysplasia. *Proc Natl Acad Sci U S A.* 97:10549-10554.
- Zhao, C., N. Irie, Y. Takada, K. Shimoda, T. Miyamoto, T. Nishiwaki, T. Suda, and K. Matsuo. 2006. Bidirectional ephrinB2-EphB4 signaling controls bone homeostasis. *Cell Metab.* 4:111-121.
- Zhao, L., J.W. Shim, T.R. Dodge, A.G. Robling, and H. Yokota. 2013. Inactivation of Lrp5 in osteocytes reduces young's modulus and responsiveness to the mechanical loading. *Bone.* 54:35-43.
- Zhao, Q., H. Eberspaecher, V. Lefebvre, and B. De Crombrughe. 1997. Parallel expression of Sox9 and Col2a1 in cells undergoing chondrogenesis. *Dev Dyn.* 209:377-386.
- Zheng, Q., G. Zhou, R. Morello, Y. Chen, X. Garcia-Rojas, and B. Lee. 2003. Type X collagen gene regulation by Runx2 contributes directly to its hypertrophic chondrocyte-specific expression in vivo. *J Cell Biol.* 162:833-842.
- Zhou, G., Y. Chen, L. Zhou, K. Thirunavukkarasu, J. Hecht, D. Chitayat, B.D. Gelb, S. Pirinen, S.A. Berry, C.R. Greenberg, G. Karsenty, and B. Lee. 1999. CBFA1 mutation analysis and functional correlation with phenotypic variability in cleidocranial dysplasia. *Hum Mol Genet.* 8:2311-2316.

Zhou, X., Z. Zhang, J.Q. Feng, V.M. Dusevich, K. Sinha, H. Zhang, B.G. Darnay, and B. de Crombrughe. 2010. Multiple functions of Osterix are required for bone growth and homeostasis in postnatal mice. *Proc Natl Acad Sci U S A.* 107:12919-12924.

Zimmermann, H., M. Zebisch, and N. Strater. 2012. Cellular function and molecular structure of ecto-nucleotidases. *Purinergic Signal.* 8:437-502.

## CHAPTER TWO

### **P2 RECEPTOR NETWORKS REGULATE SIGNALING DURATION OVER A WIDE DYNAMIC RANGE OF ATP CONCENTRATIONS<sup>1</sup>**

---

<sup>1</sup> This Chapter has been reproduced with permission from:  
Grol, M.W., A. Pereverzev, S. M. Sims, and S.J. Dixon. 2013. P2 receptor networks regulate signaling duration over a wide dynamic range of ATP concentrations. *J. Cell Sci.* 126:3615-3626, with some modifications.

## 2.1 Chapter Summary

The primordial intercellular signaling molecule ATP acts through two families of cell-surface P2 receptors – the P2Y family of G protein-coupled receptors and the P2X family of ligand-gated cation channels. Multiple P2 receptors are expressed in a variety of cell-types. However, the significance of these networks of receptors in any biological system remains unknown. Using osteoblasts as a model system, we found that a low concentration of ATP (10  $\mu$ M, ATP<sub>low</sub>) induced transient elevation of cytosolic Ca<sup>2+</sup>; whereas, a high concentration of ATP (1 mM, ATP<sub>high</sub>) elicited more sustained elevation. Moreover, graded increases in the Ca<sup>2+</sup> signal were achieved over a remarkable million-fold range of ATP concentrations (1 nM to 1 mM). Next, we demonstrated that ATP<sub>low</sub> caused transient nuclear localization of the transcription factor NFATc1; whereas, ATP<sub>high</sub> elicited more sustained localization. When stimulated with ATP<sub>high</sub>, osteoblasts from P2X7 loss-of-function mice showed only transient Ca<sup>2+</sup>/NFATc1 signaling; in contrast, sustained signaling was observed in wild-type cells. Additional experiments revealed a role for P2Y receptors in mediating transient signaling induced by low ATP concentrations. Thus, distinct P2 receptors with varying affinities for ATP account for this wide range of sensitivity to extracellular nucleotides. Finally, ATP<sub>high</sub>, but not ATP<sub>low</sub>, was shown to elicit robust expression of the NFAT target gene *Ptgs2* (encoding COX-2), consistent with a crucial role for the duration of Ca<sup>2+</sup>/NFAT signaling in regulating target gene expression. Taken together, ensembles of P2 receptors provide a mechanism by which cells sense ATP over a wide concentration range, and transduce this input into distinct cellular signals.

## 2.2 Introduction

Purine and pyrimidine nucleotides represent a primordial and pervasive class of intercellular chemical messengers (Burnstock and Verkhratsky, 2009). Many stimuli, including shear stress, mechanical stretch, osmotic swelling and hypoxia, trigger release of nucleotides from cells via mechanisms such as vesicular exocytosis and plasma membrane channels or transporters (Burnstock, 2007b). Once in the extracellular milieu, nucleotides act on target cells through two families of P2 nucleotide receptors – the P2Y family of G protein-coupled receptors and the P2X family of ligand-gated cation channels (Abbracchio et al., 2006; Khakh and North, 2006).

Eight P2Y subtypes (P2Y<sub>1</sub>, P2Y<sub>2</sub>, P2Y<sub>4</sub>, P2Y<sub>6</sub>, P2Y<sub>11-14</sub>) and seven subtypes of P2X (P2X<sub>1-7</sub>) have been identified in mammals, and are involved in regulating processes such as secretion, cell proliferation, differentiation, motility and death (Khakh and North, 2006; Burnstock, 2007a; Burnstock and Verkhratsky, 2010). Many P2Y receptors, including P2Y<sub>1</sub>, P2Y<sub>2</sub>, P2Y<sub>4</sub> and P2Y<sub>6</sub>, couple to activation of phospholipase C (PLC), resulting in formation of inositol 1,4,5-trisphosphate (IP<sub>3</sub>) and subsequent release of Ca<sup>2+</sup> from intracellular stores (Burnstock, 2007a). In contrast, homo- or heteromultimers of three ionotropic P2X receptor subunits form functional channels permeable to Na<sup>+</sup>, K<sup>+</sup> and Ca<sup>2+</sup> (Browne et al., 2010). Consequently, activation of P2X receptors results in membrane depolarization and, in many cases, Ca<sup>2+</sup> influx. P2Y receptors are activated by one or more of adenosine 5'-triphosphate (ATP), adenosine 5'-diphosphate (ADP), uridine 5'-triphosphate (UTP), uridine 5'-diphosphate (UDP) or UDP-glucose, with P2Y<sub>1</sub>, P2Y<sub>2</sub>, P2Y<sub>4</sub>, and P2Y<sub>11-13</sub> exhibiting some degree of sensitivity for ATP; in contrast, members of the P2X receptor family are activated solely by ATP (Burnstock, 2007a).

All mammalian cell-types express multiple P2 receptor subtypes, each with varying affinities for purine and pyrimidine nucleotides (Volonte et al., 2006; Burnstock and Verkhratsky, 2009). Bone-forming osteoblasts can express P2Y<sub>1</sub>, P2Y<sub>2</sub>, P2Y<sub>6</sub>, P2Y<sub>12-14</sub> and P2X<sub>1-7</sub>, and several have been shown to regulate distinct processes in these cells (Orriss et al., 2010). For instance, activation of P2Y<sub>1</sub> or P2Y<sub>2</sub> enhances osteoblast responses to systemic factors such as parathyroid hormone (PTH) (Bowler et al., 1999; Bowler et al., 2001). ATP or UTP, acting through P2Y<sub>2</sub>, inhibit matrix mineralization in cultures of differentiating osteoblasts (Hoebertz et al., 2002; Orriss et al., 2007). In contrast, activated P2X<sub>7</sub> receptors enhance osteoblast differentiation and increase bone formation (Ke et al., 2003; Panupinthu et al., 2008). More recently, P2Y<sub>12</sub> and P2Y<sub>13</sub> have also been shown to positively regulate osteoblast proliferation and differentiation *in vitro* and *in vivo* (Syberg et al., 2012; Wang et al., 2012). Though the functions of individual P2Y and P2X receptors have been examined in osteoblasts and other cell-types, mechanisms by which multiple P2 receptor subtypes act in concert to regulate cellular differentiation and function remain unclear in any system (Volonte et al., 2006).

The nuclear factor of activated T-cells (NFAT) family of transcription factors includes four members that are regulated by cytosolic Ca<sup>2+</sup> (NFATc1-4) (Crabtree and Olson, 2002). In resting cells, NFATc1-4 are phosphorylated and localized to the cytosol. Receptor-mediated elevation in cytosolic free Ca<sup>2+</sup> concentration ([Ca<sup>2+</sup>]<sub>i</sub>) leads to activation of calcineurin, a serine/threonine phosphatase that dephosphorylates NFATc1-4, resulting in their nuclear translocation and transcriptional activation (Hogan et al., 2003). Though classically described as master regulators of T-cell development and function, NFATc1-4 also play essential roles in the differentiation and function of

neuronal, muscle and bone cells, including osteoblasts and osteoclasts (Hogan et al., 2003; Sitara and Aliprantis, 2010; Moore and Goldberg, 2011). However, whether P2 receptors signal through NFAT in bone-forming osteoblasts remains unexplored.

In the present study, we show that endogenous co-expression of multiple P2Y and P2X receptors provides a novel mechanism for dose-to-duration encoding of  $\text{Ca}^{2+}$ /NFAT signaling. Using osteoblasts as a model system, we found that increases in  $\text{Ca}^{2+}$  signaling could be achieved over a million-fold range of ATP concentrations. Low concentrations of ATP acting through P2Y receptors caused transient elevation of  $\text{Ca}^{2+}$  and brief nuclear localization of NFATc1, but failed to induce expression of NFAT target genes. In contrast, high ATP concentrations acting through P2X7 elicited sustained  $\text{Ca}^{2+}$ /NFATc1 signaling and robust NFAT transcriptional activity. Taken together, these data show that P2 receptor networks provide a mechanism by which cells sense ATP over a wide range of concentrations and transduce this input into distinct cellular signals.

## 2.3 Materials and Methods

### 2.3.1 Materials and Solutions

$\alpha$ -Minimum essential medium ( $\alpha$ -MEM), heat-inactivated fetal bovine serum (FBS), antibiotic solution (10,000 U/ml penicillin, 10,000  $\mu$ g/ml streptomycin, and 25  $\mu$ g/ml amphotericin B), trypsin solution, Dulbecco's phosphate buffered saline (DPBS), Medium 199 buffered with 4-(2-hydroxyethyl)-1-piperazineethanesulfonic acid (HEPES) (25 mM) and  $\text{HCO}_3^-$  (4 mM) (M199),  $\text{HCO}_3^-$ -free MEM, Dulbecco's modified Eagle medium (high glucose) (DMEM), UltraPure<sup>TM</sup> distilled water (DNase/RNase-free) and HEPES were obtained from GIBCO (Life Technologies Inc., Burlington, ON, Canada). Fluo-4 acetoxymethyl ester (fluo-4-AM), indo-1-AM and Pluronic F-127 were obtained from Molecular Probes (Life Technologies Inc.). FuGENE 6 and X-tremeGENE 9 were from Roche Diagnostics (Laval, QC, Canada). TRIzol reagent and were obtained from Invitrogen (Life Technologies Inc.). RNeasy Mini Kit was from QIAGEN (Toronto, ON, Canada). TaqMan One-Step reverse transcriptase-polymerase chain reaction (RT-PCR) Master Mix Reagents kit, cyclooxygenase-2 (COX-2 or *Ptgs2*) primers and probe (Mm00478374\_m1) and 18S ribosomal RNA primers and probe were obtained from Applied Biosystems (Life Technologies Inc.). Passive Lysis Buffer, 5X and Bright-Glo<sup>TM</sup> Luciferase Assay System were purchased from Promega (Madison, WI, USA). Biotinylated goat anti-mouse antibody, fluorescein-conjugated streptavidin (FITC) and Vectashield mounting medium with 4,6-diamidino-2-phenylindole (DAPI) were obtained from Vector Laboratories (Burlingame, CA, USA). NFATc1 mouse monoclonal antibody was obtained from Santa Cruz Biotechnology (Santa Cruz, CA, USA). Normal goat serum, collagenase type II, ethylene glycol-bis( $\beta$ -aminoethylether)-*N,N,N',N'*-tetraacetic



acid tetrasodium salt (EGTA), ATP disodium salt, UTP trisodium salt hydrate, 2'-3'-*O*-(4-benzoylbenzoyl)adenosine 5'-triphosphate (BzATP) triethylammonium salt, 1-oleoyl-*sn*-glycero-3-phosphate (LPA) and suramin sodium salt were obtained from Sigma-Aldrich (St. Louis, MO, USA). U 73122 was from Enzo Life Sciences (Plymouth Meeting, PA, USA). 3-[[5-(2,3-Dichlorophenyl)-1H-tetrazol-1-yl]methyl]pyridine hydrochloride (A 438079 HCl) was from Tocris Bioscience (Ellisville, MO, USA). HEPES buffer consisted of (in mM): 135 NaCl, 5 KCl, 1 MgCl<sub>2</sub>, 1 CaCl<sub>2</sub>, 20 HEPES and 10 glucose, adjusted to pH 7.30±0.02, 290±5 mosmol/L. CaCl<sub>2</sub> was omitted where indicated.

### 2.3.2 Animals and Cell Culture

The P2X7 loss-of-function (knockout) mouse, generated as previously described (Solle et al., 2001), was obtained from Pfizer. Though P2X7 is present in this genetically modified mouse model, the protein is truncated at its COOH-terminus resulting in greatly diminished receptor function (Masin et al., 2012). Colonies of both wild-type and knockout mice were maintained in a mixed genetic background (129/Ola × C57BL/6 × DBA/2) by crossbreeding of heterozygous mice. All procedures were approved by the Council on Animal Care at the University of Western Ontario and were in accordance with the guidelines of the Canadian Council on Animal Care.

Calvarial osteoblasts were isolated from 5- to 7-d-old mice using sequential collagenase digestion, as previously described (Panupinthu et al., 2008). Freshly isolated calvarial osteoblasts were plated at a density of 1.0-1.5 × 10<sup>4</sup> cells/cm<sup>2</sup> on Nunc six-well plates (Thermo Fisher Scientific, Rochester, NY, USA) and maintained in  $\alpha$ -MEM

supplemented with 10% FBS and 1% antibiotic solution (culture medium) at 37°C and 5% CO<sub>2</sub>. After confluence was reached (~3-5 days), cells were trypsinized and plated for experiments.

The MC3T3-E1 osteoblast-like cell line was obtained from the American Type Culture Collection (Rockville, MD). A clonal non-transformed cell line established from newborn mouse calvaria (Sudo et al., 1983), variants of MC3T3-E1 cells have since been isolated that exhibit different phenotypic characteristics *in vitro* (Wang et al., 1999). For the present studies, the MC3T3-E1 Subclone 4 line was selected as these cells exhibit properties of osteoblasts, including elevation of adenosine 3',5'-cyclic monophosphate (cAMP) in response to PTH and expression of transcripts for runt-related transcription factor 2 (RUNX2), bone sialoprotein (BSP) and osteocalcin (OCN). Moreover, cultures form mineralized bone-like nodules upon supplementation with ascorbic acid and phosphate (Wang et al., 1999). Expression of P2X7 receptors in these cells has been demonstrated previously (Li et al., 2005; Qi et al., 2007; Okumura et al., 2008).

### **2.3.3 Fluorescence Measurement of [Ca<sup>2+</sup>]<sub>i</sub>**

For confocal microscopy, MC3T3-E1 cells or calvarial osteoblasts were plated at a density of  $1.5 \times 10^4$  cells/cm<sup>2</sup> on 35-mm glass bottom dishes (MatTek Corporation, Ashland, MA, USA) in culture medium. After 2 d, cells were placed in serum-free medium and incubated overnight. For experiments, cells were loaded with fluo-4 by incubation with fluo-4-AM (2 µg/ml) and 0.1% Pluronic F-127 for 30-45 min at 37°C and 5% CO<sub>2</sub>. Medium was then replaced with M199 supplemented with 1% antibiotic solution, and cells were observed by live-cell confocal microscopy (model LSM 510; Carl

Zeiss Inc., Jena, Germany) at  $\sim 28^{\circ}\text{C}$  using a Plan-Apochromat 40 $\times$  objective (1.2 NA) with 488-nm Ar<sup>+</sup> ion laser excitation. The emission wavelength was filtered at 500-550 nm band pass and images were captured every 500 ms in time-lapse mode.

For spectrofluorimetry, MC3T3-E1 cells were loaded with indo-1 as previously described (Grol et al., 2012). For measurement of  $[\text{Ca}^{2+}]_i$ , 1 ml aliquots of indo-1-loaded cell suspensions ( $\sim 1.0 \times 10^6$  cells) were sedimented and resuspended in 2 ml  $\text{Ca}^{2+}$ -containing or  $\text{Ca}^{2+}$ -free  $\text{Na}^+$ -HEPES buffer in a fluorometric cuvette at room temperature. Changes in  $[\text{Ca}^{2+}]_i$  were then monitored using a dual-wavelength spectrofluorimeter (Model RF-M2004; Photon Technology International, South Brunswick, NJ, USA) at 355 nm excitation and emission wavelengths of 405 and 485 nm.

#### **2.3.4 Expression and Localization of NFATc1-EGFP**

The enhanced green fluorescent protein (EGFP)-tagged NFATc1 (NFATc1-EGFP) fusion protein expression vector was purchased from GE Healthcare (Amersham Place, UK). For live-cell studies, MC3T3-E1 cells were plated at a density of  $1.5 \times 10^4$  cells/cm<sup>2</sup> on 35-mm glass bottom dishes in culture medium. After 1 d, cells were transfected with the NFATc1-EGFP expression vector using FuGENE 6 according to manufacturer's instructions. At 1 d post-transfection, cells were placed in serum-free medium and incubated overnight. On the day of the experiment, medium was replaced with M199 supplemented with 1% antibiotic solution, and cells were observed by confocal microscopy at  $\sim 28^{\circ}\text{C}$  using a Zeiss Plan-Apochromat 40 $\times$  objective (1.2 NA) with 488-nm Ar<sup>+</sup> ion laser excitation. The emission wavelength was filtered at 500-550 nm band pass, and image stacks of 2- $\mu\text{m}$  slices were captured every 5 min in time-lapse

mode. Changes in subcellular localization were quantified by comparing the average fluorescence intensity in the nucleus ( $F_N$ ) to the average fluorescence intensity of an area of equal size in the cytosol ( $F_C$ ). Values of the ratio  $F_N/F_C$  were plotted as a function of time, and values for  $F_N/F_C$  exceeding 1 were taken to indicate nuclear localization.

For fixed-cell studies, MC3T3-E1 cells were plated at a density of  $1.5 \times 10^4$  cells/cm<sup>2</sup> on 12-mm glass coverslips in Falcon 24-well plates (BD Biosciences, Mississauga, ON, Canada) in culture medium. After 1 d, cells were transfected with the NFATc1-EGFP expression vector as described above. At 1 d post-transfection, cells were placed in serum-free medium and incubated overnight. On the day of the experiment, cells were incubated with test substances for the indicated times. Cells were then fixed with paraformaldehyde (4%) in sucrose solution (2%), sealed using Vectashield mounting medium with DAPI, and visualized by fluorescence microscopy. Cells were categorized as positive for nuclear localization of NFATc1-EGFP if fluorescence intensity of the nucleus exceeded that of the cytoplasm. The proportion of cells exhibiting nuclear localization was then calculated. Representative images were acquired using a Zeiss Plan-Apochromat 40 $\times$  objective (1.2 NA) at a slice thickness of 2  $\mu$ m with one of the following configurations: 1) 405-nm diode or 488-nm Ar<sup>+</sup> ion laser excitation with emission wavelengths filtered at 420-480 or 505-550 nm band pass, respectively; or 2) 730-nm Chameleon multiphoton or 488-nm Ar<sup>+</sup> ion laser excitation with emission wavelengths filtered at 390-465 or 500-550 nm band pass, respectively.

### **2.3.5 Immunofluorescence Localization of Native NFATc1**

Calvarial osteoblasts were plated at a density of  $1.5 \times 10^4$  cells/cm<sup>2</sup> on 12-mm

glass coverslips in Falcon 24-well plates in culture medium. After 2 d, cells were placed in serum-free medium and incubated overnight. On the day of the experiment, cells were incubated with test substances for the indicated times. Cells were then fixed with paraformaldehyde (4%) in sucrose solution (2%), permeabilized with 0.1% Triton X-100 in DPBS for 10 min, and blocked for 1 h with 1% normal goat serum in DPBS (blocking solution). To detect subcellular localization of native NFATc1, cells were incubated overnight at 4°C with a mouse monoclonal antibody (1:100 in blocking solution). The next day, cells were incubated with a biotinylated goat anti-mouse antibody (1:200 in blocking solution) for 2 h followed by 15 min incubation with fluorescein-conjugated streptavidin (FITC; 1:100 in DPBS). Stained samples were then sealed using Vectashield mounting medium with DAPI, and visualized by fluorescence microscopy. Cells were categorized as positive for nuclear localization of NFATc1 if fluorescence intensity of the nucleus exceeded that of the cytoplasm. Representative images were acquired using a Zeiss Plan-Apochromat 40× objective (1.2 NA) at a slice thickness of 2 μm with the appropriate excitation wavelengths and emission filters as described above.

### **2.3.6 Real-time RT-PCR Analyses**

MC3T3-E1 or calvarial osteoblasts were plated at a density of  $1.5 \times 10^4$  cells/cm<sup>2</sup> on Falcon 6-well plates in culture medium. After 2 d, cells were placed in serum-free medium and incubated overnight. On the day of the experiment, cells were incubated with test substances for the indicated times. Total RNA was isolated using TRIzol reagent and the RNeasy Mini Kit according to manufacturer's instructions. Real-time PCR was performed using the ABI Prism 7900 HT Sequence Detector (PerkinElmer) with 15 μl

final reaction volumes containing 50 ng RNA sample, TaqMan One-Step RT-PCR Master Mix Reagents, and one of *Ptgs2* or 18S ribosomal RNA primers and probes. Reverse transcription was performed at 48°C for 30 min followed by 40 cycles of amplification at an annealing temperature of 60°C. Reactions for each sample were performed in triplicate. All samples were normalized to 18S ribosomal RNA, and time 0 or vehicle-treated controls using the delta-delta cycle threshold ( $\Delta\Delta C_t$ ) method.

### **2.3.7 Luciferase Reporter Assay for NFATc1**

The NFAT luciferase reporter plasmid (pGL3-NFAT luciferase, plasmid 17870) was obtained from Addgene (Cambridge, MA, USA). This plasmid possesses three copies of the NFAT site cloned upstream of the minimal interleukin (IL)-2 promoter (Clipstone and Crabtree, 1992). MC3T3-E1 and calvarial osteoblasts were transfected in suspension with the NFAT luciferase reporter vector using FuGENE 6 or X-tremeGENE 9 according to manufacturers' instructions. Cells were subsequently plated at a density of  $3.0 \times 10^4$  cells/cm<sup>2</sup> on Falcon 48-well plates in culture medium. At 1 d post-transfection, cells were placed in serum-free medium and incubated overnight. On the day of the experiment, cells were treated with test substances and subsequently incubated for 24 h. Cell lysates were then prepared by incubation with 65  $\mu$ l of Passive Lysis Buffer, 1X per well at room temperature for a minimum of 30 min with agitation. To assess luminescence, 15  $\mu$ l of lysate was combined with 15  $\mu$ l of Bright-Glo Luciferase Reagent in a 96-well white plate (Greiner Bio-One, Monroe, NC, USA). Reactions for each sample were performed in triplicate. Luminescence was measured using 2-s integration per well on a LMAX II<sup>384</sup> microplate reader (Molecular Devices, Downingtown, PA, USA).

### 2.3.8 Statistical Analyses

Data are shown as means  $\pm$  S.E.M. Differences between two groups were assessed using *t* tests. Differences among three or more groups were evaluated by one-way analysis of variance followed by a Tukey multiple comparisons test, or two-way analysis of variance (ANOVA) followed by a Bonferroni multiple comparisons test. Differences were accepted as statistically significant at  $p < 0.05$ .

## 2.4 Results

### 2.4.1 Effect of ATP Concentration on the Duration of Cytosolic Ca<sup>2+</sup> Signals

Cells of the osteoblast lineage express multiple subtypes of P2Y and P2X nucleotide receptors (Orriss et al., 2012). Given the central role for Ca<sup>2+</sup> in P2 receptor signaling, we investigated the functional significance of endogenous P2 receptor networks by assessing Ca<sup>2+</sup> signaling elicited by extracellular ATP. MC3T3-E1 osteoblast-like cells were loaded with the Ca<sup>2+</sup>-sensitive dye fluo-4, and changes in [Ca<sup>2+</sup>]<sub>i</sub> were monitored using real-time imaging of live cells by confocal microscopy (Figure 2.1 A). A low concentration of ATP (10 μM, which activates some P2Y and all P2X receptor subtypes *except* P2X7; ATP<sub>low</sub>) induced large, transient elevations in [Ca<sup>2+</sup>]<sub>i</sub> that recovered to baseline within ~240 s after stimulation (data are whole-field Ca<sup>2+</sup> responses, Figure 2.1 A, B; Video 2.1, video legend in Appendix A). In contrast, a higher ATP concentration (1 mM, which activates some P2Y and all P2X receptor subtypes *including* P2X7; ATP<sub>high</sub>) elicited larger, more sustained elevations in [Ca<sup>2+</sup>]<sub>i</sub> exceeding 20 min in duration (Figure 2.1 A, B; Video 2.2, video legend in Appendix A). Vehicle elicited a small elevation in [Ca<sup>2+</sup>]<sub>i</sub> (Figure 2.1 A, B), consistent with fluid shear-induced release of ATP and slight P2 receptor activation (Figures 2.2 and 2.3), as described previously (Ke et al., 2003; Li et al., 2005).

To further characterize ATP-induced Ca<sup>2+</sup> signaling, changes in [Ca<sup>2+</sup>]<sub>i</sub> were assessed in response to ATP concentrations from 1 nM to 10 mM. We first plotted the peak amplitude of the Ca<sup>2+</sup> signal against ATP concentration (Figure 2.1 C). Remarkably, graded increases in the peak Ca<sup>2+</sup> response were observed over a million-fold range of ATP concentrations (1 nM to 1 mM). The amplitude at 10 mM ATP was



**Figure 2.1 P2 Nucleotide Receptor-induced Elevations in Cytosolic Free  $\text{Ca}^{2+}$  are Dependent on ATP Concentration.**

MC3T3-E1 cells were loaded with the  $\text{Ca}^{2+}$ -sensitive dye fluo-4 and changes in  $[\text{Ca}^{2+}]_i$  were monitored by confocal microscopy. Concentrations of ATP indicated are final concentrations in the bath. Each concentration was tested on separate cell samples. A, representative fields of cells treated with vehicle,  $\text{ATP}_{\text{low}}$  (10  $\mu\text{M}$ ) or  $\text{ATP}_{\text{high}}$  (1 mM). Scale bar is 20  $\mu\text{m}$ . Videos 2.1 and 2.2 show responses to  $\text{ATP}_{\text{low}}$  and  $\text{ATP}_{\text{high}}$ , respectively (video legends in Appendix A). B, changes in  $[\text{Ca}^{2+}]_i$  were quantified from the average responses of cells in a single field as  $(F/F_0)-1$ , where F is fluorescence intensity and  $F_0$  is baseline fluorescence observed prior to treatment. At the point indicated by the arrows, cells were treated with vehicle (Veh),  $\text{ATP}_{\text{low}}$  or  $\text{ATP}_{\text{high}}$  were added. Traces are representative of responses from 8 independent preparations. C, peak amplitude was quantified as the maximal rise in  $[\text{Ca}^{2+}]_i$  above basal levels. Responses to vehicle are indicated by the letter V. D, the sustained phase was quantified as the amplitude of the  $\text{Ca}^{2+}$  response at 10 min post-treatment. E, change in  $[\text{Ca}^{2+}]_i$  was also quantified as the area under the curve, providing a combined measure of amplitude and duration. The area was determined from the beginning of agonist-induced elevation in  $[\text{Ca}^{2+}]_i$  until cytosolic  $\text{Ca}^{2+}$  recovered to within 15% of baseline. The inset shows an expanded view. Data in C-E are means  $\pm$  S.E.M. ( $n = 8$  independent preparations).

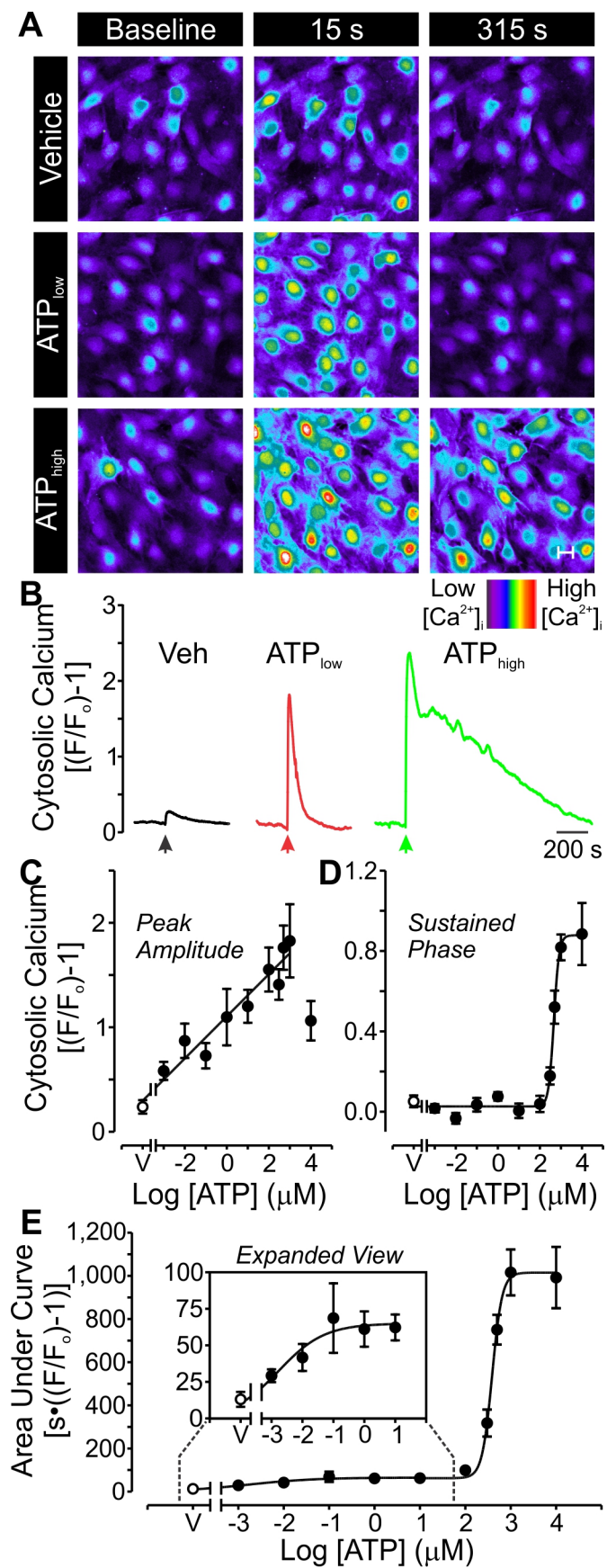


**Figure 2.2 Vehicle-induced Elevations in  $[Ca^{2+}]_i$  are Suppressed by ATP.**

MC3T3-E1 cells were loaded with the  $Ca^{2+}$ -sensitive dye fluo-4 and changes in  $[Ca^{2+}]_i$  were monitored by confocal microscopy. A and C, where indicated by the arrows, cells were treated with vehicle (Veh) or  $ATP_{low}$  (10  $\mu$ M). After  $\sim$ 7.5 min, the same fields of cells were treated with  $ATP_{low}$  or vehicle. Pre-addition of  $ATP_{low}$  suppressed  $Ca^{2+}$  responses elicited by vehicle addition. Traces are representative of responses from 4 independent preparations. B and D,  $Ca^{2+}$  elevations were analyzed for their peak amplitude. Pre-addition of vehicle did not significantly affect subsequent responses to  $ATP_{low}$  (B). In contrast, pre-addition of  $ATP_{low}$  significantly suppressed subsequent responses to vehicle (D). These data suggest that small elevations in  $[Ca^{2+}]_i$  induced by addition of vehicle may arise from fluid shear-induced release of ATP.  $\alpha$  indicates significant difference between treatments ( $p < 0.05$ ). Data are means  $\pm$  S.E.M. ( $n = 8-9$  samples from 4 independent preparations).

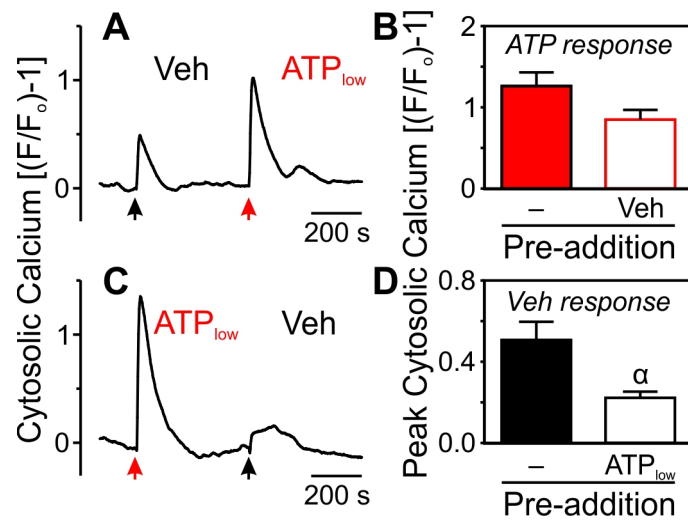
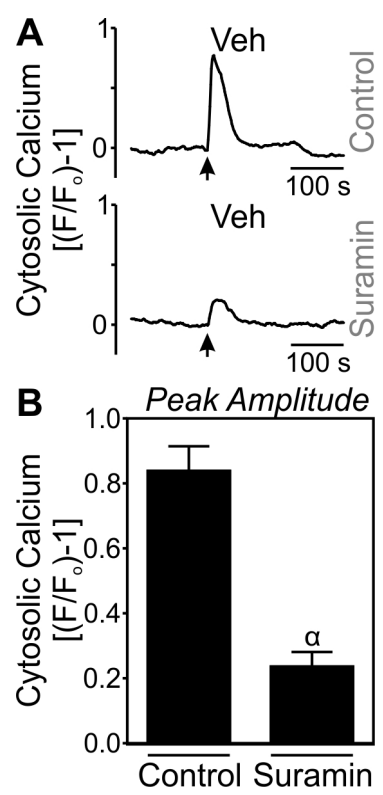


**Figure 2.3 Vehicle-induced Elevations in  $[Ca^{2+}]_i$  are Blocked by a P2 Nucleotide Receptor Antagonist.**

$[Ca^{2+}]_i$  of MC3T3-E1 cells loaded with fluo-4 was monitored using confocal microscopy. A, cells were incubated for a minimum of 45 min in the absence (Control) or presence of the P2 receptor antagonist suramin (100  $\mu$ M). Where indicated by the arrows, cells were then treated with vehicle (Veh). Suramin suppressed  $Ca^{2+}$  responses elicited by vehicle addition. Traces are representative of responses from 3 independent preparations. B,  $Ca^{2+}$  elevations were analyzed for their peak amplitude.  $\alpha$  indicates significant effect of P2 antagonist compared to control ( $p < 0.05$ ). Data are means  $\pm$  S.E.M. ( $n = 9$  samples from 3 independent preparations). Taken together with the results presented in Figure 2.2, these data further support the notion that addition of vehicle creates fluid shear, leading to release of endogenous ATP and subsequent P2 receptor signaling. Consistent with this conclusion, there was virtually no  $Ca^{2+}$  response to vehicle when added to cells suspended in a fluorometric cuvette with continuous stirring (Figure 2.6 A, D), a condition in which cells were constantly exposed to an unchanging fluid shear stimulus.



slightly reduced, likely reflecting chelation of extracellular  $\text{Ca}^{2+}$  by this high concentration of ATP. In contrast, only ATP concentrations  $>100 \mu\text{M}$  elicited a sustained  $\text{Ca}^{2+}$  signal (measured as amplitude 10 min post-treatment, Figure 2.1 D).<sup>2</sup> Finally, we quantified the magnitude of responses as the area under the fluorescence-time curve, providing a combined measure of both amplitude and duration. In this case, concentration dependence was clearly biphasic (Figure 2.1 E). The first phase began at  $\sim 1 \text{ nM}$  and plateaued at  $\sim 1 \mu\text{M}$  ATP, whereas the second phase began at  $\sim 100 \mu\text{M}$  and plateaued at  $\sim 1 \text{ mM}$  ATP.

#### **2.4.2 P2X7 is Essential for Sustained Cytosolic $\text{Ca}^{2+}$ Signaling Elicited by High Concentrations of ATP**

Extracellular ATP activates a number of P2Y and P2X receptor subtypes at concentrations within the nM to  $\mu\text{M}$  range; in contrast, P2X7 is stimulated solely at ATP concentrations exceeding  $100 \mu\text{M}$  (Khakh and North, 2006; Burnstock, 2007a). Therefore, we investigated whether P2X7 receptors mediate the effects of high ATP concentrations. Changes in  $[\text{Ca}^{2+}]_i$  were examined following treatment of osteoblast-like cells with vehicle,  $\text{ATP}_{\text{low}}$  or BzATP ( $300 \mu\text{M}$ ) in the absence or presence of A 438079 ( $10 \mu\text{M}$ ), a specific P2X7 antagonist (Nelson et al., 2006; Donnelly-Roberts and Jarvis, 2007) (Figure 2.5 A-C). Although not specific for P2X7, BzATP is a more potent agonist than ATP at the P2X7 receptor (North, 2002). In the absence of antagonist, BzATP elicited a large, sustained elevation in cytosolic  $\text{Ca}^{2+}$ , whereas  $\text{ATP}_{\text{low}}$  induced a more

---

<sup>2</sup> Similar patterns of concentration dependence were observed when percentages of cells exhibiting elevation of  $[\text{Ca}^{2+}]_i$  were examined (Figure 2.4).

**Figure 2.4 The Percentage of Cells Exhibiting P2 Nucleotide Receptor-induced Elevations in  $[Ca^{2+}]_i$  is Dependent on ATP Concentration.**

$[Ca^{2+}]_i$  of MC3T3-E1 cells loaded with fluo-4 was monitored using confocal microscopy. Concentrations of ATP indicated are final concentrations in the bath. Each concentration was tested on separate cell samples. Responses to vehicle are indicated by the letter V. A, data are the percentage of responding cells in a field at the indicated concentration of ATP. In this case, cells were considered to have responded when the peak amplitude (i.e. maximal rise in  $[Ca^{2+}]_i$ ) was  $\geq 100\%$  of basal levels. B, data are the percentage of cells in a field exhibiting a sustained  $Ca^{2+}$  response at the indicated concentration of ATP. In this case, cells were considered to have a sustained response when the amplitude at 10 min post-treatment was  $\geq 50\%$  of basal levels. Data for both A and B are means  $\pm$  S.E.M. ( $n = 8$  independent preparations). These single cell data closely resemble  $Ca^{2+}$  responses seen in whole-field analyses presented in Figure 1 C, D. Thus, the dependence of  $Ca^{2+}$  signaling on ATP concentration is due, at least in part, to changes in the proportion of responding cells.



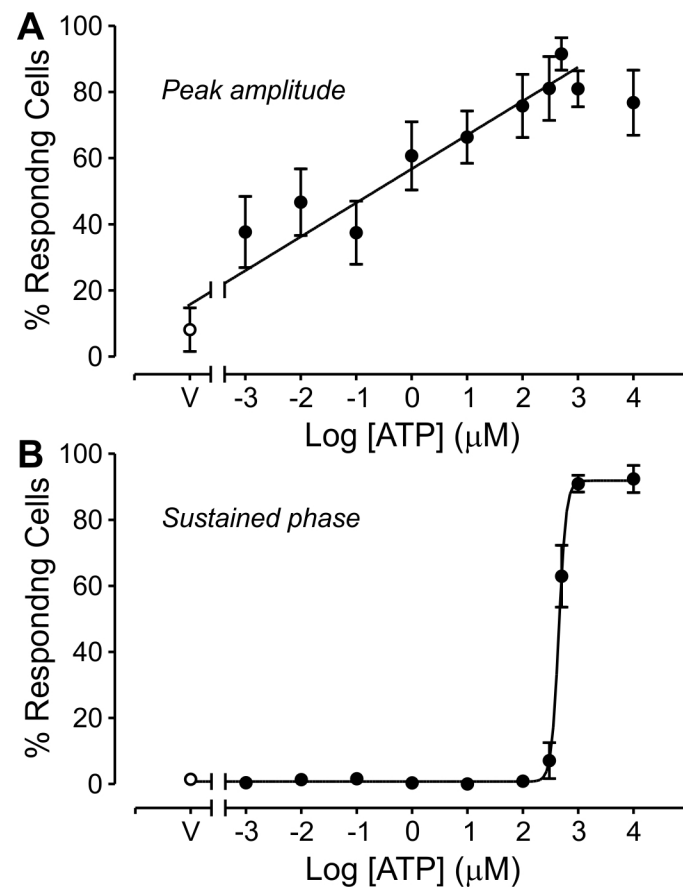
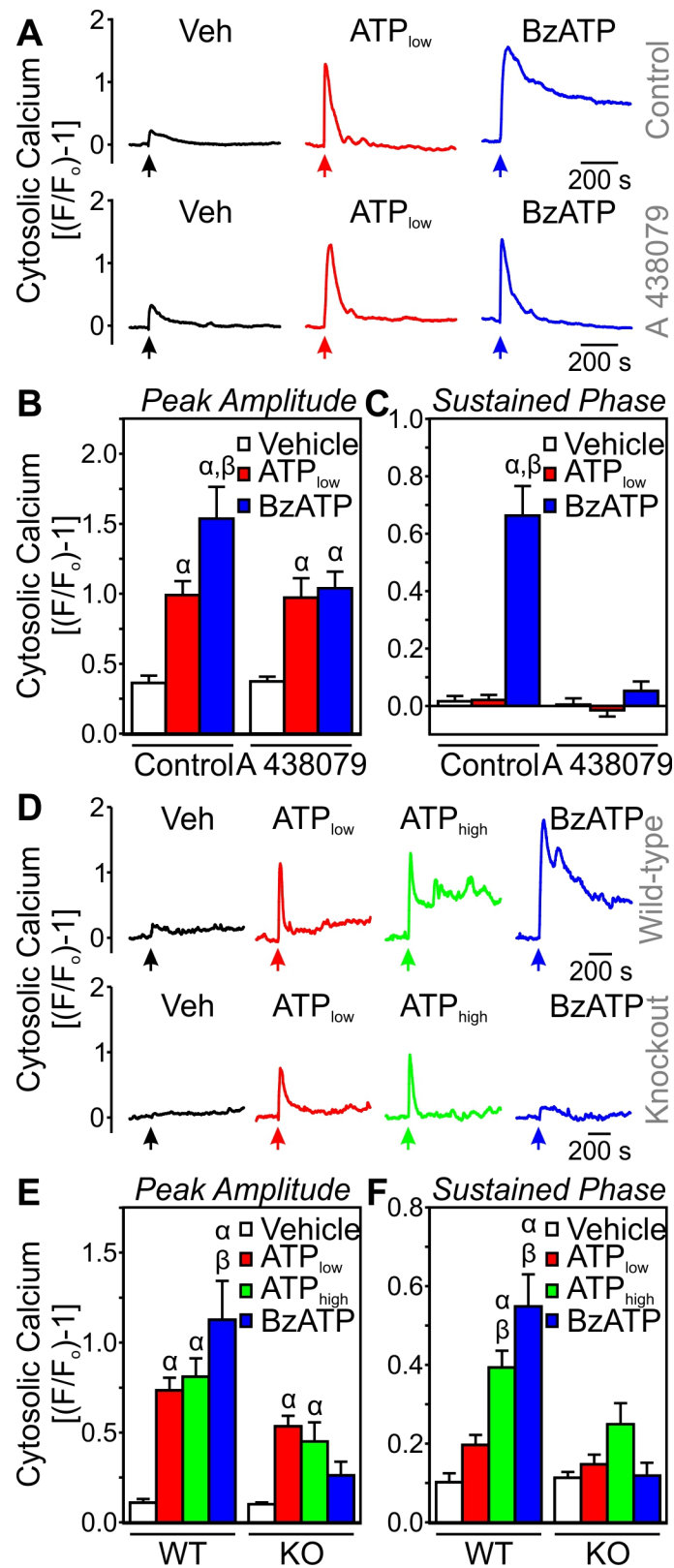


**Figure 2.5 The P2X7 Receptor is Required for Sustained Elevations in  $[Ca^{2+}]_i$ .**

A,  $[Ca^{2+}]_i$  of MC3T3-E1 cells loaded with fluo-4 was monitored using confocal microscopy. Cells were incubated for 5-10 min in the absence or presence of the specific P2X7 antagonist A 438079 (10  $\mu$ M). At the point indicated by the arrows, cells were then treated with vehicle (Veh), ATP<sub>low</sub> (10  $\mu$ M) or BzATP (300  $\mu$ M). Traces are representative of responses from 6 independent preparations. B and C, Ca<sup>2+</sup> elevations were analyzed for their (B) peak amplitude and (C) sustained phase.  $\alpha$  indicates significant difference from vehicle;  $\beta$  indicates significant difference between ATP<sub>low</sub> and BzATP ( $p < 0.05$ ). Data are means  $\pm$  S.E.M. ( $n = 12$  samples from 6 independent preparations). D, calvarial osteoblasts from wild-type and P2X7 knockout mice were loaded with fluo-4 and changes in  $[Ca^{2+}]_i$  were monitored. Where indicated by the arrows, cells were treated with Vehicle (Veh), ATP<sub>low</sub> (10  $\mu$ M), ATP<sub>high</sub> (1 mM) or BzATP (300  $\mu$ M). Traces are representative of responses from 6 independent preparations. E and F, Ca<sup>2+</sup> elevations in calvarial osteoblasts were analyzed for amplitudes of the peak (E) and sustained phase (F).  $\alpha$  indicates significant difference from Vehicle within the same genotype;  $\beta$  indicates significant difference between ATP<sub>high</sub> or BzATP and ATP<sub>low</sub> within the same genotype ( $p < 0.05$ ). Data are means  $\pm$  S.E.M. ( $n = 10-11$  samples from 6 independent preparations).



transient increase (Figure 2.5 A-C). A 438079 abolished the sustained phase of the BzATP-induced response, converting it to a transient increase comparable to that elicited by ATP<sub>low</sub> (Figure 2.5 A-C). A 438079 had no effect on Ca<sup>2+</sup> elevation induced by ATP<sub>low</sub>, consistent with the specificity of this P2X7 receptor antagonist.

To confirm the role of P2X7 in mediating effects of high concentrations of ATP or BzATP on cytosolic Ca<sup>2+</sup> signaling, changes in [Ca<sup>2+</sup>]<sub>i</sub> were examined in primary calvarial osteoblasts isolated from wild-type mice and mice with loss of P2X7 function (knockout) (Figure 2.5 D-F). Stimulation of wild-type calvarial osteoblasts with ATP<sub>low</sub> induced transient elevations in [Ca<sup>2+</sup>]<sub>i</sub> that returned to baseline within ~240 s, whereas ATP<sub>high</sub> and BzATP (300 μM) both elicited more sustained elevations of [Ca<sup>2+</sup>]<sub>i</sub> exceeding 20 min in duration. In contrast, responses to ATP<sub>high</sub> in calvarial osteoblasts from knockout mice were comparable to those induced by ATP<sub>low</sub>, and treatment with BzATP had no significant effect on [Ca<sup>2+</sup>]<sub>i</sub> (Figure 2.5 D-F). Taken together, pharmacological and genetic evidence establish that the sustained elevations in [Ca<sup>2+</sup>]<sub>i</sub> induced by BzATP or high concentrations of ATP are mediated by activation of P2X7 receptors.

### **2.4.3 Source of Ca<sup>2+</sup> Underlying the Transient and Sustained Elevations of [Ca<sup>2+</sup>]<sub>i</sub> Elicited by ATP**

Several P2Y receptors couple to activation of PLC, resulting in release of Ca<sup>2+</sup> from intracellular stores (Burnstock, 2007a). In contrast, P2X receptors form channels that in many cases permit Ca<sup>2+</sup> influx (Browne et al., 2010). We next determined the source of Ca<sup>2+</sup> required for the transient and sustained elevations of [Ca<sup>2+</sup>]<sub>i</sub>. To assess the

contribution of intracellular stores, changes in  $[Ca^{2+}]_i$  were examined following treatment with vehicle,  $ATP_{low}$  or BzATP (300  $\mu M$ ) in the absence or presence of the PLC inhibitor U 73122 (1  $\mu M$ ) (Figure 2.6 A-C). U 73122 abolished the response induced by  $ATP_{low}$  and the transient component of the  $Ca^{2+}$  signal elicited by BzATP. In contrast, the inhibitor had no significant effect on the sustained phase of the BzATP-induced response (Figure 2.6 A-C).

To determine the role of extracellular  $Ca^{2+}$ , changes in  $[Ca^{2+}]_i$  were examined following treatment of cells with vehicle,  $ATP_{low}$  or BzATP (300  $\mu M$ ) in the presence or absence of extracellular  $Ca^{2+}$  (Figure 2.6 D-F). Removal of extracellular  $Ca^{2+}$  abolished the sustained phase of the BzATP-induced response. In contrast, there was no significant effect on the transient component of the responses to  $ATP_{low}$  and BzATP (Figure 2.6 D-F). Taken together, these data are consistent with  $ATP_{low}$  activating P2Y receptors, leading to release of  $Ca^{2+}$  from intracellular stores. On the other hand, BzATP activates both P2Y receptors and P2X7, leading to transient release of  $Ca^{2+}$  from intracellular stores and sustained influx, respectively.

We further investigated the nature of the P2Y receptors mediating transient  $Ca^{2+}$  signaling. UTP (10  $\mu M$ ) elicited responses comparable to those elicited by  $ATP_{low}$ , providing further evidence for involvement of P2Y receptors. Next, we examined responses to sequential addition of  $ATP_{low}$  and UTP and observed marked cross-desensitization (Figure 2.7), consistent with the agonist specificities of P2Y<sub>2</sub> and/or P2Y<sub>4</sub> (Burnstock, 2007a).

**Figure 2.6 Distinct Sources of  $\text{Ca}^{2+}$  Underlie Transient and Sustained Elevations in  $[\text{Ca}^{2+}]_i$ .**

MC3T3-E1 cells were loaded with the  $\text{Ca}^{2+}$ -sensitive dye indo-1 and suspended in HEPES buffer in a fluorometric cuvette with continuous stirring. Changes in  $[\text{Ca}^{2+}]_i$  were monitored by fluorescence spectrophotometry, and quantified as the ratio of emission intensity at 405 nm to that at 485 nm. A, cells were incubated for 300 s in the absence or presence of the PLC inhibitor U 73122 (1  $\mu\text{M}$ ) in  $\text{Ca}^{2+}$ -containing HEPES buffer. At the point indicated by the arrows, cells were then treated with Vehicle (Veh),  $\text{ATP}_{\text{low}}$  (10  $\mu\text{M}$ ) or BzATP (300  $\mu\text{M}$ ). Traces are representative of responses from 4 independent preparations. B and C,  $\text{Ca}^{2+}$  elevations were analyzed for their (B) peak amplitude and (C) sustained phase.  $\alpha$  indicates significant difference from Vehicle;  $\beta$  indicates significant difference between  $\text{ATP}_{\text{low}}$  and BzATP ( $p < 0.05$ ). Data are means  $\pm$  S.E.M. ( $n = 7$  samples from four independent preparations). D, cells were incubated for 100 s in the absence or presence of the  $\text{Ca}^{2+}$  chelator EGTA (0.5 mM) in  $\text{Ca}^{2+}$ -containing or nominally  $\text{Ca}^{2+}$ -free HEPES buffer, respectively. At the point indicated by the arrows, cells were then treated with Vehicle (Veh),  $\text{ATP}_{\text{low}}$  (10  $\mu\text{M}$ ) or BzATP (300  $\mu\text{M}$ ). Traces are representative of responses from four independent preparations. E and F,  $\text{Ca}^{2+}$  elevations were analyzed for amplitudes of the peak (E) and sustained phase (F).  $\alpha$  indicates significant difference from Vehicle;  $\beta$  indicates significant difference between  $\text{ATP}_{\text{low}}$  and BzATP ( $p < 0.05$ ). Data are means  $\pm$  S.E.M. ( $n = 6$  samples from four independent preparations).

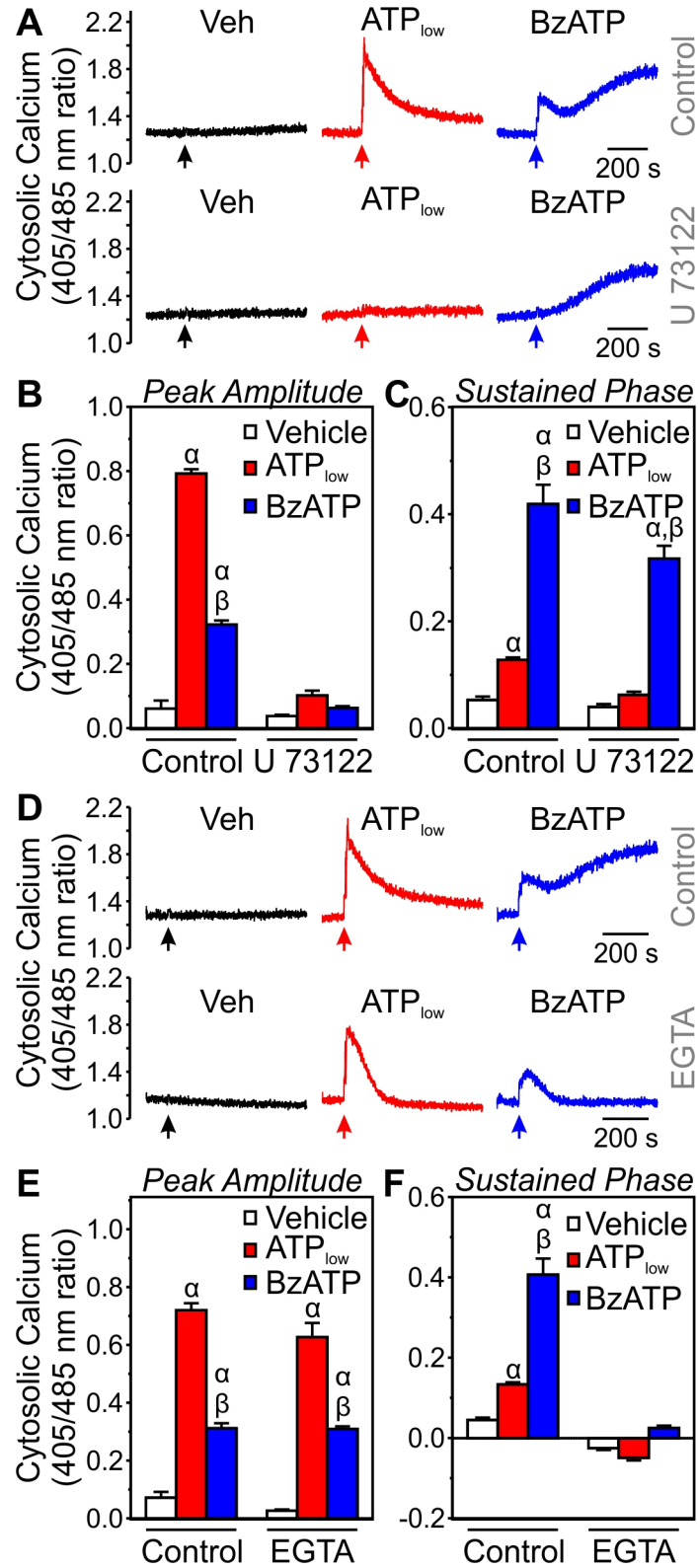
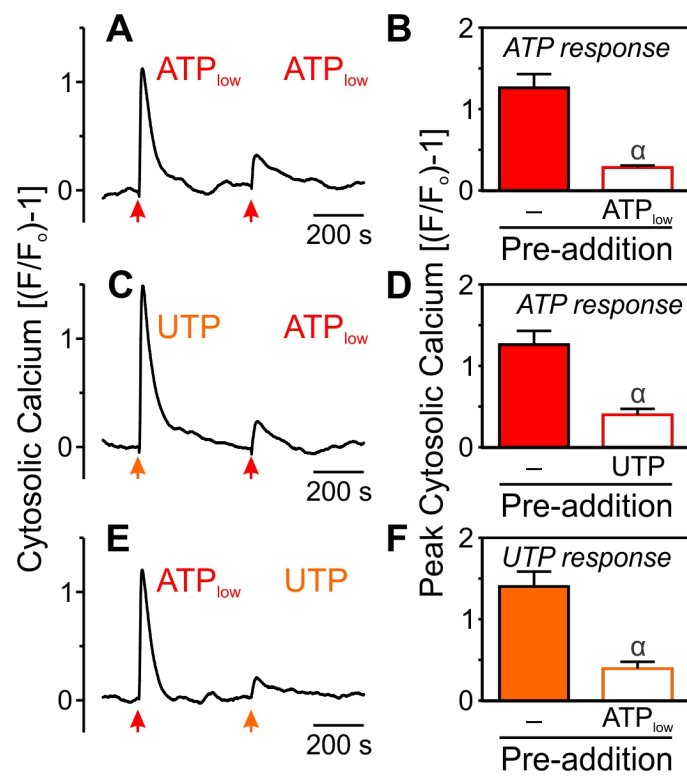


**Figure 2.7 P2Y<sub>2</sub> and/or P2Y<sub>4</sub> Mediate Elevations in [Ca<sup>2+</sup>]<sub>i</sub> Elicited by ATP<sub>low</sub>.**

[Ca<sup>2+</sup>]<sub>i</sub> of MC3T3-E1 cells loaded with fluo-4 was monitored using confocal microscopy. A, C and E, where indicated by the arrows, cells were treated with ATP<sub>low</sub> (10 μM) or UTP (10 μM). After ~7.5 min, the same cells were treated again with ATP<sub>low</sub> or UTP. B, D and F, Ca<sup>2+</sup> elevations were analyzed for their peak amplitude. Pre-addition of ATP<sub>low</sub> significantly attenuated a second response to ATP<sub>low</sub> (B). Interestingly, pre-addition of UTP significantly attenuated a subsequent response to ATP<sub>low</sub> (D). Similarly, pre-addition of ATP<sub>low</sub> significantly attenuated a subsequent response to UTP (F), indicating cross-desensitization. For control experiments, pre-addition of ATP<sub>low</sub> was followed by treatment of lysophosphatidic acid (10 μM), which acts through distinct Ca<sup>2+</sup> mobilizing G protein-coupled receptors on osteoblasts (not shown). In this case, the degree of cross-desensitization was significantly less. These control data argue against the possibility that cross-desensitization of nucleotide responses are due simply to depletion of intracellular Ca<sup>2+</sup> stores. Taken together with the data presented in A-F, this suggests that ATP and UTP interact with a common receptor, likely P2Y<sub>2</sub> and/or P2Y<sub>4</sub>. Traces are representative of responses from 4 independent preparations. α indicates significant difference between treatments (*p* < 0.05). Data are means ± S.E.M. (*n* = 8 samples from 4 independent preparations).





#### **2.4.4 Effect of ATP Concentration on the Duration of NFATc1 Nuclear Localization**

Elevations in  $[Ca^{2+}]_i$  can activate calcineurin, resulting in NFATc1 translocation from the cytoplasm to the nucleus (Crabtree and Olson, 2002; Hogan et al., 2003). To characterize the dynamics of NFATc1 activation in response to ATP, osteoblast-like cells were transfected with EGFP-tagged NFATc1, and subcellular localization was monitored by confocal imaging of live cells. In the absence of agonists, NFATc1-EGFP was uniformly distributed throughout the cytoplasm, with little if any fluorescence in the nucleus (Figure 2.8). ATP (0.01-1 mM) and BzATP (300  $\mu$ M) all induced prompt translocation of NFATc1-EGFP to the nucleus. Low concentrations of ATP (10-100  $\mu$ M) elicited transient nuclear localization of NFATc1-EGFP, with recovery of cytosolic fluorescence less than 90 min after stimulation (Figure 2.8; Video 2.3, video legend in Appendix A). In contrast, ATP<sub>high</sub> and BzATP both induced more sustained nuclear localization of NFATc1-EGFP that persisted for at least 2 h (Figure 2.8; Video 2.4, video legend in Appendix A).

To quantify NFATc1 activation, osteoblast-like cells expressing NFATc1-EGFP were treated and fixed at various time points. The percentage of cells exhibiting nuclear localization of NFATc1-EGFP was determined and expressed as a function of nucleotide concentration or time. When assessed 15 min after addition of nucleotide, nuclear localization of NFATc1-EGFP was induced in a concentration-dependent manner over a relatively narrow range for ATP and UTP (from ~0.1 to 1  $\mu$ M) and BzATP (from ~1 to 100  $\mu$ M) (Figure 2.9 A). Responses to low concentrations of ATP and UTP and higher concentrations of BzATP indicate involvement of multiple P2 receptor subtypes.

**Figure 2.8 Live-Cell Confocal Microscopy Reveals that Duration of NFATc1 Nuclear Localization is Dependent on ATP Concentration.**

MC3T3-E1 cells were transfected with plasmids encoding EGFP-tagged NFATc1 and changes in subcellular localization of NFATc1-EGFP were monitored by confocal microscopy. A, representative fields of cells treated with Vehicle, ATP<sub>low</sub> (10  $\mu$ M), ATP<sub>high</sub> (1 mM) or BzATP (300  $\mu$ M). Scale bars are 20  $\mu$ m. Videos 3 and 4 show responses to ATP<sub>low</sub> and BzATP, respectively (video legends in Appendix A). B, to quantify subcellular localization of NFATc1-EGFP, the average pixel intensity of the nucleus ( $F_N$ ) and the average pixel intensity of an area of equal size in the cytosol ( $F_C$ ) were determined. Values of the ratio  $F_N/F_C$  were plotted as a function of time, and values for  $F_N/F_C$  exceeding 1 were taken to indicate nuclear localization. Plots are representative time courses of nuclear localization for the cells marked with a white asterisk in (A). The time of addition of test substance is indicated by the vertical broken line. Data are representative responses of cells from a minimum of 4 independent transfections.

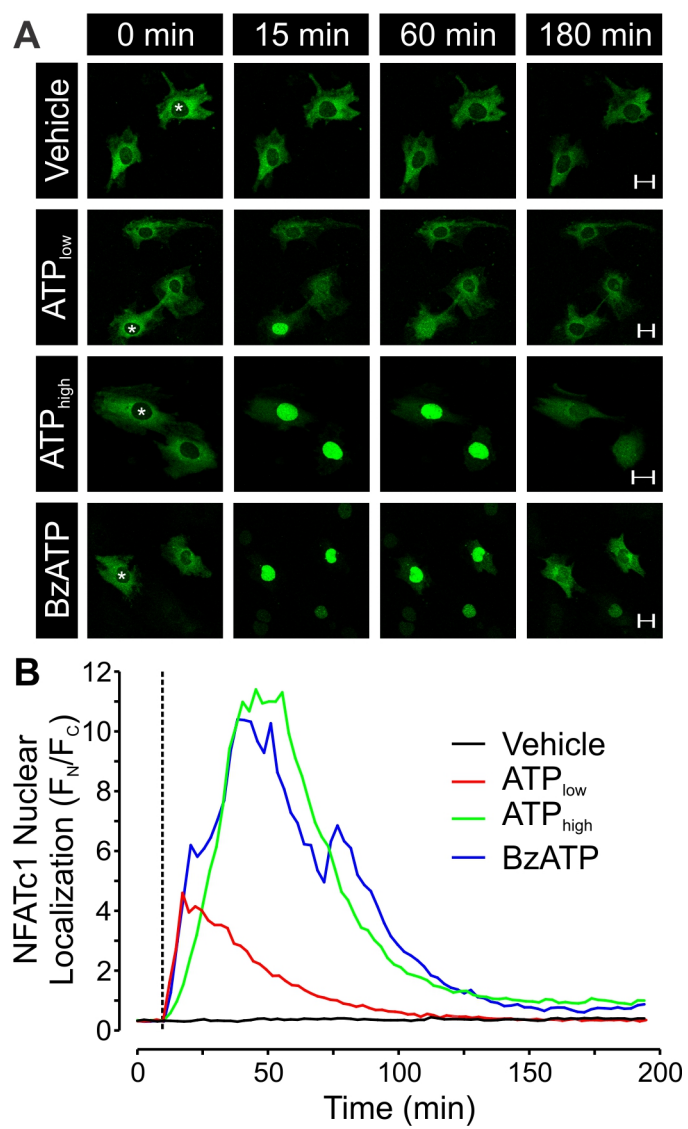
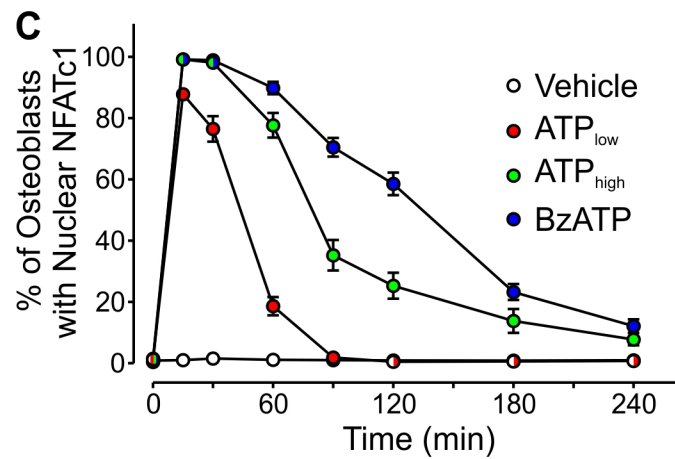
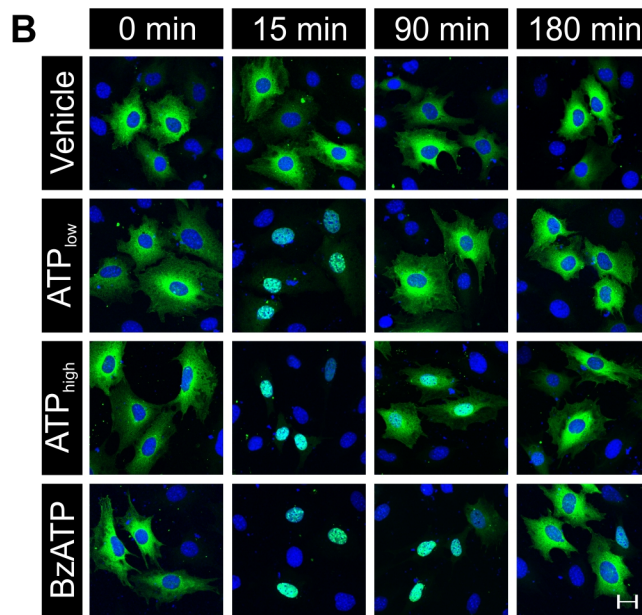
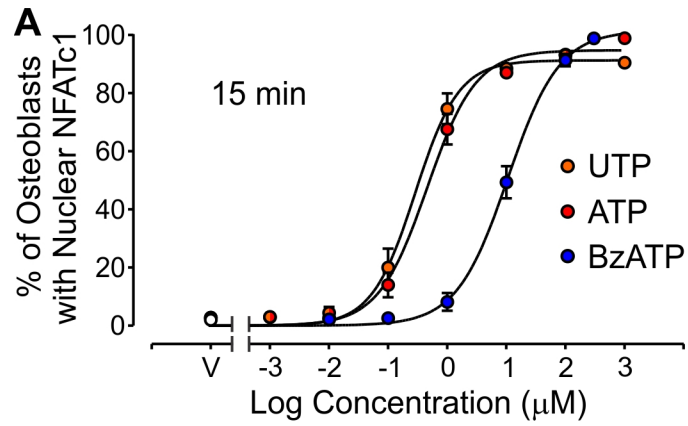


**Figure 2.9 Duration of NFATc1 Nuclear Localization is Dependent on ATP Concentration.**

MC3T3-E1 cells were transfected with plasmids encoding EGFP-tagged NFATc1. A, cells were treated with the indicated concentrations of UTP, ATP or BzATP and fixed at 15 min. The number of cells exhibiting nuclear localization was expressed as a percentage of the total number of transfected cells. Data are means  $\pm$  S.E.M. ( $n = 3$  independent experiments performed in triplicate). B, cells were treated with Vehicle, ATP<sub>low</sub> (10  $\mu$ M), ATP<sub>high</sub> (1 mM) or BzATP (300  $\mu$ M) and fixed at the indicated times. Nuclei were stained with DAPI (**blue**). Images are representative of responses from 4 independent preparations. Scale bar is 20  $\mu$ m. C, cells were treated with vehicle, ATP<sub>low</sub>, ATP<sub>high</sub> or BzATP, and fixed at time points from 0 to 240 min. The percentage of cells exhibiting nuclear localization of NFATc1 was quantified. Data are means  $\pm$  S.E.M. ( $n = 4$  independent experiments performed in triplicate).



Moreover, at this early time point, NFATc1 responds to ATP over a relatively narrow dynamic range of concentrations.

We next examined the time course of NFATc1 nuclear translocation. Consistent with the live-cell data (Figure 2.8), nuclear localization of NFATc1-EGFP elicited by  $ATP_{low}$  was transient, with recovery of cytosolic localization in all cells by 90 min (Figure 2.9 B, C). In contrast,  $ATP_{high}$  and BzATP both induced sustained localization of NFATc1-EGFP to the nucleus that persisted for up to 3 h (Figure 2.9 B, C). Thus, elevations in  $[Ca^{2+}]_i$  elicited by increasing ATP concentrations are transduced into graded increases in the duration of NFATc1 nuclear localization. Moreover, effects of BzATP and  $ATP_{high}$  implicate the P2X7 receptor in mediating prolonged NFATc1 nuclear localization.

#### **2.4.5 P2X7 is Essential for Sustained NFATc1 Nuclear Localization Elicited by High Concentrations of ATP**

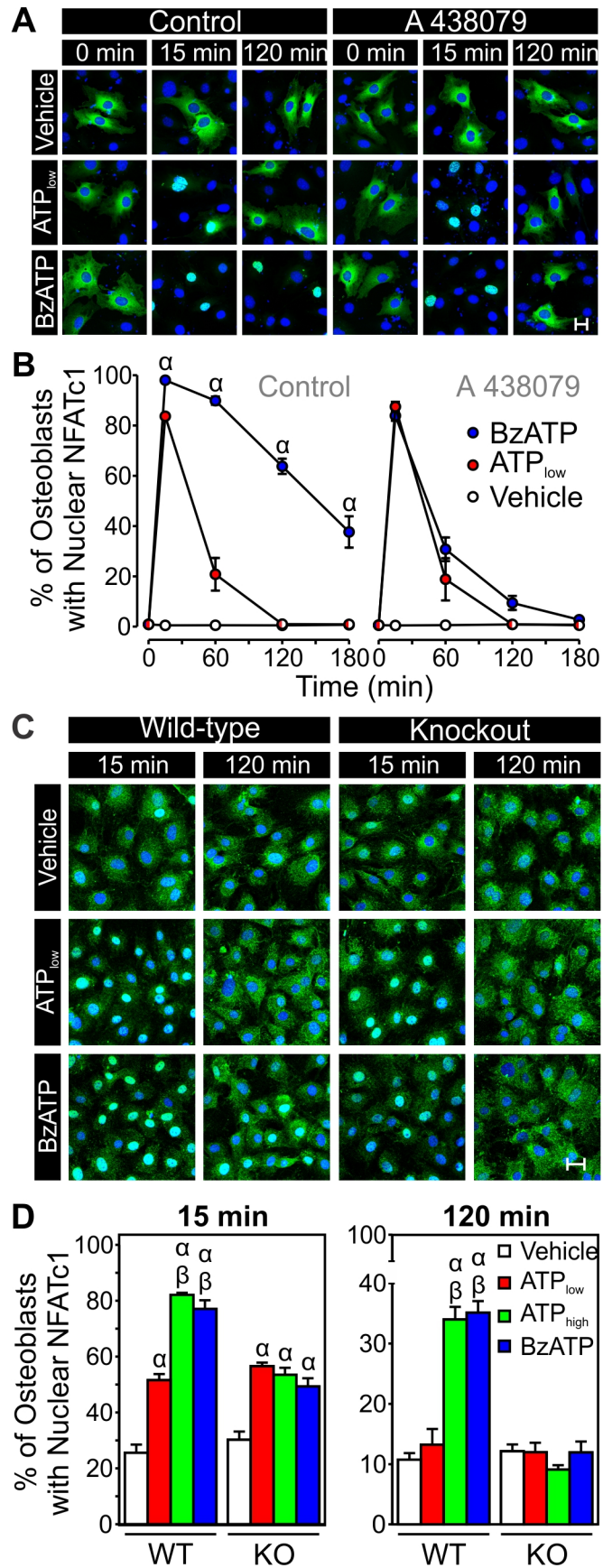
To investigate whether P2X7 receptors mediate sustained NFATc1 nuclear localization, MC3T3-E1 cells were transfected with EGFP-tagged NFATc1 and treated with vehicle,  $ATP_{low}$  or BzATP (300  $\mu$ M) in the absence or presence of A 438079 (10  $\mu$ M). A 438079 abolished the sustained phase of the BzATP-induced response, converting it to a transient response comparable to that elicited by  $ATP_{low}$  (Figure 2.10 A, B). In contrast, this antagonist had no effect on the transient nuclear localization of NFATc1-EGFP stimulated by  $ATP_{low}$ .

To confirm the role of P2X7 receptors in mediating sustained nuclear localization of NFATc1, primary calvarial osteoblasts were isolated from P2X7 knockout and wild-

**Figure 2.10 The P2X7 Receptor is Required for Sustained NFATc1 Nuclear Localization.**

A, MC3T3-E1 cells were transfected with plasmids encoding EGFP-tagged NFATc1. Cells were incubated for 5-10 min in the absence or presence of A 438079 (10  $\mu$ M). Next, cells were treated with Vehicle, ATP<sub>low</sub> (10  $\mu$ M) or BzATP (300  $\mu$ M) and fixed at the indicated times. Images are representative responses of cells from six independent preparations. Scale bar is 20  $\mu$ m. B, the percentage of MC3T3-E1 cells exhibiting NFATc1 nuclear localization was quantified.  $\alpha$  indicates significant difference between BzATP and ATP<sub>low</sub> ( $p < 0.05$ ). Data are means  $\pm$  S.E.M. ( $n = 6$  independent experiments performed in triplicate). C, calvarial osteoblasts from wild-type (WT) and P2X7 knockout (KO) mice were treated with Vehicle, ATP<sub>low</sub> (10  $\mu$ M), ATP<sub>high</sub> (1 mM) or BzATP (300  $\mu$ M) and fixed at 15 or 120 min. Subcellular localization of endogenous NFATc1 was detected by immunofluorescence (**green**). Nuclei were stained with DAPI (**blue**). Images are representative responses from 3-4 separate preparations. Scale bar is 20  $\mu$ m. D, The percentage of calvarial osteoblasts exhibiting NFATc1 nuclear localization was quantified.  $\alpha$  indicates significant difference from vehicle within the same genotype;  $\beta$  indicates significant difference between ATP<sub>high</sub> or BzATP and ATP<sub>low</sub> within the same genotype ( $p < 0.05$ ). Note the expanded y-axis scale in right panel. Data are means  $\pm$  S.E.M. ( $n = 6-8$  samples from 3-4 independent preparations).





type mice. Cultures were treated with vehicle, ATP<sub>low</sub>, ATP<sub>high</sub> or BzATP (300 μM), and fixed at 15 or 120 min (Figure 2.10 C, D). Endogenous NFATc1 was labeled using a monoclonal antibody and localized by immunofluorescence (Figure 2.10 C). The percentage of cells exhibiting nuclear localization was determined for each treatment at 15 and 120 min (Figure 2.10 D). Stimulation of wild-type calvarial osteoblasts with ATP<sub>low</sub> induced transient NFATc1 nuclear localization, whereas ATP<sub>high</sub> and BzATP both elicited sustained localization (Figure 2.10 C, D). In contrast, responses of osteoblasts from knockout mice to ATP<sub>high</sub> and BzATP were transient and comparable to those elicited by ATP<sub>low</sub> (Figure 2.10 C, D). Approximately 35% of wild-type osteoblasts responded to ATP<sub>high</sub> and BzATP at 120 min (Figure 2.10 D, *right panel*), in keeping with the percentage of primary calvarial osteoblasts reported previously to express functional P2X7 receptors (Panupinthu et al., 2007).

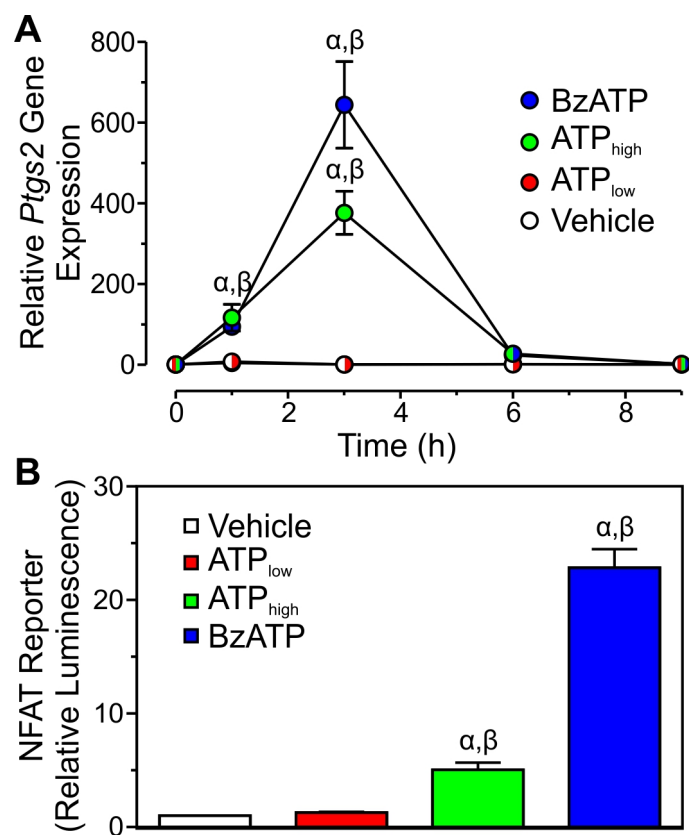
Taken together, these experiments establish that the sustained nuclear localization of NFATc1 elicited by BzATP or high concentrations of ATP is mediated by activation of P2X7 receptors; whereas, transient localization induced by low concentrations of ATP is due to activation of higher affinity P2 receptors.

#### **2.4.6 Effects of Nucleotides on NFAT Transcriptional Activity**

To determine if differences in duration of P2 receptor-induced Ca<sup>2+</sup>/NFATc1 signaling give rise to corresponding alterations in expression of NFAT target genes, MC3T3-E1 cells were treated with vehicle, ATP<sub>low</sub>, ATP<sub>high</sub> or BzATP (300 μM). Total RNA was isolated at various times, and expression of the NFATc1 target gene *Ptgs2* (encoding COX-2) was assessed by real-time RT-PCR (Figure 2.11 A). BzATP and

**Figure 2.11 P2 Nucleotide Receptor-induced Changes in NFAT Transcriptional Activity are Dependent on ATP Concentration.**

A, MC3T3-E1 cells were treated with vehicle, ATP<sub>low</sub> (10  $\mu$ M), ATP<sub>high</sub> (1 mM) or BzATP (300  $\mu$ M), and total RNA was isolated at the indicated times. Real-time RT-PCR was performed to assess expression levels of the NFATc target gene *Ptgs2* (encoding COX-2). Data were normalized to levels of 18S, and are shown relative to values for vehicle-treated cultures at 0 min.  $\alpha$  indicates significant difference from vehicle at each time point;  $\beta$  indicates significant difference between ATP<sub>high</sub> or BzATP and ATP<sub>low</sub> at each time point ( $p < 0.05$ ). Data are means  $\pm$  S.E.M. ( $n = 9$  samples from 3 independent preparations). B, MC3T3-E1 cells were transfected with an NFAT luciferase reporter plasmid and treated with vehicle, ATP<sub>low</sub>, ATP<sub>high</sub> or BzATP. After 24 h, cell lysates were collected and luminescence was assessed as a measure of NFAT transcriptional activity. Luminescence was expressed relative to vehicle.  $\alpha$  indicates significant difference from vehicle;  $\beta$  indicates significant difference between ATP<sub>high</sub> or BzATP and ATP<sub>low</sub> ( $p < 0.05$ ). Data are means  $\pm$  S.E.M. ( $n = 12$  samples from 4 independent preparations).



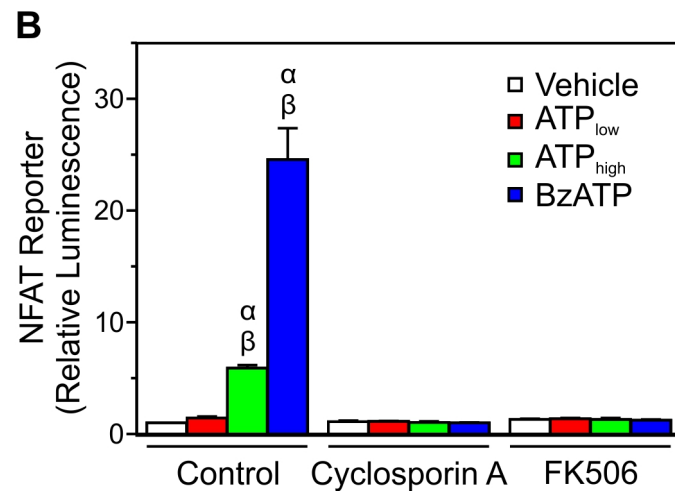
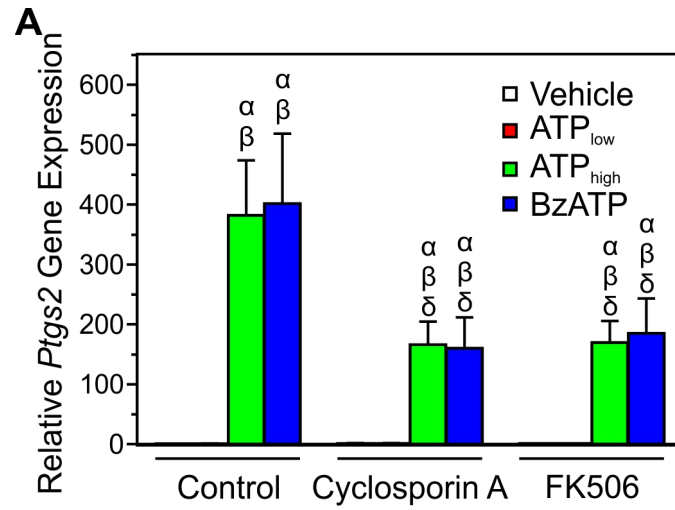
ATP<sub>high</sub> elicited dramatic increases in expression of *Ptgs2* that peaked at 3 h before returning to baseline by 6 h after treatment. In contrast, ATP<sub>low</sub> did not induce any increase in *Ptgs2* expression.

The *Ptgs2* promoter contains binding sites for many transcription factors in addition to NFAT (Kang et al., 2007). To more specifically assess changes in NFAT transcriptional activity, osteoblast-like cells were transfected with an NFAT luciferase reporter and treated with vehicle, ATP<sub>low</sub>, ATP<sub>high</sub> or BzATP (300  $\mu$ M). After 24 h, cell lysates were collected and luminescence was assessed as a measure of NFAT transcriptional activity (Figure 2.11 B). Similar to the pattern observed for *Ptgs2*, BzATP and ATP<sub>high</sub> both elicited significant increases in NFAT transcriptional activity. In contrast, ATP<sub>low</sub> did not induce any significant change compared to vehicle (Figure 2.11 B). Taken together, sustained Ca<sup>2+</sup>/NFATc1 signaling elicited by high concentrations of ATP or BzATP is associated with robust expression of NFAT target genes.

To confirm a role for the Ca<sup>2+</sup>/calcineurin pathway in regulation of NFAT transcriptional activity, changes in *Ptgs2* expression and NFAT reporter activity were examined (Figure 2.12). Osteoblast-like cells were treated with vehicle, ATP<sub>low</sub>, ATP<sub>high</sub> or BzATP (300  $\mu$ M) in the presence or absence of the calcineurin inhibitors cyclosporin A (1  $\mu$ M) or FK506 (1  $\mu$ M). Both cyclosporin A and FK506 significantly suppressed expression of *Ptgs2* induced by ATP<sub>high</sub> and BzATP (Figure 2.12 A). Moreover, in osteoblast-like cells transfected with the NFAT luciferase reporter, the effects of BzATP and ATP<sub>high</sub> were abolished by inhibition of calcineurin (Figure 2.12 B). These observations are consistent with nucleotide-induced changes in *Ptgs2* expression and NFAT reporter activity being mediated by activation of the Ca<sup>2+</sup>/calcineurin pathway.

**Figure 2.12 P2 Nucleotide Receptor-induced Changes in NFAT Transcriptional Activity are Mediated by Ca<sup>2+</sup>/Calcineurin Signaling.**

A, MC3T3-E1 cells were incubated for 30 min in the absence or presence of calcineurin inhibitors cyclosporin A (1  $\mu$ M) or FK506 (1  $\mu$ M). Next, cells were treated for 3 h with vehicle, ATP<sub>low</sub>, ATP<sub>high</sub> or BzATP in the continued absence (Control) or presence of inhibitor. Total RNA was then isolated and real-time RT-PCR was performed to assess expression levels of *Ptgs2*. Data are normalized to levels of 18S and are shown relative to values for control cultures treated with vehicle.  $\alpha$  indicates a significant difference from vehicle;  $\beta$  indicates significant difference between ATP<sub>high</sub> or BzATP and ATP<sub>low</sub>.  $\delta$  indicates significant effect of inhibitor ( $p < 0.05$ ). Data are means  $\pm$  S.E.M. ( $n = 6$  samples from 3 independent preparations). B, MC3T3-E1 cells transfected with the NFAT luciferase reporter plasmid were incubated for 30 min in the absence (Control) or presence of cyclosporin A (1  $\mu$ M) or FK506 (1  $\mu$ M). Next, cells were treated with vehicle, ATP<sub>low</sub>, ATP<sub>high</sub> or BzATP in the continued absence or presence of inhibitor. After 24 h, cell lysates were collected and luminescence was assessed. Luminescence was expressed relative to values for control cultures treated with vehicle.  $\alpha$  indicates significant difference from vehicle;  $\beta$  indicates significant difference between ATP<sub>high</sub> or BzATP and ATP<sub>low</sub> ( $p < 0.05$ ). Data are means  $\pm$  S.E.M. ( $n = 9$  samples from 3 independent preparations).



#### **2.4.7 P2X7 is Essential for Mediating Effects of High Concentrations of ATP on NFAT Transcriptional Activity**

Changes in *Ptgs2* expression and NFAT reporter activity were examined in osteoblast-like cells following treatment with vehicle, ATP<sub>low</sub>, ATP<sub>high</sub> or BzATP (300 μM) in the absence or presence of A 438079 (10 μM). A 438079 completely abolished the effects of ATP<sub>high</sub> and BzATP both on expression of *Ptgs2* (Figure 2.13 A) and on luminescence in osteoblast-like cells transfected with the NFAT luciferase reporter (Figure 2.13 B).

To confirm the involvement of P2X7 receptors, changes in *Ptgs2* expression and NFAT reporter activity were examined in primary calvarial osteoblasts isolated from P2X7 knockout and wild-type mice. Stimulation of wild-type calvarial osteoblasts with ATP<sub>high</sub> or BzATP (300 μM) induced significant expression of *Ptgs2* at 3 h, whereas ATP<sub>low</sub> had no effect (Figure 2.13 C). In contrast, ATP<sub>low</sub>, ATP<sub>high</sub> and BzATP all failed to elicit expression of *Ptgs2* in calvarial osteoblasts from knockout mice (Figure 2.13 C). Moreover, in primary calvarial osteoblasts transfected with the NFAT luciferase reporter, ATP<sub>high</sub> induced an increase in luminescence that was absent in cells from knockout mice (Figure 2.13 D)<sup>3</sup>. These observations establish that the increase in NFAT transcriptional activity and target gene expression elicited by BzATP or high concentrations of ATP is mediated by activation of the P2X7 receptor.

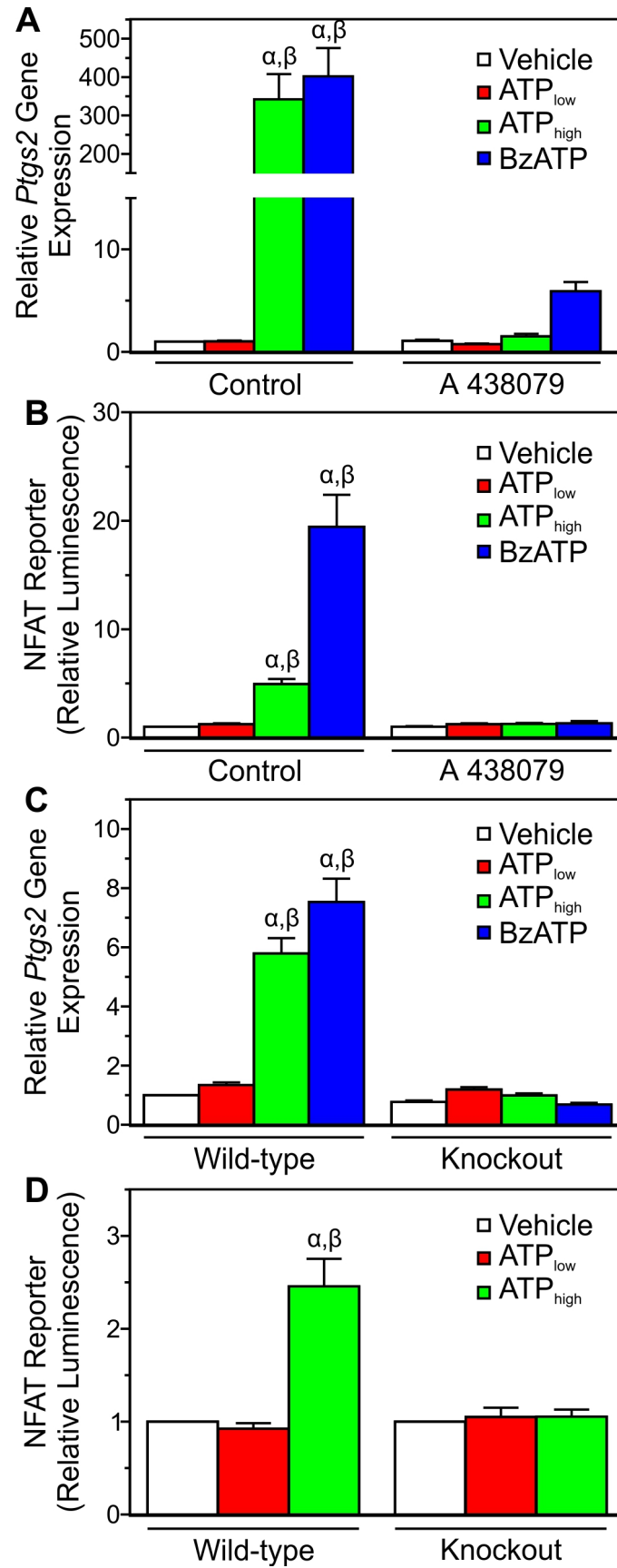
---

<sup>3</sup> In primary calvarial cell cultures from wild-type and P2X7 knockout mice, BzATP has toxic effects unrelated to P2X7 receptor signaling (unpublished observations). These effects are not observed in cultures of MC3T3-E1 cells. As a result, ATP<sub>high</sub> but not BzATP was used to activate P2X7 in experiments employing calvarial cells transfected with the NFAT reporter plasmid.



**Figure 2.13 The P2X7 Receptor is Required for Changes in NFAT Transcriptional Activity Elicited by ATP<sub>high</sub> or BzATP.**

A, MC3T3-E1 cells were incubated for 5-10 min in the absence (Control) or presence of A 438079 (10  $\mu$ M). Next, cells were treated for 3 h with vehicle, ATP<sub>low</sub> (10  $\mu$ M), ATP<sub>high</sub> (1 mM) or BzATP (300  $\mu$ M) in the continued absence or presence of antagonist. Real-time RT-PCR was performed to assess expression levels of *Ptgs2*. Data were normalized to levels of 18S and are shown relative to values for control cultures treated with vehicle. Note the expanded y-axis scale. B, MC3T3-E1 cells transfected with the NFAT luciferase reporter plasmid were incubated for 5-10 min in the absence or presence of A 438079 (10  $\mu$ M). Next, cells were treated with Vehicle, ATP<sub>low</sub>, ATP<sub>high</sub> or BzATP in the continued absence or presence of antagonist. After 24 h, cell lysates were collected and luminescence was assessed. Luminescence was expressed relative to values for control cultures treated with vehicle. For both (A) and (B),  $\alpha$  indicates significant difference from vehicle;  $\beta$  indicates significant difference between ATP<sub>high</sub> or BzATP and ATP<sub>low</sub> ( $p < 0.05$ ). Data are means  $\pm$  S.E.M. ( $n = 9$  samples from three independent preparations). C, primary osteoblasts from wild-type and P2X7 knockout mice were treated with vehicle, ATP<sub>low</sub>, ATP<sub>high</sub> or BzATP, and total RNA was isolated at 3 h. Real-time RT-PCR was performed to assess expression levels of *Ptgs2*. Data were normalized to levels of 18S and are shown relative to values for wild-type cultures treated with vehicle. D, primary osteoblasts were transfected with an NFAT luciferase reporter plasmid and treated with vehicle, ATP<sub>low</sub> or ATP<sub>high</sub>. After 24 h, cell lysates were collected and luminescence was assessed. Luminescence was expressed relative to values for wild-type cultures treated with vehicle. For both (C) and (D),  $\alpha$  indicates significant difference from vehicle within the same genotype;  $\beta$  indicates significant difference between ATP<sub>high</sub> or BzATP and ATP<sub>low</sub> within the same genotype ( $p < 0.05$ ). Data are means  $\pm$  S.E.M. ( $n = 9-12$  samples from 3-4 independent preparations).



## 2.5 Discussion

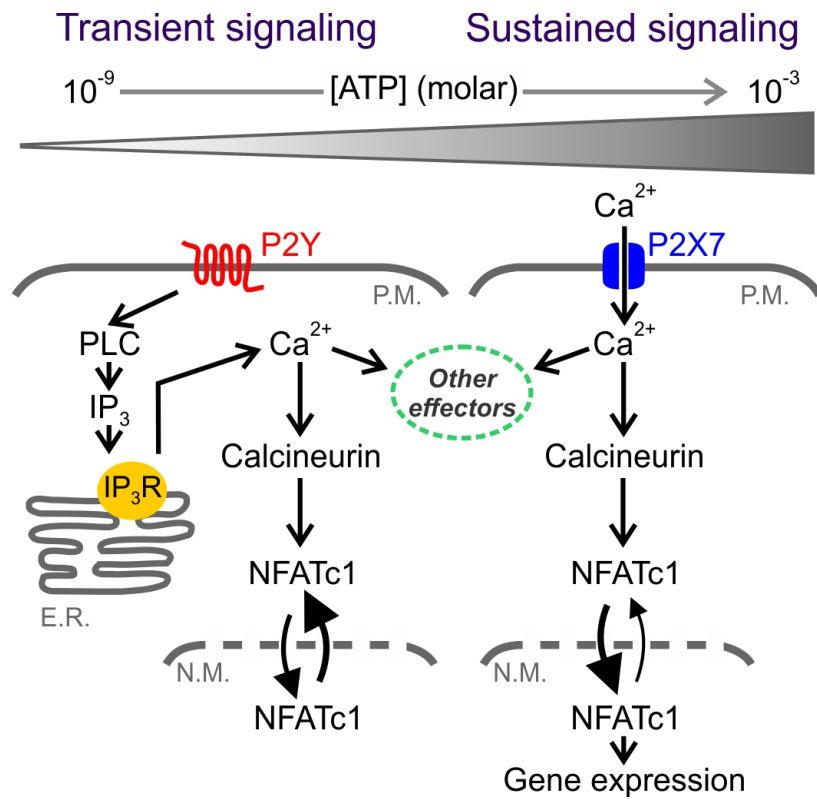
In this study, we examined ATP-induced  $\text{Ca}^{2+}$ /NFAT signaling through a network of endogenously expressed P2 nucleotide receptors. We show that ensembles of P2Y and P2X receptor subtypes impart sensitivity over a wide range of ATP concentrations, and provide a mechanism by which cells transduce ATP levels into distinct cellular signals (Figure 2.14). Specifically, low concentrations of ATP act through P2Y receptors to elicit transient  $\text{Ca}^{2+}$ /NFAT signaling; whereas, high ATP concentrations act through P2X7 to induce more sustained  $\text{Ca}^{2+}$ /NFAT signaling that culminates in robust target gene expression. These findings demonstrate that the  $\text{Ca}^{2+}$ /NFAT pathway functions in dose-to-duration encoding of P2 receptor stimuli.

### 2.5.1 P2 Receptor Networks Impart Sensitivity over a Wide Dynamic Range of ATP Concentrations

Previous studies examining the characteristics of individual P2Y and P2X receptor subtypes have demonstrated that each exhibits distinct affinities for purine and pyrimidine nucleotides. Of the P2 receptor subtypes sensitive to ATP, P2Y<sub>2</sub>, P2X<sub>1</sub>, P2X<sub>3</sub> and P2X<sub>5</sub> have the highest affinities, with responses seen at relatively low ATP concentrations (<1  $\mu\text{M}$ ); in contrast, P2X<sub>7</sub> has the lowest affinity with activation occurring at much higher concentrations of ATP (Ralevic and Burnstock, 1998). Though informative, many of these earlier studies used heterologous expression to characterize individual P2 receptor subtypes. However, expression of a single P2Y or P2X subtype does not recapitulate responses mediated by a network of P2 receptors. Moreover, overexpression of a single receptor could perturb interactions among endogenous P2 receptors, such as P2Y

**Figure 2.14 Proposed Role for the P2 nucleotide Receptor Network in ‘Dose-to-Duration’ Encoding of  $\text{Ca}^{2+}$ /NFATc1 Signaling.**

Expression of multiple P2 receptor subtypes provides a novel mechanism by which cells can sense ATP over a million-fold concentration range, and transduce these inputs into distinct cellular signals. Stimulation of one or more P2Y receptor subtypes by low ATP concentrations leads to activation of phospholipase C (PLC) and subsequent formation of inositol 1,4,5-trisphosphate ( $\text{IP}_3$ ).  $\text{IP}_3$  binds the  $\text{IP}_3$  receptor ( $\text{IP}_3\text{R}$ ) on the membrane of the endoplasmic reticulum (E.R.), resulting in transient release of  $\text{Ca}^{2+}$ . This transient elevation of  $[\text{Ca}^{2+}]_i$  causes brief NFATc1 nuclear localization, but fails to elicit expression of NFAT target genes (*left*). In contrast, activation of the P2X7 receptor by high ATP concentrations triggers sustained influx of  $\text{Ca}^{2+}$  and prolonged NFATc1 nuclear localization, resulting in robust NFAT target gene expression (*right*). Although transient elevation of  $[\text{Ca}^{2+}]_i$  does not induce NFAT target gene expression, it activates other effectors that regulate important functions such as cytoskeletal remodeling, cell motility and secretion. P.M. stands for plasma membrane; N.M. stands for nuclear membrane.



dimerization and the formation of heteromeric P2X receptors. Thus, results of these earlier studies may not represent the physiological behavior of P2 receptor networks. For these reasons, we examined concentration-dependent responses to ATP mediated by a network of P2 receptors endogenously expressed in osteoblasts.

Characterization of the concentration dependence of ATP-induced  $\text{Ca}^{2+}$  signaling in osteoblasts revealed, for the first time in any system, that graded increases in the  $\text{Ca}^{2+}$  response could be achieved over a remarkably broad range of ATP concentrations (1 nM to 1 mM). The physiological effects of many other intercellular messengers are also mediated by multiple receptor subtypes. However, few if any of these receptor families exhibit as wide a range of affinities as those observed for ATP in the purinergic system. For instance, prostaglandin  $\text{E}_2$  ( $\text{PGE}_2$ ) acts through four G protein-coupled receptors (EP1–4), which exhibit an ~100-fold range in  $\text{EC}_{50}$  for  $\text{PGE}_2$  (Abramovitz et al., 2000; Hata and Breyer, 2004). LPA, another lipid mediator, acts through at least five G protein-coupled receptors, LPA1-5, with a similar 100-fold range in  $\text{EC}_{50}$  (Bandoh et al., 2000; Anliker and Chun, 2004; Lee et al., 2006). On the other hand, the excitatory neurotransmitter L-glutamate, which like ATP signals through families of metabotropic and ionotropic receptors, elicits responses at low and high concentrations of L-glutamate (Conn and Pin, 1997; Traynelis et al., 2010). However, it has not been reported that L-glutamate can induce graded, dose-dependent increases in the amplitude or duration of a common intracellular signal. Nevertheless, given its similarities to the purinergic system, the principles described in the present study for ATP signaling may also be applicable to the glutaminergic system.

### **2.5.2 P2 Receptor Networks Enable Dose-to-Duration Encoding of Ca<sup>2+</sup>/NFAT Signaling**

In addition to relaying qualitative information about the presence or absence of a stimulus, receptors and their associated signaling pathways must also transmit quantitative information about stimulus intensity. “Dose-to-duration” encoding refers to the process by which information about the concentration of a stimulus is transduced as duration of the signal, permitting distinct cellular responses to different agonist concentrations (Behar et al., 2008). In yeast, the switch from proliferation to differentiation and/or mating is dependent both on pheromone concentration and the duration of downstream mitogen-activated protein kinase (MAPK) activity. Behar et al. (2008) proposed a model in which negative feedback regulation of the yeast pheromone receptor causes dose-dependent decreases in its affinity for ligand to allow for signaling beyond initial saturation.

As opposed to regulating the affinity of a single receptor, we describe a novel mechanism for dose-to-duration encoding in which the presence of multiple P2Y and P2X receptors, with different affinities for ATP, determine the duration of Ca<sup>2+</sup>/NFATc1 signaling. We demonstrated that low concentrations of ATP (1 nM to 100 μM) induce transient Ca<sup>2+</sup> elevation and NFATc1 activation, whereas higher ATP concentrations (300 μM to 10 mM) elicit more sustained Ca<sup>2+</sup>/NFATc1 signaling.

Ca<sup>2+</sup> signaling is a central mechanism by which P2 receptors elicit changes in cell behaviour in response to extracellular nucleotides. A number of groups have shown that ATP and other nucleotides can elicit transient or sustained Ca<sup>2+</sup> signals in a variety of other cell-types (Oshimi et al., 1999; Moller et al., 2000; Nobile et al., 2003; Korcok et

al., 2004). The role of the  $\text{Ca}^{2+}$ -regulated NFAT transcription factors in P2 receptor signaling has also been examined previously (Ferrari et al., 1999; Abbott et al., 2000; Kataoka et al., 2009; Shiratori et al., 2010). However, no previous studies have employed a concentration range capable of revealing the relationship between ATP dose and  $\text{Ca}^{2+}$ /NFAT signal duration described in the present study. Moreover, we provide the first evidence demonstrating that P2 receptors utilize the duration of  $\text{Ca}^{2+}$ /NFAT signaling to elicit distinct responses to different concentrations of extracellular ATP.

In general, signal duration can control distinct cell functions in a variety of biological systems. In the neuronal PC12 cell line, transient activation of extracellular signal-regulated kinase (ERK) by epidermal growth factor stimulates proliferation; whereas prolonged ERK activation, elicited by nerve growth factor, promotes differentiation (Vaudry et al., 2002). Similarly, in yeast, vegetative growth patterns are mediated by transient MAPK signaling at low pheromone levels; whereas, growth arrest and mating are initiated by sustained MAPK signaling in response to high levels of pheromone (Dohlman and Thorner, 2001). In the present study, we found that transient  $\text{Ca}^{2+}$ /NFAT signaling elicited by low concentrations of ATP resulted in no measureable increase in NFAT transcriptional activity. Nevertheless, these  $\text{Ca}^{2+}$  transients regulate other important aspects of osteoblast function. For example, such  $\text{Ca}^{2+}$  events activate ion channels, regulate cytoskeletal remodeling and stimulate secretion in other cell-types (Berridge, 2012). In this regard, low concentrations of ATP have been reported to induce functional changes in cells of the osteoblast lineage. For instance, stimulation of P2 receptors with micromolar concentrations of ATP increases the proliferation of osteoblasts and osteoblast-like cells (Nakamura et al., 2000; Katz et al., 2011). In



addition, micromolar concentrations of ATP and UTP activate the osteoblast master transcription factor runt-related transcription factor 2 (RUNX2) in the osteoblast-like HOBIT cell line (Costessi et al., 2005). In addition to these previously reported effects of low ATP concentrations, we found that high concentrations of ATP elicited sustained  $\text{Ca}^{2+}$ /NFATc1 signaling to stimulate NFAT transcriptional activity. Thus, we demonstrate that different ATP concentrations are transduced into distinct cellular signals.

### **2.5.3 Potential Physiological Roles of P2 Receptor Networks in Osteoblasts**

Mechanotransduction, the process by which mechanical stimuli are translated into cellular responses, has been suggested to be mediated by nucleotide release and subsequent P2 receptor signaling in bone (Dixon and Sims, 2000; Robling et al., 2006). Phenotypic examination of knockout mouse strains for various P2Y and P2X receptor subtypes has indeed revealed a number of skeletal phenotypes, helping to solidify the importance of purinergic signaling in bone. Whole-body deletion of P2Y<sub>6</sub>, P2Y<sub>12</sub> or P2Y<sub>13</sub> results in decreased bone resorption, and loss of P2Y<sub>13</sub> leads to decreased bone formation (Orriss et al., 2011a; Orriss et al., 2011b; Su et al., 2012; Wang et al., 2012). Furthermore, genetically modified mice carrying a non-functional P2X7 receptor exhibit diminished periosteal bone formation, excessive trabecular bone resorption, and impaired skeletal responses to mechanical loading (Ke et al., 2003; Li et al., 2005). The findings of the present study provide the first evidence that expression of multiple P2 receptor subtypes increases the range over which differences in ATP concentration can be sensed by a cell. This phenomenon provides a novel mechanism by which osteoblasts may transduce differences in ATP concentration and, therefore, intensity of mechanical stimuli

over a remarkably wide dynamic range.

We also demonstrate for the first time that P2X7 receptors couple to the  $\text{Ca}^{2+}$ /NFATc1 pathway in osteoblasts. Our lab has previously demonstrated that activation of P2X7 receptors by exogenous nucleotides leads to production of LPA and  $\text{PGE}_2$  by osteoblasts, culminating in enhanced differentiation and matrix mineralization (Panupinthu et al., 2008). The  $\text{Ca}^{2+}$ /NFATc1 pathway also plays an important role in the regulation of osteoblast differentiation (Koga et al., 2005; Winslow et al., 2006), but until now the pathways underlying NFATc1 activation in osteoblasts have remained obscure. In the present study, we found that  $\text{Ca}^{2+}$ /NFATc1 signaling stimulates expression of COX-2 downstream of the P2X7 receptor in osteoblasts. Given the important role of COX-2 and  $\text{PGE}_2$  in osteoblast differentiation and responses to mechanical stimuli (Blackwell et al., 2010), we propose that the  $\text{Ca}^{2+}$ /NFATc1 axis may play an important role in mediating P2X7 receptor signaling during skeletal development and mechanotransduction.

The ability of ATP to elicit distinct responses over a wide dynamic range of concentrations, as described for osteoblasts in the present study, may also occur in other cell-types, many of which express multiple subtypes of P2 receptors. In this regard, greatly varying amounts of ATP are released into the extracellular fluid under different circumstances – smaller amounts during neurotransmission and paracrine signaling, and massive amounts in response to trauma and cell lysis (Burnstock, 2007b). The presence of an ensemble of P2 receptors would allow osteoblasts and other cell-types to respond appropriately in each of these different situations.

## 2.6 References

- Abbott, K.L., J.R. Loss, 2nd, A.M. Robida, and T.J. Murphy. 2000. Evidence that Galpha(q)-coupled receptor-induced interleukin-6 mRNA in vascular smooth muscle cells involves the nuclear factor of activated T cells. *Mol Pharmacol.* 58:946-953.
- Abbracchio, M.P., G. Burnstock, J.M. Boeynaems, E.A. Barnard, J.L. Boyer, C. Kennedy, G.E. Knight, M. Fumagalli, C. Gachet, K.A. Jacobson, and G.A. Weisman. 2006. International Union of Pharmacology LVIII: update on the P2Y G protein-coupled nucleotide receptors: from molecular mechanisms and pathophysiology to therapy. *Pharmacol Rev.* 58:281-341.
- Abramovitz, M., M. Adam, Y. Boie, M. Carriere, D. Denis, C. Godbout, S. Lamontagne, C. Rochette, N. Sawyer, N.M. Tremblay, M. Belley, M. Gallant, C. Dufresne, Y. Gareau, R. Ruel, H. Juteau, M. Labelle, N. Ouimet, and K.M. Metters. 2000. The utilization of recombinant prostanoid receptors to determine the affinities and selectivities of prostaglandins and related analogs. *Biochim Biophys Acta.* 1483:285-293.
- Anliker, B., and J. Chun. 2004. Lysophospholipid G protein-coupled receptors. *J Biol Chem.* 279:20555-20558.
- Bandoh, K., J. Aoki, A. Taira, M. Tsujimoto, H. Arai, and K. Inoue. 2000. Lysophosphatidic acid (LPA) receptors of the EDG family are differentially activated by LPA species. Structure-activity relationship of cloned LPA receptors. *FEBS Lett.* 478:159-165.
- Behar, M., N. Hao, H.G. Dohlman, and T.C. Elston. 2008. Dose-to-duration encoding and signaling beyond saturation in intracellular signaling networks. *PLoS Comput Biol.* 4:e1000197.
- Berridge, M.J. 2012. Calcium signalling remodelling and disease. *Biochem Soc Trans.* 40:297-309.
- Blackwell, K.A., L.G. Raisz, and C.C. Pilbeam. 2010. Prostaglandins in bone: bad cop, good cop? *Trends Endocrinol Metab.* 21:294-301.
- Bowler, W.B., K.A. Buckley, A. Gartland, R.A. Hipskind, G. Bilbe, and J.A. Gallagher. 2001. Extracellular nucleotide signaling: a mechanism for integrating local and systemic responses in the activation of bone remodeling. *Bone.* 28:507-512.
- Bowler, W.B., C.J. Dixon, C. Halleux, R. Maier, G. Bilbe, W.D. Fraser, J.A. Gallagher, and R.A. Hipskind. 1999. Signaling in human osteoblasts by extracellular nucleotides. Their weak induction of the c-fos proto-oncogene via Ca<sup>2+</sup> mobilization is strongly potentiated by a parathyroid hormone/cAMP-dependent

- protein kinase pathway independently of mitogen-activated protein kinase. *J Biol Chem.* 274:14315-14324.
- Browne, L.E., L.H. Jiang, and R.A. North. 2010. New structure enlivens interest in P2X receptors. *Trends Pharmacol Sci.* 31:229-237.
- Burnstock, G. 2007a. Physiology and pathophysiology of purinergic neurotransmission. *Physiol Rev.* 87:659-797.
- Burnstock, G. 2007b. Purine and pyrimidine receptors. *Cell Mol Life Sci.* 64:1471-1483.
- Burnstock, G., and A. Verkhratsky. 2009. Evolutionary origins of the purinergic signalling system. *Acta Physiol (Oxf).* 195:415-447.
- Burnstock, G., and A. Verkhratsky. 2010. Long-term (trophic) purinergic signalling: purinoceptors control cell proliferation, differentiation and death. *Cell Death Dis.* 1:e9.
- Clipstone, N.A., and G.R. Crabtree. 1992. Identification of calcineurin as a key signalling enzyme in T-lymphocyte activation. *Nature.* 357:695-697.
- Conn, P.J., and J.P. Pin. 1997. Pharmacology and functions of metabotropic glutamate receptors. *Annu Rev Pharmacol Toxicol.* 37:205-237.
- Costessi, A., A. Pines, P. D'Andrea, M. Romanello, G. Damante, L. Cesaratto, F. Quadrifoglio, L. Moro, and G. Tell. 2005. Extracellular nucleotides activate Runx2 in the osteoblast-like HOBIT cell line: a possible molecular link between mechanical stress and osteoblasts' response. *Bone.* 36:418-432.
- Crabtree, G.R., and E.N. Olson. 2002. NFAT signaling: choreographing the social lives of cells. *Cell.* 109 Suppl:S67-79.
- Dixon, S.J., and S.M. Sims. 2000. P2 purinergic receptors on osteoblasts and osteoclasts: Potential targets for drug development. *Drug Dev Res.* 49:187-200.
- Dohlman, H.G., and J.W. Thorner. 2001. Regulation of G protein-initiated signal transduction in yeast: paradigms and principles. *Annu Rev Biochem.* 70:703-754.
- Donnelly-Roberts, D.L., and M.F. Jarvis. 2007. Discovery of P2X7 receptor-selective antagonists offers new insights into P2X7 receptor function and indicates a role in chronic pain states. *Br J Pharmacol.* 151:571-579.
- Ferrari, D., C. Stroh, and K. Schulze-Osthoff. 1999. P2X7/P2Z purinoreceptor-mediated activation of transcription factor NFAT in microglial cells. *J Biol Chem.* 274:13205-13210.

- Grol, M.W., I. Zelner, and S.J. Dixon. 2012. P2X(7)-mediated calcium influx triggers a sustained, PI3K-dependent increase in metabolic acid production by osteoblast-like cells. *Am J Physiol Endocrinol Metab.* 302:E561-575.
- Hata, A.N., and R.M. Breyer. 2004. Pharmacology and signaling of prostaglandin receptors: multiple roles in inflammation and immune modulation. *Pharmacol Ther.* 103:147-166.
- Hoebertz, A., S. Mahendran, G. Burnstock, and T.R. Arnett. 2002. ATP and UTP at low concentrations strongly inhibit bone formation by osteoblasts: a novel role for the P2Y2 receptor in bone remodeling. *J Cell Biochem.* 86:413-419.
- Hogan, P.G., L. Chen, J. Nardone, and A. Rao. 2003. Transcriptional regulation by calcium, calcineurin, and NFAT. *Genes Dev.* 17:2205-2232.
- Kang, Y.J., U.R. Mbonye, C.J. DeLong, M. Wada, and W.L. Smith. 2007. Regulation of intracellular cyclooxygenase levels by gene transcription and protein degradation. *Prog Lipid Res.* 46:108-125.
- Kataoka, A., H. Tozaki-Saitoh, Y. Koga, M. Tsuda, and K. Inoue. 2009. Activation of P2X7 receptors induces CCL3 production in microglial cells through transcription factor NFAT. *J Neurochem.* 108:115-125.
- Katz, S., V. Ayala, G. Santillan, and R. Boland. 2011. Activation of the PI3K/Akt signaling pathway through P2Y(2) receptors by extracellular ATP is involved in osteoblastic cell proliferation. *Arch Biochem Biophys.* 513:144-152.
- Ke, H.Z., H. Qi, A.F. Weidema, Q. Zhang, N. Panupinthu, D.T. Crawford, W.A. Grasser, V.M. Paralkar, M. Li, L.P. Audoly, C.A. Gabel, W.S. Jee, S.J. Dixon, S.M. Sims, and D.D. Thompson. 2003. Deletion of the P2X<sub>7</sub> nucleotide receptor reveals its regulatory roles in bone formation and resorption. *Mol Endocrinol.* 17:1356-1367.
- Khakh, B.S., and R.A. North. 2006. P2X receptors as cell-surface ATP sensors in health and disease. *Nature.* 442:527-532.
- Koga, T., Y. Matsui, M. Asagiri, T. Kodama, B. de Crombrughe, K. Nakashima, and H. Takayanagi. 2005. NFAT and Osterix cooperatively regulate bone formation. *Nat Med.* 11:880-885.
- Korcok, J., L.N. Raimundo, H.Z. Ke, S.M. Sims, and S.J. Dixon. 2004. Extracellular nucleotides act through P2X7 receptors to activate NF- $\kappa$ B in osteoclasts. *J Bone Miner Res.* 19:642-651.
- Lee, C.W., R. Rivera, S. Gardell, A.E. Dubin, and J. Chun. 2006. GPR92 as a new G12/13- and Gq-coupled lysophosphatidic acid receptor that increases cAMP, LPA5. *J Biol Chem.* 281:23589-23597.

- Li, J., D. Liu, H.Z. Ke, R.L. Duncan, and C.H. Turner. 2005. The P2X<sub>7</sub> nucleotide receptor mediates skeletal mechanotransduction. *J Biol Chem.* 280:42952-42959.
- Masin, M., C. Young, K. Lim, S.J. Barnes, X.J. Xu, V. Marschall, W. Brutkowski, E.R. Mooney, D.C. Gorecki, and R. Murrell-Lagnado. 2012. Expression, assembly and function of novel C-terminal truncated variants of the mouse P2X<sub>7</sub> receptor: re-evaluation of P2X<sub>7</sub> knockouts. *Br J Pharmacol.* 165:978-993.
- Moller, T., O. Kann, A. Verkhratsky, and H. Kettenmann. 2000. Activation of mouse microglial cells affects P2 receptor signaling. *Brain Res.* 853:49-59.
- Moore, D.L., and J.L. Goldberg. 2011. Multiple transcription factor families regulate axon growth and regeneration. *Dev Neurobiol.* 71:1186-1211.
- Nakamura, E., Y. Uezono, K. Narusawa, I. Shibuya, Y. Oishi, M. Tanaka, N. Yanagihara, T. Nakamura, and F. Izumi. 2000. ATP activates DNA synthesis by acting on P2X receptors in human osteoblast-like MG-63 cells. *Am J Physiol Cell Physiol.* 279:C510-519.
- Nelson, D.W., R.J. Gregg, M.E. Kort, A. Perez-Medrano, E.A. Voight, Y. Wang, G. Grayson, M.T. Namovic, D.L. Donnelly-Roberts, W. Niforatos, P. Honore, M.F. Jarvis, C.R. Faltynek, and W.A. Carroll. 2006. Structure-activity relationship studies on a series of novel, substituted 1-benzyl-5-phenyltetrazole P2X<sub>7</sub> antagonists. *J Med Chem.* 49:3659-3666.
- Nobile, M., I. Monaldi, S. Alloisio, C. Cugnoli, and S. Ferroni. 2003. ATP-induced, sustained calcium signalling in cultured rat cortical astrocytes: evidence for a non-capacitative, P2X<sub>7</sub>-like-mediated calcium entry. *FEBS Lett.* 538:71-76.
- North, R.A. 2002. Molecular physiology of P2X receptors. *Physiol Rev.* 82:1013-1067.
- Okumura, H., D. Shiba, T. Kubo, and T. Yokoyama. 2008. P2X<sub>7</sub> receptor as sensitive flow sensor for ERK activation in osteoblasts. *Biochem Biophys Res Commun.* 372:486-490.
- Orriss, I., S. Syberg, N. Wang, B. Robaye, A. Gartland, N. Jorgensen, T. Arnett, and J.M. Boeynaems. 2011a. Bone phenotypes of P2 receptor knockout mice. *Front Biosci (Schol Ed).* 3:1038-1046.
- Orriss, I.R., G. Burnstock, and T.R. Arnett. 2010. Purinergic signalling and bone remodelling. *Curr Opin Pharmacol.* 10:322-330.
- Orriss, I.R., M.L. Key, A. Brandao-Burch, J.J. Patel, G. Burnstock, and T.R. Arnett. 2012. The regulation of osteoblast function and bone mineralisation by extracellular nucleotides: The role of p2x receptors. *Bone.*

- Orriss, I.R., J.C. Utting, A. Brandao-Burch, K. Colston, B.R. Grubb, G. Burnstock, and T.R. Arnett. 2007. Extracellular nucleotides block bone mineralization in vitro: evidence for dual inhibitory mechanisms involving both P2Y2 receptors and pyrophosphate. *Endocrinology*. 148:4208-4216.
- Orriss, I.R., N. Wang, G. Burnstock, T.R. Arnett, A. Gartland, B. Robaye, and J.M. Boeynaems. 2011b. The P2Y(6) receptor stimulates bone resorption by osteoclasts. *Endocrinology*. 152:3706-3716.
- Oshimi, Y., S. Miyazaki, and S. Oda. 1999. ATP-induced  $Ca^{2+}$  response mediated by P2U and P2Y purinoceptors in human macrophages: signalling from dying cells to macrophages. *Immunology*. 98:220-227.
- Panupinthu, N., J.T. Rogers, L. Zhao, L.P. Solano-Flores, F. Possmayer, S.M. Sims, and S.J. Dixon. 2008. P2X7 receptors on osteoblasts couple to production of lysophosphatidic acid: a signaling axis promoting osteogenesis. *J Cell Biol*. 181:859-871.
- Panupinthu, N., L. Zhao, F. Possmayer, H.Z. Ke, S.M. Sims, and S.J. Dixon. 2007. P2X7 nucleotide receptors mediate blebbing in osteoblasts through a pathway involving lysophosphatidic acid. *J Biol Chem*. 282:3403-3412.
- Qi, J., L. Chi, J. Faber, B. Koller, and A.J. Banes. 2007. ATP reduces gel compaction in osteoblast-populated collagen gels. *J Appl Physiol*. 102:1152-1160.
- Ralevic, V., and G. Burnstock. 1998. Receptors for purines and pyrimidines. *Pharmacol Rev*. 50:413-492.
- Robling, A.G., A.B. Castillo, and C.H. Turner. 2006. Biomechanical and molecular regulation of bone remodeling. *Annu Rev Biomed Eng*. 8:455-498.
- Shiratori, M., H. Tozaki-Saitoh, M. Yoshitake, M. Tsuda, and K. Inoue. 2010. P2X7 receptor activation induces CXCL2 production in microglia through NFAT and PKC/MAPK pathways. *J Neurochem*. 114:810-819.
- Sitara, D., and A.O. Aliprantis. 2010. Transcriptional regulation of bone and joint remodeling by NFAT. *Immunol Rev*. 233:286-300.
- Solle, M., J. Labasi, D.G. Perregaux, E. Stam, N. Petrushova, B.H. Koller, R.J. Griffiths, and C.A. Gabel. 2001. Altered cytokine production in mice lacking P2X7 receptors. *J Biol Chem*. 276:125-132.
- Su, X., D.H. Floyd, A. Hughes, J. Xiang, J.G. Schneider, O. Uluckan, E. Heller, H. Deng, W. Zou, C.S. Craft, K. Wu, A.C. Hirbe, D. Grabowska, M.C. Eagleton, S. Townsley, L. Collins, D. Piwnica-Worms, T.H. Steinberg, D.V. Novack, P.B. Conley, M.A. Hurchla, M. Rogers, and K.N. Weilbaecher. 2012. The ADP

- receptor P2RY12 regulates osteoclast function and pathologic bone remodeling. *J Clin Invest.*
- Sudo, H., H.A. Kodama, Y. Amagai, S. Yamamoto, and S. Kasai. 1983. In vitro differentiation and calcification in a new clonal osteogenic cell line derived from newborn mouse calvaria. *J Cell Biol.* 96:191-198.
- Syberg, S., A. Brandao-Burch, J.J. Patel, M. Hajjawi, T.R. Arnett, P. Schwarz, N.R. Jorgensen, and I.R. Orriss. 2012. Clopidogrel (Plavix(R)), a P2Y(12) receptor antagonist, inhibits bone cell function in vitro and decreases trabecular bone in vivo. *J Bone Miner Res.*
- Traynelis, S.F., L.P. Wollmuth, C.J. McBain, F.S. Menniti, K.M. Vance, K.K. Ogden, K.B. Hansen, H. Yuan, S.J. Myers, and R. Dingledine. 2010. Glutamate receptor ion channels: structure, regulation, and function. *Pharmacol Rev.* 62:405-496.
- Vaudry, D., P.J. Stork, P. Lazarovici, and L.E. Eiden. 2002. Signaling pathways for PC12 cell differentiation: making the right connections. *Science.* 296:1648-1649.
- Volonte, C., S. Amadio, N. D'Ambrosi, M. Colpi, and G. Burnstock. 2006. P2 receptor web: complexity and fine-tuning. *Pharmacol Ther.* 112:264-280.
- Wang, D., K. Christensen, K. Chawla, G. Xiao, P.H. Krebsbach, and R.T. Franceschi. 1999. Isolation and characterization of MC3T3-E1 preosteoblast subclones with distinct in vitro and in vivo differentiation/mineralization potential. *J Bone Miner Res.* 14:893-903.
- Wang, N., B. Robaye, A. Agrawal, T.M. Skerry, J.M. Boeynaems, and A. Gartland. 2012. Reduced bone turnover in mice lacking the P2Y(13) receptor of ADP. *Mol Endocrinol.* 26:142-152.
- Winslow, M.M., M. Pan, M. Starbuck, E.M. Gallo, L. Deng, G. Karsenty, and G.R. Crabtree. 2006. Calcineurin/NFAT signaling in osteoblasts regulates bone mass. *Dev Cell.* 10:771-782.



## CHAPTER THREE

### **P2X7-MEDIATED CALCIUM INFLUX TRIGGERS A SUSTAINED, PI3K-DEPENDENT INCREASE IN METABOLIC ACID PRODUCTION BY OSTEOBLAST-LIKE CELLS<sup>1</sup>**

---

<sup>1</sup> This Chapter has been reproduced with permission from:

Grol, M.W., I. Zelner, and S.J. Dixon. 2012. P2X7-mediated calcium influx triggers a sustained, PI3K-dependent increase in metabolic acid production by osteoblast-like cells. *Am. J. Physiol. Endocrinol. Metab.* 302:E561-E575, with some modifications.

### 3.1 Chapter Summary

The P2X7 receptor is an ATP-gated cation channel expressed by a number of cell-types including osteoblasts. Genetically modified mice with loss of P2X7 function exhibit altered bone formation. Moreover, activation of P2X7 *in vitro* stimulates osteoblast differentiation and matrix mineralization, though underlying mechanisms remain unclear. As osteogenesis is associated with enhanced cellular metabolism, our goal was to characterize the effects of nucleotides on metabolic acid production (proton efflux) by osteoblasts. The P2X7 agonist BzATP (300  $\mu$ M) induced dynamic membrane blebbing in MC3T3-E1 osteoblast-like cells (consistent with activation of P2X7 receptors), but did not induce cell death. Using a Cytosensor microphysiometer, we found that 9-min exposure to BzATP (300  $\mu$ M) caused a dramatic increase in proton efflux from MC3T3-E1 cells (~2-fold), which was sustained for at least 1 h. In contrast, ATP or UTP (100  $\mu$ M), which activate P2 receptors other than P2X7, failed to elicit a sustained increase in proton efflux. Specific P2X7 receptor antagonists, A 438079 and A 740003, inhibited the sustained phase of the BzATP-induced response. Extracellular  $\text{Ca}^{2+}$  was required during P2X7 receptor stimulation for initiation of sustained proton efflux; and removal of extracellular glucose within the sustained phase abolished the elevation elicited by BzATP. In addition, inhibition of phosphatidylinositol-3-kinase blocked the maintenance, but not initiation of the sustained phase. Taken together, we conclude that brief activation of P2X7 receptors on osteoblast-like cells triggers a dramatic,  $\text{Ca}^{2+}$ -dependent stimulation of metabolic acid production. This increase in proton efflux is sustained, and dependent on glucose and phosphatidylinositol-3-kinase activity.

### 3.2 Introduction

Bone remodeling is a dynamic process that relies on a delicate balance between formation and resorption by osteoblasts and osteoclasts, respectively. A combination of local and systemic factors, including parathyroid hormone (PTH), insulin-like growth factors (IGFs), estrogen and bone morphogenetic proteins (BMPs), act in concert with mechanical stimuli to modulate skeletal homeostasis (Harada and Rodan, 2003). Mechanical load enhances bone formation resulting in improved skeletal strength (Robling et al., 2006). Osteoblasts release adenosine 5'-triphosphate (ATP) and other nucleotides in response to mechanical stimuli (Genetos et al., 2005; Li et al., 2005), and it has been suggested that these molecules mediate mechanotransduction in bone (Dixon and Sims, 2000).

Extracellular nucleotides signal through P2 receptors expressed in a variety of cell-types, including osteoblasts and osteoclasts. These receptors are divided into two families – the P2Y family of G protein-coupled receptors and the P2X family of ligand-gated cation channels (Khakh and North, 2006; Burnstock, 2007). Currently, eight P2Y subtypes (P2Y<sub>1, 2, 4, 6, 11-14</sub>) and seven subtypes of P2X (P2X<sub>1-7</sub>) have been identified in mammals. The metabotropic P2Y receptors possess an extracellular NH<sub>2</sub>-terminus, an intracellular COOH-terminus, and seven transmembrane domains, and signal through heterotrimeric G proteins (Burnstock, 2007). In contrast, ionotropic P2X receptor subunits are composed of two transmembrane domains, a large N-glycosylated extracellular loop, and intracellular NH<sub>2</sub>- and COOH-termini. Functional channels, composed of homo- or heteromultimers of three P2X subunits (Khakh and North, 2006), are permeable to cations, resulting in membrane depolarization and, in many cases, Ca<sup>2+</sup>

influx upon receptor activation. Unlike P2Y family members that are activated by adenine or uracil nucleotides, or both, P2X receptors are activated solely by adenine nucleotides (Burnstock, 2007).

Relative to other P2X family members, the P2X7 receptor is unique in that i) it is activated only by relatively high concentrations of extracellular ATP (>100  $\mu$ M); ii) it possesses an extended intracellular COOH-terminus, containing putative interaction domains for structural and signaling proteins (Kim et al., 2001); and iii) it causes dynamic blebbing of the plasma membrane in numerous cell-types (Qu and Dubyak, 2009). The P2X7 receptor is expressed in cells of the osteoblast lineage (Gartland et al., 2001; Grol et al., 2009) together with other P2X and P2Y subtypes (Dixon and Sims, 2000; Orriss et al., 2010). Ke *et al.* (2003) demonstrated that genetically modified mice, in which P2X7 function is disrupted, exhibit diminished periosteal bone formation and excessive trabecular bone resorption. Moreover, Li *et al.* (2005) found that these same mice also exhibit impaired skeletal responses to mechanical load, implicating P2X7 in mechanotransduction *in vivo*. Interestingly, other investigators have described a distinct skeletal phenotype in a second mouse model in which P2X7 expression is disrupted (Gartland et al., 2003). However, recent studies have revealed this second model to be an inadvertent tissue-specific knockout (Nicke et al., 2009; Taylor et al., 2009), in which the presence or absence of P2X7 in osteoblasts has yet to be determined. In keeping with the phenotype of the first mouse model (Ke et al., 2003), our lab has shown that activation of P2X7 receptors by exogenous nucleotides couples to production of the potent lipid mediator lysophosphatidic acid (LPA) in cells of the osteoblast lineage, resulting in dynamic membrane blebbing and enhanced osteogenesis (Panupinthu et al., 2007;

Panupinthu et al., 2008). However, many of the signaling pathways and downstream effects of P2X7 activation in osteoblasts remain to be elucidated.

Numerous metabolic demands are placed on osteoblasts during differentiation, and in the production and mineralization of osteoid. In this regard, osteoblast differentiation is associated with a striking increase in cellular metabolism (Komarova et al., 2000; Chen et al., 2008). Whereas osteoblast progenitors rely primarily on glycolytic metabolism, induction of osteoblast differentiation leads to increases in aerobic respiration and ATP production (Komarova et al., 2000). In addition, differentiated osteoblasts possess an increased number of mitochondria with hyperpolarized transmembrane potentials, indicative of enhanced mitochondrial activity (Komarova et al., 2000; Chen et al., 2008). Heterologous expression of P2X7 in HEK293 and HeLa cells hyperpolarizes the mitochondrial membrane, and increases basal mitochondrial  $\text{Ca}^{2+}$  levels and intracellular ATP content (Adinolfi et al., 2005a). However, it is not known whether activation of P2X7 influences metabolism in cells, such as osteoblasts, which express these receptors endogenously.

In the present study, we used a Cytosensor microphysiometer to monitor metabolic acid production (proton efflux) from osteoblasts in real time as a measure of cellular metabolism (McConnell et al., 1992). We show that activation of P2X7 elicits a large and sustained increase in proton efflux. Initiation of the response is dependent on  $\text{Ca}^{2+}$  influx through activated P2X7 receptors, whereas its maintenance is dependent on phosphatidylinositol 3-kinase (PI3K) activity and the availability of glucose. These data show for the first time that stimulation of P2X7 elicits a dramatic increase in metabolic acid production and efflux, which is triggered by elevation of cytosolic free  $\text{Ca}^{2+}$

concentration ( $[Ca^{2+}]_i$ ) and is sustained in part by PI3K-activated glucose metabolism.

### 3.3 Materials and Methods

#### 3.3.1 Materials and Solutions

$\alpha$ -Minimum essential medium ( $\alpha$ -MEM) buffered with  $\text{HCO}_3^-$  (26 mM), heat-inactivated fetal bovine serum (FBS), antibiotic solution (10,000 units/ml penicillin, 10,000  $\mu\text{g}/\text{ml}$  streptomycin, and 25  $\mu\text{g}/\text{ml}$  amphotericin B), trypsin solution, Dulbecco's phosphate buffered saline (DPBS),  $\text{HCO}_3^-$ -free MEM, MEM amino acids solution (50 $\times$ ), L-glutamine, 4-(2-hydroxyethyl)-1-piperazineethanesulfonic acid (HEPES), HEPES buffer solution (1 M), and UltraPure<sup>TM</sup> distilled water (DNase/RNase-free) were obtained from GIBCO (Life Technologies Inc., Burlington, ON, Canada). BSA (fraction V, fatty-acid free) was from Roche Diagnostics (Laval, QC, Canada).  $\text{HCO}_3^-$ - and glucose-free Dulbecco's modified Eagle medium (DMEM), ATP disodium salt, uridine 5'triphosphate (UTP) trisodium salt hydrate, 2',3'-*O*-(4-benzoylbenzoyl)ATP (BzATP) triethylammonium salt, lactate dehydrogenase,  $\beta$ -NAD, glycine buffer, and ethylene glycol-bis( $\beta$ -aminoethylether)-*N,N,N',N'*-tetraacetic acid tetrasodium salt (EGTA) were from Sigma-Aldrich (St. Louis, MO, USA). FM4-64 and indo-1 acetoxymethyl ester (indo-1-AM) were from Molecular Probes (Life Technologies Inc.). Click-iT<sup>®</sup> terminal deoxynucleotidyl transferase-mediated dUTP nick-end labeling (TUNEL) Alexa Fluor<sup>®</sup> 488 imaging assay was from Invitrogen (Life Technologies Inc.). Vectashield mounting medium with 4,6-diamidino-2-phenylindole (DAPI) was from Vector Laboratories (Burlingame, CA, USA). 3-(5-(2,3-Dichlorophenyl)-1*H*-tetrazol-1-yl)methyl pyridine hydrochloride (A 438079 HCl) and N-[1-[[[(cyanoamino)(5-quinolinylamino)methylene]amino]-2,2-dimethylpropyl]-3,4 dimethoxybenzene-acetamide (A 740003) were from Tocris Bioscience (Ellisville, MO, USA). Wortmannin, 2-(4-morpholinyl)-8-

phenyl-4*H*-1-benzopyran-4-one (LY 294002), and staurosporine were from Calbiochem (EMD Biosciences, Inc., San Diego, CA, USA). Nucleotides were dissolved in the appropriate buffer, A 438079 HCl was dissolved in water and stored in aliquots at -20 °C, and FM4-64, A 740003, wortmannin, LY 294002, and staurosporine were dissolved in dimethyl sulfoxide (DMSO) and stored in aliquots at -20 °C.

Standard superfusion medium, used in experiments monitoring proton efflux, was HCO<sub>3</sub><sup>-</sup>-free MEM supplemented with HEPES (1 mM) and BSA (1 mg/ml). Glucose dependence was investigated using DMEM supplemented with HEPES (1 mM) and BSA (1 mg/ml) with or without glucose (5.5 mM, glucose-containing and glucose-free medium, respectively). Ca<sup>2+</sup>-dependence experiments were performed using Ca<sup>2+</sup>-containing and Ca<sup>2+</sup>-free buffers. Ca<sup>2+</sup>-containing buffer consisted of (in mM): 5.4 KCl, 1.8 CaCl<sub>2</sub>, 0.8 MgSO<sub>4</sub>, 116.4 NaCl, 1 NaH<sub>2</sub>PO<sub>4</sub>·H<sub>2</sub>O, 2 L-glutamine, 5.5 glucose and 1 HEPES, supplemented with MEM amino acids solution (1X) and BSA (1 mg/ml). Ca<sup>2+</sup>-free buffer contained no added CaCl<sub>2</sub> and was supplemented with EGTA (0.5 mM). For morphological assessments, culture medium was removed and replaced with nominally divalent cation-free buffer containing (in mM): 140 NaCl, 5 KCl, 20 HEPES and 10 glucose. For measurements of [Ca<sup>2+</sup>]<sub>i</sub>, indo-1-loaded cells were suspended in HEPES buffer containing (in mM): 135 NaCl, 5 KCl, 1 MgCl<sub>2</sub>, 1 CaCl<sub>2</sub>, 10 glucose, and 20 HEPES. All media and buffers described above were adjusted to 290 ± 5 mOsm/L and pH 7.30 ± 0.02.

### 3.3.2 Cells and Culture

The MC3T3-E1 osteoblast-like cell line (subclone 4) was obtained from the



American Type Culture Collection (Rockville, MD, USA). The UMR-106 cell line, isolated from a rat osteosarcoma, was also obtained from the American Type Culture Collection (Rockville, MD). Like the MC3T3-E1 cell line, UMR-106 cells exhibit several properties of osteoblasts, including collagen type 1 (COL1) production, high alkaline phosphatase (ALP) activity, responsiveness to PTH and formation of mineralized tumors *in vivo* (Partridge et al., 1983). However, unlike the MC3T3-E1 cells, UMR-106 cells do not express P2X7 (Panupinthu et al., 2008). MC3T3-E1 and UMR-106 cells were subcultured twice weekly and maintained in  $\alpha$ -MEM containing  $\text{HCO}_3^-$  (26 mM) supplemented with 10% FBS and 1% antibiotic solution in humidified 5%  $\text{CO}_2$  at 37 °C.

### 3.3.3 Morphological Assessments

For time-lapse recordings, cells were trypsinized, plated at a density of  $1.0\text{-}1.5 \times 10^4$  cells/cm<sup>2</sup> on 35-mm culture dishes (Nunc, Thermo Fisher Scientific, Rochester, NY, USA) in supplemented  $\alpha$ -MEM, and cultured for 24-48 h. For recordings, culture medium was removed and replaced with nominally divalent cation-free buffer. Dishes were placed on a heater stage (~35 °C) mounted on an inverted phase-contrast microscope (Nikon Plan-Fluor  $\times 20$  objective, 0.45 numerical aperture). For quantitative analysis, the percentages of cells in each field exhibiting membrane blebbing before and after addition of test substances were determined. A single field was analyzed from each cell preparation. Experiments were performed on at least three independent preparations.

For live-cell confocal microscopy, MC3T3-E1 cells were plated at a density of  $1.5 \times 10^4$  cells/cm<sup>2</sup> on 35-mm glass bottom culture dishes (MatTek Corporation, Ashland, MA, USA) for 24 h in supplemented  $\alpha$ -MEM. Membranes were labelled by incubation

with lipophilic fluorescent probe FM4-64 (2  $\mu\text{g/ml}$ ) in medium for 15 min at 37  $^{\circ}\text{C}$ . Medium was then replaced with nominally divalent cation-free buffer, and cells were observed by confocal microscopy at  $\sim 28\text{--}30$   $^{\circ}\text{C}$  (Zeiss model LSM 510, Jena, Germany). Images were acquired using Zeiss Plan-Apochromat  $\times 63$  objective (1.4 numerical aperture) and 488 nm  $\text{Ar}^+$  ion laser excitation. The emission was filtered at 560 nm long pass, and images were captured using time-lapse mode.

### 3.3.4 Measurement of Proton Efflux

MC3T3-E1 and UMR-106 cells were seeded on porous polycarbonate membranes (Transwell, 12-mm diameter, 3- $\mu\text{m}$  pore size; Corning Inc. Costar, Corning, NY) in supplemented  $\alpha$ -MEM at a density of  $8.8 \times 10^4$  cells/ $\text{cm}^2$  and  $3.5 \times 10^4$  cells/ $\text{cm}^2$ , respectively. After 48 h, cells adhering to the polycarbonate membranes were placed in microflow chambers and positioned above silicon-based potentiometric sensors, which detect changes in extracellular pH ( $\text{pH}_o$ ) of as little as  $10^{-3}$  units (Cytosensor microphysiometer, Molecular Devices, Sunnyvale, CA) (McConnell et al., 1992). Cells were continuously superfused at a rate of 100  $\mu\text{l/min}$  with medium at 37  $^{\circ}\text{C}$ . Superfusion media with low buffering power were used to enhance the small alterations in  $\text{pH}_o$  arising by efflux of protons from cells. Each chamber was supplied with medium from one of two reservoirs selected by a computer-controlled valve. Test substances were directly introduced in superfusion medium, and changes in proton efflux were monitored. The lag time between a valve switch and the arrival of test solutions at the microflow chambers was 4–5 s.

Surface potential of each silicon sensor, corresponding to the  $\text{pH}_o$ , was plotted as a

voltage-time trace. At 37 °C, 61 mV corresponds to 1 pH unit. To measure the rate of acidification (net cellular efflux of proton equivalents), fluid flow to cells was stopped periodically for 30 s. During this time, acid accumulated in the microflow chamber (volume 2.8  $\mu$ l) causing  $\text{pH}_o$  to decrease. Measurement of acidification rate was obtained by linear least-squares fit to the slope of the  $\text{pH}_o$ -time trace during the time when fluid flow to the cells was stopped. Due to an artefact arising from changing medium, the first data point after beginning superfusion with agonist was sometimes omitted from the trace.

### **3.3.5 Measurement of Lactate Efflux**

Extracellular lactate was measured using a spectrophotometric assay based on generation of NADH via the catalytic action of lactate dehydrogenase [modified from (Santhanagopal et al., 2001)]. Briefly, cells were seeded at a density of  $1.5 \times 10^4$  cells/cm<sup>2</sup> on 60-mm culture dishes (BD Biosciences, Franklin Lakes, NJ, USA) in supplemented  $\alpha$ -MEM for 48 h. On the day of the experiment, growth medium was replaced by  $\alpha$ -MEM supplemented with BSA (1 mg/ml) and 1% antibiotic solution (serum-free) in 5% CO<sub>2</sub> at 37 °C. After 3 h, cultures were incubated with BzATP or vehicle. Samples of media (100  $\mu$ l) were then collected for lactate determination. To measure lactate concentration, 6.9  $\mu$ l of each sample was combined with 193.1  $\mu$ l of lactate assay solution (50 mg  $\beta$ -NAD dissolved in 10 ml glycine buffer, 20 ml deionized H<sub>2</sub>O and 17 U/ml lactate dehydrogenase) in a 96-well UV-plate (Corning Inc., Costar, Corning, NY, USA). The plate was incubated at 37 °C for 15-30 min and absorbance at 340 nm was quantified with a microplate reader (Tecan, Durham, NC, USA). The concentration of lactate in each

sample was determined from a standard curve of absorbance for known lactate concentrations.

### 3.3.6 Spectrofluorometric Measurement of $[Ca^{2+}]_i$

Changes in  $[Ca^{2+}]_i$  were measured using spectrofluorimetry, as previously described (Santhanagopal et al., 2001). Briefly, MC3T3-E1 cells were seeded at a density of  $1.5 \times 10^4$  cells/cm<sup>2</sup> on 60-mm culture dishes (BD Biosciences) in supplemented  $\alpha$ -MEM for 48 h. On the day of the experiment, cells were loaded with indo-1 by incubation in serum-supplemented medium with indo-1-AM (2  $\mu$ g/ml) for 30 min at 37 °C and 5% CO<sub>2</sub>. After loading, cells were washed with PBS and harvested by trypsinization. Supplemented medium was added to neutralize the trypsin, and cells were then sedimented and resuspended in HEPES-buffered MEM (catalog no. 41200). For measurement of  $[Ca^{2+}]_i$ , 1 ml aliquots of indo-1-loaded cell suspensions ( $\sim 1.0 \times 10^6$  cells/ml) maintained at room temperature in HEPES-buffered MEM were sedimented and resuspended in 2 ml HEPES buffer in a fluorometric cuvette at room temperature. Test substances were added directly to the cuvette.

$[Ca^{2+}]_i$  was monitored using a dual-wavelength spectrofluorimeter (Model RF-M2004, from Photon Technology International, South Brunswick, NJ) at 355 nm excitation and emission wavelengths of 405 and 485 nm. The system software was used to calculate the ratio, R, which is the fluorescence intensity at 405 nm divided by the intensity at 485 nm.  $[Ca^{2+}]_i$  was determined from the relationship  $[Ca^{2+}] = K_d[(R - R_{min})/(R_{max} - R)]\beta$ , where  $K_d$  (for the indo-1- $Ca^{2+}$  complex) was taken as 250 nM,  $R_{min}$  and  $R_{max}$  were the values of R at low and saturating concentrations of  $Ca^{2+}$ , respectively, and

$\beta$  was the ratio fluorescence at 485 nm measured at low and saturating  $\text{Ca}^{2+}$  concentrations.

### 3.3.7 Assessment of Apoptosis

MC3T3-E1 cells were seeded at a density of  $1.5 \times 10^4$  cells/cm<sup>2</sup> on 12-mm glass coverslips (Fisher Scientific, Ottawa, ON, CANADA) in 24-well culture plates (BD Biosciences) in supplemented  $\alpha$ -MEM for 48 h. On the day of the experiment, growth medium was replaced by  $\alpha$ -MEM supplemented with BSA (1 mg/ml) and 1% antibiotic solution (serum-free) in 5% CO<sub>2</sub> at 37 °C. Three hours later, cultures were incubated with test substances. After 24 h, cells were fixed with paraformaldehyde (4%) in sucrose solution (2%), permeabilized with 0.25% Triton X-100 in PBS, and assessed for apoptosis using the Click-iT® TUNEL Alexa Fluor® 488 imaging assay according to manufacturer's instructions. Selected untreated samples from each experiment were incubated with DNase I before staining as a positive control for the TUNEL assay. After staining, coverslips were sealed using Vectashield mounting medium with DAPI and visualized by confocal microscopy (Zeiss model LSM 510). Images were acquired using Zeiss Plan-Apochromat  $\times 40$  objective (1.2 numerical aperture) with 730-nm Chameleon multi-photon or 488-nm Ar<sup>+</sup> ion laser excitation, and the emission was filtered at 390-465 nm or 500-550 nm band pass, respectively. The total number of cells and the number of TUNEL-positive cells were determined from randomly selected fields.

### 3.3.8 Statistical Analyses

Proton efflux was normalized as a percentage of basal efflux in standard

superfusion medium before addition of test substance or change of superfusion solution. This normalization compensated for differences in cell numbers among the chambers. Results are presented as means  $\pm$  S.E.M. Differences between two groups were evaluated by *t* test. Differences among three or more groups were evaluated by one-way or two-way analysis of variance (ANOVA) followed by Tukey or Bonferroni multiple comparison tests. Differences were accepted as statistically significant at  $p < 0.05$ .

## 3.4 Results

### 3.4.1 The P2X7 Agonist BzATP Induces Dynamic Membrane Blebbing in MC3T3-E1 Osteoblast-like Cells

Among P2 nucleotide receptors, the ability to induce membrane blebbing is a unique property of P2X7 (North, 2002). Using primary cultures of rat and murine calvarial cells, we have shown previously that activation of P2X7 elicits dynamic and reversible blebbing of the plasma membrane in only a subpopulation of these cells (Panupinthu et al., 2007). To investigate the proportion of MC3T3-E1 cells expressing functional P2X7 receptors, we monitored morphology using time-lapse phase-contrast microscopy. Prior to addition of agonist, few cells exhibited membrane blebs (Figure 3.1 A, *Before*). Cultures were then treated with the P2X7 agonist BzATP (300  $\mu$ M) or vehicle for 20 min. BzATP caused cellular retraction followed by dynamic plasma membrane blebbing (Figure 3.1 A, *BzATP*; Video 3.1, video legend in Appendix A). In contrast, UMR-106 cells exhibited cellular retraction but no membrane blebbing in response to BzATP (Figure 3.1 A, *BzATP*; Video 3.2, video legend in Appendix A), consistent with the absence of P2X7 in these cells.

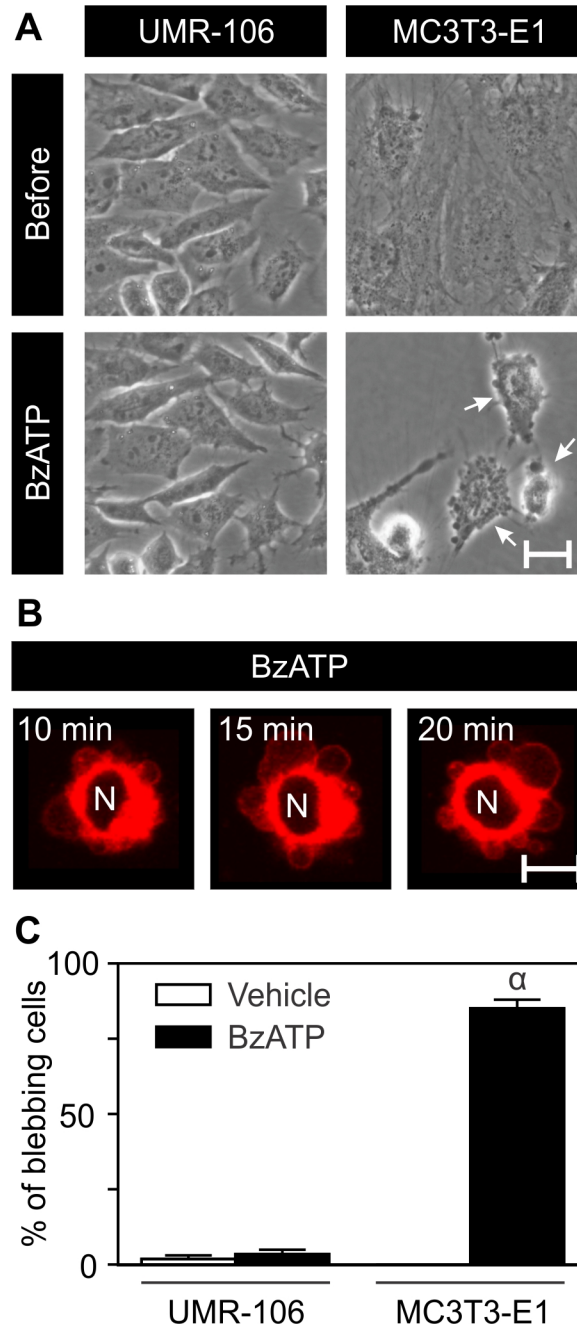
To further characterize the dynamic changes in morphology of individual MC3T3-E1 cells exposed to BzATP, membranes were stained with the fluorescent lipophilic dye FM4-64, and cells were observed by live-cell confocal microscopy. BzATP (300  $\mu$ M) induced the formation of multiple membrane blebs that enlarged and shrunk asynchronously (Figure 3.1 B). These blebs occurred over the entire cell surface and did not contain FM4-64-stained intracellular membranes.

We used the time-lapse recordings to quantify the percentage of cells exhibiting

**Figure 3.1 The P2X7 Agonist BzATP Induces Membrane Blebbing in MC3T3-E1 Osteoblast-like, but not UMR-106 Osteosarcoma Cells.**

A, morphology of MC3T3-E1 and UMR-106 osteoblast-like cells was monitored by time-lapse phase-contrast microscopy. Cultures were bathed in nominally divalent cation-free buffer at ~35 °C for 10 min (*Before*). Cells were then treated with BzATP (300 μM). Data are representative fields of cells from 4 independent preparations. Scale bar is 20 μm. *White arrows* indicate blebbing cells. Videos 3.1 and 3.2 show responses of MC3T3-E1 cells and UMR-106 cells to BzATP, respectively (video legends in Appendix A). B, to examine bleb morphology, MC3T3-E1 cells were loaded with FM4-64 to stain membranes, and observed using confocal microscopy. Cells were bathed in nominally divalent cation-free buffer. BzATP (300 μM) was added at time 0 min. Images show 2-μm-thick optical sections through a single cell at 5 min intervals ( $N$  = nucleus). Images are representative of cells demonstrating dynamic membrane blebbing from 4 independent preparations. Scale bar is 20 μm. C, percentage of MC3T3-E1 and UMR-106 cells exhibiting dynamic membrane blebbing determined from time-lapse movies obtained before and during 20 min of treatment with vehicle or BzATP (300 μM).  $\alpha$  indicates significant difference compared with respective vehicle for each cell line ( $p < 0.05$ ). Data are means  $\pm$  S.E.M. ( $n = 8$  samples from 6 independent preparations for MC3T3-E1 cells,  $n = 6$  samples from 4 independent preparations for UMR-106 cells).





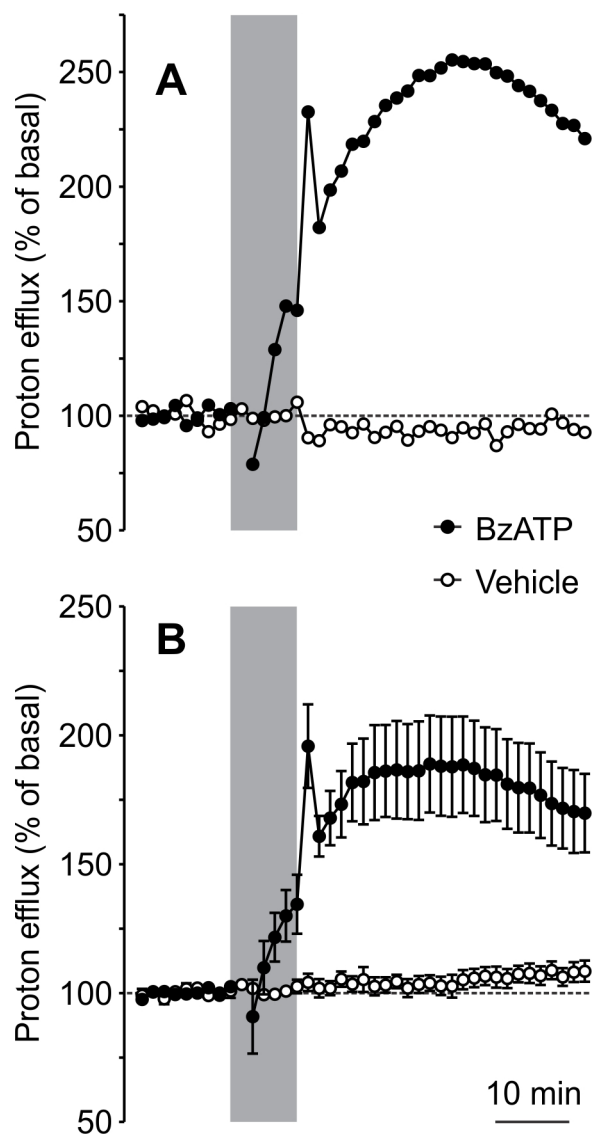
membrane blebbing. BzATP induced significant blebbing of the plasma membrane in MC3T3-E1 cells ( $85 \pm 3\%$ ; Figure 3.1 C), thereby establishing the expression of functional P2X7 receptors in the majority of these cells. As expected, no significant increase in the percentage of blebbing cells was seen following treatment of UMR-106 cells with BzATP (Figure 3.1 C). Thus, in contrast to UMR-106 cells (which do not express P2X7) and primary bone cell systems (in which only a subpopulation of cells express functional P2X7 receptors), the vast majority MC3T3-E1 osteoblasts expressed functional P2X7 receptors. Consequently, we used the MC3T3-E1 cell line to characterize the effects of P2X7 activation on metabolic acid production by osteoblasts.

### **3.4.2 Effects of BzATP on Proton Efflux from MC3T3-E1 Cells**

To assess changes in cellular metabolism, proton efflux from MC3T3-E1 cells was monitored by microphysiometry. Basal proton efflux in standard superfusion medium remained steady for periods of  $> 60$  min. Superfusion with BzATP ( $300 \mu\text{M}$ ) for 9 min caused dramatic changes in proton efflux (Figure 3.2). The first phase of the BzATP-induced response (initial phase) consisted of a variable, transient depression in proton efflux, which reached its maximum at 1.5-3 min after addition of BzATP, followed by a slow increase to levels above basal by 9 min in the presence of agonist. The second phase (sustained phase) occurred following removal of BzATP, and was characterized by a large sustained increase in proton efflux that lasted for  $> 1$  h following agonist removal (Figure 3.2). A transient overshoot in proton efflux was also observed immediately upon

**Figure 3.2 BzATP Causes a Sustained Increase in Proton Efflux from MC3T3-E1 Cells.**

MC3T3-E1 cells were cultured on porous polycarbonate membranes, and proton efflux was monitored by microphysiometry. Cells were superfused with standard medium, and at 1.5 min intervals, superfusion was interrupted for 30 s to measure acidification rate. Net efflux of proton equivalents (proton efflux) was calculated from the acidification rate and expressed as a percentage of basal proton efflux. Where indicated by the *shaded area*, MC3T3-E1 cells were superfused with BzATP (300  $\mu$ M, *closed symbols*) or vehicle (*open symbols*) in standard medium for 9 min. A, data are representative traces from 4 independent preparations. B, data are means  $\pm$  S.E.M. of 8 samples from 4 independent preparations. Data points for BzATP from 22.5-60 min are significantly different compared with vehicle at the same time points ( $p < 0.05$ ).



washout of BzATP<sup>2</sup>. Treatment with vehicle did not cause any appreciable change in proton efflux. To exclude the possibility that responses to BzATP were due to direct interaction with the silicon sensor, cells were devitalized with 1% Triton X-100 and then superfused with agonist. The basal proton efflux from non-vital cells was zero, and no changes were observed upon superfusion with BzATP (300  $\mu$ M), ruling out the possibility of interaction with the silicon sensor.

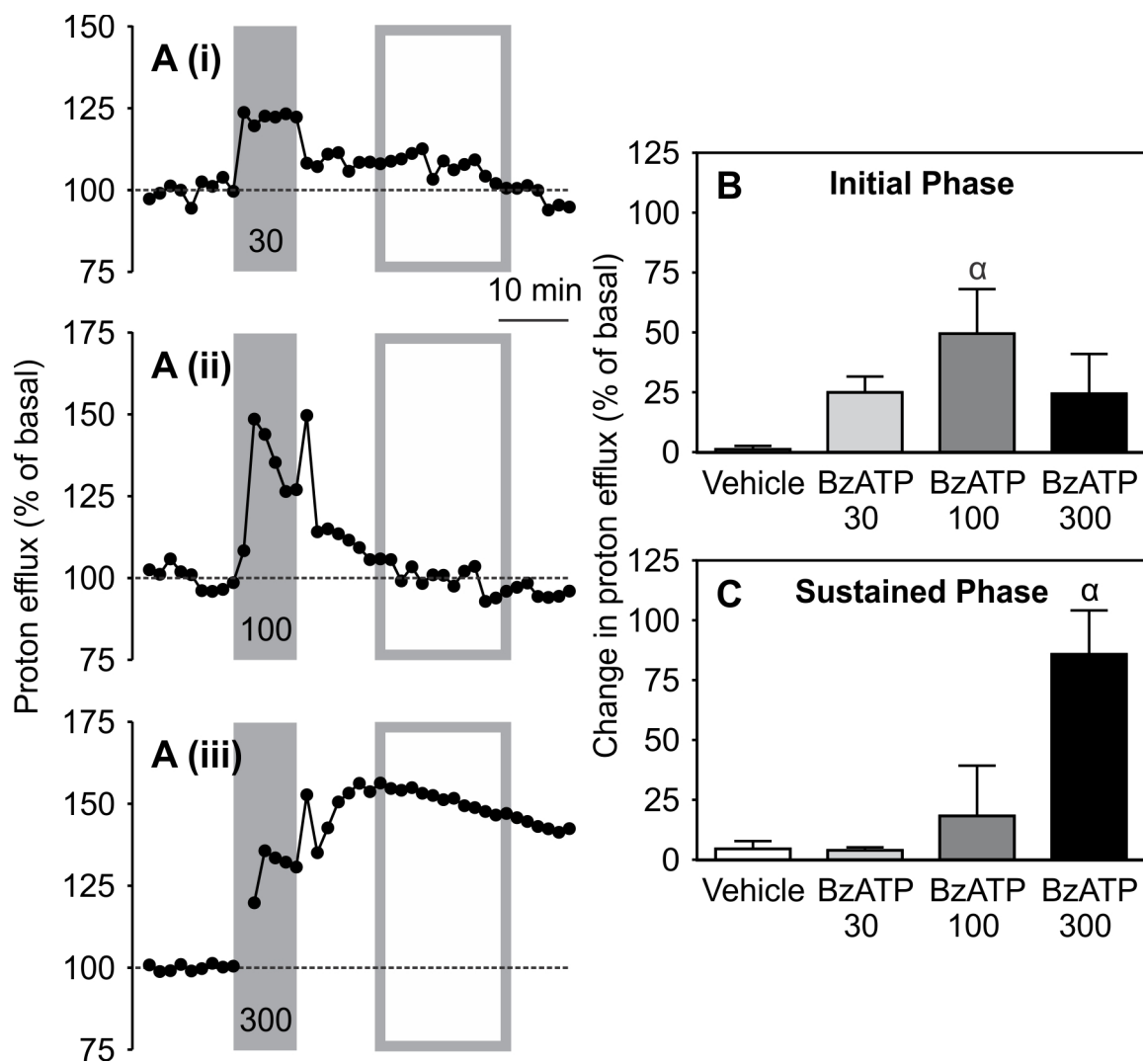
We next investigated the dependence of these changes in proton efflux on BzATP concentration (Figure 3.3). The initial phase of the BzATP response was quantified as the average increase in proton efflux above basal within the 9 min during which BzATP was applied. The sustained phase was quantified as the average increase in proton efflux above basal, 12-30 min after washout of BzATP. BzATP (100  $\mu$ M, a concentration sufficient to fully activate several P2 receptors, but only partially activate P2X7) elicited an initial, transient increase in proton efflux ( $49 \pm 19\%$ ,  $p < 0.05$ ; Figure 3.3 B), but no significant sustained phase (Figure 3.3 C). In contrast, BzATP (300  $\mu$ M, a concentration sufficient to fully activate P2X7) induced a large sustained elevation in proton efflux ( $86 \pm 18\%$ ,  $p < 0.05$ ; Figure 3.3 C). These data are consistent with a role for P2X7 in triggering the sustained increase in proton efflux, and subsequent studies were performed using a concentration of 300  $\mu$ M BzATP.

---

<sup>2</sup> The transient depression in proton efflux upon exposure to BzATP and subsequent overshoot in proton efflux upon washout of BzATP are due to the presence of triethylammonium in the BzATP preparation. Upon superfusion with BzATP solution, influx of unprotonated triethylammonium transiently increases  $pH_i$ , leading to brief suppression of proton efflux. On the other hand, upon washout, efflux of unprotonated triethylammonium transiently decreases  $pH_i$ , leading to a transitory increase in proton efflux (Reyes, J.P., M.W. Grol, S.M. Sims, and S.J. Dixon. 2013. Receptor-independent effects of 2'(3')-O-(4-benzoylbenzoyl)ATP triethylammonium salt on cytosolic pH. *Purinergic Signal*. [Epub ahead of print; DOI:10.1007/s11302-013-9365-4]).

**Figure 3.3 Increases in Proton Efflux are Dependent on BzATP Concentration.**

MC3T3-E1 cells were superfused with standard medium, and proton efflux was monitored. A, where indicated by the *shaded areas*, MC3T3-E1 cells were challenged with indicated concentrations ( $\mu\text{M}$ ) of BzATP or vehicle (not shown) in standard medium for 9 min. Data are representative traces from 4 independent preparations. B, amplitude of the initial phase, quantified as the average increase in proton efflux above basal during application of BzATP or vehicle. C, amplitude of the sustained phase, quantified as the average increase in proton efflux above basal, 12-30 min following removal of BzATP or vehicle (indicated by *gray-outlined boxes* in A (i-iii)). For both B and C,  $\alpha$  indicates significant difference compared with vehicle ( $p < 0.05$ ). Data are means  $\pm$  S.E.M. ( $n = 4-8$  samples from 4 independent preparations).



### 3.4.3 Role of P2X7 in Mediating Nucleotide-induced Increases in Proton Efflux

In addition to P2X7, cells of the osteoblast lineage express a number of other P2X and P2Y nucleotide receptors. BzATP is not specific for P2X7 as it also activates a number of other P2 receptors (North, 2002), including P2Y<sub>11</sub>, P2X1, P2X3 and P2X4 (Bianchi et al., 1999; Communi et al., 1999; Naemsch et al., 2001), with similar potency. Thus, responses to BzATP alone cannot be used to establish involvement of the P2X7 receptor. To investigate the nucleotide receptors mediating the effects of BzATP on proton efflux, we first tested the effects of other P2 receptor agonists. Parallel samples of cells were superfused with low concentrations of ATP (100  $\mu$ M, which activates P2X1-5 and many P2Y receptors) and UTP (100  $\mu$ M, which activates P2Y<sub>2</sub>, P2Y<sub>4</sub> and P2Y<sub>6</sub> receptors), and high concentrations of ATP (1 mM) and BzATP (300  $\mu$ M), both of which also activate P2X7. Responses to UTP and a low concentration of ATP (100  $\mu$ M) consisted only of a transient elevation in proton efflux during agonist application (Figure 3.4 Ai and ii). On the other hand, the response to a higher concentration of ATP (1 mM) consisted of both initial transient and sustained elevations in proton efflux (Figure 3.4 Aiii)<sup>3</sup>. Transient elevations in proton efflux caused by UTP (100  $\mu$ M) and ATP (0.1-1 mM) during the initial phase were significantly different compared to vehicle-treated cultures (Figure 3.4 Bi). Consistent with the involvement of P2X7, only a high concentration of ATP (1 mM) elicited a significant and sustained increase in proton efflux following washout of agonist, similar to that seen with BzATP (300  $\mu$ M) (Figure 3.4 Bii). Since UTP (and uridine 5'-diphosphate (UDP)) can only activate certain members of the P2Y receptor family, the initial transient phase is most likely due to activation of P2Y

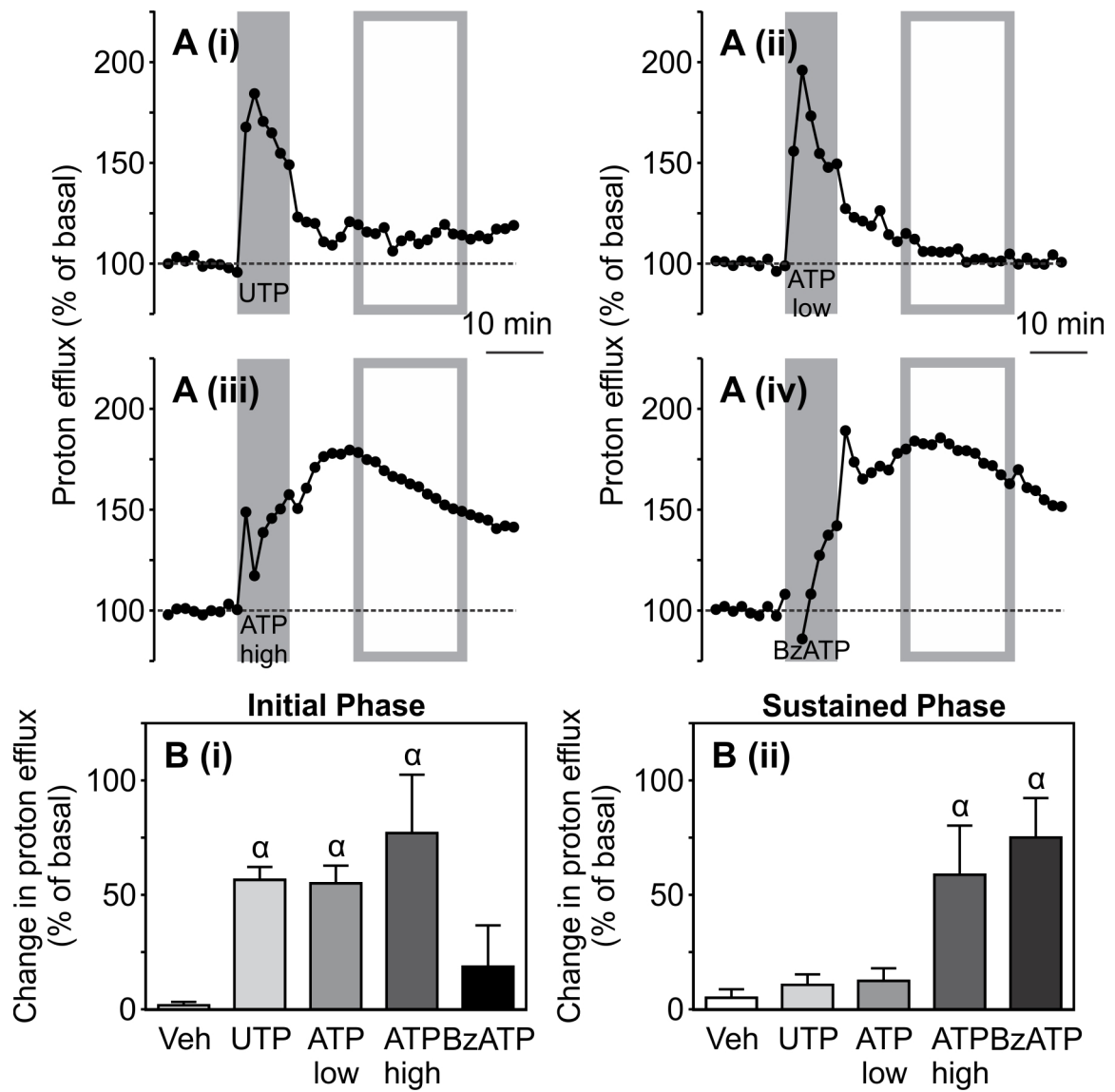
---

<sup>3</sup> The transient depression and overshoot in proton efflux observed with the triethylammonium<sup>+</sup> salt of BzATP were not observed with ATP, which was applied as a Na<sup>+</sup> salt.



**Figure 3.4 P2X7 Receptor Agonists alone Induce Sustained Increases in Proton Efflux.**

MC3T3-E1 cells were superfused with standard medium, and proton efflux was monitored. A, where indicated by the *shaded areas*, MC3T3-E1 cells were challenged with BzATP (300  $\mu$ M), ATP (100  $\mu$ M or 1 mM), UTP (100  $\mu$ M) or vehicle (not shown) in standard medium for 9 min. Data are representative traces from 3-5 independent preparations. B (i), amplitude of the initial phase, quantified as the average increase in proton efflux above basal during application of agonist. B (ii), amplitude of the sustained phase, quantified as the average increase in proton efflux above basal, 12-30 min after application of agonist (indicated by *gray-outlined boxes* in A). For both B and C,  $\alpha$  indicates significant difference compared with vehicle ( $p < 0.05$ ). Data are means  $\pm$  S.E.M. ( $n = 5-8$  samples from 3-5 independent preparations).



receptors. On the other hand, the sustained phase is most likely triggered by P2X7.

We used two approaches to confirm the involvement of P2X7 receptors in triggering the sustained phase of BzATP-induced proton efflux. First, we compared responses of MC3T3-E1 cells (which express P2X7) and UMR-106 cells (which do not express P2X7). Parallel samples of MC3T3-E1 and UMR-106 cells were superfused with BzATP (300  $\mu$ M) or vehicle (Figure 3.5 A). Proton efflux from UMR-106 cells was suppressed in the presence of BzATP (~60% of basal levels). However, BzATP failed to elicit the sustained increase seen in MC3T3-E1 cells (Figure 3.5 B). Second, we examined the effects of A 438079 and A 740003, two specific P2X7 antagonists (Nelson et al., 2006; Donnelly-Roberts and Jarvis, 2007). Although treatment with A 438079 or A 740003 (10  $\mu$ M) had no appreciable effect on basal proton efflux (Figure 3.6 A, C), both significantly blocked the sustained phase of the BzATP-induced response (Figure 3.6 B, D). Taken together, we conclude that the sustained phase of nucleotide-induced increase in proton efflux from osteoblast-like cells is triggered by activation of P2X7.

#### **3.4.4 Effects of P2X7 Agonists on Survival and Apoptosis of MC3T3-E1 Cells**

Activation of P2X7 promotes apoptosis in a number of cell systems (Adinolfi et al., 2005b), though its ability to promote cell death in osteoblasts is controversial. ATP and BzATP have been shown to induce delayed release of lactate dehydrogenase from osteoblast-like cells (Gartland et al., 2001), indicating cell death. However, we have reported previously that BzATP-induced membrane blebbing of murine calvarial cells was reversible upon removal of agonist, suggesting that P2X7 receptors do not induce

**Figure 3.5 BzATP Induces an Increase in Proton Efflux from MC3T3-E1 but not UMR-106 Cells.**

MC3T3-E1 and UMR-106 cells were superfused with standard medium, and proton efflux was monitored. A, parallel samples of MC3T3-E1 (A (i)) and UMR-106 (A (ii)) cells were challenged with BzATP (300  $\mu$ M, *closed symbols*) or vehicle (*open symbols*) in standard medium for 9 min, where indicated by the *shaded areas*. Data are representative traces from 3 independent preparations. B, amplitude of the sustained phase, quantified as the average increase in proton efflux above basal, 12-30 min following application of vehicle (Veh) or BzATP (Bz) (indicated by *gray-outlined boxes* in A (i-ii)).  $\alpha$  indicates significant difference compared with respective vehicle for each cell line ( $p < 0.05$ ). Data are means  $\pm$  S.E.M. ( $n = 3-9$  samples from 3 independent preparations).

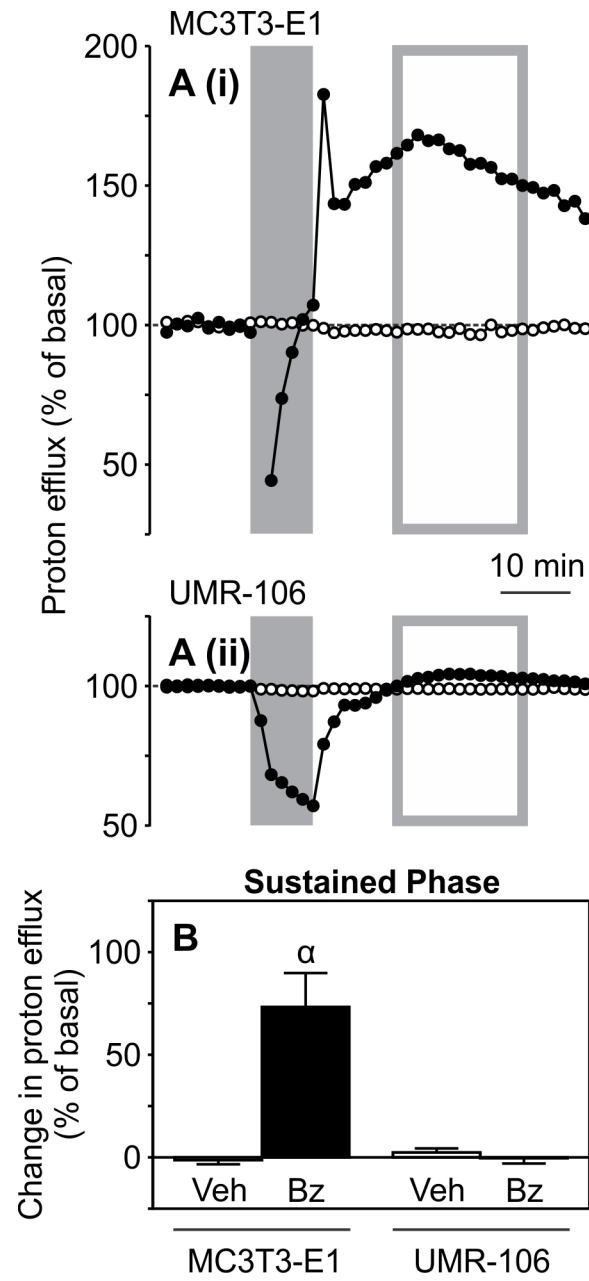
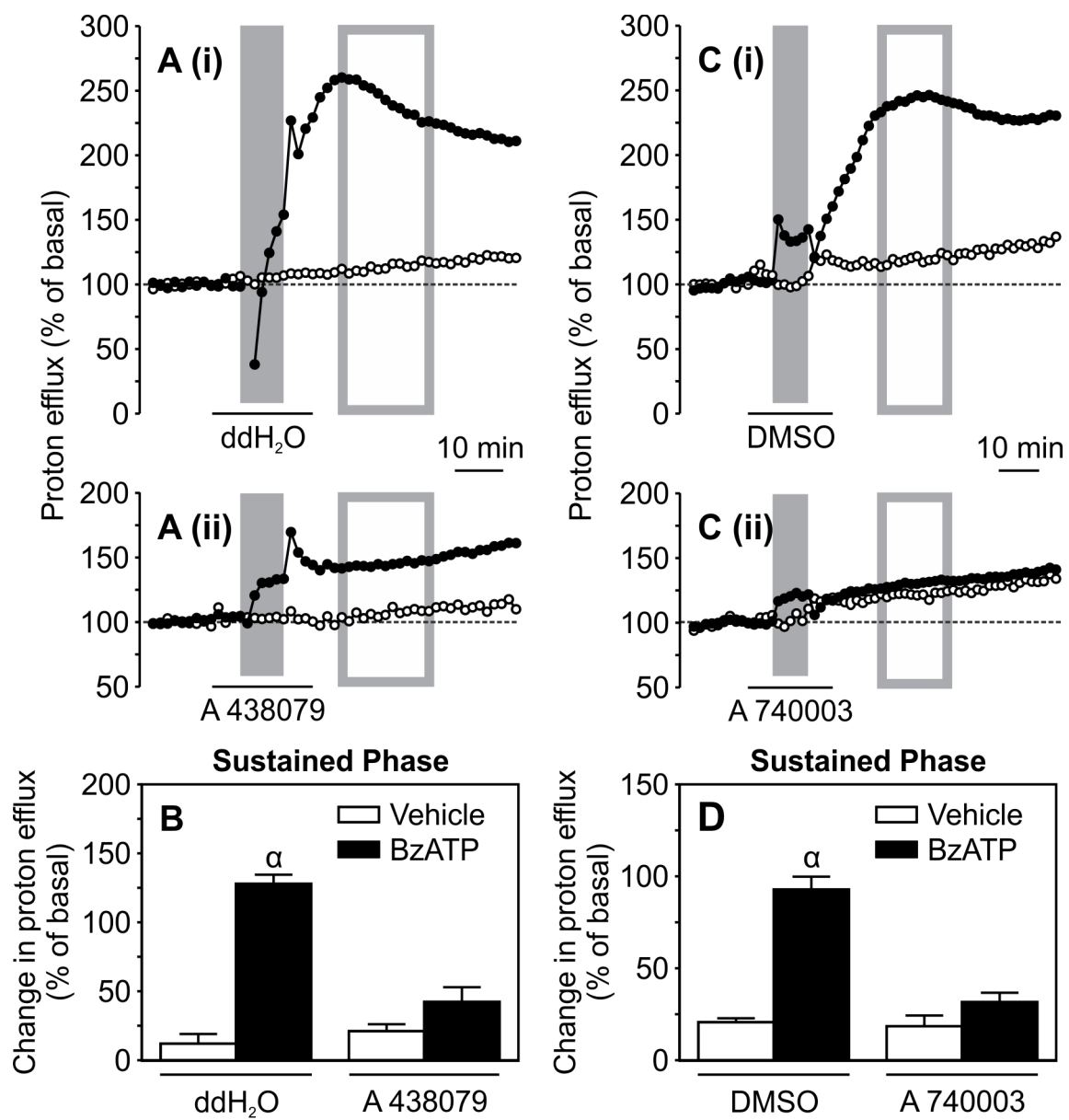


**Figure 3.6 Blockade of P2X7 Receptors Suppresses the Increase in Proton Efflux Induced by BzATP.**

MC3T3-E1 cells were superfused with standard medium, and proton efflux was monitored. A, parallel samples of MC3T3-E1 cells were initially superfused with standard medium. Subsequently, samples were superfused with either control (ddH<sub>2</sub>O, A (i)) or the P2X7 antagonist, A 438079 (10 μM, A (ii)), for the period indicated by the *horizontal bar beneath the graph*. After 6 min, cultures in both A (i) and A (ii) were superfused with either vehicle (*open symbols*) or BzATP (300 μM, *closed symbols*) where indicated by the *shaded area*, in the continued presence of the appropriate medium. B, amplitude of the sustained phase, quantified as the average increase in proton efflux above basal, 12-30 min after application of vehicle or BzATP (indicated by *gray-outlined boxes* in A (i-ii)). C, parallel samples of MC3T3-E1 cells were initially superfused with standard medium. Subsequently, samples were superfused with either control (DMSO, C (i)) or the P2X7 antagonist, A 740003 (10 μM, C (ii)), for the period indicated by the *horizontal bar beneath the graph*. After 6 min, cultures in both C (i) and C (ii) were superfused with either vehicle (*open symbols*) or BzATP (300 μM, *closed symbols*) where indicated by the *shaded area*, in the continued presence of the appropriate medium. D, amplitude of the sustained phase, quantified as the average increase in proton efflux above basal, 12-30 min after application of vehicle or BzATP (indicated by *gray-outlined boxes* in C (i-ii)). For both A and C, data are representative traces from 3-4 independent preparations. For both B and D, α indicates significant difference compared to respective vehicle ( $p < 0.05$ ). Data are means ± S.E.M. ( $n = 5-12$  samples from 3-4 independent preparations).

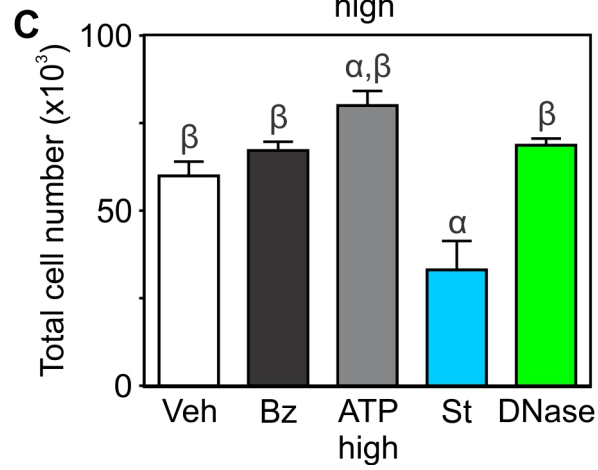
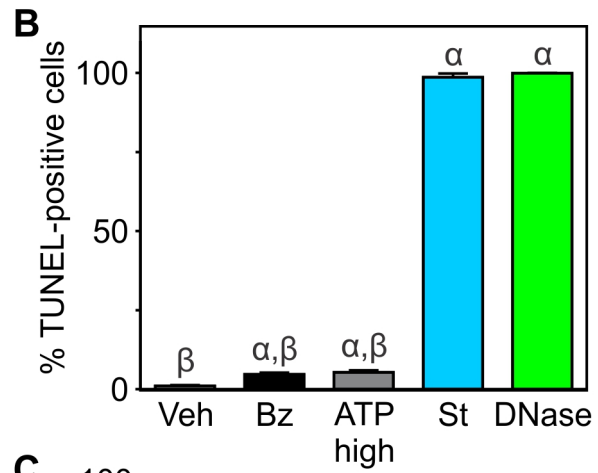
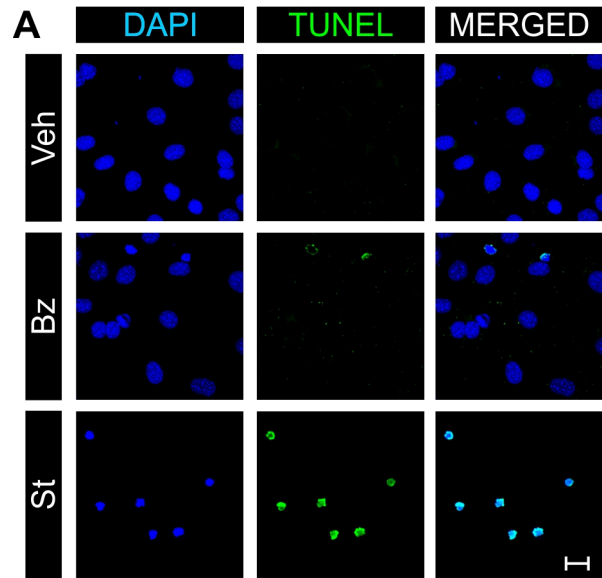


acute cell death (Panupinthu et al., 2007). Moreover, stimulation of P2X7 receptors in MC3T3-E1 cells does not activate caspase 3 (Li et al., 2005), a key mediator of apoptosis, arguing against a pro-apoptotic effect. To determine whether the increased proton efflux elicited by activation of P2X7 might be associated with induction of apoptosis, we investigated the effects of prolonged P2X7 stimulation on apoptosis and survival of MC3T3-E1 cells. Cultures were incubated with vehicle, BzATP (300  $\mu$ M), ATP (1 mM) or staurosporine (1  $\mu$ M, positive control) for 24 h in the absence of serum. Cultures were then fixed, permeabilized, subjected to TUNEL, and visualized by confocal microscopy (Figure 3.7 A). Staurosporine induced apoptosis in close to 99% of cells, whereas BzATP or ATP caused only a slight increase in the percentage of TUNEL-positive cells compared to vehicle (Figure 3.7 B). In this regard, staurosporine alone induced a significant decrease in total cell number, whereas treatment with BzATP had no significant effect (Figure 3.7 C). Interestingly, ATP slightly increased the total number of cells per coverslip compared to vehicle (Figure 3.7 C), consistent with an increase in proliferation. In summary: i) the percentage of cells exhibiting TUNEL staining after treatment with BzATP or ATP (~5%) was substantially less than the total number of cells expressing functional P2X7 receptors (~85%, Figure 3.1); and ii) neither BzATP nor a high concentration of ATP caused a decrease in the total number of cells. These findings rule out the possibility that the P2X7-induced increase in proton efflux is associated with induction of apoptosis or cell death.



**Figure 3.7 P2X7 Agonists do not Induce Death of MC3T3-E1 cells.**

Cultures of MC3T3-E1 cells were bathed in serum-free  $\alpha$ -MEM supplemented with bovine albumin (1 mg/ml) and 1% antibiotic solution for 3 h, and subsequently treated with vehicle (Veh), BzATP (300  $\mu$ M, Bz), ATP (1 mM, ATP high), or staurosporine (1  $\mu$ M, St). After 24 h, cells were fixed, permeabilized and subjected to TUNEL to identify apoptotic cells (**green**). Nuclei were stained with DAPI (**blue**). A, samples were visualized by confocal microscopy. Data are representative images from 3 independent preparations performed in duplicate. Scale bar is 20  $\mu$ m. B, to quantify apoptosis, the number of TUNEL-positive cells was expressed as a percentage of the total number of cells in a field. C, the total number of cells per coverslip for each treatment was determined. For both B and C,  $\alpha$  indicates significant difference compared with vehicle ( $p < 0.05$ ).  $\beta$  indicates a significant difference compared to staurosporine. Data are means  $\pm$  S.E.M. ( $n = 3$  independent preparations each performed in duplicate).



### 3.4.5 Role of Glucose Metabolism in Generating Sustained Nucleotide-induced Proton Efflux

Transient changes in proton efflux can arise from the activation or inhibition of transporters mediating the movement of proton equivalents across the plasma membrane; however, sustained increases in proton efflux reflect increases in the production of proton equivalents and their subsequent extrusion. Therefore, we considered the possibility that the sustained phase was due to enhanced glucose metabolism. We first investigated dependence of the sustained phase on extracellular glucose. Parallel samples of MC3T3-E1 cells were treated with BzATP (300  $\mu$ M) or vehicle in standard superfusion medium (containing 5.5 mM glucose). Subsequently, when BzATP-treated cells were within the sustained phase, samples were superfused with glucose-free medium, resulting in a large, rapid decrease in proton efflux in both vehicle- and BzATP-treated samples to comparable levels (Figure 3.8). Thus, most if not all of the sustained phase of the nucleotide-induced response is dependent on the presence of extracellular glucose.

Next, we assessed the effects of BzATP on extracellular lactate levels. MC3T3-E1 cells were incubated with BzATP (300  $\mu$ M) or vehicle, and medium samples were collected for analysis over a 3-h period. BzATP caused a significant increase in extracellular lactate concentration (indicative of lactate efflux), compared with vehicle-treated cultures (Figure 3.9)<sup>4</sup>. In MC3T3-E1 cells, the observed ~250% increase in lactate efflux (from 0.5 to 3 h) is comparable to the magnitude of the sustained increase in proton efflux induced by BzATP. Taken together, these data are consistent with the sustained

---

<sup>4</sup> When tested in UMR-106 cells, neither BzATP (300  $\mu$ M) nor ATP (1 mM) induced a significant increase in extracellular lactate concentration relative to vehicle-treated cultures (*data not shown*), in keeping with a role for the P2X7 receptor in mediating this response.

**Figure 3.8 Sustained Increase in Proton Efflux Induced by BzATP is Dependent on Extracellular Glucose.**

MC3T3-E1 cells were superfused with standard medium, and proton efflux was monitored. A, where indicated by the *shaded area*, parallel samples of MC3T3-E1 cells were challenged with BzATP (300  $\mu$ M, *closed symbols*) or vehicle (*open symbols*) in standard running medium for 9 min. Subsequently, both samples were superfused with glucose-free medium for 9 min, where indicated by the *horizontal bar beneath the graph*. Data are representative traces from 3 independent preparations. B, amplitude of the response, quantified as the change in proton efflux relative to basal, calculated at the times indicated by *I* and *II* in panel A.  $\alpha$  indicates significant difference compared with respective vehicle ( $p < 0.05$ ). Data are means  $\pm$  S.E.M. ( $n = 6-8$  samples from 3 independent preparations).

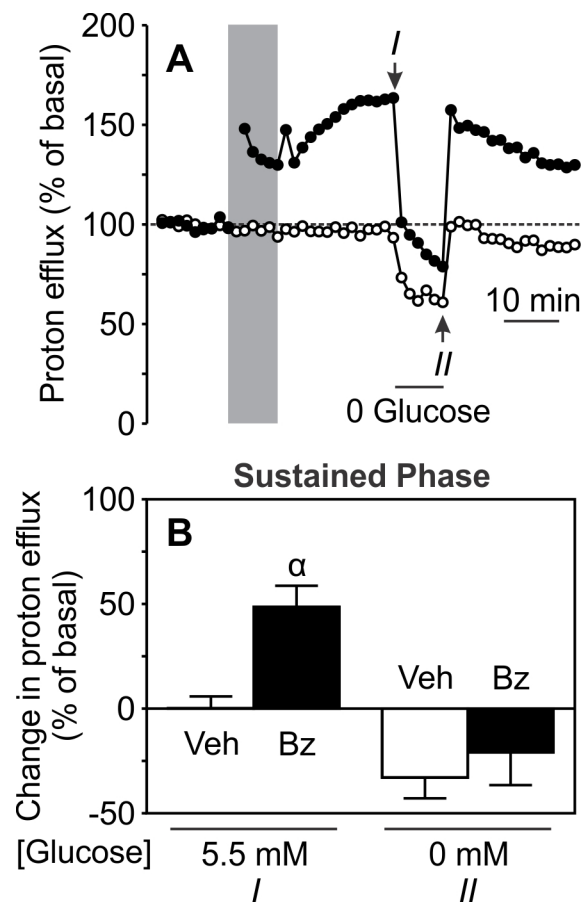
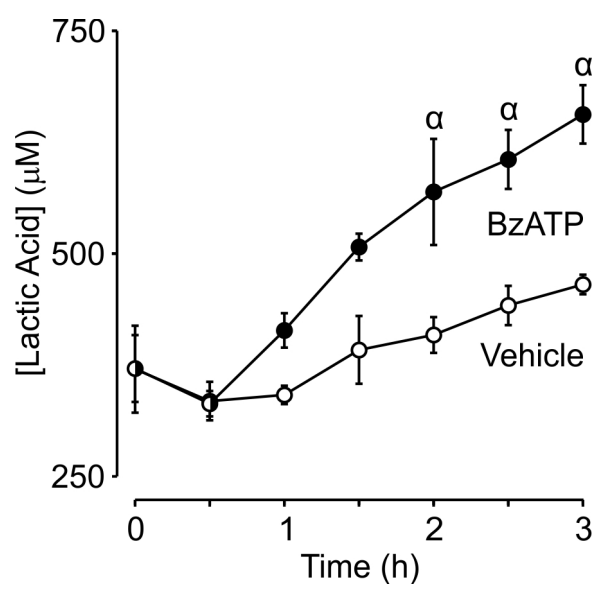


**Figure 3.9 BzATP Increases Lactate Production by MC3T3-E1 Cells.**

Cultures of MC3T3-E1 cells were bathed in serum-free  $\alpha$ -MEM supplemented with bovine albumin (1 mg/ml) and 1% antibiotic solution for 3 h, and subsequently treated with BzATP (300  $\mu$ M) or vehicle (beginning at time 0). Samples of extracellular medium were collected for lactate determination at the indicated times. To calculate lactate efflux (change in extracellular lactate concentration per hour), data were fit by linear regression from 0.5-3 h.  $\alpha$  indicates significant difference compared with vehicle at the same time point ( $p < 0.05$ ). Data are means  $\pm$  S.E.M. ( $n = 3$  samples from 3 independent preparations).



phase arising from enhanced rates of glycolytic metabolism.

### 3.4.6 Dependence of Nucleotide-induced Proton Efflux on $\text{Ca}^{2+}$

To characterize signaling mechanisms underlying the actions of nucleotides on proton efflux, we investigated the role of  $\text{Ca}^{2+}$  influx through P2X7 receptors. Since P2X7-induced  $\text{Ca}^{2+}$  signaling in cells of the osteoblast lineage had not been characterized previously, we first examined changes in  $[\text{Ca}^{2+}]_i$  of indo-1-loaded cells by fluorescence spectrophotometry. In MC3T3-E1 cells, BzATP (300  $\mu\text{M}$ ) induced both a transient and sustained increase in  $[\text{Ca}^{2+}]_i$ , whereas UTP or ATP (100  $\mu\text{M}$ ) elicited only a transient elevation (Figure 3.10 A). The initial transient increase in  $[\text{Ca}^{2+}]_i$  is likely due to activation of P2Y receptors, causing release of  $\text{Ca}^{2+}$  from intracellular stores. A 438079 (10  $\mu\text{M}$ ) blocked the sustained increase in  $[\text{Ca}^{2+}]_i$  elicited by BzATP in MC3T3-E1 cells (*not shown*). Moreover, UTP or ATP (100  $\mu\text{M}$ ) both elicited a transient elevation in  $[\text{Ca}^{2+}]_i$  in UMR-106 cells, whereas BzATP (300  $\mu\text{M}$ ) had no effect (Figure 3.10 B), consistent with a role for P2X7 in sustained  $\text{Ca}^{2+}$  signaling.

We next assessed the role of  $\text{Ca}^{2+}$  influx through P2X7 in initiating nucleotide-induced proton efflux. Parallel samples of MC3T3-E1 cells were superfused with  $\text{Ca}^{2+}$ -containing or  $\text{Ca}^{2+}$ -free medium. Superfusion with  $\text{Ca}^{2+}$ -free medium had no appreciable effect on basal proton efflux (Figure 3.11 A). Subsequently, cells were treated with BzATP (300  $\mu\text{M}$ ) or vehicle in the continued presence or absence of extracellular  $\text{Ca}^{2+}$ . Removal of  $\text{Ca}^{2+}$  from the superfusion medium abolished the BzATP-induced response (Figure 3.11 A). Upon reintroduction of  $\text{Ca}^{2+}$  to the superfusion medium, BzATP-induced proton efflux remained completely inhibited ( $10 \pm 9\%$ ) when compared with the sustained



**Figure 3.10 Patterns of  $[Ca^{2+}]_i$  Elevation Elicited by P2 Receptor Agonists.**

MC3T3-E1 cells (A) or UMR-106 cells (B) were loaded with the  $Ca^{2+}$ -sensitive dye indo-1 and suspended in  $Ca^{2+}$ -containing HEPES buffer in a fluorometric cuvette with continuous stirring.  $[Ca^{2+}]_i$  of parallel samples was monitored by fluorescence spectrophotometry. Where indicated by the arrows, vehicle, UTP (100  $\mu$ M), ATP (100  $\mu$ M, ATP low) or BzATP (300  $\mu$ M) was added directly to the cuvette. Data are representative traces from 3 to 4 independent preparations, each assayed in duplicate.

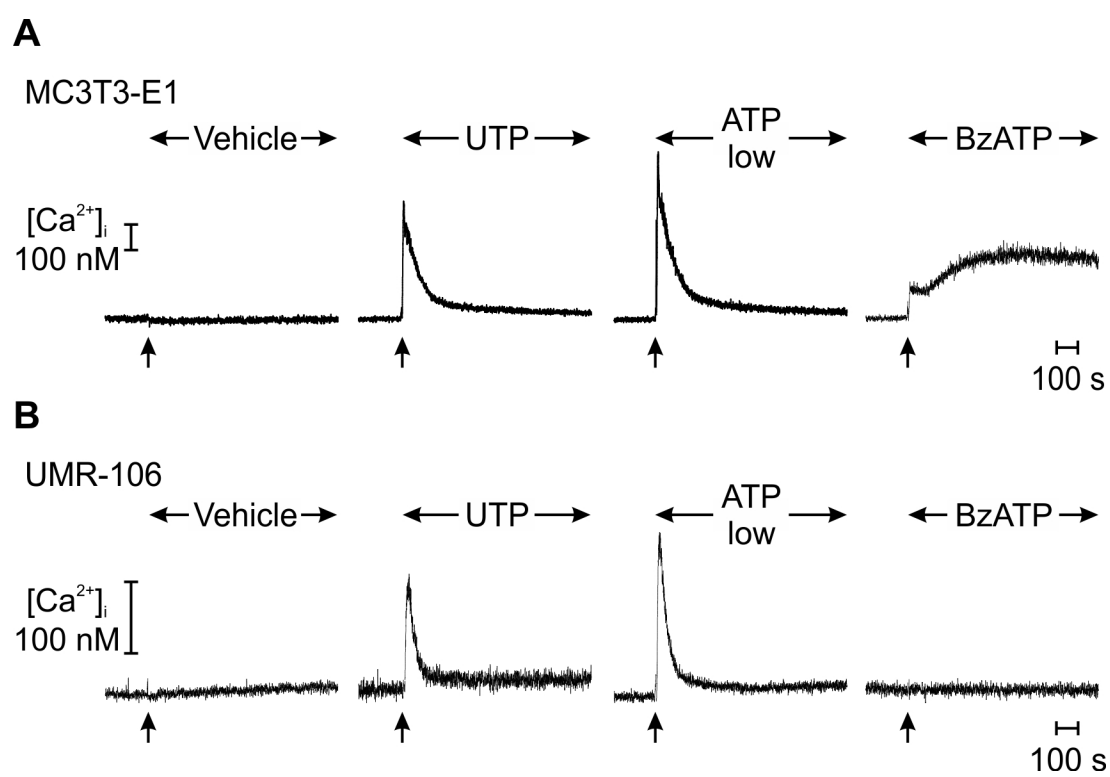
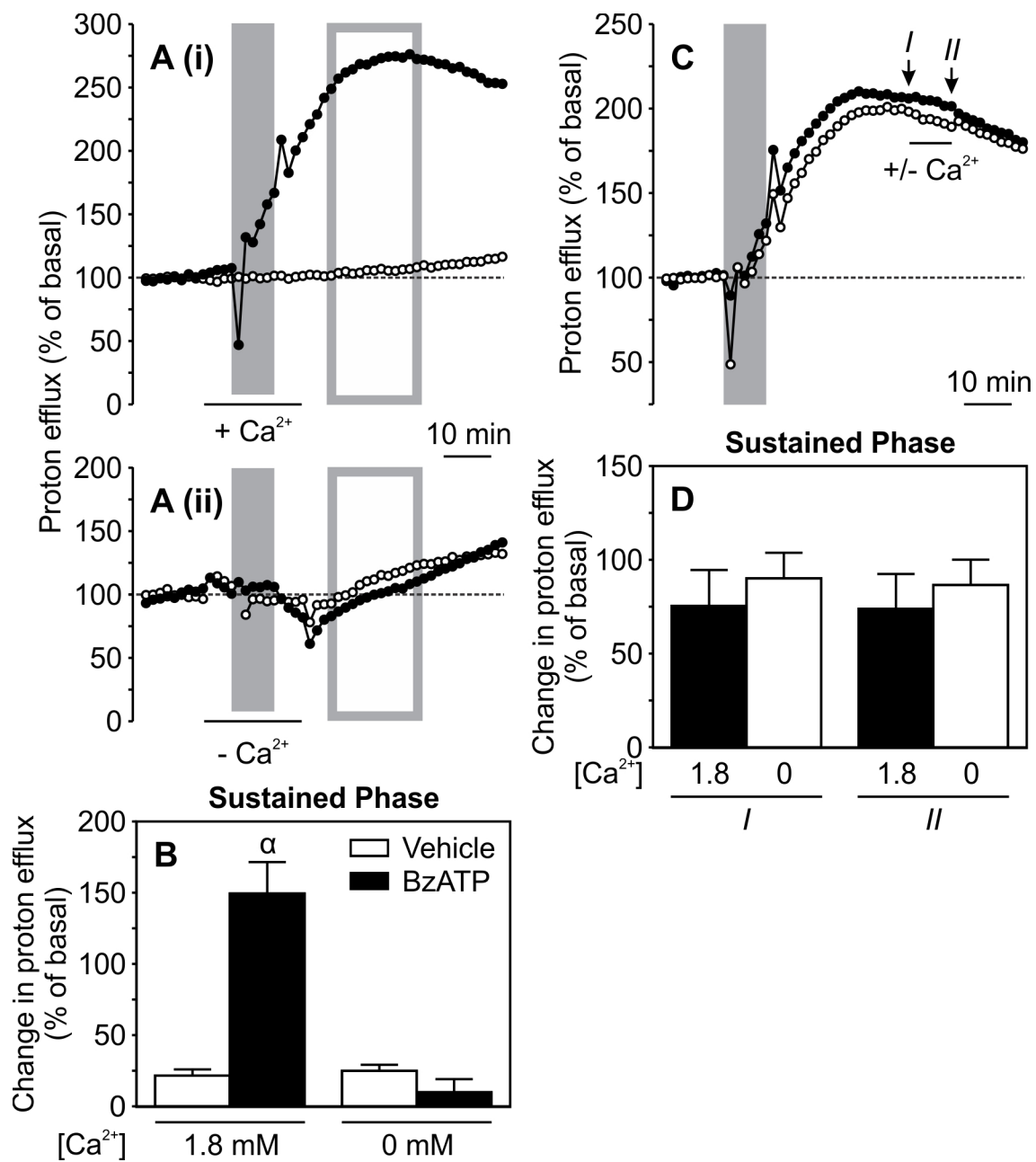


**Figure 3.11 Initiation of the BzATP-induced Increase in Proton Efflux is Dependent on Extracellular Ca<sup>2+</sup>.**

MC3T3-E1 cells were superfused with standard medium, and proton efflux was monitored. A, parallel samples of MC3T3-E1 cells were initially superfused with standard medium. Subsequently, samples were superfused with either Ca<sup>2+</sup>-containing medium (1.8 mM Ca<sup>2+</sup> (+ Ca<sup>2+</sup>), A (i)) or calcium-free medium with 0.5 mM EGTA (- Ca<sup>2+</sup>, A (ii)) for the period indicated by the *horizontal bar beneath the graph*. After 6 min, cultures in both A (i) and A (ii) were superfused with vehicle (*open symbols*) or BzATP (300 μM, *closed symbols*) where indicated by the *shaded areas*, in the continued presence of the appropriate medium. Data are representative traces from 5 independent preparations. B, amplitude of the sustained phase, quantified as the average increase in proton efflux above basal, 12-30 min after application of vehicle or BzATP (indicated by *gray-outlined boxes* in A (i-ii)).  $\alpha$  indicates significant difference compared with respective vehicle ( $p < 0.05$ ). Data are means  $\pm$  S.E.M. ( $n = 9-10$  samples from 5 independent preparations). C, where indicated by the *shaded area*, parallel samples of MC3T3-E1 cells were challenged with BzATP (300 μM) in standard running medium for 9 min. Subsequently, samples were superfused with either Ca<sup>2+</sup>-containing medium (1.8 mM Ca<sup>2+</sup> (+ Ca<sup>2+</sup>), *closed symbols*) or calcium-free medium with 0.5 mM EGTA (- Ca<sup>2+</sup>, *open symbols*) for 9 min, where indicated by the *horizontal bar beneath the graph*. Data are representative traces from 3-5 independent preparations. D, amplitude of the response, quantified as the change in proton efflux relative to basal, calculated at the times indicated by *I* and *II* in C. The *filled bars* represent responses of cells in the continuous presence of 1.8 mM Ca<sup>2+</sup>. The *unfilled bars* represent responses of cells exposed to Ca<sup>2+</sup>-free medium. Data are means  $\pm$  S.E.M. ( $n = 6-13$  samples from 3-5 independent preparations).



phase in control cells exposed to BzATP in the presence of extracellular  $\text{Ca}^{2+}$  ( $149 \pm 22\%$ ,  $p < 0.05$ ; Figure 3.11 B).

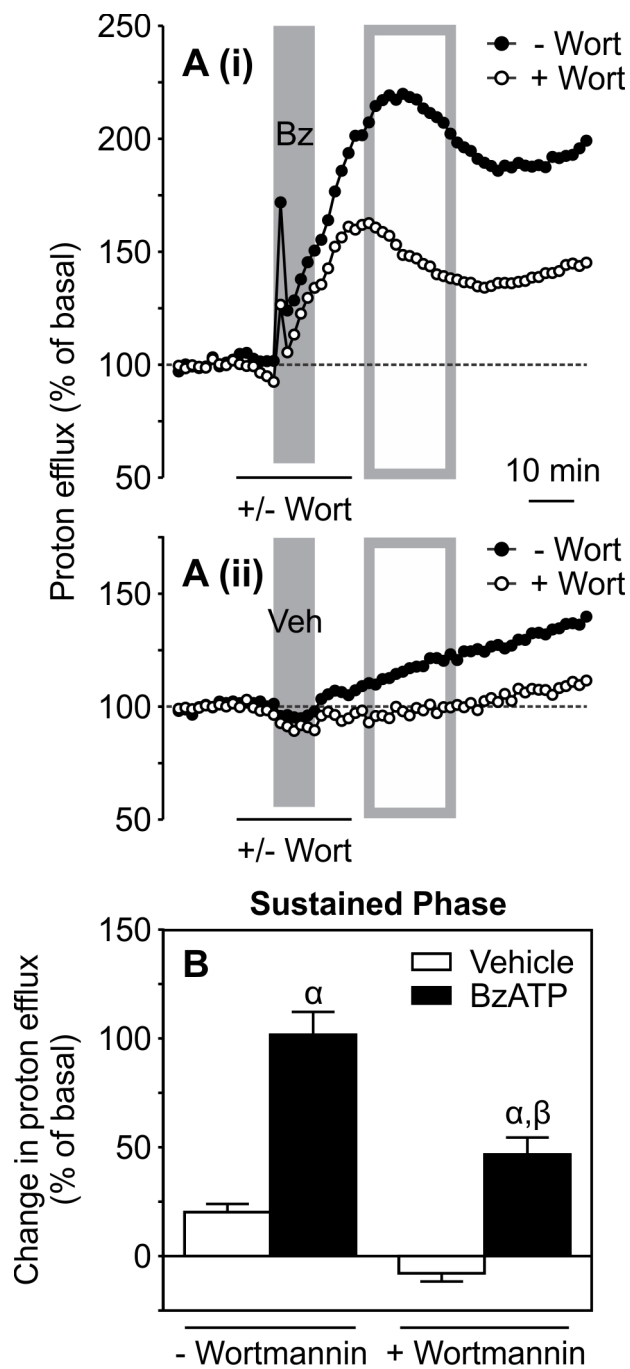
We then investigated the role of extracellular  $\text{Ca}^{2+}$  in maintaining the sustained phase of the BzATP-induced response (subsequent to its initiation). Parallel samples of MC3T3-E1 cells were treated with BzATP (300  $\mu\text{M}$ ) in standard medium and, during the sustained phase, BzATP-treated cells were superfused with either standard medium or  $\text{Ca}^{2+}$ -free medium. Removal of extracellular  $\text{Ca}^{2+}$  had no appreciable effect on proton efflux (Figure 3.11 C, D). Thus, initiation (but not maintenance) of the sustained phase requires the presence of extracellular  $\text{Ca}^{2+}$ , indicating that influx of  $\text{Ca}^{2+}$  through activated P2X7 receptors is necessary to trigger sustained proton efflux.

#### **3.4.7 Dependence of Nucleotide-induced Proton Efflux on PI3K Signaling**

Many growth factors and hormones stimulate cellular metabolism through activation of the PI3K-AKT pathway (Engelman et al., 2006; Hammerman et al., 2004). PI3K signaling also plays important roles in osteoblast differentiation (Fujita et al., 2004; Ghosh-Choudhury et al., 2002; Peng et al., 2003). Moreover, the PI3K pathway in osteoblasts mediates the increase in metabolic acid production induced by IGF-1 (Santhanagopal and Dixon, 1999). Consequently, it was of interest to explore whether P2X7 activates PI3K signaling in osteoblasts. To characterize the role of PI3K signaling in mediating the effects of nucleotides on proton efflux, parallel samples of MC3T3-E1 cells were first treated with the irreversible PI3K inhibitor wortmannin (100 nM) or its vehicle (DMSO) in standard superfusion medium for 9 min. Wortmannin slightly decreased basal proton efflux (Figure 3.12 A), suggesting that unstimulated metabolism

**Figure 3.12 The Irreversible PI3K Inhibitor Wortmannin Inhibits the Sustained Increase in Proton Efflux Induced by BzATP.**

MC3T3-E1 cells were superfused with standard medium, and proton efflux was monitored. A, parallel samples of MC3T3-E1 cells were initially superfused with standard medium. Subsequently, samples were superfused with either control (- Wort, *closed symbols*) or the irreversible PI3K inhibitor, wortmannin (100 nM, + Wort, *open symbols*), for the period indicated by the *horizontal bars beneath the graphs*. After 9 min, cultures were superfused with either BzATP (300  $\mu$ M, Bz, A (i)) or Vehicle (Veh, A (ii)) where indicated by the *shaded areas*, in the continued presence of the appropriate medium. Data are representative traces from 4 independent preparations. B, amplitude of the sustained phase, quantified as the average increase in proton efflux above basal, 12-30 min after application of vehicle or BzATP (indicated by *gray-outlined boxes* in panel A).  $\alpha$  indicates significant difference compared to respective vehicle ( $p < 0.05$ ).  $\beta$  indicates significant effect of wortmannin ( $p < 0.05$ ). Data are means  $\pm$  S.E.M. ( $n = 6-8$  samples from 4 independent preparations).



in osteoblast-like cells is partially dependent on PI3K activity. Subsequently, cells were treated with BzATP (300  $\mu$ M) or vehicle in the continued presence of wortmannin or DMSO (Figure 3.12 A). The PI3K inhibitor partially blocked the sustained phase of the BzATP response ( $41 \pm 8\%$ ) compared to parallel cultures treated with BzATP alone ( $104 \pm 13\%$ ,  $p < 0.05$ ; Figure 3.12 B)<sup>5</sup>.

To examine the role of PI3K signaling in initiation and maintenance of the sustained phase of the BzATP-induced response, we used LY 294002 – a specific and reversible PI3K inhibitor, structurally unrelated to wortmannin. To assess initiation, parallel samples of MC3T3-E1 cells were treated with LY 294002 (30  $\mu$ M) or its vehicle (DMSO) in standard superfusion medium for 15 min. Like wortmannin, LY 294002 decreased basal proton efflux (Figure 3.13 A), confirming that baseline metabolism in osteoblast-like cells is partially dependent on the PI3K activity. Subsequently, cells were treated with BzATP (300  $\mu$ M) or vehicle in the continued presence of LY 294002 or DMSO (Figure 3.13 A). LY 294002 significantly inhibited the sustained phase of the BzATP response ( $34 \pm 6\%$ ; *Point I*, Figure 3.13 B) compared to parallel cultures treated with BzATP in the absence of the inhibitor ( $82 \pm 10\%$ ; *Point I*, Figure 3.13 B)<sup>6</sup>. Interestingly, upon washout of LY 294002, proton efflux recovered to levels comparable with those observed in control cells exposed to BzATP in the presence of DMSO (*Point II*, Figure 3.13 B). Thus, PI3K activity is not essential to trigger the sustained phase of

---

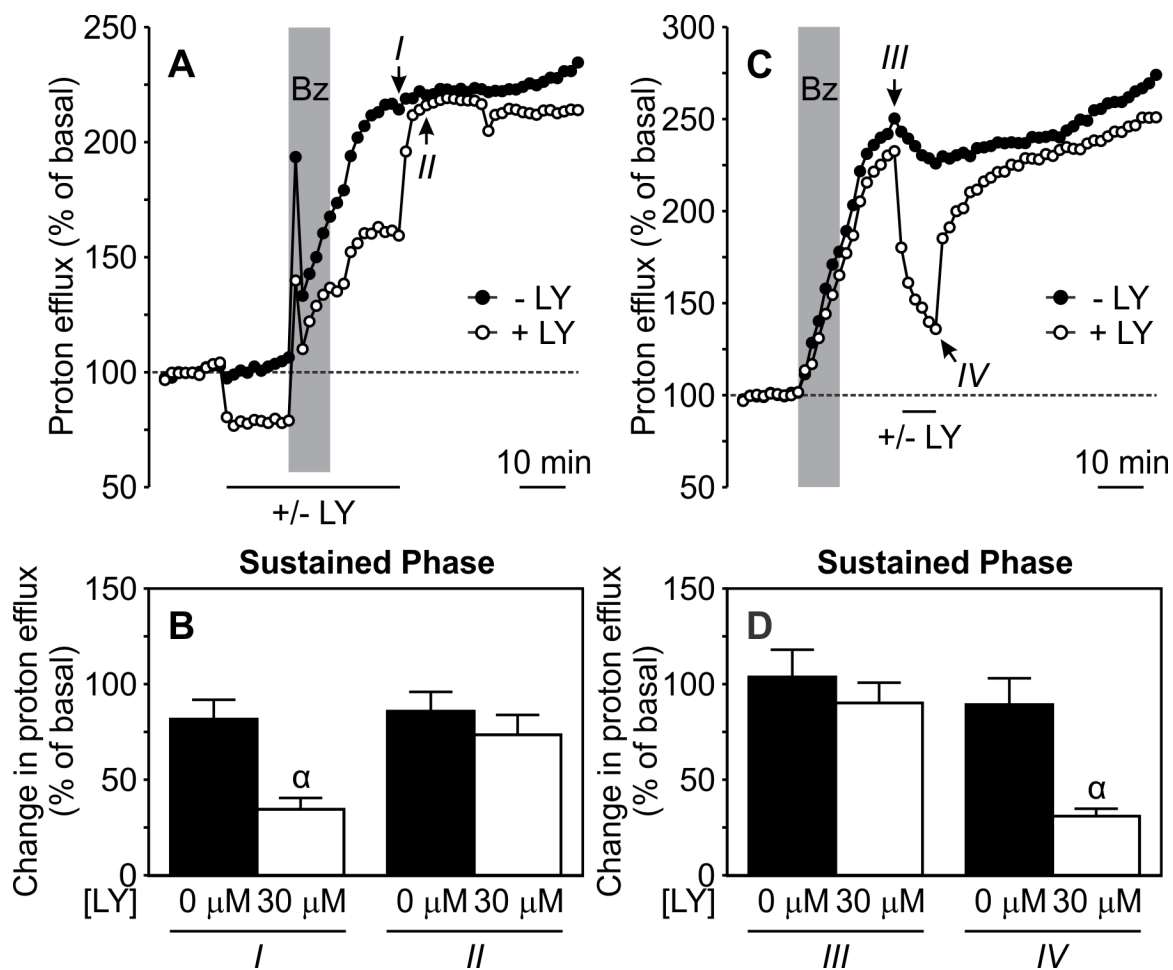
<sup>5</sup> Since wortmannin suppressed basal proton efflux compared to DMSO alone, data were also corrected for the effects of wortmannin on baseline at the sustained phase. Even with values corrected, the PI3K inhibitor still significantly blocked the sustained phase of the BzATP response ( $69 \pm 16\%$ ) compared to parallel cultures treated with BzATP in the absence of inhibitor ( $104 \pm 20\%$ ).

<sup>6</sup> Since LY294002 suppressed basal proton efflux compared to DMSO alone, data were also corrected for the effects of LY 294002 on baseline. Even with values corrected, the PI3K inhibitor still significantly blocked the sustained phase of the BzATP response ( $50 \pm 12\%$ ) compared to parallel cultures treated with BzATP in absence of inhibitor ( $90 \pm 17\%$ ).



**Figure 3.13 The Reversible PI3K Inhibitor LY 294002 Inhibits Maintenance of the Sustained Increase in Proton Efflux Induced by BzATP.**

MC3T3-E1 cells were superfused with standard medium, and proton efflux was monitored. A, parallel samples of MC3T3-E1 cells were initially superfused with standard medium. Subsequently, samples were superfused with either control (- LY, *closed symbols*) or the reversible PI3K inhibitor, LY 294002 (30  $\mu$ M, + LY, *open symbols*), for the period indicated by the *horizontal bar beneath the graph*. After 15 min, cultures were superfused with BzATP (300  $\mu$ M, Bz) or vehicle (not shown) where indicated by the *shaded areas*, in the continued presence of the appropriate medium. Data are representative traces from 5 independent preparations. B, amplitude of the response, quantified as the change in proton efflux relative to basal, calculated at the times indicated by *I* and *II* in panel A.  $\alpha$  indicates significant effect of LY 294002 ( $p < 0.05$ ). Data are means  $\pm$  S.E.M. ( $n = 7-10$  samples from 5 independent preparations). C, where indicated by the *shaded area*, parallel samples of MC3T3-E1 cells were challenged with BzATP (300  $\mu$ M, Bz) in standard running medium for 9 min. Subsequently, samples were superfused with either control (- LY, *closed symbols*) or LY 294002 (+ LY, *open symbols*) for 9 min, where indicated by the *horizontal bar beneath the graph*. Data are representative traces from 3 independent preparations. D, amplitude of the response, quantified as the change in proton efflux relative to basal, calculated at the times indicated by *III* and *IV* in panel C.  $\alpha$  indicates significant effect of LY 294002 ( $p < 0.05$ ). Data are means  $\pm$  S.E.M. ( $n = 7$  samples from 3 independent preparations).



nucleotide-induced proton efflux.

To assess the role of PI3K signaling in maintenance of the sustained phase of the BzATP-induced proton efflux, parallel samples were treated with BzATP (300  $\mu$ M) and subsequently superfused with either LY 294002 (30  $\mu$ M) or DMSO for 9 min, before returning to standard superfusion medium (Figure 3.13 C). LY 294002 caused a significant decrease in proton efflux ( $31 \pm 4\%$ ; *Point IV*, Figure 3.13 D) compared to cells treated with BzATP in the absence of inhibitor ( $89 \pm 14\%$ ; *Point IV*, Figure 3.13 D)<sup>7</sup>. Consistent with its reversibility, removal of LY 294002 from the superfusion medium resulted in complete recovery of proton efflux to levels comparable with the sustained phase observed in cells exposed to BzATP in the absence of inhibitor (Figure 3.13 C). Thus, maintenance of the sustained phase, but not its initiation, is dependent on PI3K activity.

---

<sup>7</sup> Since LY294002 suppressed basal proton efflux compared to DMSO alone (not shown), data were corrected for the effects of LY 294002 on baseline. With values corrected, LY294002 still significantly blocked the sustained phase of the BzATP response ( $37 \pm 6\%$ ) compared to parallel cultures treated with BzATP alone ( $105 \pm 21\%$ ).

### **3.5 Discussion**

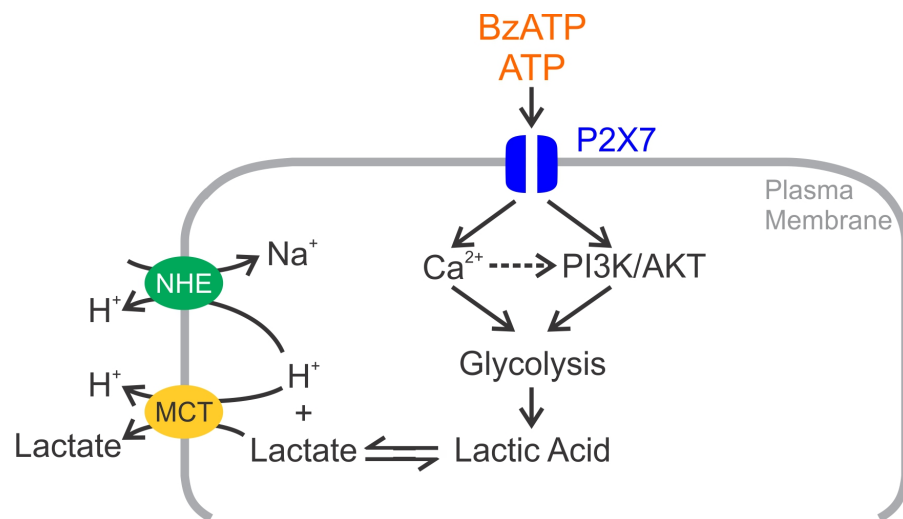
The P2X7 receptor plays a role in the regulation of osteogenesis (Ke et al., 2003; Panupinthu et al., 2008) and is required for full response of the skeleton to mechanical loading (Li et al., 2005), but the mechanisms underlying its effects in osteoblasts are poorly understood. In this study, we examined changes in cellular metabolism triggered by activation of endogenous P2 nucleotide receptors in osteoblast-like cells. We show for the first time in any system that brief activation of P2X7 elicits a large and sustained increase in metabolic acid production that requires  $\text{Ca}^{2+}$  for initiation and is maintained by PI3K signaling, resulting in enhanced glucose metabolism (Figure 3.14). As well, this is the first report that, in osteoblast-like cells, P2X7 couples to sustained  $\text{Ca}^{2+}$  and PI3K signaling – pathways known to enhance osteoblast differentiation, leading to increased bone formation.

#### **3.5.1 BzATP Elicits Membrane Blebbing in Osteoblast-like Cells Expressing the P2X7 Receptor**

In this study, we investigated the effects of P2X7 receptor activation on osteoblast metabolism. Whereas UMR-106 cells do not express P2X7 (Panupinthu et al., 2008), studies by others have confirmed expression of this receptor in MC3T3-E1 cells by RT-PCR (Qi et al., 2007; Okumura et al., 2008), Western blot and pore formation assays (Li et al., 2005). However, as pore formation has been observed for other P2X receptor subtypes, including P2X2, P2X2/3 and P2X4 (North, 2002), it cannot be used to demonstrate specifically the expression of functional P2X7 receptors. Membrane blebbing is a characteristic unique to activation of P2X7 (North, 2002). In the present

**Figure 2.14 Proposed Role for P2X7 Receptor Signaling in Regulation of the PI3K/AKT Pathway and Cellular Metabolism.**

Osteoblasts are subjected to a number of metabolic demands during differentiation and in the production and mineralization of the bone extracellular matrix. The P2X7 nucleotide receptor promotes osteoblast differentiation and matrix mineralization. Brief activation of P2X7 in osteoblast-like cells elicits a large sustained increase in proton efflux, which is associated with elevated lactic acid production. Initiation of this metabolic response is dependent on  $\text{Ca}^{2+}$  influx through activated P2X7 receptors, whereas maintenance is dependent on PI3K activity and availability of extracellular glucose. Interestingly,  $\text{Ca}^{2+}$  has been shown to activate PI3K in other systems through Pyk2 and Ras. Taken together, this study shows for the first time that P2X7 signaling promotes aerobic glycolysis and PI3K/AKT signaling in cells of the osteoblast lineage – two processes known to enhance osteoblast differentiation, leading to increased bone formation.



study, we demonstrated that MC3T3-E1 osteoblast-like cells, but not UMR-106 osteosarcoma cells, display blebbing in response to BzATP. Previous work from our lab has shown that BzATP or high concentrations of ATP induce formation of plasma membrane blebs in approximately 40% of cultured rat and murine calvarial cells (Panupinthu et al., 2007), providing evidence for heterogeneous expression of functional P2X7 receptors in calvarial cell cultures. In contrast, over 85% of MC3T3-E1 cells exhibited membrane blebbing following stimulation of P2X7, indicating that these cells represent a more homogenous population with respect to expression of functional P2X7. Thus, the MC3T3-E1 cell line was an ideal model with which to assess signaling and metabolic pathways activated by stimulation of endogenous P2X7 receptors.

### **3.5.2 P2X7 Receptors Stimulate Sustained Proton Efflux**

In the present study, we demonstrated that the P2X7 agonist BzATP (300  $\mu$ M) elicits a sustained increase in metabolic acid production by osteoblast-like cells. However, as osteoblasts express multiple P2 receptor subtypes, it was possible that the sustained increase in proton efflux elicited by BzATP was not activated specifically by P2X7 receptors. In this regard, low concentrations of ATP or UTP (100  $\mu$ M), which activate other P2 receptors but not P2X7, elicited only a transient increase in proton efflux that, upon removal of either agonist, returned to basal levels. These responses are in keeping with changes in proton efflux previously reported for ATP or UTP (10  $\mu$ M) in primary astrocyte cultures (Dixon et al., 2004). In contrast, a high concentration of ATP (1 mM), known to activate the P2X7 receptor, recapitulated the sustained increase in proton efflux elicited by BzATP. Providing further evidence for involvement of P2X7,

BzATP did not elicit a sustained increase in proton efflux from UMR-106 cells, which do not express the P2X7 receptor. Moreover, we showed that the BzATP-induced response in MC3T3-E1 cells was blocked by A 438079 and A 740003, recently developed antagonists that specifically block P2X7 (Nelson et al., 2006; Donnelly-Roberts and Jarvis, 2007).

The sustained phase of P2X7-induced proton efflux observed in this study is consistent with a net increase in metabolic acid production, rather than simply activation of proton efflux pathways. Had only proton efflux mechanisms been activated, the response would have been transient, lasting only until a more alkaline steady-state cytosolic pH was established. Such transient responses are often mediated by activation of Na<sup>+</sup>/H<sup>+</sup> exchangers (NHEs), associated with phospholipase C (PLC)-mediated mobilization of Ca<sup>2+</sup> from intracellular stores. In contrast, sustained proton efflux with delayed onset that persists even after removal of the agonist (as observed in this study) generally involves activation of protein kinases (McConnell et al., 1992) (*see below*).

The mechanisms underlying P2X7-induced acid production are unclear, but may involve increased ATP hydrolysis or efflux (Burnstock, 2008), lipolysis or glycogenolysis, followed by glycolysis (producing lactic acid) or oxidative phosphorylation (producing carbonic acid). In the present study, the sustained increase in proton efflux was dependent on the presence of extracellular glucose. Moreover, activation of P2X7 was associated with an increase in lactate efflux that was sustained for at least 3 h, establishing that the response was due, at least in part, to stimulation of glycolytic metabolism. These findings are in contrast to those previously reported for growth factor effects in osteoblasts, in which IGF-1-induced proton efflux was



independent of extracellular glucose (Santhanagopal and Dixon, 1999).

### **3.5.3 Dependence of P2X7-induced Proton Efflux on $\text{Ca}^{2+}$**

Stimulation of P2X7 triggers rapid and sustained elevations of  $[\text{Ca}^{2+}]_i$  in HEK293 cells heterologously expressing P2X7 receptors (Gudipaty et al., 2003). Such elevations in  $[\text{Ca}^{2+}]_i$  mediate a number of important physiological functions in many cell-types, including inhibition of neuritogenesis in the Neuro-2a neuroblastoma cell line (Gomez-Villafuertes et al., 2009), neuroprotection in primary cerebellar granular neurons (Ortega et al., 2009), and regulation of interleukin (IL)-1 $\beta$  secretion from monocytes and macrophages (Gudipaty et al., 2003). In the present study, we demonstrated that stimulation of osteoblasts with BzATP elicits a biphasic elevation in  $[\text{Ca}^{2+}]_i$ , consisting of an initial transient and sustained phase. The initial transient increase in  $[\text{Ca}^{2+}]_i$  induced by nucleotides has been shown previously to be due to activation of P2Y receptors, leading to release of  $\text{Ca}^{2+}$  from intracellular stores (Reimer and Dixon, 1992; Gudipaty et al., 2003). Consistent with these reports, we showed that activation of P2Y receptors by UTP elicited only an initial transient increase in proton efflux in osteoblasts. That BzATP also elicited a rapid  $\text{Ca}^{2+}$  transient in osteoblasts is consistent with BzATP activating P2 receptors other than P2X7 in MC3T3-E1 cells. In contrast, the sustained  $\text{Ca}^{2+}$  elevation elicited by BzATP is mediated specifically by the P2X7 receptor and arises by influx of  $\text{Ca}^{2+}$  from the extracellular milieu.

The similarity in patterns of  $\text{Ca}^{2+}$  signaling and proton efflux induced by exogenous nucleotides suggests a role for  $\text{Ca}^{2+}$  in regulation of proton production downstream of P2 receptors in osteoblasts. In this regard, we observed that extracellular

$\text{Ca}^{2+}$  is required to initiate, but not maintain, BzATP-induced proton efflux.  $\text{Ca}^{2+}$  influx through activated P2X7 receptors may directly stimulate proton efflux, independent of cellular metabolism. For instance,  $\text{Ca}^{2+}$  can acidify the cytosol by displacing protons from common binding sites (Austin and Wray, 2000).  $\text{Ca}^{2+}$  also increases the rate at which NHE1 transports protons from the cytosol to the extracellular fluid (Okada et al., 2002). However, these two mechanisms would only give rise to transient increases in proton efflux. Thus, influx of  $\text{Ca}^{2+}$  through the P2X7 receptor appears to modulate cellular metabolism.

Cytosolic  $\text{Ca}^{2+}$  is a known regulator of ATP synthesis and utilization, thereby affecting the formation of acid metabolites (lactic and carbonic acids) (Balaban, 1990; Smart and Wood, 2000). Several dehydrogenases of the citric acid cycle, including pyruvate dehydrogenase, isocitrate dehydrogenase,  $\alpha$ -ketoglutarate dehydrogenase, succinate dehydrogenase and malate dehydrogenase, are positively regulated by elevations in mitochondrial  $[\text{Ca}^{2+}]$ , resulting in enhanced rates of oxidative phosphorylation (Denton, 2009; Griffiths and Rutter, 2009). Mitochondrial  $[\text{Ca}^{2+}]$  may also directly regulate the ATP synthase complex to increase ATP production (Denton, 2009). In this regard, HEK293 and HeLa cells heterologously expressing P2X7 exhibit more mitochondria with hyperpolarized transmembrane potentials, and greater basal mitochondrial  $\text{Ca}^{2+}$  and intracellular ATP content than non-transfected cells (Adinolfi et al., 2005a). These effects are presumably dependent on tonic stimulation of P2X7 by secreted ATP, and implicate P2X7 in the positive regulation of cellular metabolism. On the other hand, Adinolfi and coworkers (Adinolfi et al., 2005a) provide evidence that stimulation of these heterologous P2X7 receptors by exogenous ATP causes

depolarization of the mitochondrial transmembrane potential that is accompanied by a large increase in mitochondrial  $[Ca^{2+}]$ , mitochondrial fragmentation and cell death. Interestingly, we confirmed a previous report (Li et al., 2005) that stimulation of endogenous P2X7 receptors in MC3T3-E1 cells does not elicit cell death. This discrepancy highlights potential differences in signaling by endogenously *versus* heterologously expressed P2X7 receptors.

#### **3.5.4 Role of PI3K in Mediating P2X7-induced Proton Efflux**

There are few reports concerning regulation of the PI3K-AKT pathway by P2X7 in any cell type, and opposing effects have been described. For instance, stimulation of P2X7 in non-small cell lung cancer, HepG2 liver hepatocyte and Panc1 human pancreatic cell lines decreases constitutive and insulin-induced total and nuclear phosphorylated AKT (Mistafa et al., 2008; Mistafa and Stenius, 2009). Moreover, in Neuro-2a neuroblastoma cells, inhibition or knockdown of P2X7 led to increased AKT phosphorylation and activity (Gomez-Villafuertes et al., 2009). In contrast, BzATP acts through P2X7 receptors to stimulate PI3K-dependent AKT phosphorylation in cultures of rat astrocytes and cerebellar granular neurons (Jacques-Silva et al., 2004; Liu et al., 2010; Ortega et al., 2010). Consistent with the latter, we observed that PI3K activity is required to maintain proton efflux downstream of the P2X7 receptor, demonstrating that PI3K signaling is sustained for an extended period of time following activation of P2X7 in osteoblast-like cells.

Several mechanisms may underlie the coupling of P2X7 to activation of the PI3K-AKT pathway. In cultures of rat cortical astrocytes, activation of P2X7, as well as other

P2 receptors, stimulated AKT phosphorylation in a manner dependent upon extracellular and cytosolic  $\text{Ca}^{2+}$ , PI3K and a Src family kinase (Jacques-Silva et al., 2004; Liu et al., 2010). The lipid kinase PI4K is one of many signaling proteins that form the P2X7 receptor complex; a complex that, in part, is responsible for signaling downstream of P2X7 (Kim et al., 2001). It has been suggested that phosphatidylinositol-4-phosphate (generated by PI4K following stimulation of the P2X7 receptor) may serve as a substrate for PI3K leading to activation of AKT (Jacques-Silva et al., 2004). Elevations in  $[\text{Ca}^{2+}]_i$  also appear critical in coupling P2X7 to activation of the PI3K-AKT pathway. In this regard, heterologously expressed P2X7 activates the proline-rich/ $\text{Ca}^{2+}$ -activated tyrosine kinase Pyk2 (Gendron et al., 2003), a kinase that associates with Src tyrosine kinases to stimulate the Ras-PI3K pathway (Kodaki et al., 1994).  $\text{Ca}^{2+}$  can also trigger AKT phosphorylation through CaMKK, independent of Pyk2, Src tyrosine kinases or PI3K (Yano et al., 1998). Ultimately, additional studies will be needed to determine how P2X7 couples to PI3K signaling in cells of the osteoblast lineage.

The PI3K-AKT pathway regulates several cellular processes that may contribute to proton efflux; these include uptake of nutrients such as amino acids and glucose, the activity of several glycolytic enzymes and ATP production (Hammerman et al., 2004; Engelman et al., 2006). For example, AKT directly increases activities of the glycolytic enzymes hexokinase and phosphofructokinase-2 in Rat1a fibroblasts and cardiac muscle, respectively. The importance of the PI3K-AKT pathway in regulation of glycolytic metabolism is in keeping with our results demonstrating that BzATP-induced increase in proton efflux is dependent on extracellular glucose and PI3K activity, and arises at least in part from increased rates of lactic acid production and efflux.

### **3.5.5 Potential Physiological Roles of P2X7-induced Ca<sup>2+</sup> Elevation, PI3K Signaling and Proton Efflux in Osteoblast Regulation and Function**

To the best of our knowledge, the present study is the first to report that P2X7 couples to sustained Ca<sup>2+</sup> and PI3K signaling in osteoblasts. Interestingly, both the Ca<sup>2+</sup>-NFATc1 (Koga et al., 2005) and PI3K-AKT (Fujita et al., 2004) pathways play important roles in osteoblast differentiation. Activation of the PI3K-AKT pathway also enhances survival in many cell-types (Hammerman et al., 2004; Engelman et al., 2006); a phenomenon that may explain the resistance of osteoblasts to P2X7-induced apoptosis seen in several other cell-types (Adinolfi et al., 2005a).

It is possible that metabolic acid production induced by P2X7 plays a role in osteoblast function. During the synthesis and secretion of osteoid by active osteoblasts *in vivo*, the pH<sub>o</sub> in the region between the osteoblast layer and the mineralizing front affects both the rate of mineral formation and its phase transformation. An acidic zone beneath the active osteoblast layer may prevent premature mineralization of the osteoid seam during bone formation. It is also possible that acid production by cells of the osteoblast lineage activates osteoclastic bone resorption (Arnett and Spowage, 1996; Komarova et al., 2005; Pereverzev et al., 2008). *In vitro* studies of pit formation by rat osteoclasts have shown that there is little, if any, resorptive activity at values of pH<sub>o</sub> >7.3. Slight decreases in pH<sub>o</sub> markedly stimulate osteoclastic resorption, which is maximally active at values <7.0 (Arnett and Spowage, 1996). Taken together, the effects of P2X7 on Ca<sup>2+</sup> and PI3K signaling, as well as metabolic acid production, described in the present study may help to explain the mechanism by which P2X7 promotes osteogenesis *in vivo*.

### 3.6 References

- Adinolfi, E., M.G. Callegari, D. Ferrari, C. Bolognesi, M. Minelli, M.R. Wieckowski, P. Pinton, R. Rizzuto, and F. Di Virgilio. 2005a. Basal activation of the P2X7 ATP receptor elevates mitochondrial calcium and potential, increases cellular ATP levels, and promotes serum-independent growth. *Mol Biol Cell*. 16:3260-3272.
- Adinolfi, E., C. Pizzirani, M. Idzko, E. Panther, J. Norgauer, F. Di Virgilio, and D. Ferrari. 2005b. P2X(7) receptor: Death or life? *Purinergic Signal*. 1:219-227.
- Arnett, T.R., and M. Spowage. 1996. Modulation of the resorptive activity of rat osteoclasts by small changes in extracellular pH near the physiological range. *Bone*. 18:277-279.
- Austin, C., and S. Wray. 2000. Interactions between  $\text{Ca}^{2+}$  and  $\text{H}^{+}$  and functional consequences in vascular smooth muscle. *Circ Res*. 86:355-363.
- Balaban, R.S. 1990. Regulation of oxidative phosphorylation in the mammalian cell. *Am J Physiol*. 258:C377-389.
- Bianchi, B.R., K.J. Lynch, E. Touma, W. Niforatos, E.C. Burgard, K.M. Alexander, H.S. Park, H. Yu, R. Metzger, E. Kowaluk, M.F. Jarvis, and T. van Biesen. 1999. Pharmacological characterization of recombinant human and rat P2X receptor subtypes. *Eur J Pharmacol*. 376:127-138.
- Burnstock, G. 2007. Physiology and pathophysiology of purinergic neurotransmission. *Physiol Rev*. 87:659-797.
- Burnstock, G. 2008. Unresolved issues and controversies in purinergic signalling. *J Physiol*. 586:3307-3312.
- Chen, C.T., Y.R. Shih, T.K. Kuo, O.K. Lee, and Y.H. Wei. 2008. Coordinated changes of mitochondrial biogenesis and antioxidant enzymes during osteogenic differentiation of human mesenchymal stem cells. *Stem Cells*. 26:960-968.
- Communi, D., B. Robaye, and J.M. Boeynaems. 1999. Pharmacological characterization of the human P2Y<sub>11</sub> receptor. *Br J Pharmacol*. 128:1199-1206.
- Denton, R.M. 2009. Regulation of mitochondrial dehydrogenases by calcium ions. *Biochim Biophys Acta*. 1787:1309-1316.
- Dixon, S.J., and S.M. Sims. 2000. P2 purinergic receptors on osteoblasts and osteoclasts: Potential targets for drug development. *Drug Dev Res*. 49:187-200.
- Dixon, S.J., R. Yu, N. Panupinthu, and J.X. Wilson. 2004. Activation of P2 nucleotide receptors stimulates acid efflux from astrocytes. *Glia*. 47:367-376.

- Donnelly-Roberts, D.L., and M.F. Jarvis. 2007. Discovery of P2X7 receptor-selective antagonists offers new insights into P2X7 receptor function and indicates a role in chronic pain states. *Br J Pharmacol.* 151:571-579.
- Engelman, J.A., J. Luo, and L.C. Cantley. 2006. The evolution of phosphatidylinositol 3-kinases as regulators of growth and metabolism. *Nat Rev Genet.* 7:606-619.
- Fujita, T., Y. Azuma, R. Fukuyama, Y. Hattori, C. Yoshida, M. Koida, K. Ogita, and T. Komori. 2004. Runx2 induces osteoblast and chondrocyte differentiation and enhances their migration by coupling with PI3K-Akt signaling. *J Cell Biol.* 166:85-95.
- Gartland, A., K.A. Buckley, R.A. Hipskind, M.J. Perry, J.H. Tobias, G. Buell, I. Chessell, W.B. Bowler, and J.A. Gallagher. 2003. Multinucleated osteoclast formation *in vivo* and *in vitro* by P2X7 receptor-deficient mice. *Crit Rev Eukaryot Gene Expr.* 13:243-253.
- Gartland, A., R.A. Hipskind, J.A. Gallagher, and W.B. Bowler. 2001. Expression of a P2X7 receptor by a subpopulation of human osteoblasts. *J Bone Miner Res.* 16:846-856.
- Gendron, F.P., J.T. Neary, P.M. Theiss, G.Y. Sun, F.A. Gonzalez, and G.A. Weisman. 2003. Mechanisms of P2X7 receptor-mediated ERK1/2 phosphorylation in human astrocytoma cells. *Am J Physiol Cell Physiol.* 284:C571-581.
- Genetos, D.C., D.J. Geist, D. Liu, H.J. Donahue, and R.L. Duncan. 2005. Fluid shear-induced ATP secretion mediates prostaglandin release in MC3T3-E1 osteoblasts. *J Bone Miner Res.* 20:41-49.
- Ghosh-Choudhury, N., S.L. Abboud, R. Nishimura, A. Celeste, L. Mahimainathan, and G.G. Choudhury. 2002. Requirement of BMP-2-induced phosphatidylinositol 3-kinase and Akt serine/threonine kinase in osteoblast differentiation and Smad-dependent BMP-2 gene transcription. *J Biol Chem.* 277:33361-33368.
- Gomez-Villafuertes, R., A. del Puerto, M. Diaz-Hernandez, D. Bustillo, J.I. Diaz-Hernandez, P.G. Huerta, A.R. Artalejo, J.J. Garrido, and M.T. Miras-Portugal. 2009. Ca<sup>2+</sup>/calmodulin-dependent kinase II signalling cascade mediates P2X7 receptor-dependent inhibition of neuritegenesis in neuroblastoma cells. *FEBS J.* 276:5307-5325.
- Griffiths, E.J., and G.A. Rutter. 2009. Mitochondrial calcium as a key regulator of mitochondrial ATP production in mammalian cells. *Biochim Biophys Acta.* 1787:1324-1333.
- Grol, M.W., N. Panupinthu, J. Korcok, S.M. Sims, and S.J. Dixon. 2009. Expression, signaling, and function of P2X7 receptors in bone. *Purinergic Signal.*

- Gudipaty, L., J. Munetz, P.A. Verhoef, and G.R. Dubyak. 2003. Essential role for  $\text{Ca}^{2+}$  in regulation of IL-1 $\beta$  secretion by P2X<sub>7</sub> nucleotide receptor in monocytes, macrophages, and HEK-293 cells. *Am J Physiol Cell Physiol*. 285:C286-299.
- Hammerman, P.S., C.J. Fox, and C.B. Thompson. 2004. Beginnings of a signal-transduction pathway for bioenergetic control of cell survival. *Trends Biochem Sci*. 29:586-592.
- Harada, S., and G.A. Rodan. 2003. Control of osteoblast function and regulation of bone mass. *Nature*. 423:349-355.
- Jacques-Silva, M.C., R. Rodnight, G. Lenz, Z. Liao, Q. Kong, M. Tran, Y. Kang, F.A. Gonzalez, G.A. Weisman, and J.T. Neary. 2004. P2X<sub>7</sub> receptors stimulate AKT phosphorylation in astrocytes. *Br J Pharmacol*. 141:1106-1117.
- Ke, H.Z., H. Qi, A.F. Weidema, Q. Zhang, N. Panupinthu, D.T. Crawford, W.A. Grasser, V.M. Paralkar, M. Li, L.P. Audoly, C.A. Gabel, W.S. Jee, S.J. Dixon, S.M. Sims, and D.D. Thompson. 2003. Deletion of the P2X<sub>7</sub> nucleotide receptor reveals its regulatory roles in bone formation and resorption. *Mol Endocrinol*. 17:1356-1367.
- Khakh, B.S., and R.A. North. 2006. P2X receptors as cell-surface ATP sensors in health and disease. *Nature*. 442:527-532.
- Kim, M., L.H. Jiang, H.L. Wilson, R.A. North, and A. Surprenant. 2001. Proteomic and functional evidence for a P2X<sub>7</sub> receptor signalling complex. *EMBO J*. 20:6347-6358.
- Kodaki, T., R. Woscholski, B. Hallberg, P. Rodriguez-Viciana, J. Downward, and P.J. Parker. 1994. The activation of phosphatidylinositol 3-kinase by Ras. *Curr Biol*. 4:798-806.
- Koga, T., Y. Matsui, M. Asagiri, T. Kodama, B. de Crombrughe, K. Nakashima, and H. Takayanagi. 2005. NFAT and Osterix cooperatively regulate bone formation. *Nat Med*. 11:880-885.
- Komarova, S.V., F.I. Ataulakhanov, and R.K. Globus. 2000. Bioenergetics and mitochondrial transmembrane potential during differentiation of cultured osteoblasts. *Am J Physiol Cell Physiol*. 279:C1220-1229.
- Komarova, S.V., A. Pereverzev, J.W. Shum, S.M. Sims, and S.J. Dixon. 2005. Convergent signaling by acidosis and receptor activator of NF- $\kappa$ B ligand (RANKL) on the calcium/calcineurin/NFAT pathway in osteoclasts. *Proc Natl Acad Sci U S A*. 102:2643-2648.
- Li, J., D. Liu, H.Z. Ke, R.L. Duncan, and C.H. Turner. 2005. The P2X<sub>7</sub> nucleotide receptor mediates skeletal mechanotransduction. *J Biol Chem*. 280:42952-42959.



- Liu, Y.P., C.S. Yang, M.C. Chen, S.H. Sun, and S.F. Tzeng. 2010.  $\text{Ca}^{2+}$ -dependent reduction of glutamate aspartate transporter GLAST expression in astrocytes by P2X<sub>7</sub> receptor-mediated phosphoinositide 3-kinase signaling. *J Neurochem.* 113:213-227.
- McConnell, H.M., J.C. Owicki, J.W. Parce, D.L. Miller, G.T. Baxter, H.G. Wada, and S. Pitchford. 1992. The cytosensor microphysiometer: biological applications of silicon technology. *Science.* 257:1906-1912.
- Mistafa, O., J. Hogberg, and U. Stenius. 2008. Statins and ATP regulate nuclear pAkt via the P2X<sub>7</sub> purinergic receptor in epithelial cells. *Biochem Biophys Res Commun.* 365:131-136.
- Mistafa, O., and U. Stenius. 2009. Statins inhibit Akt/PKB signaling via P2X<sub>7</sub> receptor in pancreatic cancer cells. *Biochem Pharmacol.* 78:1115-1126.
- Naemsch, L.N., S.J. Dixon, and S.M. Sims. 2001. Activity-dependent development of P2X<sub>7</sub> current and  $\text{Ca}^{2+}$  entry in rabbit osteoclasts. *J Biol Chem.* 276:39107-39114.
- Nelson, D.W., R.J. Gregg, M.E. Kort, A. Perez-Medrano, E.A. Voight, Y. Wang, G. Grayson, M.T. Namovic, D.L. Donnelly-Roberts, W. Niforatos, P. Honore, M.F. Jarvis, C.R. Faltynek, and W.A. Carroll. 2006. Structure-activity relationship studies on a series of novel, substituted 1-benzyl-5-phenyltetrazole P2X<sub>7</sub> antagonists. *J Med Chem.* 49:3659-3666.
- Nicke, A., Y.H. Kuan, M. Masin, J. Rettinger, B. Marquez-Klaka, O. Bender, D.C. Gorecki, R.D. Murrell-Lagnado, and F. Soto. 2009. A functional P2X<sub>7</sub> splice variant with an alternative transmembrane domain 1 escapes gene inactivation in P2X<sub>7</sub> knock-out mice. *J Biol Chem.* 284:25813-25822.
- North, R.A. 2002. Molecular physiology of P2X receptors. *Physiol Rev.* 82:1013-1067.
- Okada, Y., T. Taniguchi, Y. Akagi, and I. Muramatsu. 2002. Two-phase response of acid extrusion triggered by purinoceptor in Chinese hamster ovary cells. *Eur J Pharmacol.* 455:19-25.
- Okumura, H., D. Shiba, T. Kubo, and T. Yokoyama. 2008. P2X<sub>7</sub> receptor as sensitive flow sensor for ERK activation in osteoblasts. *Biochem Biophys Res Commun.* 372:486-490.
- Orriss, I.R., G. Burnstock, and T.R. Arnett. 2010. Purinergic signalling and bone remodelling. *Curr Opin Pharmacol.* 10:322-330.
- Ortega, F., R. Perez-Sen, E.G. Delicado, and M.T. Miras-Portugal. 2009. P2X<sub>7</sub> nucleotide receptor is coupled to GSK-3 inhibition and neuroprotection in cerebellar granule neurons. *Neurotox Res.* 15:193-204.

- Ortega, F., R. Perez-Sen, V. Morente, E.G. Delicado, and M.T. Miras-Portugal. 2010. P2X7, NMDA and BDNF receptors converge on GSK3 phosphorylation and cooperate to promote survival in cerebellar granule neurons. *Cell Mol Life Sci.* 67:1723-1733.
- Panupinthu, N., J.T. Rogers, L. Zhao, L.P. Solano-Flores, F. Possmayer, S.M. Sims, and S.J. Dixon. 2008. P2X7 receptors on osteoblasts couple to production of lysophosphatidic acid: a signaling axis promoting osteogenesis. *J Cell Biol.* 181:859-871.
- Panupinthu, N., L. Zhao, F. Possmayer, H.Z. Ke, S.M. Sims, and S.J. Dixon. 2007. P2X7 nucleotide receptors mediate blebbing in osteoblasts through a pathway involving lysophosphatidic acid. *J Biol Chem.* 282:3403-3412.
- Partridge, N.C., D. Alcorn, V.P. Michelangeli, G. Ryan, and T.J. Martin. 1983. Morphological and biochemical characterization of four clonal osteogenic sarcoma cell lines of rat origin. *Cancer Res.* 43:4308-4314.
- Peng, X.D., P.Z. Xu, M.L. Chen, A. Hahn-Windgassen, J. Skeen, J. Jacobs, D. Sundararajan, W.S. Chen, S.E. Crawford, K.G. Coleman, and N. Hay. 2003. Dwarfism, impaired skin development, skeletal muscle atrophy, delayed bone development, and impeded adipogenesis in mice lacking Akt1 and Akt2. *Genes Dev.* 17:1352-1365.
- Pereverzev, A., S.V. Komarova, J. Korcok, S. Armstrong, G.B. Tremblay, S.J. Dixon, and S.M. Sims. 2008. Extracellular acidification enhances osteoclast survival through an NFAT-independent, protein kinase C-dependent pathway. *Bone.* 42:150-161.
- Qi, J., L. Chi, J. Faber, B. Koller, and A.J. Banes. 2007. ATP reduces gel compaction in osteoblast-populated collagen gels. *J Appl Physiol.* 102:1152-1160.
- Qu, Y., and G.R. Dubyak. 2009. P2X7 receptors regulate multiple types of membrane trafficking responses and non-classical secretion pathways. *Purinergic Signal.* 5:163-173.
- Reimer, W.J., and S.J. Dixon. 1992. Extracellular nucleotides elevate  $[Ca^{2+}]_i$  in rat osteoblastic cells by interaction with two receptor subtypes. *Am J Physiol.* 263:C1040-1048.
- Reyes, J.P., M.W. Grol, S.M. Sims, and S.J. Dixon. 2013. Receptor-independent effects of 2'(3')-O-(4-benzoylbenzoyl)ATP triethylammonium salt on cytosolic pH. *Purinergic Signal.* [Epub ahead of print; DOI:10.1007/s11302-013-9365-4]
- Robling, A.G., A.B. Castillo, and C.H. Turner. 2006. Biomechanical and molecular regulation of bone remodeling. *Annu Rev Biomed Eng.* 8:455-498.

- Santhanagopal, A., P. Chidiac, W.C. Horne, R. Baron, and S.J. Dixon. 2001. Calcitonin (CT) rapidly increases  $\text{Na}^+/\text{H}^+$  exchange and metabolic acid production: effects mediated selectively by the C1a CT receptor isoform. *Endocrinology*. 142:4401-4413.
- Santhanagopal, A., and S.J. Dixon. 1999. Insulin-like growth factor I rapidly enhances acid efflux from osteoblastic cells. *Am J Physiol*. 277:E423-432.
- Smart, D., and M.D. Wood. 2000. Cytosensor techniques for examining signal transduction of neurohormones. *Biochem Cell Biol*. 78:281-288.
- Taylor, S.R., M. Gonzalez-Begne, D.K. Sojka, J.C. Richardson, S.A. Sheardown, S.M. Harrison, C.D. Pusey, F.W. Tam, and J.I. Elliott. 2009. Lymphocytes from P2X7-deficient mice exhibit enhanced P2X7 responses. *J Leukoc Biol*. 85:978-986.
- Yano, S., H. Tokumitsu, and T.R. Soderling. 1998. Calcium promotes cell survival through CaM-K kinase activation of the protein-kinase-B pathway. *Nature*. 396:584-587.

## **CHAPTER FOUR**

### **P2X7 NUCLEOTIDE RECEPTOR SIGNALING POTENTIATES THE WNT/ $\beta$ -CATENIN PATHWAY IN OSTEOBLASTS**

## 4.1 Chapter Summary

The P2X7 and Wnt/ $\beta$ -catenin pathways regulate osteoblast differentiation and are critical for anabolic responses of bone to mechanical loading. However, whether these pathways interact to control osteoblast activity is unknown. The purpose of this study was to investigate effects of P2X7 activation on Wnt/ $\beta$ -catenin signaling in osteoblasts. Using MC3T3-E1 osteoblast-like cells, we found that canonical Wnt3a elicited an increase in  $\beta$ -catenin nuclear localization that peaked at 3 h and slowly returned to baseline within 24 h. In contrast, BzATP caused transient nuclear localization only at 0.5 h post-treatment. Notably, Wnt3a and BzATP together elicited a dramatically sustained  $\beta$ -catenin nuclear localization compared to Wnt3a alone. Wnt3a also induced an increase in transcriptional activity of  $\beta$ -catenin that was potentiated by treatment with BzATP. On the other hand, BzATP alone did not increase  $\beta$ -catenin transcriptional activity. Consistent with involvement of P2X7, a high ATP concentration (1 mM) potentiated  $\beta$ -catenin transcriptional activity elicited by Wnt3a, whereas low concentrations of ATP, ADP or UTP (10  $\mu$ M) failed to elicit a response. BzATP-induced potentiation of  $\beta$ -catenin transcriptional activity elicited by Wnt3a was inhibited by two distinct P2X7 antagonists. Moreover, responses to Wnt3a in calvarial cells from *P2rx7* knockout mice were significantly less than in cells from wild-type controls. This potentiation was associated with GSK3 $\beta$  inhibitory phosphorylation induced downstream of activated P2X7 receptors, suggesting that P2X7 may potentiate canonical Wnt signaling through GSK3 $\beta$ . Taken together, we show for the first time that P2X7 activation prolongs and potentiates Wnt/ $\beta$ -catenin signaling. Thus, crosstalk between P2X7 and Wnt/ $\beta$ -catenin pathways may modulate osteoblast activity in response to mechanically-induced ATP release in bone.

## 4.2 Introduction

Mechanical loading of the skeleton greatly influences bone remodeling, a process that relies on the coordinated removal of old or damaged bone by osteoclasts and formation of new bone by osteoblasts (Robling et al., 2006). In cells of the osteoblast lineage, a variety of mechanical stimuli, including fluid shear stress and tensile strain, regulate proliferation, differentiation, survival and function both *in vitro* and *in vivo* (Thompson et al., 2012). The process by which these mechanical stimuli are translated into cellular responses, termed mechanotransduction, is thought to be mediated by the release of autocrine and paracrine factors, including adenosine 5'-triphosphate (ATP), nitric oxide (NO) and prostaglandin E<sub>2</sub> (PGE<sub>2</sub>), that in turn activate a number of downstream signaling pathways such as Ca<sup>2+</sup>/nuclear factor of activated T-cells (NFAT), adenosine 3',5'-cyclic monophosphate (cAMP)/protein kinase A (PKA), phosphatidylinositol 3-kinase (PI3K)/AKT and Wnt/ $\beta$ -catenin (Papachristou et al., 2009; Thompson et al., 2012).

The canonical Wnt/ $\beta$ -catenin pathway plays a critical role in osteoblast differentiation (Westendorf et al., 2004; Bodine and Komm, 2006; Hartmann, 2006; Krishnan et al., 2006; Long, 2012; Baron and Kneissel, 2013), and in response of the skeleton to mechanical loading (Bonewald and Johnson, 2008; Bonewald, 2011; Baron and Kneissel, 2013). In resting cells,  $\beta$ -catenin forms a complex with glycogen synthase kinase 3 $\beta$  (GSK3 $\beta$ ) and other proteins, resulting in its phosphorylation and subsequent degradation (MacDonald et al., 2009). Upon binding of canonical Wnt ligands to the appropriate Frizzled receptor (Fzd)-lipoprotein receptor-related protein (LRP) 5/6 co-receptor complex, GSK3 $\beta$  activity is suppressed and  $\beta$ -catenin is stabilized. As a result,  $\beta$ -

catenin accumulates within the cytosol and translocates to the nucleus to activate target gene expression (MacDonald et al., 2009). The absence of mechanical loading *in vivo* leads to a rapid loss in bone mass associated with release of the LRP5/6 antagonist sclerostin (SOST) from osteocytes (Robling et al., 2008; Lin et al., 2009; Tu et al., 2012) concomitant with decreased bone formation and increased bone resorption (Robling et al., 2006). On the other hand, increased loading reduces SOST levels (Robling et al., 2008; Lin et al., 2009; Tu et al., 2012) and activates canonical Wnt signaling (Robinson et al., 2006; Lin et al., 2009; Tu et al., 2012) to promote bone formation resulting in greater bone mass (Robling et al., 2006). Mice with either deletion of LRP5 or overexpression of SOST in osteocytes exhibit impaired anabolic responses to mechanical load (Sawakami et al., 2006; Tu et al., 2012; Zhao et al., 2013), confirming a critical role for the Wnt/ $\beta$ -catenin pathway in skeletal mechanotransduction.

Activation of  $\beta$ -catenin is elicited following fluid shear stress or tensile strain in a number of osteoblast and osteocyte cell culture systems (Norvell et al., 2004; Armstrong et al., 2007; Case et al., 2008; Sen et al., 2008; Santos et al., 2009; Sen et al., 2009; Case et al., 2010; Case et al., 2011). At the same time, primary calvarial osteoblasts from LRP5-deficient mice exhibit no differences in ATP release, PGE<sub>2</sub> production or extracellular signal-regulated kinase (ERK) 1/2 activation in response to fluid shear stress (Sawakami et al., 2006). The canonical Wnt antagonist dickkopf 1 (DKK1) also fails to inhibit  $\beta$ -catenin nuclear localization elicited by tensile strain in CIMC-4 osteoblast-like cells (Case et al., 2008). Thus, mechanisms independent of canonical Wnt signaling appear to mediate activation of  $\beta$ -catenin in osteoblast lineage cells downstream of mechanical stimulation.

Extracellular nucleotides, released in response to mechanical stimuli, signal through P2 receptors expressed in osteoblasts and most other cell types. These receptors are further divided into two subfamilies: the P2Y family of G protein-coupled receptors, and the P2X family of ligand-gated cation channels (Abbracchio et al., 2006; Khakh and North, 2006; Burnstock, 2007). Mice in which P2X7 receptor function is disrupted (knockout) exhibit diminished periosteal bone formation and increased trabecular bone resorption (Ke et al., 2003), and impaired anabolic responses of the skeleton to mechanical load (Li et al., 2005). P2X7 couples to production of lysophosphatidic acid (LPA) and PGE<sub>2</sub> in cells of the osteoblast lineage to promote osteoblast differentiation and matrix mineralization *in vitro* (Panupinthu et al., 2008). Additionally, P2X7 is required to mediate the effects of fluid shear stress in cultures of osteoblast-like and osteocyte-like cells (Li et al., 2005). We have recently demonstrated that P2X7 activates PI3K/AKT signaling in MC3T3-E1 osteoblast-like cells (Grol et al., 2012), a pathway that inhibits GSK3 $\beta$  in other systems. However, it is not known whether P2X7 receptors couple to inhibition of GSK3 $\beta$  in osteoblasts. Moreover, though GSK3 $\beta$  inhibition is linked to activation of  $\beta$ -catenin, no studies to date have evaluated whether P2X7 may cross-talk with Wnt signaling to enhance  $\beta$ -catenin target gene expression.

In the present study, we show that stimulation of P2X7 receptors by exogenous nucleotides in MC3T3-E1 osteoblast-like cells promotes transient  $\beta$ -catenin nuclear localization with no detectable change in transcriptional activity. On the other hand, P2X7 activation prolongs  $\beta$ -catenin nuclear localization and potentiates transcriptional activation elicited by canonical Wnt signaling. Moreover, this potentiation is associated with the inhibitory phosphorylation of GSK3 $\beta$  induced by activated P2X7 receptors,



suggesting that P2X7 may promote Wnt/ $\beta$ -catenin signaling through GSK3 $\beta$ . Taken together, these data show for the first time in any system that P2X7 activation can potentiate Wnt/ $\beta$ -catenin signaling, a mechanism through which osteoblast activity may be modulated in response to mechanically-induced ATP release in bone.

## 4.3 Materials and Methods

### 4.3.1 Materials and Solutions

$\alpha$ -Minimum essential medium ( $\alpha$ -MEM), heat-inactivated fetal bovine serum (FBS), antibiotic solution (10,000 U/ml penicillin, 10,000  $\mu$ g/ml streptomycin, and 25  $\mu$ g/ml amphotericin B), trypsin solution, Dulbecco's phosphate buffered saline (DPBS) and Dulbecco's modified Eagle medium (high glucose) (DMEM) were obtained from GIBCO (Life Technologies Inc., Burlington, ON, Canada).  $\beta$ -catenin (L54E2) mouse monoclonal and phospho-GSK3 $\alpha/\beta$  (Ser21/9) rabbit polyclonal antibodies were from Cell Signaling Technologies Inc. (Danvers, MA, USA). GSK3 $\alpha/\beta$  mouse monoclonal, horse radish peroxidase (HRP)-conjugated goat anti-rabbit and HRP-conjugated goat anti-mouse antibodies were obtained from Santa Cruz Biotechnology Inc. (Dallas, TX, USA). Alexa Fluor® 488 goat anti-mouse antibody was from Molecular Probes (Life Technologies Inc.). Vectashield mounting medium with 4,6-diamidino-2-phenylindole (DAPI) was obtained from Vector Laboratories Inc. (Burlingame, CA, USA). BCA Protein Assay Kit, SuperSignal West Pico Chemiluminescent Substrate and Restore PLUS Western Blot Stripping Buffer were obtained from Pierce (Thermo Fisher Scientific, Inc., Rockland, IL, USA). Precision Plus Protein™ Kaleidoscope Standards and nitrocellulose transfer membranes were from Bio-Rad Laboratories Inc. (Hercules, CA, USA). Phospho-GSK3 $\alpha/\beta$  (Tyr279/216) rabbit polyclonal antibody, NuPAGE® LDS Sample Buffer, 4X, NuPAGE® Sample Reducing Agent, 10X, NuPAGE® Antioxidant, NuPAGE® MOPS SDS Running Buffer, 20X, NuPAGE® Transfer Buffer, 20X and NuPAGE® Bis-Tris Gels, 1.5 mm, 10 well were obtained from Novex (Life Technologies Inc.). Gel blot paper was from Whatman (GE Healthcare Life Sciences,

Piscataway, NJ, USA). KODAK® BioMax® light autoradiography film was obtained from VWR International (Mississauga, ON, Canada). Mini-Complete Protease Inhibitor tablets, FuGENE 6 and X-tremeGENE 9 were from Roche Diagnostics (Laval, QC, Canada). Passive Lysis Buffer, 5X and Bright-Glo™ Luciferase Assay System were obtained from Promega (Madison, WI, USA). Bovine albumin (BSA), Fraction V was from Fisher Scientific (Thermo Fisher Scientific Inc.). Recombinant mouse Wnt3a was obtained from either R&D Systems, Inc. (Minneapolis, MN, USA) or Abcam, Inc. (Cambridge, MA, USA). Normal goat serum, collagenase type II, Phosphatase Inhibitor Cocktail II, ATP disodium salt, adenosine 5'-diphosphate (ADP) disodium salt, uridine 5'-triphosphate (UTP) trisodium salt hydrate and 2'-3'-O-(4-benzoylbenzoyl)adenosine 5'-triphosphate (BzATP) triethylammonium salt were obtained from Sigma-Aldrich (St. Louis, MO, USA). 3-[[5-(2,3-Dichlorophenyl)-1*H*-tetrazol-1-yl]methyl]pyridine hydrochloride (A 438079 HCl) and N-[1-[[[(cyanoamino)(5-quinolinylamino)methylene]amino]-2,2-dimethylpropyl]-3,4-dimethoxybenzeneacetamide (A 740003) were from Tocris Bioscience (Ellisville, MO, USA). Phosphatase Inhibitor Cocktail IV was from Calbiochem (EMD Biosciences, San Diego, CA).

RIPA buffer (for protein isolation) consisted of: 50 mM Tris pH 7.5, 150 mM NaCl, 1% Triton X-100, 1% sodium deoxycholate, 0.1% sodium dodecyl sulphate (SDS), and 2 mM EDTA, pH 8.0 supplemented with 2 Mini-Complete Protease Inhibitor tablets (Roche Diagnostics), 200 µl Phosphatase Inhibitor Cocktail II (Sigma-Aldrich) and 400 µl Phosphatase Inhibitor Cocktail IV (Calbiochem) in 20 ml total volume.

### 4.3.2 Animals and Cell Culture

The P2X7 loss-of-function (knockout) mouse, generated as previously described (Solle et al., 2001), was obtained from Pfizer. Though P2X7 is present in this genetically modified mouse model, the protein has a COOH-terminal truncation that greatly diminishes receptor function (Masin et al., 2012). Colonies of wild-type and knockout mice were maintained in a mixed genetic background (129/Ola  $\times$  C57BL/6  $\times$  DBA/2) by crossbreeding of heterozygous mice. All procedures were approved by the Council on Animal Care at the University of Western Ontario and were in accordance with the guidelines of the Canadian Council on Animal Care.

Calvarial osteoblasts were isolated from 5- to 7-d-old mice using sequential collagenase digestion, as previously described (Panupinthu et al., 2008). Freshly isolated calvarial osteoblasts were plated at a density of  $1.0\text{-}1.5 \times 10^4$  cells/cm<sup>2</sup> on Nunc six-well plates (Thermo Fisher Scientific, Rochester, NY, USA) and maintained in  $\alpha$ -MEM supplemented with 10% FBS and 1% antibiotic solution (culture medium) at 37°C and 5% CO<sub>2</sub>. After confluence was reached (~3-5 days), cells were trypsinized and plated for experiments.

The MC3T3-E1 osteoblast-like cell line (subclone 4) was obtained from the American Type Culture Collection (Rockville, MD, USA). MC3T3-E1 cells were subcultured twice weekly and maintained in culture medium at 37°C and 5% CO<sub>2</sub>. These cells endogenously express P2X7 and Wnt signaling components, and are responsive to canonical Wnt3a (Li et al., 2005; Spencer et al., 2006; Qi et al., 2007; Okumura et al., 2008; Caverzasio et al., 2013).

### 4.3.3 Immunofluorescence Localization of $\beta$ -catenin

MC3T3-E1 cells were plated at a density of  $1.5 \times 10^4$  cells/cm<sup>2</sup> on 12-mm glass coverslips in Falcon 24-well plates in culture medium. After 2 d, cells were placed in serum-free medium and incubated overnight. On the day of the experiment, cells were incubated with test substances for the indicated times. Cells were then fixed with paraformaldehyde (4%) in sucrose solution (2%), permeabilized with 0.1% Triton X-100 in DPBS for 10 min, and blocked for 1 h with 1% normal goat serum in DPBS (blocking solution). To detect subcellular localization of  $\beta$ -catenin, cells were first incubated for 1 h with a mouse monoclonal antibody (1:200 in blocking solution) followed by a 2 h incubation with an Alexa Fluor® 488 goat anti-mouse antibody (1:200 in blocking solution) at room temperature. Stained samples were then sealed using Vectashield mounting medium with DAPI, and visualized by confocal microscopy (model LSM 510; Carl Zeiss Inc., Jena, Germany) using a Zeiss Plan-Apochromat 40 $\times$  objective (1.2 NA) at a slice thickness of 2  $\mu$ m with 488-nm Ar<sup>+</sup> ion laser excitation and emission wavelengths filtered at 500-550 nm band pass. To quantify subcellular localization of  $\beta$ -catenin, the average fluorescence intensity of an area in the nucleus ( $F_N$ ) and the average fluorescence intensity of an area of equal size in the cytosol ( $F_C$ ) were determined. Values of the ratio  $F_N/F_C$  greater than or equal to 1.25 were taken to indicate nuclear localization of  $\beta$ -catenin protein. Twelve images were obtained per coverslip for each treatment, and the  $F_N/F_C$  ratios for all cells within a field were analyzed (~20-30 cells per field).

### 4.3.4 Luciferase Reporter Assay for $\beta$ -catenin Transcriptional Activity

The  $\beta$ -catenin luciferase reporter plasmid (pBARK) was obtained from Dr.

Randall Moon (University of Washington, Seattle, WA, USA). This plasmid consists of twelve TCF response elements (or  $\beta$ -catenin binding sites) cloned upstream of Promega's minP© minimal promoter (Biechele and Moon, 2008). MC3T3-E1 and calvarial osteoblasts were transfected in suspension with the  $\beta$ -catenin luciferase reporter vector using FuGENE 6 or X-tremeGENE 9 according to manufacturers' instructions. Cells were subsequently plated at a density of  $3.0 \times 10^4$  cells/cm<sup>2</sup> on Falcon 48-well plates (or Nunc 48-well plates for calvarial cells) in culture medium. At 1 d post-transfection, cells were placed in serum-free medium and incubated overnight. On the day of the experiment, cells were treated with test substances and subsequently incubated for 24 h. Cell lysates were then prepared by incubation with 65  $\mu$ l (or 100  $\mu$ l for calvarial cells) of Passive Lysis Buffer, 1X per well at room temperature for a minimum of 30 min with agitation. To assess luminescence, 15  $\mu$ l of lysate was combined with 15  $\mu$ l of Bright-Glo Luciferase Reagent in a 96-well white plate (Greiner Bio-One, Monroe, NC, USA). Reactions for each sample were performed in triplicate. Luminescence was measured using 2-s integration per well on a LMAX II<sup>384</sup> microplate reader (Molecular Devices, Downingtown, PA, USA).

#### **4.3.5 Western Blot Analysis of GSK3 $\alpha$ / $\beta$ Phosphorylation**

MC3T3-E1 cells were plated at a density of  $1.5 \times 10^4$  cells/cm<sup>2</sup> on Falcon 60-mm dishes in culture medium. After 1 d, cells were placed in serum-free medium and incubated overnight. On the day of the experiment, cells were incubated with test substances for the indicated times. Cellular protein was then collected by lysing cells on ice in RIPA lysis buffer supplemented with protease and phosphatase inhibitors. Cell

lysates were homogenized by sonication at 20% for 5 s on ice using a Sonic Dismembrator (Model 500; Fisher Scientific) followed by sedimentation at 13,000×g for 10 min at 4 °C. The resulting supernatant was used for Western blot analysis. Protein concentration was determined with the Pierce BCA protein assay kit. Equivalent amounts of protein (10-15 µg) were prepared with NuPAGE® Sample Reducing Agent (1X) and NuPAGE® LDS Sample Buffer (1X), and resolved on NuPAGE® Bis-Tris polyacrylamide gels in 1X NuPAGE® MOPS SDS Running Buffer (1X). Proteins were then transferred to nitrocellulose membranes by electroblotting at 30 V for 90 min at 4° C.

After transfer, membranes were washed for 5 min in Tris-buffered saline (TBS) with 0.05% Tween 20 (TBST; washing solution) before being blocked for 1 h with 5% BSA in TBST (blocking solution) at RT. To detect phospho-GSK3α/β (Ser21/9), phospho-GSK3α/β (Tyr279/216) or total GSK3α/β, membranes were incubated overnight at 4 °C with a phospho-GSK3α/β (Ser21/9) rabbit polyclonal antibody (1:1000 in blocking solution), phospho-GSK3α/β (Tyr216/279) rabbit polyclonal antibody (1:1000 in blocking solution), or GSK3α/β mouse monoclonal antibody (1:5000 in blocking solution), respectively. The next day, membranes were subjected to three 5-min washes in TBST, incubated with the appropriate secondary antibody at a dilution of 1:20000 in blocking solution at RT and washed three more times for 5 min each in TBST. Antibody/protein complexes were visualized by 1, 3 or 5 min incubations of the membrane in SuperSignal West Pico Chemiluminescent Substrate followed by exposure using KODAK® BioMax® light autoradiography film and a KODAK® M35A X-OMAT processor. Band intensities on immunoblots were quantified by densitometry using Quantity One v4.5.2 (Bio-Rad Laboratories Inc.), and normalized to total GSK3α/β signal

(loading control). For repeated probing, membranes were stripped with Restore PLUS Western Blot Stripping Buffer for 5-20 min at RT (or 37 °C) followed by one wash with TBST.

#### **4.3.6 Statistical Analyses**

Data are shown as means  $\pm$  S.E.M. Differences between two groups were assessed using *t* tests. Differences among three or more groups were evaluated by one-way analysis of variance (ANOVA) followed by a Tukey multiple comparisons test, or two-way ANOVA followed by a Bonferroni multiple comparisons test. Differences were accepted as statistically significant at  $p < 0.05$ .



## 4.4 Results

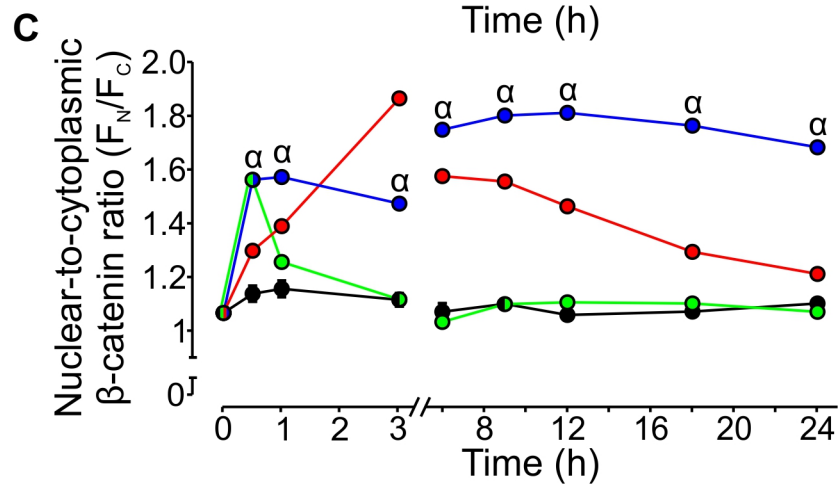
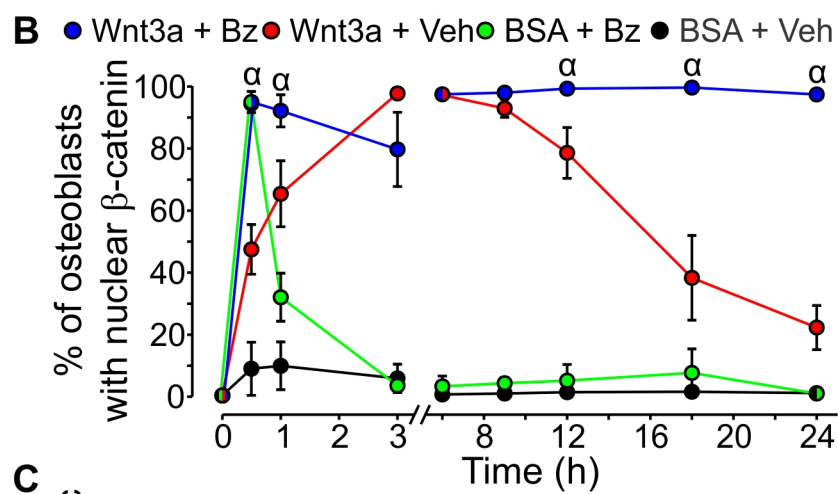
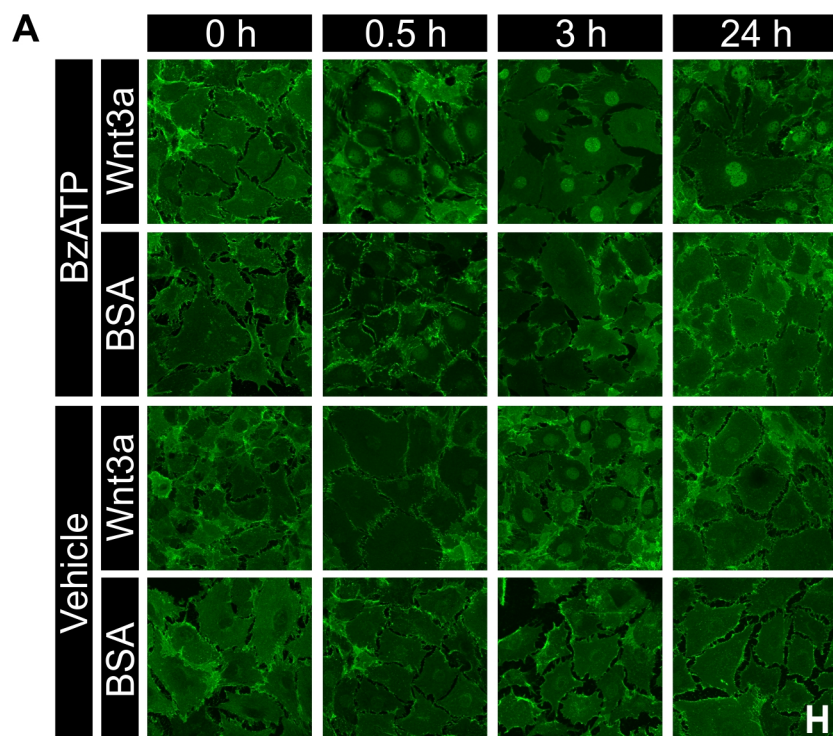
### 4.4.1 Effect of the P2X7 Agonist BzATP on Wnt-induced $\beta$ -catenin Nuclear Localization

Canonical Wnt ligands signal through Fzd-LRP5/6 co-receptor complexes within the plasma membrane, leading to stabilization and subsequent translocation of  $\beta$ -catenin from the cytoplasm to the nucleus (MacDonald et al., 2009). To assess whether P2X7 receptor signaling could influence Wnt-induced nuclear localization of  $\beta$ -catenin in osteoblasts, MC3T3-E1 cells were treated with canonical Wnt3a (20 ng/ml) or its vehicle, and the P2X7 receptor agonist BzATP (300  $\mu$ M) or its vehicle, alone or in combination. Samples were fixed at various time points, processed for  $\beta$ -catenin immunofluorescence, and visualized by confocal microscopy (Figure 4.1 A). To quantify subcellular localization of  $\beta$ -catenin, average pixel intensity for areas of equal size within the nucleus ( $F_N$ ) and the cytosol ( $F_C$ ) were determined. Values of  $F_N/F_C$  exceeding 1.25 were taken to indicate nuclear localization (Figure 4.1 B). In the absence of agonists,  $\beta$ -catenin localized to cell junctions and the cytoplasm, with little or no fluorescence in the nucleus (Figure 4.1 A, B). Wnt3a alone elicited a gradual increase in the percentage of osteoblasts with  $\beta$ -catenin nuclear localization, which peaked at 3 h and slowly returned to baseline by 24 h (Figure 4.1 A, B). In contrast, BzATP alone caused transient nuclear localization in nearly all cells only at 0.5 h after treatment (Figure 4.1 A, B). Notably, when cells were treated with Wnt3a and BzATP in combination,  $\beta$ -catenin nuclear localization was more rapid and sustained compared to Wnt3a alone (Figure 4.1 A, B).

To assess the degree (or intensity) of  $\beta$ -catenin nuclear localization at each time point, the average value for  $F_N/F_C$  in a field was determined and plotted. In keeping with

**Figure 4.1 The P2X7 Agonist BzATP Potentiates  $\beta$ -catenin Nuclear Localization Elicited by Canonical Wnt3a.**

A, MC3T3-E1 osteoblast-like cells were seeded at a density of  $1.5 \times 10^4$  cells/cm<sup>2</sup> on glass coverslips and cultured for 2 days. Cells were then placed in serum-free media and incubated overnight. The next day, cells were treated under serum-free conditions with recombinant mouse canonical Wnt3a (20 ng/ml) or its vehicle (0.2% BSA; BSA) in the presence of either BzATP (300  $\mu$ M) or its vehicle (Vehicle), and fixed at the indicated times. To observe changes in subcellular localization of  $\beta$ -catenin, immunofluorescence was performed using a  $\beta$ -catenin monoclonal antibody (green) and visualized by confocal microscopy. Data are representative images from 4 independent preparations each performed in duplicate. Scale bar is 20  $\mu$ m. B,  $\beta$ -catenin nuclear localization was assessed by measuring the average pixel intensity of an area in the nucleus ( $F_N$ ) and an area of equal size in the cytosol ( $F_C$ ). The proportion of all cells within 24 fields (12 per coverslip) exhibiting  $\beta$ -catenin nuclear localization was analyzed for each condition. Values of the ratio  $F_N/F_C$  greater than or equal to 1.25 were taken as indicating nuclear localization. The number of cells exhibiting nuclear localization was expressed as a percentage of the total number of cells for each treatment group. C, the ratio of  $F_N/F_C$  (an indication of the intensity of  $\beta$ -catenin nuclear localization) for all cells analyzed was plotted for each treatment at times indicated. For both B and C,  $\alpha$  indicates a significant effect of BzATP on Wnt3a-induced  $\beta$ -catenin nuclear localization compared to Wnt3a alone at the same time point ( $p < 0.05$ ). Data are means  $\pm$  S.E.M. ( $n = 4$  independent preparations each performed in duplicate).



observations made when assessing the percentage of responding cells, the intensity of  $\beta$ -catenin nuclear localization was significantly greater at all-time points other than 3 h in cultures treated with Wnt3a and BzATP compared to Wnt3a alone (Figure 4.1 A, C). Thus, stimulation of only P2X7 promotes brief, transient  $\beta$ -catenin nuclear localization, whereas activated P2X7 receptors prolong and increase nuclear localization of  $\beta$ -catenin elicited by canonical Wnt signaling.

#### **4.4.2 Effect of BzATP on Wnt-induced $\beta$ -catenin Transcriptional Activity**

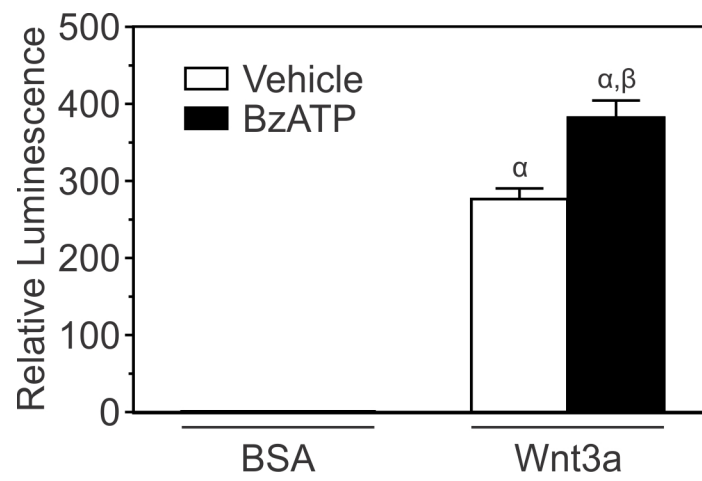
To determine if BzATP affects  $\beta$ -catenin transcriptional activity elicited by canonical Wnt signaling, MC3T3-E1 cells were transfected with a  $\beta$ -catenin luciferase reporter and treated with Wnt3a (20 ng/ml) or its vehicle, and BzATP (300  $\mu$ M) or its vehicle, alone or in combination. After 24 h, cell lysates were collected and luminescence was assessed as a measure of  $\beta$ -catenin transcriptional activity (Figure 4.2). Wnt3a alone induced a dramatic increase in  $\beta$ -catenin transcriptional activity (Figure 4.2). Interestingly, although BzATP alone induced nuclear localization of  $\beta$ -catenin at 0.5 h, it did not increase  $\beta$ -catenin transcriptional activity in these cells. In keeping with the analysis of  $\beta$ -catenin subcellular localization, the combination of Wnt3a and BzATP significantly enhanced transcriptional activity compared to that induced by Wnt3a alone (Figure 4.2).

#### **4.4.3 P2X7 is Essential for Mediating Effects of Nucleotides on Wnt-induced $\beta$ -catenin Transcriptional Activity**

Since BzATP can activate other P2 nucleotide receptors in addition to P2X7

**Figure 4.2 BzATP Potentiates  $\beta$ -catenin Transcriptional Activity Elicited by Wnt3a.**

MC3T3-E1 osteoblast-like cells were transfected in suspension with a  $\beta$ -catenin luciferase reporter plasmid, seeded at a density of  $3.0 \times 10^4$  cells/cm<sup>2</sup> in a 48-well plate, and cultured for 1 day. Cells were then placed in serum-free media and incubated overnight. The next day, cells were treated under serum-free conditions with recombinant mouse Wnt3a (20 ng/ml) or its vehicle (0.2% BSA; BSA) in the presence of either BzATP (300  $\mu$ M) or its vehicle (Vehicle). After 24 h, cell lysates were collected and luminescence was assessed as a measure of  $\beta$ -catenin transcriptional activity. The luminescence for each treatment was expressed relative to BSA + Vehicle.  $\alpha$  indicates a significant effect of treatment on  $\beta$ -catenin transcriptional activity compared to BSA + Vehicle ( $p < 0.05$ ).  $\beta$  indicates significant effect of BzATP on Wnt3a-induced  $\beta$ -catenin transcriptional activity ( $p < 0.05$ ). Data are means  $\pm$  S.E.M. ( $n = 21$  samples from 7 independent preparations).



(North, 2002), the effects of additional P2 agonists on Wnt-induced  $\beta$ -catenin transcriptional activity were assessed. MC3T3-E1 cells transfected with the  $\beta$ -catenin luciferase reporter were treated with Wnt3a (20 ng/ml) or its vehicle and varying concentrations of ATP, ADP, UTP or their vehicle, alone or in combination (Figure 4.3 A-C). Whether in the absence or presence of Wnt3a, neither ADP nor UTP altered  $\beta$ -catenin transcriptional activity (Figure 4.3 B, C). A low concentration of ATP (10  $\mu$ M) also failed to elicit a response (Figure 4.3 A). In contrast, a high ATP concentration (1 mM) significantly potentiated  $\beta$ -catenin transcriptional activity compared to Wnt3a alone (Figure 4.3 A), consistent with involvement of the low-affinity P2X7 receptor.

To further assess the role of P2X7, pharmacological and genetic approaches were utilized. First, MC3T3-E1 cells transfected with the  $\beta$ -catenin luciferase reporter were treated with Wnt3a (20 ng/ml) or its vehicle and BzATP (300  $\mu$ M) or its vehicle, alone or in combination, in the presence or absence of the P2X7 antagonists A 438079 (10  $\mu$ M) or A 740003 (10  $\mu$ M) (Figure 4.4). A 438079 (Figure 4.4 A) and A 740003 (Figure 4.4 B) both abolished the BzATP-induced potentiation of Wnt3a signaling, but did not significantly alter the effects elicited by Wnt3a alone. Next, changes in Wnt signaling were assessed in primary osteoblasts isolated from wild-type mice and mice with loss of P2X7 function (knockout) (Figure 4.5). Both wild-type and knockout calvarial osteoblasts transfected with the  $\beta$ -catenin luciferase reporter displayed significant increases in  $\beta$ -catenin transcriptional activity in response to Wnt3a (20 ng/ml) (Figure 4.5). However, the response to Wnt3a was significantly less in knockout cells compared to wild-type (Figure 4.5). Taken together, these findings demonstrate that P2X7 receptor signaling cross-talks with the Wnt/ $\beta$ -catenin pathway to enhance its activity in cells of the

**Figure 4.3 P2X7 Receptor Agonists Potentiate  $\beta$ -catenin Transcriptional Activity Elicited by Wnt3a.**

MC3T3-E1 osteoblast-like cells transfected with the  $\beta$ -catenin luciferase reporter plasmid were treated under serum-free conditions. A, cells were treated with recombinant mouse Wnt3a (20 ng/ml) or its vehicle (0.2% BSA; BSA) in the presence of either 10  $\mu$ M ATP (ATP<sub>low</sub>), 1 mM ATP (ATP<sub>high</sub>) or their vehicle (Vehicle). After 24 h, cell lysates were collected and luminescence was assessed. Luminescence for each treatment was expressed relative to BSA + Vehicle. B, cells were treated with recombinant canonical Wnt3a (20 ng/ml) or its vehicle (0.2% BSA; BSA) in the presence of either 10  $\mu$ M ADP (ADP<sub>low</sub>), 1 mM ADP (ATP<sub>high</sub>) or their vehicle (Vehicle). After 24 h, luminescence was assessed as described in (A). C, cells were treated with recombinant canonical Wnt3a (20 ng/ml) or its vehicle (0.2% BSA; BSA) in the presence of either 10  $\mu$ M UTP (UTP) or its vehicle (Vehicle). After 24 h, luminescence was assessed as described in (A). For A, B and C,  $\alpha$  indicates a significant effect of treatment on  $\beta$ -catenin transcriptional activity compared to BSA + Vehicle ( $p < 0.05$ ).  $\beta$  indicates significant effect of nucleotide on Wnt3a-induced  $\beta$ -catenin transcriptional activity ( $p < 0.05$ ). Data are means  $\pm$  S.E.M. ( $n = 21$  samples from 7 independent experiments).



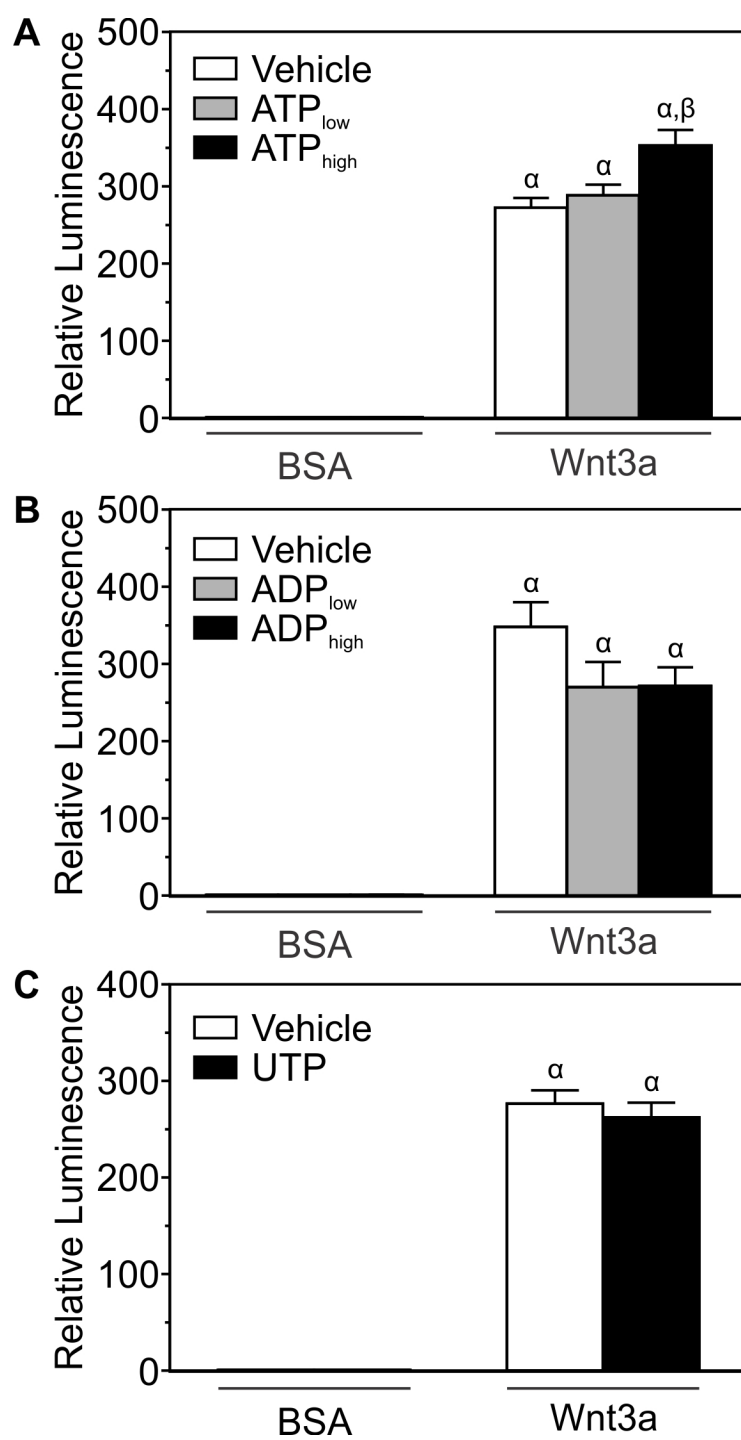


**Figure 4.4 P2X7 Receptor Antagonists Block the Effects of BzATP on Wnt3a-induced  $\beta$ -catenin Transcriptional Activity.**

MC3T3-E1 osteoblast-like cells transfected with the  $\beta$ -catenin luciferase reporter plasmid were treated under serum-free conditions. Cells were incubated for 5-10 min in the absence or presence of the specific P2X7 antagonist A 438079 (10  $\mu$ M, Panel A) or a second P2X7 antagonist A 740003 (10  $\mu$ M, Panel B). Next, cells were treated with recombinant mouse Wnt3a (20 ng/ml) or its vehicle (0.2% BSA; BSA) in the presence of either BzATP (300  $\mu$ M) or its vehicle (Vehicle). After 24 h, cell lysates were collected and luminescence was assessed. Luminescence for each treatment was expressed relative to DMSO + BSA + Vehicle. For both A and B,  $\alpha$  indicates a significant effect of treatment on  $\beta$ -catenin transcriptional activity compared to Control + BSA + Vehicle ( $p < 0.05$ ).  $\beta$  indicates significant effect of BzATP on Wnt3a-induced  $\beta$ -catenin transcriptional activity ( $p < 0.05$ ).  $\delta$  indicates significant effect of the antagonist ( $p < 0.05$ ). Data are means  $\pm$  S.E.M. ( $n = 18$  samples from 6 independent experiments).

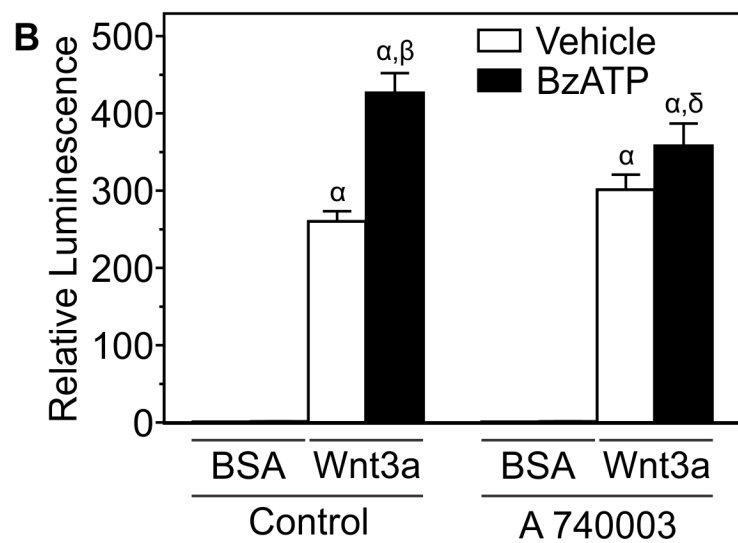
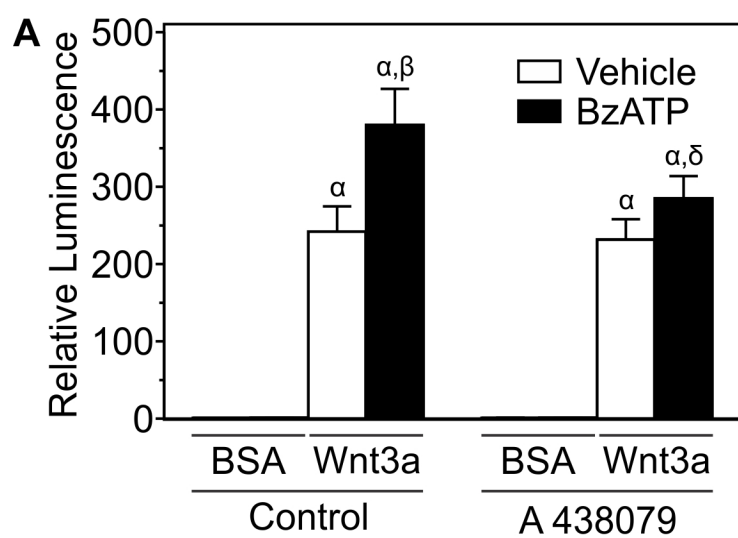
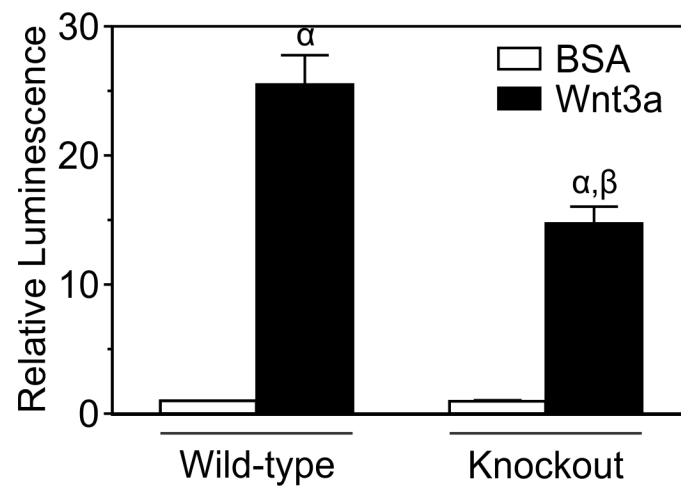


**Figure 4.5 Functional P2X7 Receptors are Required for Complete Activation of Wnt3a-induced  $\beta$ -catenin Transcriptional Activity.**

Calvarial osteoblasts from wild-type and P2X7 loss-of-function (knockout) mice were transfected with the  $\beta$ -catenin luciferase reporter plasmid, and treated under serum-free conditions with recombinant mouse Wnt3a (20 ng/ml) or its vehicle (0.2% BSA; BSA). After 24 h, cell lysates were collected and luminescence was assessed. Luminescence for each treatment was expressed relative to BSA treatment in wild-type cells.  $\alpha$  indicates a significant effect of Wnt3a on  $\beta$ -catenin transcriptional activity compared to BSA treatment ( $p < 0.05$ ).  $\beta$  indicates significant effect of genotype ( $p < 0.05$ ). Data are means  $\pm$  S.E.M. ( $n = 21$  samples from 7 independent experiments).



osteoblast lineage.

#### **4.4.4 Activation of P2X7 Increases Inhibitory Phosphorylation of GSK3 $\alpha/\beta$**

During canonical Wnt signaling, stabilization of  $\beta$ -catenin is achieved in part through inhibition of GSK3 $\beta$  (MacDonald et al., 2009). To determine whether P2X7 couples to inhibition of GSK3 $\beta$  in cells of the osteoblast lineage, the effects of BzATP on GSK3 $\alpha/\beta$  phosphorylation were examined (Figure 4.6). Treatment of MC3T3-E1 cells with BzATP (300  $\mu$ M) inhibited GSK3 $\alpha/\beta$  as indicated by the significant increase in inhibitory phosphorylation of both GSK3 $\alpha$  and GSK3 $\beta$  at serines 21 and 9, respectively (Figure 4.6 A, B). On the other hand, BzATP had no effect on the phosphorylation status of tyrosine residues 279 (GSK3 $\alpha$ ) or 216 (GSK3 $\beta$ ), both of which are associated with activation of GSK3 (Figure 4.6 A). Consistent with involvement of P2X7, A 438079 (10  $\mu$ M) suppressed the inhibitory phosphorylation of GSK3 $\alpha/\beta$  induced by BzATP (Figure 4.7 A, B). Thus, P2X7 may potentiate canonical Wnt signaling through inhibition of GSK3 $\beta$ , though further experiments are required.

**Figure 4.6 BzATP Induces Inhibitory Phosphorylation of GSK3 $\alpha/\beta$ .**

A, MC3T3-E1 osteoblast-like cells were seeded at a density of  $1.5 \times 10^4$  cells/cm<sup>2</sup> in a 6-well plate and cultured for 1 day. Cells were then placed in serum-free media and incubated overnight. The next day, cells were treated under serum-free conditions with vehicle (V) or BzATP (300  $\mu$ M; BzATP) for the times indicated, and total protein was harvested. Samples were subjected to immunoblot analyses using specific phospho-serine 21/9 and phospho-tyrosine 279/216 GSK3 $\alpha/\beta$  antibodies. As a loading control, blots were also probed for total GSK3 $\alpha/\beta$ . Bands were visualized by the ECL method. Images are representative blots from 3-5 independent preparations. B, phospho-serine 21/9, phospho-tyrosine 279/216 and total GSK3 $\alpha/\beta$  bands were evaluated by densitometry. The ratio of phospho-GSK3 $\alpha/\beta$  to total GSK3 $\alpha/\beta$  was determined for serine and tyrosine residues, and results were normalized to vehicle. Treatment with BzATP had no significant effect on the phosphorylation status of tyrosine 279/216 (*data not shown*). Interestingly, additional bands not consistent with the molecular weight of GSK3 $\alpha/\beta$  were also detected with this antibody after treatment with BzATP. It is likely that the antibody is non-specific, and detected a distinct phosphorylation event on a second protein of unknown identity.  $\alpha$  indicates a significant difference from 0 min ( $p < 0.05$ ). Data are means  $\pm$  S.E.M. ( $n = 3-5$  independent preparations).

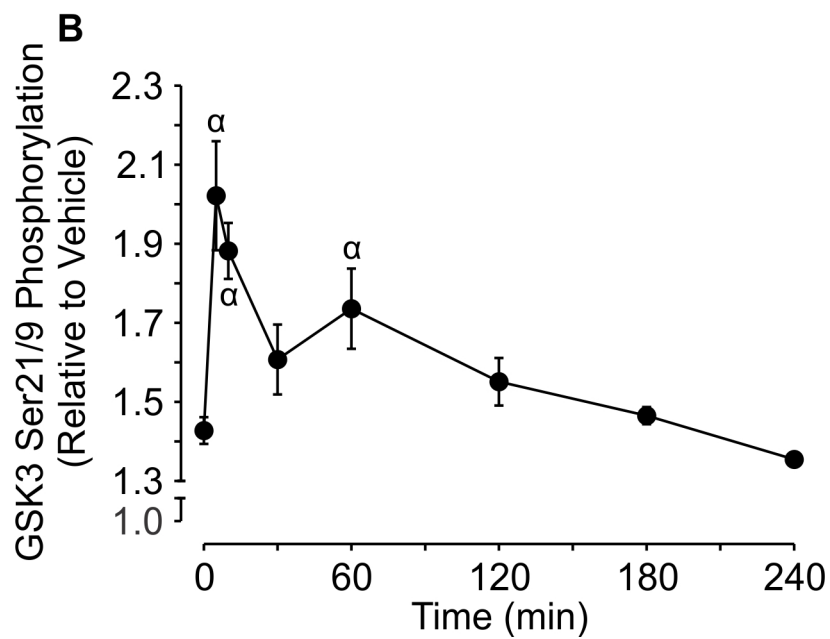
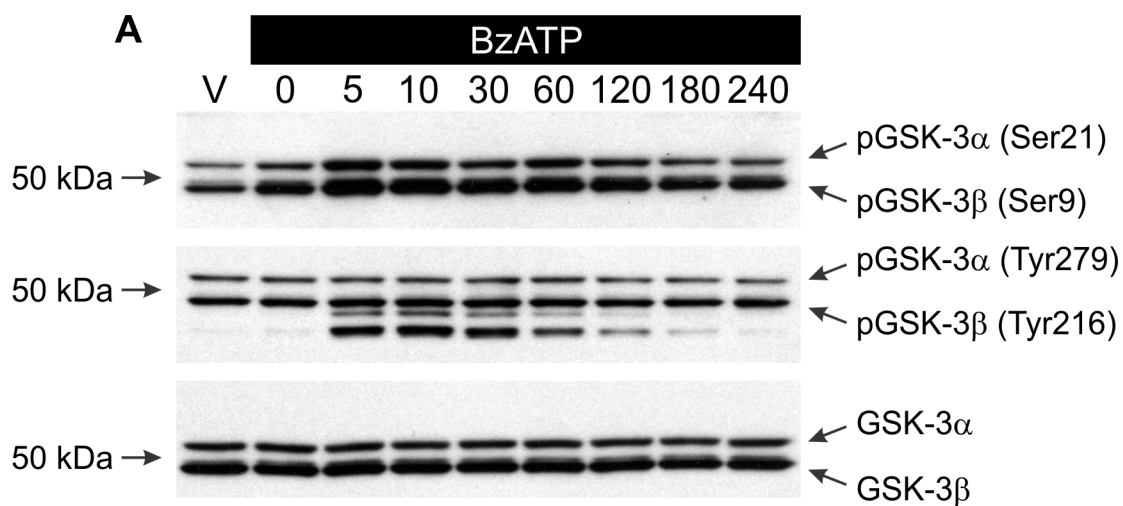
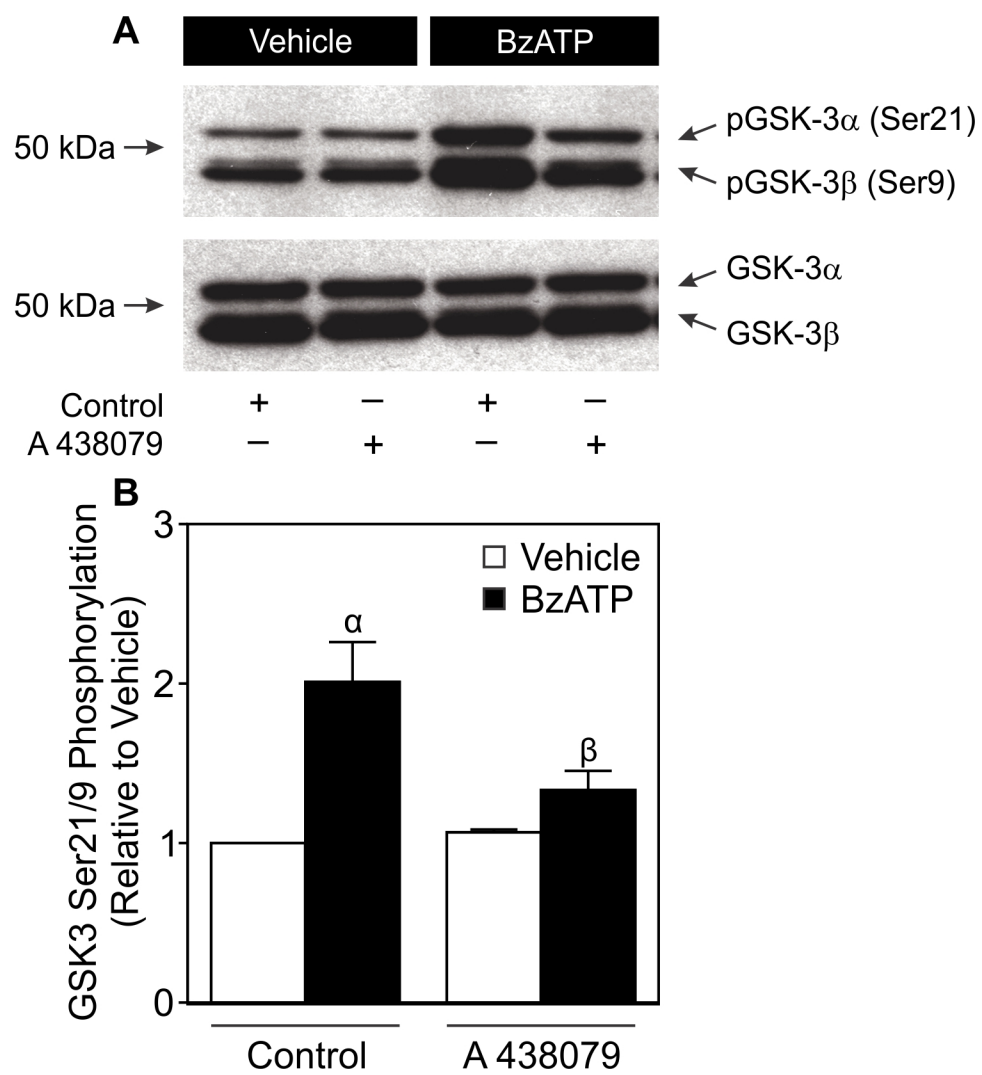




**Figure 4.7 A P2X7 Antagonist Blocks BzATP-induced Inhibitory Phosphorylation of GSK3 $\alpha$ / $\beta$ .**

A, MC3T3-E1 osteoblast-like cells were incubated for 20 min in the presence of the P2X7 antagonist A 438079 (10  $\mu$ M) or its vehicle (Control). Next, cells were treated with vehicle or BzATP (300  $\mu$ M; BzATP) for 5 min, and total protein was subsequently harvested. Samples were subjected to immunoblot analyses using a specific phosphoserine 21/9 GSK3 $\alpha$ / $\beta$  antibody. As a loading control, blots were also probed for total GSK3 $\alpha$ / $\beta$ . Bands were visualized by the ECL method. Images are representative blots from 3 independent preparations. B, phospho-serine 21/9 and total GSK3 $\alpha$ / $\beta$  bands were evaluated by densitometry. The ratio of phospho-GSK3 $\alpha$ / $\beta$  to total GSK3 $\alpha$ / $\beta$  was determined, and results were normalized to Control + Vehicle.  $\alpha$  indicates a significant difference from Control + Vehicle ( $p < 0.05$ ).  $\beta$  indicates a significant effect of the antagonist ( $p < 0.05$ ). Data are means  $\pm$  S.E.M. ( $n = 3$  independent preparations).



## 4.5 Discussion

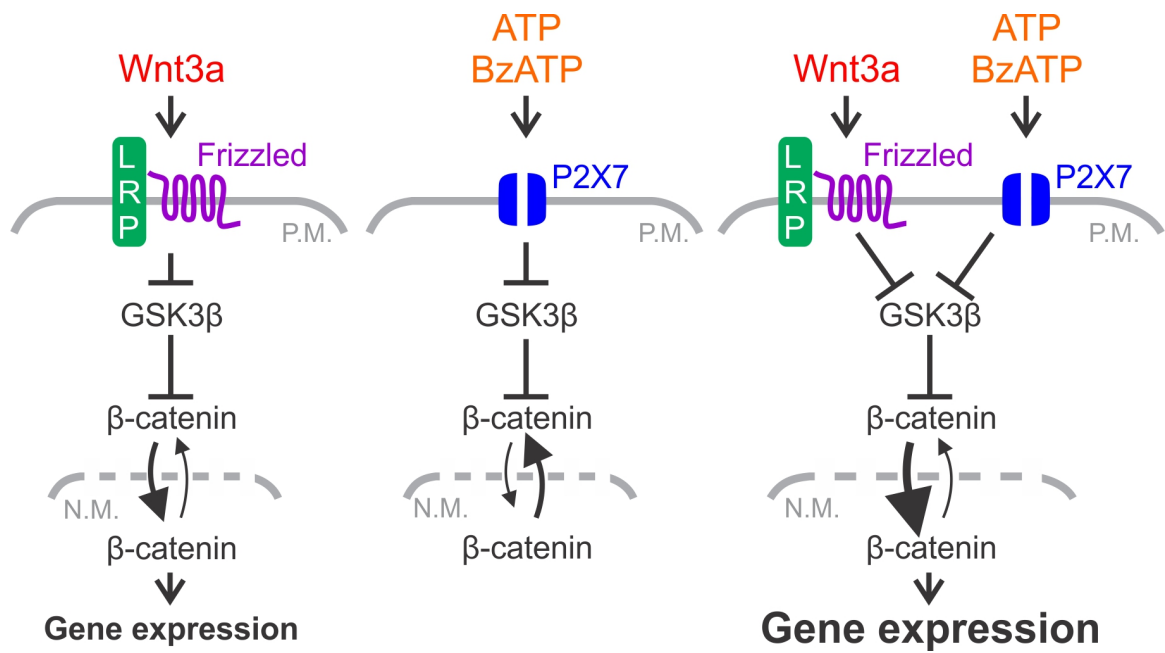
In the present study, we investigated the effects of P2X7 receptor activation on Wnt/ $\beta$ -catenin signaling in cells of the osteoblast lineage. We show for the first time in any system that activation of P2X7 by exogenous nucleotides promotes transient  $\beta$ -catenin nuclear localization. Notably, stimulation of P2X7 prolongs  $\beta$ -catenin nuclear localization and potentiates transcriptional activation elicited by canonical Wnt signaling (Figure 4.8). This potentiation is associated with the inhibitory phosphorylation of GSK3 $\beta$  induced by activated P2X7 receptors, suggesting that P2X7 may potentiate Wnt/ $\beta$ -catenin signaling through GSK3 $\beta$ . P2X7-induced potentiation of Wnt/ $\beta$ -catenin signaling is a novel mechanism through which osteoblast activity may be modulated in response to mechanically-induced ATP release in bone.

### 4.5.1 P2X7 Potentiates the Wnt/ $\beta$ -catenin Pathway

A number of P2 receptors have been shown to modulate signaling mediated by growth factors and hormones leading to changes in osteoblast proliferation, differentiation and function. For instance, P2Y<sub>2</sub> potentiates c-fos expression elicited by parathyroid hormone (PTH)/cAMP signaling (Bowler et al., 1999; Bowler et al., 2001). ATP also synergistically enhances platelet-derived growth factor (PDGF) and insulin-like growth factor (IGF)-1-induced proliferation of human MG-63 osteoblast-like cells through an unidentified P2 receptor (Nakamura et al., 2000). Micromolar concentrations of ATP activate runt-related transcription factor 2 (RUNX2) in the osteoblast-like HOBIT cell line (Costessi et al., 2005), and  $\beta$ -catenin has been shown to interact with RUNX2 to enhance osteoblast gene expression (Gaur et al., 2005). In this regard, stimulation of the

**Figure 4.8 Possible Mechanism for Cross-talk between P2X7 Nucleotide Receptor and Canonical Wnt Signaling Pathways in Cells of the Osteoblast Lineage.**

The P2X7 and Wnt/ $\beta$ -catenin pathways regulate osteoblast differentiation, and are critical for anabolic responses of the skeleton to mechanical load. Activation of canonical Wnt signaling by Wnt3a alone elicits a sustained increase in  $\beta$ -catenin nuclear localization and transcriptional activity (*left panel*). Activation of P2X7 receptor signaling causes inhibitory phosphorylation of GSK3 $\beta$  and promotes transient nuclear localization of  $\beta$ -catenin, but fails to elicit changes in  $\beta$ -catenin transcriptional activity (*middle panel*). Notably, stimulation of P2X7 receptors in the presence of Wnt3a leads to a dramatic potentiation of  $\beta$ -catenin nuclear localization and transcriptional activity compared to Wnt3a alone (*right panel*). Taken together, this study provides the first evidence of crosstalk between the P2X7 and Wnt/ $\beta$ -catenin pathways, a novel mechanism through which osteoblast activity may be modulated in response to mechanically-induced ATP release in bone.



ADP-sensitive P2Y<sub>13</sub> receptor in cerebellar granule neurons leads to PI3K/AKT-dependent inhibition of GSK3 $\beta$ , resulting in nuclear localization of  $\beta$ -catenin (Ortega et al., 2008). As transcripts for P2Y<sub>13</sub> have been detected in cultures of MC3T3-E1 cells and primary rat calvarial osteoblasts (Qi et al., 2007; Orriss et al., 2010), P2Y<sub>13</sub> may also modulate canonical Wnt signaling in our system. However, we found that low concentrations of ATP, UTP and ADP did not potentiate  $\beta$ -catenin transcriptional activity in the presence or absence of Wnt3a. In contrast, both BzATP and high ATP concentrations elicited potentiation indicating that P2X<sub>7</sub> alone modulates canonical Wnt signaling in osteoblasts. At the same time, mechanisms underlying the effects P2X<sub>7</sub> on the Wnt/ $\beta$ -catenin pathway remain to be elucidated.

PTH, bone morphogenetic proteins (BMPs) and other bone anabolic pathways modulate Wnt/ $\beta$ -catenin signaling to regulate the proliferation, differentiation and function of osteoblast lineage cells. In the present study, we demonstrate that P2X<sub>7</sub> receptors can induce transient nuclear localization of  $\beta$ -catenin and additively increase  $\beta$ -catenin nuclear localization elicited by Wnt3a at early time points. The speed with which  $\beta$ -catenin is activated downstream of P2X<sub>7</sub> suggests its effects are mediated by modulation of intracellular signaling pathways upstream of changes in gene expression. In this regard, the PTH 1 receptor (PTH1R) interacts with dishevelled (Dvl) when bound to PTH, resulting in rapid stabilization and nuclear localization of  $\beta$ -catenin independent of Wnt ligands or LRP5/6 (Romero et al., 2010). The PTH-PTH1R complex also couples to the cAMP/PKA pathway to facilitate canonical Wnt signaling through inhibition of GSK3 $\beta$  in osteoblast-like SaOS-2 cells (Suzuki et al., 2008). Previous work by our lab demonstrated that the P2X<sub>7</sub> receptor couples to production of PGE<sub>2</sub> to promote osteoblast

differentiation and matrix mineralization (Panupinthu et al., 2008). Moreover, studies by others have shown that P2X7 is required for fluid shear stress-induced release of PGE<sub>2</sub> and associated signaling *in vitro* (Li et al., 2005). Like PTH, PGE<sub>2</sub> also signals at least in part through Gα<sub>s</sub> downstream of fluid shear stress to activate cAMP/PKA and PI3K/AKT signaling, both of which inhibit GSK3β leading to activation of β-catenin in the absence of canonical Wnts (Kitase et al., 2010; Xia et al., 2010). Thus, the early, rapid potentiation of the Wnt/β-catenin pathway elicited by P2X7 may involve PGE<sub>2</sub> signaling.

In addition to its transient effects, stimulation of P2X7 prolonged Wnt3a-induced β-catenin nuclear localization compared to Wnt3a alone. Notably, prolonged (but not transient) activation of canonical Wnt signaling was associated with increases in β-catenin transcriptional activity. Nucleotides are rapidly degraded once released into the extracellular environment by actions of ecto-nucleotidases present on the cell surface (Zimmermann et al., 2012). Thus, it is likely that the prolonged potentiation of canonical Wnt signaling mediated by P2X7 is due at least in part to changes in expression of secondary factors such as canonical Wnt ligands and antagonists. In this regard, intermittent PTH signaling decreases expression of Wnt pathway antagonists such as SOST and DKK1 (Bellido et al., 2005; Keller and Kneissel, 2005; Guo et al., 2010; Yao et al., 2011). Additionally, BMP-2 has been shown to activate β-catenin transcriptional activity leading to increased expression of Wnt ligands and their receptors in differentiating cultures of primary calvarial osteoblasts (Chen et al., 2007). At the same time, BMP can stimulate expression of canonical Wnt antagonists such as DKK1 and SOST, and mice deficient in either the BMP receptor type 1A or the BMP-7 receptor ACVR1 specifically in osteoblasts exhibit increased Wnt/β-catenin signaling (Kamiya et

al., 2010; Kamiya et al., 2011). We have demonstrated previously that prolonged  $\text{Ca}^{2+}$ /NFATc1 signaling downstream of P2X7 leads to prolonged expression of cyclooxygenase-2 (COX-2) (Grol et al., 2013). Interestingly, NFATc1 has been shown to function downstream of strontium ranelate *in vitro* to elicit expression of canonical Wnt3a and non-canonical Wnt5a (Fromigue et al., 2010). Taken together, whereas transient activation of  $\beta$ -catenin downstream of P2X7 is likely due to modulation of intracellular signaling, the prolonged potentiation may be mediated by longer-term changes in the expression of canonical Wnt pathway components.

#### **4.5.2 P2X7 Promotes Inhibitory Phosphorylation of GSK3 $\beta$**

One mechanism through which anabolic factors such as PTH and  $\text{PGE}_2$  modulate  $\beta$ -catenin activity is by inhibiting GSK3 $\beta$  through cAMP/PKA and PI3K/AKT signaling (Suzuki et al., 2008; Kitase et al., 2010; Xia et al., 2010). In the present study, we found that activation of P2X7 receptors leads to inhibitory phosphorylation of GSK3 $\beta$ . These findings are consistent with observations in cultures of cerebellar granule neurons, in which activation of P2X7 inhibits GSK3 $\beta$  in a manner dependent upon protein kinase C (PKC) signaling (Ortega et al., 2009; Ortega et al., 2010). In this regard, we have shown previously that activation of P2X7 in osteoblast-like cells couples to PI3K/AKT signaling (Grol et al., 2012), a pathway that has been previously associated with GSK3 $\beta$  inhibition in osteoblast lineage cells (Xia et al., 2010). Moreover, in osteoclasts, P2X7 couples to activation of various  $\text{Ca}^{2+}$ -sensitive PKC isoforms including PKC $\alpha$  and PKC $\beta$  (Armstrong et al., 2009). Thus, both PI3K/AKT and PKC may mediate the effects of P2X7 on GSK3 $\beta$ .



Interestingly, inhibition of GSK3 $\beta$  protects cerebellar granule neurons from cell death induced by PI3K inhibition (Ortega et al., 2009; Ortega et al., 2010). In osteocytes, activation of  $\beta$ -catenin downstream of PGE<sub>2</sub> and/or fluid shear stress promotes survival in response to skeletal unloading or glucocorticoid treatment (Kitase et al., 2010; Xia et al., 2010; Bonewald, 2011). Activation of P2X7 promotes apoptosis in many, but not all cell types (Adinolfi et al., 2005). In this regard, cells of the osteoblast lineage are resistant to P2X7-induced cell death, a phenomenon that may be mediated in part by activation of PI3K/AKT signaling downstream of the P2X7 receptor in these cells (Grol et al., 2012). The finding that P2X7 also couples to inhibitory phosphorylation of GSK3 $\beta$  inhibition in osteoblasts further suggests that, in addition to serving as a potential point of cross-talk with the canonical Wnt pathway, GSK3 $\beta$  inhibition may promote osteoblast survival downstream of P2X7 activation.

#### **4.5.3 Potential Physiological Roles of P2X7-induced Potentiation of Canonical Wnt Signaling in Osteoblasts**

Homozygous deletion of either P2X7 or canonical Wnt signaling components such as LRP5 in mice reduces anabolic responses of the skeleton to mechanical load (Li et al., 2005; Sawakami et al., 2006; Zhao et al., 2013). The crosstalk identified between these two pathways in the present study may help to explain how each increases osteoblast differentiation and bone formation during mechanotransduction. Experimental evidence suggests that ATP acts upstream of LRP5-dependent signaling as an initial transducer of mechanical stimuli in cells of the osteoblast lineage (Sawakami et al., 2006). Thus, ATP signaling through P2X7 may be required to sensitize quiescent cells to

mechanical stimuli to permit activation the Wnt/ $\beta$ -catenin pathway. In this regard, microstrain increases expression of Wnt/ $\beta$ -catenin target genes in MC3T3-E1 osteoblast-like cells, an effect that can be potentiated by pretreatment with Wnt ligand (Robinson et al., 2006). Given that ATP is released from these cultures in response to mechanical stimuli (Li et al., 2005; Sawakami et al., 2006), this potentiation may in fact be mediated by signaling through P2X7.

Based on the extensive genetic data demonstrating importance of the Wnt/ $\beta$ -catenin pathway in adult bone homeostasis, a SOST antibody was recently developed for use as an anabolic therapy for the treatment of osteoporosis. In keeping with the experimental evidence, this treatment, in both humans and animal models, promotes bone formation concomitant with reduction in bone resorption markers resulting in overall increases in bone mass (Li et al., 2010; Ominsky et al., 2010; Paszty et al., 2010; Padhi et al., 2011). In the present study, we demonstrate that responses to canonical Wnt3a in calvarial cells from P2X7 knockout mice are significantly less than in cells from wild-type controls. Common loss-of-function polymorphisms in the human P2X7 receptor are associated with lower lumbar spine bone mineral density and increased fracture risk in post-menopausal women (Ohlendorff et al., 2007; Gartland et al., 2012; Jorgensen et al., 2012). Taken together with the data presented here, this suggests that individuals with reduced P2X7 receptor function could exhibit a blunted response to anabolic therapies targeting canonical Wnt signaling for the treatment of osteoporosis.

## 4.6 References

- Abbracchio, M.P., G. Burnstock, J.M. Boeynaems, E.A. Barnard, J.L. Boyer, C. Kennedy, G.E. Knight, M. Fumagalli, C. Gachet, K.A. Jacobson, and G.A. Weisman. 2006. International Union of Pharmacology LVIII: update on the P2Y G protein-coupled nucleotide receptors: from molecular mechanisms and pathophysiology to therapy. *Pharmacol Rev.* 58:281-341.
- Adinolfi, E., C. Pizzirani, M. Idzko, E. Panther, J. Norgauer, F. Di Virgilio, and D. Ferrari. 2005. P2X(7) receptor: Death or life? *Purinergic Signal.* 1:219-227.
- Armstrong, S., A. Pereverzev, S.J. Dixon, and S.M. Sims. 2009. Activation of P2X7 receptors causes isoform-specific translocation of protein kinase C in osteoclasts. *J Cell Sci.* 122:136-144.
- Armstrong, V.J., M. Muzylak, A. Sunters, G. Zaman, L.K. Saxon, J.S. Price, and L.E. Lanyon. 2007. Wnt/beta-catenin signaling is a component of osteoblastic bone cell early responses to load-bearing and requires estrogen receptor alpha. *J Biol Chem.* 282:20715-20727.
- Baron, R., and M. Kneissel. 2013. WNT signaling in bone homeostasis and disease: from human mutations to treatments. *Nat Med.* 19:179-192.
- Bellido, T., A.A. Ali, I. Gubrij, L.I. Plotkin, Q. Fu, C.A. O'Brien, S.C. Manolagas, and R.L. Jilka. 2005. Chronic elevation of parathyroid hormone in mice reduces expression of sclerostin by osteocytes: a novel mechanism for hormonal control of osteoblastogenesis. *Endocrinology.* 146:4577-4583.
- Biechele, T.L., and R.T. Moon. 2008. Assaying beta-catenin/TCF transcription with beta-catenin/TCF transcription-based reporter constructs. *Methods Mol Biol.* 468:99-110.
- Bodine, P.V., and B.S. Komm. 2006. Wnt signaling and osteoblastogenesis. *Rev Endocr Metab Disord.* 7:33-39.
- Bonewald, L.F. 2011. The amazing osteocyte. *J Bone Miner Res.* 26:229-238.
- Bonewald, L.F., and M.L. Johnson. 2008. Osteocytes, mechanosensing and Wnt signaling. *Bone.* 42:606-615.
- Bowler, W.B., K.A. Buckley, A. Gartland, R.A. Hipskind, G. Bilbe, and J.A. Gallagher. 2001. Extracellular nucleotide signaling: a mechanism for integrating local and systemic responses in the activation of bone remodeling. *Bone.* 28:507-512.
- Bowler, W.B., C.J. Dixon, C. Halleux, R. Maier, G. Bilbe, W.D. Fraser, J.A. Gallagher, and R.A. Hipskind. 1999. Signaling in human osteoblasts by extracellular

- nucleotides. Their weak induction of the c-fos proto-oncogene via  $\text{Ca}^{2+}$  mobilization is strongly potentiated by a parathyroid hormone/cAMP-dependent protein kinase pathway independently of mitogen-activated protein kinase. *J Biol Chem.* 274:14315-14324.
- Burnstock, G. 2007. Purine and pyrimidine receptors. *Cell Mol Life Sci.* 64:1471-1483.
- Case, N., M. Ma, B. Sen, Z. Xie, T.S. Gross, and J. Rubin. 2008. Beta-catenin levels influence rapid mechanical responses in osteoblasts. *J Biol Chem.* 283:29196-29205.
- Case, N., B. Sen, J.A. Thomas, M. Styner, Z. Xie, C.R. Jacobs, and J. Rubin. 2011. Steady and oscillatory fluid flows produce a similar osteogenic phenotype. *Calcif Tissue Int.* 88:189-197.
- Case, N., Z. Xie, B. Sen, M. Styner, M. Zou, C. O'Connor, M. Horowitz, and J. Rubin. 2010. Mechanical activation of beta-catenin regulates phenotype in adult murine marrow-derived mesenchymal stem cells. *J Orthop Res.* 28:1531-1538.
- Caverzasio, J., E. Biver, and C. Thouverey. 2013. Predominant role of PDGF receptor transactivation in Wnt3a-induced osteoblastic cell proliferation. *J Bone Miner Res.* 28:260-270.
- Chen, Y., H.C. Whetstone, A. Youn, P. Nadesan, E.C. Chow, A.C. Lin, and B.A. Alman. 2007. Beta-catenin signaling pathway is crucial for bone morphogenetic protein 2 to induce new bone formation. *J Biol Chem.* 282:526-533.
- Costessi, A., A. Pines, P. D'Andrea, M. Romanello, G. Damante, L. Cesaratto, F. Quadrifoglio, L. Moro, and G. Tell. 2005. Extracellular nucleotides activate Runx2 in the osteoblast-like HOBIT cell line: a possible molecular link between mechanical stress and osteoblasts' response. *Bone.* 36:418-432.
- Fromigue, O., E. Hay, A. Barbara, and P.J. Marie. 2010. Essential role of nuclear factor of activated T cells (NFAT)-mediated Wnt signaling in osteoblast differentiation induced by strontium ranelate. *J Biol Chem.* 285:25251-25258.
- Gartland, A., K.K. Skarratt, L.J. Hocking, C. Parsons, L. Stokes, N.R. Jorgensen, W.D. Fraser, D.M. Reid, J.A. Gallagher, and J.S. Wiley. 2012. Polymorphisms in the P2X7 receptor gene are associated with low lumbar spine bone mineral density and accelerated bone loss in post-menopausal women. *Eur J Hum Genet.* 20:559-564.
- Gaur, T., C.J. Lengner, H. Hovhannisyan, R.A. Bhat, P.V. Bodine, B.S. Komm, A. Javed, A.J. van Wijnen, J.L. Stein, G.S. Stein, and J.B. Lian. 2005. Canonical WNT signaling promotes osteogenesis by directly stimulating Runx2 gene expression. *J Biol Chem.* 280:33132-33140.

- Grol, M.W., A. Pereverzev, S.M. Sims, and S.J. Dixon. 2013. P2 receptor networks regulate signaling duration over a wide dynamic range of ATP concentrations. *Journal of Cell Science*. [Epub ahead of print; DOI:10.1242/jcs.122705]
- Grol, M.W., I. Zelner, and S.J. Dixon. 2012. P2X(7)-mediated calcium influx triggers a sustained, PI3K-dependent increase in metabolic acid production by osteoblast-like cells. *Am J Physiol Endocrinol Metab*. 302:E561-575.
- Guo, J., M. Liu, D. Yang, M.L. Bouxsein, H. Saito, R.J. Galvin, S.A. Kuhstoss, C.C. Thomas, E. Schipani, R. Baron, F.R. Bringhurst, and H.M. Kronenberg. 2010. Suppression of Wnt signaling by Dkk1 attenuates PTH-mediated stromal cell response and new bone formation. *Cell Metab*. 11:161-171.
- Hartmann, C. 2006. A Wnt canon orchestrating osteoblastogenesis. *Trends Cell Biol*. 16:151-158.
- Jorgensen, N.R., L.B. Husted, K.K. Skarratt, L. Stokes, C.L. Tofteng, T. Kvist, J.E. Jensen, P. Eiken, K. Brixen, S. Fuller, R. Clifton-Bligh, A. Gartland, P. Schwarz, B.L. Langdahl, and J.S. Wiley. 2012. Single-nucleotide polymorphisms in the P2X7 receptor gene are associated with post-menopausal bone loss and vertebral fractures. *Eur J Hum Genet*. 20:675-681.
- Kamiya, N., V.M. Kaartinen, and Y. Mishina. 2011. Loss-of-function of ACVR1 in osteoblasts increases bone mass and activates canonical Wnt signaling through suppression of Wnt inhibitors SOST and DKK1. *Biochem Biophys Res Commun*. 414:326-330.
- Kamiya, N., T. Kobayashi, Y. Mochida, P.B. Yu, M. Yamauchi, H.M. Kronenberg, and Y. Mishina. 2010. Wnt inhibitors Dkk1 and Sost are downstream targets of BMP signaling through the type IA receptor (BMPRIA) in osteoblasts. *J Bone Miner Res*. 25:200-210.
- Ke, H.Z., H. Qi, A.F. Weidema, Q. Zhang, N. Panupinthu, D.T. Crawford, W.A. Grasser, V.M. Paralkar, M. Li, L.P. Audoly, C.A. Gabel, W.S. Jee, S.J. Dixon, S.M. Sims, and D.D. Thompson. 2003. Deletion of the P2X<sub>7</sub> nucleotide receptor reveals its regulatory roles in bone formation and resorption. *Mol Endocrinol*. 17:1356-1367.
- Keller, H., and M. Kneissel. 2005. SOST is a target gene for PTH in bone. *Bone*. 37:148-158.
- Khakh, B.S., and R.A. North. 2006. P2X receptors as cell-surface ATP sensors in health and disease. *Nature*. 442:527-532.
- Kitase, Y., L. Barragan, H. Qing, S. Kondoh, J.X. Jiang, M.L. Johnson, and L.F. Bonewald. 2010. Mechanical induction of PGE<sub>2</sub> in osteocytes blocks glucocorticoid-induced apoptosis through both the beta-catenin and PKA

- pathways. *J Bone Miner Res.* 25:2657-2668.
- Krishnan, V., H.U. Bryant, and O.A. Macdougald. 2006. Regulation of bone mass by Wnt signaling. *J Clin Invest.* 116:1202-1209.
- Li, J., D. Liu, H.Z. Ke, R.L. Duncan, and C.H. Turner. 2005. The P2X<sub>7</sub> nucleotide receptor mediates skeletal mechanotransduction. *J Biol Chem.* 280:42952-42959.
- Li, X., K.S. Warmington, Q.T. Niu, F.J. Asuncion, M. Barrero, M. Grisanti, D. Dwyer, B. Stouch, T.M. Thway, M. Stolina, M.S. Ominsky, P.J. Kostenuik, W.S. Simonet, C. Paszty, and H.Z. Ke. 2010. Inhibition of sclerostin by monoclonal antibody increases bone formation, bone mass, and bone strength in aged male rats. *J Bone Miner Res.* 25:2647-2656.
- Lin, C., X. Jiang, Z. Dai, X. Guo, T. Weng, J. Wang, Y. Li, G. Feng, X. Gao, and L. He. 2009. Sclerostin mediates bone response to mechanical unloading through antagonizing Wnt/beta-catenin signaling. *J Bone Miner Res.* 24:1651-1661.
- Long, F. 2012. Building strong bones: molecular regulation of the osteoblast lineage. *Nat Rev Mol Cell Biol.* 13:27-38.
- MacDonald, B.T., K. Tamai, and X. He. 2009. Wnt/beta-catenin signaling: components, mechanisms, and diseases. *Dev Cell.* 17:9-26.
- Masin, M., C. Young, K. Lim, S.J. Barnes, X.J. Xu, V. Marschall, W. Brutkowski, E.R. Mooney, D.C. Gorecki, and R. Murrell-Lagnado. 2012. Expression, assembly and function of novel C-terminal truncated variants of the mouse P2X<sub>7</sub> receptor: re-evaluation of P2X<sub>7</sub> knockouts. *Br J Pharmacol.* 165:978-993.
- Nakamura, E., Y. Uezono, K. Narusawa, I. Shibuya, Y. Oishi, M. Tanaka, N. Yanagihara, T. Nakamura, and F. Izumi. 2000. ATP activates DNA synthesis by acting on P2X receptors in human osteoblast-like MG-63 cells. *Am J Physiol Cell Physiol.* 279:C510-519.
- North, R.A. 2002. Molecular physiology of P2X receptors. *Physiol Rev.* 82:1013-1067.
- Norvell, S.M., M. Alvarez, J.P. Bidwell, and F.M. Pavalko. 2004. Fluid shear stress induces beta-catenin signaling in osteoblasts. *Calcif Tissue Int.* 75:396-404.
- Ohlendorff, S.D., C.L. Tofteng, J.E. Jensen, S. Petersen, R. Civitelli, M. Fenger, B. Abrahamsen, A.P. Hermann, P. Eiken, and N.R. Jorgensen. 2007. Single nucleotide polymorphisms in the P2X<sub>7</sub> gene are associated to fracture risk and to effect of estrogen treatment. *Pharmacogenet Genomics.* 17:555-567.
- Okumura, H., D. Shiba, T. Kubo, and T. Yokoyama. 2008. P2X<sub>7</sub> receptor as sensitive flow sensor for ERK activation in osteoblasts. *Biochem Biophys Res Commun.*

372:486-490.

- Ominsky, M.S., F. Vlasseros, J. Jolette, S.Y. Smith, B. Stouch, G. Doellgast, J. Gong, Y. Gao, J. Cao, K. Graham, B. Tipton, J. Cai, R. Deshpande, L. Zhou, M.D. Hale, D.J. Lightwood, A.J. Henry, A.G. Popplewell, A.R. Moore, M.K. Robinson, D.L. Lacey, W.S. Simonet, and C. Paszty. 2010. Two doses of sclerostin antibody in cynomolgus monkeys increases bone formation, bone mineral density, and bone strength. *J Bone Miner Res.* 25:948-959.
- Orriss, I.R., G. Burnstock, and T.R. Arnett. 2010. Purinergic signalling and bone remodelling. *Curr Opin Pharmacol.* 10:322-330.
- Ortega, F., R. Perez-Sen, E.G. Delicado, and M.T. Miras-Portugal. 2009. P2X7 nucleotide receptor is coupled to GSK-3 inhibition and neuroprotection in cerebellar granule neurons. *Neurotox Res.* 15:193-204.
- Ortega, F., R. Perez-Sen, and M.T. Miras-Portugal. 2008. Gi-coupled P2Y-ADP receptor mediates GSK-3 phosphorylation and beta-catenin nuclear translocation in granule neurons. *J Neurochem.* 104:62-73.
- Ortega, F., R. Perez-Sen, V. Morente, E.G. Delicado, and M.T. Miras-Portugal. 2010. P2X7, NMDA and BDNF receptors converge on GSK3 phosphorylation and cooperate to promote survival in cerebellar granule neurons. *Cell Mol Life Sci.* 67:1723-1733.
- Padhi, D., G. Jang, B. Stouch, L. Fang, and E. Posvar. 2011. Single-dose, placebo-controlled, randomized study of AMG 785, a sclerostin monoclonal antibody. *J Bone Miner Res.* 26:19-26.
- Panupinthu, N., J.T. Rogers, L. Zhao, L.P. Solano-Flores, F. Possmayer, S.M. Sims, and S.J. Dixon. 2008. P2X7 receptors on osteoblasts couple to production of lysophosphatidic acid: a signaling axis promoting osteogenesis. *J Cell Biol.* 181:859-871.
- Papachristou, D.J., K.K. Papachroni, E.K. Basdra, and A.G. Papavassiliou. 2009. Signaling networks and transcription factors regulating mechanotransduction in bone. *Bioessays.* 31:794-804.
- Paszty, C., C.H. Turner, and M.K. Robinson. 2010. Sclerostin: a gem from the genome leads to bone-building antibodies. *J Bone Miner Res.* 25:1897-1904.
- Qi, J., L. Chi, J. Faber, B. Koller, and A.J. Banes. 2007. ATP reduces gel compaction in osteoblast-populated collagen gels. *J Appl Physiol.* 102:1152-1160.
- Robinson, J.A., M. Chatterjee-Kishore, P.J. Yaworsky, D.M. Cullen, W. Zhao, C. Li, Y. Kharode, L. Sauter, P. Babij, E.L. Brown, A.A. Hill, M.P. Akhter, M.L. Johnson,

- R.R. Recker, B.S. Komm, and F.J. Bex. 2006. Wnt/beta-catenin signaling is a normal physiological response to mechanical loading in bone. *J Biol Chem.* 281:31720-31728.
- Robling, A.G., A.B. Castillo, and C.H. Turner. 2006. Biomechanical and molecular regulation of bone remodeling. *Annu Rev Biomed Eng.* 8:455-498.
- Robling, A.G., P.J. Niziolek, L.A. Baldrige, K.W. Condon, M.R. Allen, I. Alam, S.M. Mantila, J. Gluhak-Heinrich, T.M. Bellido, S.E. Harris, and C.H. Turner. 2008. Mechanical stimulation of bone in vivo reduces osteocyte expression of Sost/sclerostin. *J Biol Chem.* 283:5866-5875.
- Romero, G., W.B. Sneddon, Y. Yang, D. Wheeler, H.C. Blair, and P.A. Friedman. 2010. Parathyroid hormone receptor directly interacts with dishevelled to regulate beta-catenin signaling and osteoclastogenesis. *J Biol Chem.* 285:14756-14763.
- Santos, A., A.D. Bakker, B. Zandieh-Doulabi, C.M. Semeins, and J. Klein-Nulend. 2009. Pulsating fluid flow modulates gene expression of proteins involved in Wnt signaling pathways in osteocytes. *J Orthop Res.* 27:1280-1287.
- Sawakami, K., A.G. Robling, M. Ai, N.D. Pitner, D. Liu, S.J. Warden, J. Li, P. Maye, D.W. Rowe, R.L. Duncan, M.L. Warman, and C.H. Turner. 2006. The Wnt co-receptor LRP5 is essential for skeletal mechanotransduction but not for the anabolic bone response to parathyroid hormone treatment. *J Biol Chem.* 281:23698-23711.
- Sen, B., M. Styner, Z. Xie, N. Case, C.T. Rubin, and J. Rubin. 2009. Mechanical loading regulates NFATc1 and beta-catenin signaling through a GSK3beta control node. *J Biol Chem.* 284:34607-34617.
- Sen, B., Z. Xie, N. Case, M. Ma, C. Rubin, and J. Rubin. 2008. Mechanical strain inhibits adipogenesis in mesenchymal stem cells by stimulating a durable beta-catenin signal. *Endocrinology.* 149:6065-6075.
- Solle, M., J. Labasi, D.G. Perregaux, E. Stam, N. Petrushova, B.H. Koller, R.J. Griffiths, and C.A. Gabel. 2001. Altered cytokine production in mice lacking P2X<sub>7</sub> receptors. *J Biol Chem.* 276:125-132.
- Spencer, G.J., J.C. Utting, S.L. Etheridge, T.R. Arnett, and P.G. Genever. 2006. Wnt signalling in osteoblasts regulates expression of the receptor activator of NFkappaB ligand and inhibits osteoclastogenesis in vitro. *J Cell Sci.* 119:1283-1296.
- Suzuki, A., K. Ozono, T. Kubota, H. Kondou, K. Tachikawa, and T. Michigami. 2008. PTH/cAMP/PKA signaling facilitates canonical Wnt signaling via inactivation of glycogen synthase kinase-3beta in osteoblastic Saos-2 cells. *J Cell Biochem.*



104:304-317.

- Thompson, W.R., C.T. Rubin, and J. Rubin. 2012. Mechanical regulation of signaling pathways in bone. *Gene*. 503:179-193.
- Tu, X., Y. Rhee, K.W. Condon, N. Bivi, M.R. Allen, D. Dwyer, M. Stolina, C.H. Turner, A.G. Robling, L.I. Plotkin, and T. Bellido. 2012. Sost downregulation and local Wnt signaling are required for the osteogenic response to mechanical loading. *Bone*. 50:209-217.
- Westendorf, J.J., R.A. Kahler, and T.M. Schroeder. 2004. Wnt signaling in osteoblasts and bone diseases. *Gene*. 341:19-39.
- Xia, X., N. Batra, Q. Shi, L.F. Bonewald, E. Sprague, and J.X. Jiang. 2010. Prostaglandin promotion of osteocyte gap junction function through transcriptional regulation of connexin 43 by glycogen synthase kinase 3/beta-catenin signaling. *Mol Cell Biol*. 30:206-219.
- Yao, G.Q., J.J. Wu, N. Troiano, and K. Insogna. 2011. Targeted overexpression of Dkk1 in osteoblasts reduces bone mass but does not impair the anabolic response to intermittent PTH treatment in mice. *J Bone Miner Metab*. 29:141-148.
- Zhao, L., J.W. Shim, T.R. Dodge, A.G. Robling, and H. Yokota. 2013. Inactivation of Lrp5 in osteocytes reduces young's modulus and responsiveness to the mechanical loading. *Bone*. 54:35-43.
- Zimmermann, H., M. Zebisch, and N. Strater. 2012. Cellular function and molecular structure of ecto-nucleotidases. *Purinergic Signal*. 8:437-502.

## **CHAPTER FIVE**

### **GENERAL DISCUSSION**

## 5.1 Summary and Conclusions

This thesis evaluated signaling downstream of P2X7 and other P2 nucleotide receptors in cells of the osteoblast lineage. We demonstrate that endogenous P2Y-P2X receptor networks allow cells to sense a wide range of adenosine 5'-triphosphate (ATP) concentrations, and transduce this input into distinct cellular responses. Additionally, we found that P2X7 couples through multiple anabolic pathways, including  $\text{Ca}^{2+}$ /nuclear factor of activated T-cells, cytoplasmic 1 (NFATc1), phosphatidylinositol 3-kinase (PI3K)/AKT, and Wnt/ $\beta$ -catenin signaling, to promote changes in gene expression and cellular metabolism. The specific objectives and findings of each data chapter are summarized below.

### 5.1.1 Role of P2 Receptor Networks in Osteoblasts: Objective, Summary and Conclusions

*Specific Objective of Chapter 2* – To characterize the P2 network expressed by cells of the osteoblast lineage by elucidating the role of P2Y and P2X receptor subtypes in regulation of  $\text{Ca}^{2+}$ /NFATc1 signaling in these cells.

#### *Summary of Methodology and Results*

1. Changes in cytosolic free  $\text{Ca}^{2+}$  concentration ( $[\text{Ca}^{2+}]_i$ ) and the subcellular localization and transcriptional activity of NFATc1 were assessed using MC3T3-E1 osteoblast-like cells and primary calvarial osteoblasts from wild-type and P2X7 knockout mice.
2. Graded increases in the magnitude and duration of cytosolic  $\text{Ca}^{2+}$  signaling were achieved over a remarkable million-fold range of ATP concentrations (1 nM to 1 mM).

3. A low concentration of ATP (10  $\mu\text{M}$ ,  $\text{ATP}_{\text{low}}$ ) activated  $\text{P2Y}_2$  and/or  $\text{P2Y}_4$  receptors to cause release of  $\text{Ca}^{2+}$  from intracellular stores resulting in transient elevation of  $[\text{Ca}^{2+}]_i$ .
4. Sustained elevations of  $[\text{Ca}^{2+}]_i$  elicited by treatment with a high concentration of ATP (1 mM,  $\text{ATP}_{\text{high}}$ ) or 2',3'-*O*-(4-benzoylbenzoyl)ATP (BzATP) were mediated by activation of  $\text{P2X}_7$  receptors and subsequent  $\text{Ca}^{2+}$  influx.
5.  $\text{ATP}_{\text{low}}$  caused transient nuclear localization of NFATc1; whereas,  $\text{ATP}_{\text{high}}$  or BzATP elicited more sustained localization.
6. Sustained nuclear localization of NFATc1 elicited by BzATP or  $\text{ATP}_{\text{high}}$  was mediated by activation of  $\text{P2X}_7$  receptors; whereas, transient localization induced by  $\text{ATP}_{\text{low}}$  was due to activation of higher affinity  $\text{P2Y}$  receptors.
7.  $\text{ATP}_{\text{high}}$  or BzATP, but not  $\text{ATP}_{\text{low}}$ , elicited robust expression of the NFAT target gene *Ptgs2* (encoding cyclooxygenase-2 (COX-2)) and increased NFAT transcriptional activity.
8. The increase in NFAT target gene expression and transcriptional activity elicited by BzATP or  $\text{ATP}_{\text{high}}$  was mediated by activation of the  $\text{P2X}_7$  receptor.

### *Conclusions and Significance*

1. Ensembles of  $\text{P2Y}$  and  $\text{P2X}$  receptor subtypes impart sensitivity over a wide range of ATP concentrations, and provide a mechanism by which cells transduce differences in ATP levels into distinct cellular signals.
2. The  $\text{Ca}^{2+}$ /NFATc1 pathway can function as a transducer in dose-to-duration encoding of  $\text{P2}$  receptor stimuli.

3. This phenomenon provides a novel mechanism by which osteoblasts may transduce differences in ATP concentration and, therefore, intensity of mechanical stimuli over a wide dynamic range.
4. The effects of P2X7 on  $\text{Ca}^{2+}$ /NFATc1 signaling may contribute to the mechanisms by which this P2 receptor promotes osteoblast differentiation and function.

### **5.1.2 Regulation of Metabolic Acid Production in Osteoblasts by P2 Receptors: Objective, Summary and Conclusions**

*Specific Objective for Chapter 3* – To determine the effects of signaling through P2X7 as well as other P2 receptor subtypes on energy metabolism in cells of the osteoblast lineage.

#### *Summary of Methodology and Results*

1. A Cytosensor microphysiometer was used to monitor metabolic acid production (proton efflux) from MC3T3-E1 osteoblast-like cells in real time as a measure of cellular metabolism. Additionally, changes in lactic acid efflux and  $[\text{Ca}^{2+}]_i$  were assessed.
2. A high concentration of ATP (1 mM) or BzATP caused a sustained increase in proton efflux; whereas, low concentrations of ATP or UTP (100  $\mu\text{M}$ ) elicited only a transient increase.
3. The sustained phase of BzATP-induced proton efflux was mediated by activation of P2X7 receptors.
4. The increase in proton efflux elicited by BzATP was not associated with

induction of apoptosis.

5. The sustained phase of BzATP-induced proton efflux was dependent on the presence of extracellular glucose.
6. BzATP elicited an increase in lactic acid efflux that was of comparable magnitude to the sustained increase in proton efflux induced by activation of P2X7.
7.  $\text{Ca}^{2+}$  influx through activated P2X7 receptors initiated sustained proton efflux.
8. Maintenance but not initiation of sustained proton efflux elicited by BzATP was dependent on activation of PI3K signaling.

#### *Conclusions and Significance*

1. Brief activation of P2X7 elicits a large and sustained increase in metabolic acid production that requires  $\text{Ca}^{2+}$  for initiation and is maintained by PI3K signaling, resulting in enhanced glucose metabolism via increased glycolytic flux.
2. As the PI3K/AKT pathway enhances cell survival, its activation in osteoblasts may explain the resistance of these cells to P2X7-induced apoptosis observed in many other cell-types.
3. The effects of P2X7 on  $\text{Ca}^{2+}$  and PI3K signaling, as well as glycolytic metabolism and lactic acid efflux, may contribute to mechanisms by which this P2 receptor promotes osteoblast differentiation and matrix mineralization.
4. Metabolic acid production induced by P2X7 may provide a coupling mechanism by which osteoblasts can activate osteoclasts to promote bone resorption.

### **5.1.3 Cross-talk between P2X7 and Wnt/ $\beta$ -catenin Pathways in Osteoblasts: Objective, Summary and Conclusions**

*Specific Objective for Chapter 4* – To investigate whether P2X7 and canonical Wnt signaling pathways interact to regulate  $\beta$ -catenin-mediated gene expression in osteoblasts.

#### *Summary of Methodology and Results*

1. Changes in the phosphorylation of glycogen synthase kinase 3 $\beta$  (GSK3 $\beta$ ), and the subcellular localization and transcriptional activity of  $\beta$ -catenin were assessed using MC3T3-E1 osteoblast-like cells and primary calvarial osteoblasts from wild-type and P2X7 knockout mice.
2. The P2X7 agonist BzATP caused brief transient nuclear localization of  $\beta$ -catenin.
3. Canonical Wnt3a and BzATP caused more rapid and sustained  $\beta$ -catenin nuclear localization compared to Wnt3a alone.
4. Wnt3a induced an increase in the transcriptional activity of  $\beta$ -catenin that was potentiated by treatment with BzATP; in contrast, BzATP alone did not increase  $\beta$ -catenin transcriptional activity.
5. A high concentration of ATP (1 mM), but not a low ATP concentration (10  $\mu$ M) or any concentration of adenosine 5'-diphosphate (ADP) or uridine 5'-triphosphate (UTP) (0.01-1 mM), potentiated  $\beta$ -catenin transcriptional activity elicited by Wnt3a.
6. The potentiation of  $\beta$ -catenin transcriptional activity elicited by BzATP was mediated by activation of the P2X7 receptor.
7. Responses to Wnt3a in calvarial cells from P2X7 knockout mice were

significantly less than in cells from wild-type controls.

8. BzATP increased inhibitory phosphorylation of GSK3 $\beta$  through activation of the P2X7 receptor.

#### *Conclusions and Significance*

1. Activation of the P2X7 receptor potentiates Wnt/ $\beta$ -catenin signaling in cells of the osteoblast lineage, a potential mechanism through which osteoblast activity may be modulated in response to mechanically-induced ATP release in bone.
2. P2X7-mediated potentiation of the Wnt/ $\beta$ -catenin pathway is associated with inhibitory phosphorylation of GSK3 $\beta$ , suggesting that P2X7 may potentiate the effects of canonical Wnt ligands through GSK3 $\beta$ .
3. Given that GSK3 $\beta$  inhibition can promote cell survival, its inhibition in osteoblasts may help to explain the resistance of these cells to P2X7-induced apoptosis observed in many other cell-types.



## 5.2 Limitations of the Research

*Assessment of P2 nucleotide receptor signaling in vitro:* The studies described in this thesis relied primarily on use of the MC3T3-E1 osteoblast-like cell line to evaluate signaling events downstream of P2 nucleotide receptors such as P2X7. As discussed in Chapter 3, only approximately 40% of cultured rat and murine calvarial cells express functional P2X7 receptors (Panupinthu et al., 2007). In contrast, P2X7 is present in over 85% of MC3T3-E1 cells. Thus, the MC3T3-E1 cell line was an ideal model with which to assess P2X7 receptor signaling. To confirm a role for P2X7 in various processes, calvarial cells from P2X7 knockout mice and specific P2X7 antagonists were also employed. Though unequivocal *in vitro* evidence for a role of P2X7 in cellular metabolism as well as  $\text{Ca}^{2+}$ /NFATc1, PI3K/AKT and Wnt/ $\beta$ -catenin signaling pathways is shown, these responses may not reflect responses of osteoblast lineage cells *in vivo*. Additionally, nucleotides were applied exogenously to cultured cells in these studies; whereas *in vivo*, release of nucleotides is elicited by mechanical loading, trauma or other stimuli. Taken together, future studies should verify activation of  $\text{Ca}^{2+}$ /NFAT and Wnt/ $\beta$ -catenin downstream of the P2X7 receptor *in vivo*. This could be accomplished by crossing NFAT luciferase or TOPGAL  $\beta$ -catenin reporter mouse strains with the P2X7 knockout mouse (DasGupta and Fuchs, 1999; Solle et al., 2001; Wilkins et al., 2004), and subjecting these mice to axial ulnar loading (induces bending of the ulna) or high frequency, low amplitude vibration (Thompson et al., 2012). Alternatively, load-bearing bones isolated from wild-type and P2X7 knockout mice following exposure to mechanical loading could be processed and analyzed by real-time reverse transcriptase-polymerase chain reaction (RT-PCR) or Western blot to assess changes in NFAT and  $\beta$ -

catenin target genes.

Though it is unlikely that changes in  $[Ca^{2+}]_i$  could be assessed *in vivo*, a method for *ex vivo* real-time imaging of  $Ca^{2+}$  signaling in calvarial bone explants was recently described (Ishihara et al., 2013). This protocol would provide a three-dimensional context in which to confirm the patterns of P2 receptor-induced  $Ca^{2+}$  signaling described in this thesis. Moreover, changes in  $[Ca^{2+}]_i$  following exposure to nucleotides could be determined in both osteoblasts on the calvarial surface and osteocytes embedded within the bone matrix.

In this thesis, undifferentiated cultures of calvarial osteoblasts were used to examine signaling downstream of P2X7 and other P2 receptors. However, evidence suggests that osteocytes are more sensitive than osteoblasts to mechanical stimuli in terms of fluid shear stress-induced prostaglandin E<sub>2</sub> (PGE<sub>2</sub>) release (Klein-Nulend et al., 1995; Kamel et al., 2010). Moreover,  $Ca^{2+}$  signaling responses to nucleotides have been shown to increase during *in vitro* osteoblast differentiation (Orriss et al., 2006), and the complement of P2 receptors and ecto-nucleotidases is also modulated during osteoblastogenesis (Orriss et al., 2006; Noronha-Matos et al., 2012; Orriss et al., 2012; Roszek et al., 2013). Thus, the studies described in this thesis should ultimately be repeated at various stages of osteoblast differentiation to assess possible differences in P2 receptor signaling.

*Genetically modified mouse models:* Calvarial osteoblasts isolated from P2X7 knockout mice were used in this thesis to confirm a role for P2X7 in various signaling events *in vitro*. These mice were generated previously by exchanging the Cys<sup>506</sup> to Pro<sup>532</sup> section of the P2X7 receptor COOH-terminal domain with a neomycin cassette oriented

in the 3'-5' direction (Solle et al., 2001). Though initial evidence suggested that protein for P2X7 was absent in these mice (Solle et al., 2001), recent work has demonstrated the existence of a COOH-terminal truncated version of the receptor in these mice (Masin et al., 2012). The truncated P2X7 receptor exhibits impaired plasma membrane trafficking as well as greatly diminished BzATP-evoked whole cell currents (Masin et al., 2012). To further complicate interpretations from this knockout mouse model, a naturally occurring P451L loss-of-function polymorphism exists in many common strains of laboratory mice such as C57Bl/6 and DBA/2 (Adriouch et al., 2002). This polymorphism occurs in the COOH-terminus of P2X7, and reduces pore formation, Ca<sup>2+</sup> signaling and ATP release elicited either by BzATP or ATP compared to controls (Adriouch et al., 2002; Suadicani et al., 2009). Given that the P2X7 knockout used in this thesis was maintained on a mixed genetic background (129/Ola × C57Bl/6 × DBA/2), the magnitude of differences between wild-type and knockout mice in our studies may be underestimated. Future development of tissue-specific knockouts for P2X7 will prove invaluable for conclusively demonstrating the function of this nucleotide receptor in bone cells.

### 5.3 Contributions of the Research to the Current State of Knowledge

*P2 receptor networks in mammalian cell-types:* Prior to this thesis, the biological significance of networks of P2Y and P2X receptors in any cell type was unknown. We show that ensembles of P2 receptors provide a mechanism by which cells sense ATP over a wide concentration range, and transduce this input into distinct patterns of  $\text{Ca}^{2+}$ /NFATc1 signaling. At the same time, the studies described here examined only one of four  $\text{Ca}^{2+}$ -regulated NFAT transcription factors. Growing evidence suggests that NFATc1-4 are differentially regulated by kinases that control their subcellular localization (Macian, 2005). The constitutive export kinases for  $\text{Ca}^{2+}$ -regulated NFAT transcription factors are casein kinase 1 (CK1) and GSK3 $\beta$  (Beals et al., 1997a; Beals et al., 1997b; Zhu et al., 1998; Okamura et al., 2004). Inducible kinases, including p38 mitogen-activated protein kinase (MAPK) and c-jun NH<sub>2</sub>-terminal kinase (JNK), differentially phosphorylate NFATc1-4 – p38 MAPK acts on NFATc2 and NFATc4, whereas JNK acts on NFATc1 and NFATc3 (Chow et al., 2000; Gomez del Arco et al., 2000; Yang et al., 2002). Phosphorylation mediated by either p38 MAPK or JNK in turn potentiates CK1 activity (Macian, 2005). Additionally, protein kinase A (PKA)-dependent phosphorylation of NFATc1 may be required prior to phosphorylation by GSK3 $\beta$  (Sheridan et al., 2002). Taken together, additional studies are needed to assess whether other  $\text{Ca}^{2+}$ -regulated NFAT transcription factors in addition to NFATc1 mediate dose-to-duration coupling downstream of endogenous P2Y-P2X receptor networks.

A number of pathways in addition to  $\text{Ca}^{2+}$ /NFATc1 signaling are activated by P2Y and P2X receptor subtypes in cells of the osteoblast lineage. Treatment of ROS 17/2.8 osteoblast-like cells with exogenous ATP activates extracellular signal-regulated

kinase (ERK)1/2 in a dose- and time-dependent manner, presumably through P2Y<sub>2</sub> (Katz et al., 2006). Moreover, fluid shear stress stimulates P2X7 via Ca<sup>2+</sup>-dependent ATP release, resulting in activation of ERK1/2 in cultures of MC3T3-E1 cells and primary calvarial osteoblasts (Liu et al., 2008; Okumura et al., 2008). Interestingly, duration of ERK activation in neuronal PC12 cells has been shown to regulate distinct cellular functions, with transient activation stimulating proliferation and prolonged activation promoting differentiation (Vaudry et al., 2002). Given the critical role for ERK in bone morphogenetic protein (BMP)- and insulin-like growth factor (IGF)-1-induced osteoblast differentiation (Gallea et al., 2001; Celil and Campbell, 2005; Ge et al., 2007; Ge et al., 2012), it would be of interest to determine whether ERK, like the Ca<sup>2+</sup>/NFATc1 pathway, functions in dose-to-duration encoding of P2 receptor stimuli.

*Effects of P2X7 activation on anabolic signaling pathways in osteoblasts:* In this thesis, P2X7 was shown to activate multiple anabolic pathways in osteoblast lineage cells, including Ca<sup>2+</sup>/NFATc1, PI3K/AKT, and Wnt/ $\beta$ -catenin signaling. Each of these pathways in turn may promote osteoblast differentiation and matrix mineralization downstream of the P2X7 receptor. In this regard, NFATc1 and PI3K/AKT signaling drive osteoblast differentiation downstream of BMP-2 at least in part through interactions with Osterix (OSX) and runt-related transcription factor 2 (RUNX2), respectively (Ghosh-Choudhury et al., 2002; Fujita et al., 2004; Koga et al., 2005).  $\beta$ -catenin also enhances RUNX2 expression and transcriptional activity (Gaur et al., 2005), and canonical Wnt signaling is essential for osteoblastogenesis during skeletal development and remodeling (Westendorf et al., 2004; Bodine and Komm, 2006; Hartmann, 2006; Krishnan et al., 2006; Long, 2012; Baron and Kneissel, 2013). Taken together, future studies examining

the role of these signaling pathways downstream of P2X7 will provide valuable insights into how this P2 receptor regulates osteoblast differentiation and function.

In addition to modulation of the anabolic pathways described above, we found that acute stimulation of the P2X7 receptor promotes metabolic acid efflux from osteoblast-like cells primarily through increased rates of glycolysis. Interestingly, recent evidence has suggested that modulation of glycolytic metabolism downstream of Wnt-lipoprotein receptor-related protein (LRP) 5 signaling provides an additional mechanism promoting osteoblast differentiation *in vitro* and *in vivo* (Esen et al., 2013) (*see below*).

*Role for cellular metabolism in regulation of osteoblast differentiation:* Many growth factors and hormones stimulate cellular metabolism through activation of the PI3K/AKT pathway, which in turn increases nutrient uptake and glycolytic enzyme activity to drive ATP production (Hammerman et al., 2004; Engelman et al., 2006). Earlier studies *in vitro* demonstrated that prolonged Wnt treatment promotes mitochondrial biogenesis through activation of  $\beta$ -catenin (Yoon et al., 2010). However, recent evidence suggests that acute treatment with Wnt3a in osteoblast lineage cells also stimulates glucose consumption, glycolytic metabolism and lactic acid production through increased expression of key glycolytic enzymes such as hexokinase, phosphofructokinase, and lactate dehydrogenase A (Esen et al., 2013). The effects of acute Wnt3a on glycolytic metabolism are mediated by LRP5-dependent activation of mTORC2/AKT downstream of Rac1, independent of  $\beta$ -catenin. Moreover, knockdown of mTORC2, lactate dehydrogenase A or phosphofructokinase 1 greatly reduces upregulation of alkaline phosphatase (ALP), collagen type 1 (COL1)  $\alpha$ 1 and bone sialoprotein (BSP) in response to Wnt3a but not BMP-2 (Esen et al., 2013). In this thesis,

it is shown that brief activation of P2X7 by exogenous nucleotides elicits a large and sustained increase in proton efflux that is maintained by PI3K signaling, resulting in enhanced glucose metabolism and increased lactic acid production. Given findings for Wnt3a described by Esen and colleagues, this suggests that increased glycolytic metabolism elicited by activation of P2X7 may contribute to its effects on osteoblast differentiation. Thus, future studies assessing the role of glycolytic metabolism in P2X7-induced osteoblast differentiation should be performed.

Besides the metabolic effects described in this thesis, activation of P2X7 was also shown to potentiate canonical Wnt signaling in cells of the osteoblast lineage. In this regard, expression of functional P2X7 receptors was required for full activation of  $\beta$ -catenin downstream of Wnt3a. However, the effect of P2X7 receptor signaling on Wnt3a-induced glycolytic metabolism remains to be investigated. It is possible that functional P2X7 receptors are required, at least in part, for the metabolic response elicited by Wnt3a in cells of the osteoblast lineage.

*P2 receptors and mechanotransduction in bone:* Our lab has proposed previously that mechanotransduction in bone is mediated, at least in part, by nucleotide release and subsequent P2 receptor signaling in osteoblasts and osteoclasts (Dixon and Sims, 2000). In this thesis, it is shown for the first time that P2Y-P2X receptor networks provide a mechanism by which cells sense ATP over a wide concentration range, and transduce this input into distinct cellular signals. This phenomenon may explain how osteoblasts transduce differences in the intensity of mechanical loads to modulate bone mass. In this regard, bone loss associated with skeletal unloading might result from the complete absence of P2 receptor signaling; whereas, modest mechanical loading would maintain

bone mass through activation of low affinity P2 receptors (equivalent to the effects of ATP<sub>low</sub>). On the other hand, large increases in loading, due to an increase in weight bearing exercise or skeletal trauma, may greatly increase ATP concentration within the bone microenvironment, resulting in P2X7-induced bone formation (equivalent to the effects of ATP<sub>high</sub>). That the P2X7 receptor potentiates Wnt/ $\beta$ -catenin signaling suggests that both the P2X7 and canonical Wnt pathways may be required for maximal anabolic responses of the skeleton to mechanical stimuli.

*Implications for cancer:* P2X7 expression is upregulated in many malignant cancers including chronic B lymphocytic leukemia (Adinolfi et al., 2002), prostate (Slater et al., 2004a), lobular and ductal breast carcinomas (Slater et al., 2004b), and thyroid papillary carcinoma (Solini et al., 2008). Though virtually undetectable in healthy tissues, extracellular ATP is in the hundreds of micromolar range in the tumor microenvironment (Pellegatti et al., 2008), a concentration sufficient to stimulate the low affinity P2X7 receptor. Mice inoculated with HEK293 or mouse CT26 carcinoma cells overexpressing P2X7 develop tumors of greater size compared to controls (Adinolfi et al., 2012). These P2X7-expressing tumors are characterized by increased cell proliferation, reduced apoptosis, elevated levels of activated NFATc1 and greater neoangiogenesis compared to control tumors (Adinolfi et al., 2012). In addition to its role in tumor size and vascular infiltration, expression of P2X7 is associated with increased rates of metastasis in papillary thyroid carcinoma (Gu et al., 2010). Moreover, TGF $\beta$ -1-induced migration of human lung cancer A549 cells is dependent on ATP release and subsequent P2X7 receptor signaling (Takai et al., 2012). The enhanced migration and invasiveness associated with expression of P2X7 is thought to be dependent on vascular endothelial



growth factor (VEGF) release and protease production (Gu and Wiley, 2006; Jelassi et al., 2011). In this thesis, we show that P2X7 stimulates sustained proton efflux associated with increased lactic acid production in response to exogenous ATP. Extracellular acidification promotes apoptosis of healthy tissues while promoting degradation of the extracellular matrix in growing tumors (Dhup et al., 2012). Additionally, lactate within the tumor microenvironment is associated with increased tumor cell migration, immunosuppression, VEGF secretion and vascular invasion (Hirschhaeuser et al., 2011; Dhup et al., 2012). Thus, P2X7 activation may also play a role in promoting tumor growth and metastasis by lowering extracellular pH ( $\text{pH}_o$ ) and providing a source of extracellular lactate.

During tumor progression, many cancer cells acquire a metabolic phenotype, described as the Warburg effect, which involves a shift from oxidative phosphorylation to glycolytic metabolism even under normal oxygen concentrations (Warburg, 1956; Cairns et al., 2011). As a result, these cells derive significant amounts of energy from aerobic glycolysis through conversion of glucose to lactate. In this thesis, P2X7 was found to induce the Warburg effect in osteoblast-like cells through a mechanism dependent upon both  $\text{Ca}^{2+}$  and PI3K signaling. Esen and colleagues also show that Wnt3a-LRP5 signaling induces glycolytic metabolism through Rac1 and mTORC2/AKT (Esen et al., 2013). In addition to P2X7, various components of the canonical Wnt signaling pathway such as  $\beta$ -catenin are upregulated or mutated in breast, colorectal and other human cancers (Anastas and Moon, 2013). The ability of P2X7 to potentiate Wnt signaling suggests that concomitant upregulation of the P2X7 and Wnt pathways may drastically increase tumor invasiveness through both canonical and potentially metabolic mechanisms. Future

studies evaluating the role of P2X7 in cancer cell migration and metabolism (both alone and together with Wnt) are likely to provide valuable insights into cancer cell biology.

## 5.4 References

- Adinolfi, E., L. Melchiorri, S. Falzoni, P. Chiozzi, A. Morelli, A. Tieghi, A. Cuneo, G. Castoldi, F. Di Virgilio, and O.R. Baricordi. 2002. P2X7 receptor expression in evolutive and indolent forms of chronic B lymphocytic leukemia. *Blood*. 99:706-708.
- Adinolfi, E., L. Raffaghello, A.L. Giuliani, L. Cavazzini, M. Capece, P. Chiozzi, G. Bianchi, G. Kroemer, V. Pistoia, and F. Di Virgilio. 2012. Expression of P2X7 receptor increases in vivo tumor growth. *Cancer Res*. 72:2957-2969.
- Adriouch, S., C. Dox, V. Welge, M. Seman, F. Koch-Nolte, and F. Haag. 2002. Cutting edge: a natural P451L mutation in the cytoplasmic domain impairs the function of the mouse P2X7 receptor. *J Immunol*. 169:4108-4112.
- Anastas, J.N., and R.T. Moon. 2013. WNT signalling pathways as therapeutic targets in cancer. *Nat Rev Cancer*. 13:11-26.
- Baron, R., and M. Kneissel. 2013. WNT signaling in bone homeostasis and disease: from human mutations to treatments. *Nat Med*. 19:179-192.
- Beals, C.R., N.A. Clipstone, S.N. Ho, and G.R. Crabtree. 1997a. Nuclear localization of NF-ATc by a calcineurin-dependent, cyclosporin-sensitive intramolecular interaction. *Genes Dev*. 11:824-834.
- Beals, C.R., C.M. Sheridan, C.W. Turck, P. Gardner, and G.R. Crabtree. 1997b. Nuclear export of NF-ATc enhanced by glycogen synthase kinase-3. *Science*. 275:1930-1934.
- Bodine, P.V., and B.S. Komm. 2006. Wnt signaling and osteoblastogenesis. *Rev Endocr Metab Disord*. 7:33-39.
- Cairns, R.A., I.S. Harris, and T.W. Mak. 2011. Regulation of cancer cell metabolism. *Nat Rev Cancer*. 11:85-95.
- Celil, A.B., and P.G. Campbell. 2005. BMP-2 and insulin-like growth factor-I mediate Osterix (Osx) expression in human mesenchymal stem cells via the MAPK and protein kinase D signaling pathways. *J Biol Chem*. 280:31353-31359.
- Chow, C.W., C. Dong, R.A. Flavell, and R.J. Davis. 2000. c-Jun NH(2)-terminal kinase inhibits targeting of the protein phosphatase calcineurin to NFATc1. *Mol Cell Biol*. 20:5227-5234.
- DasGupta, R., and E. Fuchs. 1999. Multiple roles for activated LEF/TCF transcription complexes during hair follicle development and differentiation. *Development*. 126:4557-4568.

- Dhup, S., R.K. Dadhich, P.E. Porporato, and P. Sonveaux. 2012. Multiple biological activities of lactic acid in cancer: influences on tumor growth, angiogenesis and metastasis. *Curr Pharm Des.* 18:1319-1330.
- Dixon, S.J., and S.M. Sims. 2000. P2 purinergic receptors on osteoblasts and osteoclasts: Potential targets for drug development. *Drug Dev Res.* 49:187-200.
- Engelman, J.A., J. Luo, and L.C. Cantley. 2006. The evolution of phosphatidylinositol 3-kinases as regulators of growth and metabolism. *Nat Rev Genet.* 7:606-619.
- Esen, E., J. Chen, C.M. Karner, A.L. Okunade, B.W. Patterson, and F. Long. 2013. WNT-LRP5 Signaling Induces Warburg Effect through mTORC2 Activation during Osteoblast Differentiation. *Cell Metab.* 17:745-755.
- Fujita, T., Y. Azuma, R. Fukuyama, Y. Hattori, C. Yoshida, M. Koida, K. Ogita, and T. Komori. 2004. Runx2 induces osteoblast and chondrocyte differentiation and enhances their migration by coupling with PI3K-Akt signaling. *J Cell Biol.* 166:85-95.
- Gallea, S., F. Lallemand, A. Atfi, G. Rawadi, V. Ramez, S. Spinella-Jaegle, S. Kawai, C. Faucheu, L. Huet, R. Baron, and S. Roman-Roman. 2001. Activation of mitogen-activated protein kinase cascades is involved in regulation of bone morphogenetic protein-2-induced osteoblast differentiation in pluripotent C2C12 cells. *Bone.* 28:491-498.
- Gaur, T., C.J. Lengner, H. Hovhannisyan, R.A. Bhat, P.V. Bodine, B.S. Komm, A. Javed, A.J. van Wijnen, J.L. Stein, G.S. Stein, and J.B. Lian. 2005. Canonical WNT signaling promotes osteogenesis by directly stimulating Runx2 gene expression. *J Biol Chem.* 280:33132-33140.
- Ge, C., G. Xiao, D. Jiang, and R.T. Franceschi. 2007. Critical role of the extracellular signal-regulated kinase-MAPK pathway in osteoblast differentiation and skeletal development. *J Cell Biol.* 176:709-718.
- Ge, C., Q. Yang, G. Zhao, H. Yu, K.L. Kirkwood, and R.T. Franceschi. 2012. Interactions between extracellular signal-regulated kinase 1/2 and p38 MAP kinase pathways in the control of RUNX2 phosphorylation and transcriptional activity. *J Bone Miner Res.* 27:538-551.
- Ghosh-Choudhury, N., S.L. Abboud, R. Nishimura, A. Celeste, L. Mahimainathan, and G.G. Choudhury. 2002. Requirement of BMP-2-induced phosphatidylinositol 3-kinase and Akt serine/threonine kinase in osteoblast differentiation and Smad-dependent BMP-2 gene transcription. *J Biol Chem.* 277:33361-33368.
- Gomez del Arco, P., S. Martinez-Martinez, J.L. Maldonado, I. Ortega-Perez, and J.M. Redondo. 2000. A role for the p38 MAP kinase pathway in the nuclear shuttling

of NFATp. *J Biol Chem.* 275:13872-13878.

- Gu, B.J., and J.S. Wiley. 2006. Rapid ATP-induced release of matrix metalloproteinase 9 is mediated by the P2X7 receptor. *Blood.* 107:4946-4953.
- Gu, L.Q., F.Y. Li, L. Zhao, Y. Liu, Q. Chu, X.X. Zang, J.M. Liu, G. Ning, and Y.J. Zhao. 2010. Association of XIAP and P2X7 receptor expression with lymph node metastasis in papillary thyroid carcinoma. *Endocrine.* 38:276-282.
- Hammerman, P.S., C.J. Fox, and C.B. Thompson. 2004. Beginnings of a signal-transduction pathway for bioenergetic control of cell survival. *Trends Biochem Sci.* 29:586-592.
- Hartmann, C. 2006. A Wnt canon orchestrating osteoblastogenesis. *Trends Cell Biol.* 16:151-158.
- Hirschhaeuser, F., U.G. Sattler, and W. Mueller-Klieser. 2011. Lactate: a metabolic key player in cancer. *Cancer Res.* 71:6921-6925.
- Ishihara, Y., Y. Sugawara, H. Kamioka, N. Kawanabe, S. Hayano, T.A. Balam, K. Naruse, and T. Yamashiro. 2013. Ex vivo real-time observation of Ca(2+) signaling in living bone in response to shear stress applied on the bone surface. *Bone.* 53:204-215.
- Jelassi, B., A. Chantome, F. Alcaraz-Perez, A. Baroja-Mazo, M.L. Cayuela, P. Pelegrin, A. Surprenant, and S. Roger. 2011. P2X(7) receptor activation enhances SK3 channels- and cystein cathepsin-dependent cancer cells invasiveness. *Oncogene.* 30:2108-2122.
- Kamel, M.A., J.L. Picconi, N. Lara-Castillo, and M.L. Johnson. 2010. Activation of beta-catenin signaling in MLO-Y4 osteocytic cells versus 2T3 osteoblastic cells by fluid flow shear stress and PGE2: Implications for the study of mechanosensation in bone. *Bone.* 47:872-881.
- Katz, S., R. Boland, and G. Santillan. 2006. Modulation of ERK 1/2 and p38 MAPK signaling pathways by ATP in osteoblasts: involvement of mechanical stress-activated calcium influx, PKC and Src activation. *Int J Biochem Cell Biol.* 38:2082-2091.
- Klein-Nulend, J., A. van der Plas, C.M. Semeins, N.E. Ajubi, J.A. Frangos, P.J. Nijweide, and E.H. Burger. 1995. Sensitivity of osteocytes to biomechanical stress in vitro. *FASEB J.* 9:441-445.
- Koga, T., Y. Matsui, M. Asagiri, T. Kodama, B. de Crombrughe, K. Nakashima, and H. Takayanagi. 2005. NFAT and Osterix cooperatively regulate bone formation. *Nat Med.* 11:880-885.

- Krishnan, V., H.U. Bryant, and O.A. Macdougald. 2006. Regulation of bone mass by Wnt signaling. *J Clin Invest.* 116:1202-1209.
- Liu, D., D.C. Genetos, Y. Shao, D.J. Geist, J. Li, H.Z. Ke, C.H. Turner, and R.L. Duncan. 2008. Activation of extracellular-signal regulated kinase (ERK1/2) by fluid shear is  $\text{Ca}^{2+}$ - and ATP-dependent in MC3T3-E1 osteoblasts. *Bone.* 42:644-652.
- Long, F. 2012. Building strong bones: molecular regulation of the osteoblast lineage. *Nat Rev Mol Cell Biol.* 13:27-38.
- Macian, F. 2005. NFAT proteins: key regulators of T-cell development and function. *Nat Rev Immunol.* 5:472-484.
- Masin, M., C. Young, K. Lim, S.J. Barnes, X.J. Xu, V. Marschall, W. Brutkowski, E.R. Mooney, D.C. Gorecki, and R. Murrell-Lagnado. 2012. Expression, assembly and function of novel C-terminal truncated variants of the mouse P2X7 receptor: re-evaluation of P2X7 knockouts. *Br J Pharmacol.* 165:978-993.
- Noronha-Matos, J.B., M.A. Costa, M.T. Magalhaes-Cardoso, F. Ferreira, J. Pelletier, R. Freitas, J.M. Neves, J. Sevigny, and P. Correia-de-Sa. 2012. Role of ecto-NTPDases on UDP-sensitive P2Y(6) receptor activation during osteogenic differentiation of primary bone marrow stromal cells from postmenopausal women. *J Cell Physiol.* 227:2694-2709.
- Okamura, H., C. Garcia-Rodriguez, H. Martinson, J. Qin, D.M. Virshup, and A. Rao. 2004. A conserved docking motif for CK1 binding controls the nuclear localization of NFAT1. *Mol Cell Biol.* 24:4184-4195.
- Okumura, H., D. Shiba, T. Kubo, and T. Yokoyama. 2008. P2X7 receptor as sensitive flow sensor for ERK activation in osteoblasts. *Biochem Biophys Res Commun.* 372:486-490.
- Orriss, I.R., M.L. Key, A. Brandao-Burch, J.J. Patel, G. Burnstock, and T.R. Arnett. 2012. The regulation of osteoblast function and bone mineralisation by extracellular nucleotides: The role of p2x receptors. *Bone.*
- Orriss, I.R., G.E. Knight, S. Ranasinghe, G. Burnstock, and T.R. Arnett. 2006. Osteoblast responses to nucleotides increase during differentiation. *Bone.* 39:300-309.
- Panupinthu, N., L. Zhao, F. Possmayer, H.Z. Ke, S.M. Sims, and S.J. Dixon. 2007. P2X7 nucleotide receptors mediate blebbing in osteoblasts through a pathway involving lysophosphatidic acid. *J Biol Chem.* 282:3403-3412.
- Pellegatti, P., L. Raffaghello, G. Bianchi, F. Piccardi, V. Pistoia, and F. Di Virgilio. 2008. Increased level of extracellular ATP at tumor sites: in vivo imaging with plasma membrane luciferase. *PLoS One.* 3:e2599.

- Roszek, K., A. Blaszcak, M. Wujak, and M. Komoszynski. 2013. Nucleotides metabolizing ectoenzymes as possible markers of mesenchymal stem cell osteogenic differentiation. *Biochem Cell Biol.* 91:176-181.
- Sheridan, C.M., E.K. Heist, C.R. Beals, G.R. Crabtree, and P. Gardner. 2002. Protein kinase A negatively modulates the nuclear accumulation of NF-ATc1 by priming for subsequent phosphorylation by glycogen synthase kinase-3. *J Biol Chem.* 277:48664-48676.
- Slater, M., S. Danieleto, A. Gidley-Baird, L.C. Teh, and J.A. Barden. 2004a. Early prostate cancer detected using expression of non-functional cytolytic P2X7 receptors. *Histopathology.* 44:206-215.
- Slater, M., S. Danieleto, M. Pooley, L. Cheng Teh, A. Gidley-Baird, and J.A. Barden. 2004b. Differentiation between cancerous and normal hyperplastic lobules in breast lesions. *Breast Cancer Res Treat.* 83:1-10.
- Solini, A., S. Cuccato, D. Ferrari, E. Santini, S. Gulinelli, M.G. Callegari, A. Dardano, P. Faviana, S. Madec, F. Di Virgilio, and F. Monzani. 2008. Increased P2X7 receptor expression and function in thyroid papillary cancer: a new potential marker of the disease? *Endocrinology.* 149:389-396.
- Solle, M., J. Labasi, D.G. Perregaux, E. Stam, N. Petrushova, B.H. Koller, R.J. Griffiths, and C.A. Gabel. 2001. Altered cytokine production in mice lacking P2X7 receptors. *J Biol Chem.* 276:125-132.
- Suadicani, S.O., R. Iglesias, D.C. Spray, and E. Scemes. 2009. Point mutation in the mouse P2X7 receptor affects intercellular calcium waves in astrocytes. *ASN Neuro.* 1.
- Takai, E., M. Tsukimoto, H. Harada, K. Sawada, Y. Moriyama, and S. Kojima. 2012. Autocrine regulation of TGF-beta1-induced cell migration by exocytosis of ATP and activation of P2 receptors in human lung cancer cells. *J Cell Sci.* 125:5051-5060.
- Thompson, W.R., C.T. Rubin, and J. Rubin. 2012. Mechanical regulation of signaling pathways in bone. *Gene.* 503:179-193.
- Vaudry, D., P.J. Stork, P. Lazarovici, and L.E. Eiden. 2002. Signaling pathways for PC12 cell differentiation: making the right connections. *Science.* 296:1648-1649.
- Warburg, O. 1956. On the origin of cancer cells. *Science.* 123:309-314.
- Westendorf, J.J., R.A. Kahler, and T.M. Schroeder. 2004. Wnt signaling in osteoblasts and bone diseases. *Gene.* 341:19-39.

- Wilkins, B.J., Y.S. Dai, O.F. Bueno, S.A. Parsons, J. Xu, D.M. Plank, F. Jones, T.R. Kimball, and J.D. Molkentin. 2004. Calcineurin/NFAT coupling participates in pathological, but not physiological, cardiac hypertrophy. *Circ Res.* 94:110-118.
- Yang, T.T., Q. Xiong, H. Enslen, R.J. Davis, and C.W. Chow. 2002. Phosphorylation of NFATc4 by p38 mitogen-activated protein kinases. *Mol Cell Biol.* 22:3892-3904.
- Yoon, J.C., A. Ng, B.H. Kim, A. Bianco, R.J. Xavier, and S.J. Elledge. 2010. Wnt signaling regulates mitochondrial physiology and insulin sensitivity. *Genes Dev.* 24:1507-1518.
- Zhu, J., F. Shibasaki, R. Price, J.C. Guillemot, T. Yano, V. Dotsch, G. Wagner, P. Ferrara, and F. McKeon. 1998. Intramolecular masking of nuclear import signal on NF-AT4 by casein kinase I and MEKK1. *Cell.* 93:851-861.



## **APPENDIX A**

### Supplementary Video Legends

**Video 2.1 A Low Concentration of ATP (10  $\mu$ M) Elicits a Transient Increase in Cytosolic Free  $\text{Ca}^{2+}$ .**

MC3T3-E1 cells were loaded with the  $\text{Ca}^{2+}$ -sensitive dye fluo-4 and changes in  $[\text{Ca}^{2+}]_i$  were monitored by live-cell confocal microscopy under serum-free conditions. Cultures were bathed in M199 supplemented with 1% antibiotic solution at  $\sim 25$  °C and ATP (10  $\mu$ M;  $\text{ATP}_{\text{low}}$ ) was added at 10 min. Movie begins at 0 min and ends at 30 min real-time. Image intervals are 1.5 s and frames are shown at 100 frames/s. Width of the field is 230  $\mu$ m.

**Video 2.2 A High Concentration of ATP (1 mM) Elicits a Sustained Increase in Cytosolic Free  $\text{Ca}^{2+}$ .**

MC3T3-E1 cells were loaded with the  $\text{Ca}^{2+}$ -sensitive dye fluo-4 and changes in  $[\text{Ca}^{2+}]_i$  were monitored by live-cell confocal microscopy under serum-free conditions. Cultures were bathed in M199 supplemented with 1% antibiotic solution at  $\sim 25$  °C and ATP (1 mM;  $\text{ATP}_{\text{high}}$ ) was added at 10 min. Movie begins at 0 min and ends at 30 min real-time. Image intervals are 1.5 s and frames are shown at 100 frames/s. Width of the field is 230  $\mu$ m.

**Video 2.3 A Low Concentration of ATP (10  $\mu$ M) Elicits NFATc1-EGFP Nuclear Translocation of Transient Duration.**

MC3T3-E1 cells were transfected with plasmids encoding EGFP-tagged NFATc1 and changes in subcellular localization of NFATc1-EGFP were monitored by live-cell confocal microscopy under serum-free conditions. Cultures were bathed in M199 supplemented with 1% antibiotic solution at  $\sim 25$  °C and ATP (10  $\mu$ M;  $\text{ATP}_{\text{low}}$ ) was added at 12.5 min. Movie begins at 0 min and ends at 197 min real-time. Image intervals are 2.5 min and frames are shown at 10 frames/s. Width of the field is 230  $\mu$ m.

**Video 2.4 The P2X7 Agonist BzATP Elicits NFATc1-EGFP Nuclear Translocation of Sustained Duration.**

MC3T3-E1 cells were transfected with plasmids encoding EGFP-tagged NFATc1 and changes in subcellular localization of NFATc1-EGFP were monitored by live-cell

confocal microscopy under serum-free conditions. Cultures were bathed in M199 supplemented with 1% antibiotic solution at ~25 °C and BzATP (300  $\mu$ M) was added at 12.5 min. Movie begins at 0 min and ends at 194 min real-time. Image intervals are 2.5 min and frames are shown at 10 frames/s. Width of the field is 154  $\mu$ m.

**Video 3.1 BzATP Induces Dynamic Membrane Blebbing in MC3T3-E1 Osteoblast-like Cells.**

MC3T3-E1 cells were monitored by time-lapse phase-contrast microscopy. Cultures were bathed in nominally divalent cation-free buffer at ~35 °C and BzATP (300  $\mu$ M) was added at 10 min. Movie begins at 0 min and ends at 30 min real-time. The majority of cells exhibit dynamic blebbing in response to BzATP, indicating the presence of functional P2X7 receptors. Image intervals are 3 s and frames are shown at 50 frames/s. Width of the field is 530  $\mu$ m.

**Video 3.2 BzATP Induces Retraction but not Membrane Blebbing in UMR-106 Osteosarcoma Cells.**

UMR-106 cells were monitored by time-lapse phase-contrast microscopy. Cultures were bathed in nominally divalent cation-free buffer at ~35 °C and BzATP (300  $\mu$ M) was added at 10 min. Movie begins at 0 min and ends at 30 min real-time. The majority of cells exhibit retraction, but not membrane blebbing in response to BzATP. Lack of blebbing is consistent with the absence of P2X7 receptors in these cells. Image intervals are 3 s and frames are shown at 50 frames/s. Width of the field is 530  $\mu$ m.

## **APPENDIX B**

Permission for Reproduction from Springer Science + Business Media

**SPRINGER LICENSE  
TERMS AND CONDITIONS**

Jun 03, 2013

This is a License Agreement between Matthew W Grol ("You") and Springer ("Springer") provided by Copyright Clearance Center ("CCC"). The license consists of your order details, the terms and conditions provided by Springer, and the payment terms and conditions.

**All payments must be made in full to CCC. For payment instructions, please see information listed at the bottom of this form.**

License Number	3161371147717
License date	Jun 03, 2013
Licensed content publisher	Springer
Licensed content publication	Purinergic Signalling
Licensed content title	Expression, signaling, and function of P2X7 receptors in bone
Licensed content author	Matthew W. Grol
Licensed content date	Jan 1, 2009
Volume number	5
Issue number	2
Type of Use	Thesis/Dissertation
Portion	Excerpts
Author of this Springer article	Yes and you are the sole author of the new work
Order reference number	
Title of your thesis / dissertation	P2X7 Nucleotide Receptor Signaling in Osteoblasts
Expected completion date	Jul 2013
Estimated size(pages)	300
Total	0.00 USD
Terms and Conditions	

## **APPENDIX C**

Permission for Reproduction from The Company of Biologists



## **Rights and permissions**

### **Author rights**

(these rights are retained when publishing an Open Access article)

Authors remain the owners of the copyright to the article and retain the following non-exclusive rights (for further details, please refer to the licence agreement that accompanies article proofs):

- (1) authors may reproduce the article, in whole or in part, in any printed book (including a thesis) of which they are author, provided the original article is properly and fully attributed;
- (2) authors and any academic institution where they are employed may reproduce the article, in whole or in part, for the purpose of teaching students;
- (3) authors may post a copy of the article on their website, provided that it has already been published by the Journal and is linked to the Journal's website;
- (4) authors may use data contained in the article in other works they create.

**Disclaimer:** Responsibility for (1) the accuracy of statements of fact; (2) the authenticity of scientific findings or observations; (3) expressions of scientific or other opinion; (4) any other material published in the journal rests solely with the author(s) of the article in which such statements, etc., appear. No responsibility for such matters is assumed by the Journal, its owners, publishers, referees or staff.

### **Copyright and reproduction**

Articles in JCS are published under an exclusive, worldwide licence granted to the publisher by the authors, who retain copyright.

### **Permission to use material from JCS in other publications**

Authors are free to reproduce material from their own articles in other publications.

## **APPENDIX D**

Permission for Reproduction from The American Physiological Society





## Permission Request Procedures

### Copyright

The Mandatory Submission Form serves as the Society's official copyright transfer form. The APS Journals are copyrighted for the protection of authors and the Society.

### Rights of Authors of APS Articles

For educational purposes only, authors may make copies of their own articles or republish parts of these articles (e.g., figures, tables), without charge and without requesting permission, provided that full acknowledgement of the source is given in the new work. Also, authors may e-mail a PDF of their article to fellow researchers for educational purposes. However, authors may not post a PDF of their published article on any website; instead, links may be posted to the article on the APS journal website where it resides. Posting of articles or parts of articles is restricted and subject to the conditions below.

### Rights of Authors for Reuse of Content from their Articles

**Theses and dissertations.** APS permits whole published articles to be reproduced without charge in dissertations, which may be posted to theses repositories. Full citation is required.

**Open courseware.** Articles, or parts of articles, may be posted to a public access courseware website. Permission must be requested from the APS. A copyright fee will apply during the first 12 months of the article's publication by the APS. The APS requires full citation for all permissions granted.

**Institutional websites.** The author's published article (in whole or in part) may not be posted to an institutional website, neither at the institutional nor departmental level. This exclusion includes, but is not limited to, library websites and national government websites. Instead, a link to the article on the APS journal website should be used. (See also the APS Policy on Funding Agencies, below.)

**Institutional repositories (non-theses).** The author's published article (in whole or in part) may not be posted to any institutional repository. This exclusion includes, but is not limited to, library repositories and national government repositories. Instead, a link to the APS journal website should be used. (See also the APS Policy on Funding Agencies, below.)

**Author's article in presentations.** Authors may use their articles (in whole or in part) for presentations (e.g., at meetings and conferences). These presentations may be reproduced (e.g., in monographs) on any type of media including, but not limited to, CDs, DVDs, and flash drives, for educational use only in materials arising from the meeting or conference such as the proceedings of a meeting or conference. A copyright fee will apply if there is a charge to the user or if the materials arising are directly or indirectly commercially supported.

**Reuse in another journal before final publication is prohibited.** Permission for reuse of an article (whether in whole or in part) in another publication is restricted to the final published version of the article. If an article is currently published on the APS "publish ahead of print" website (Articles in PresS), then the author must wait to request permission to reuse the article, or any part of the article, until such time when the article appears in final-published form on the APS journal website.

Authors who do not have access to a subscription and/or who are not APS members may

- purchase the article through the pay-per-view option, or
- purchase a Toll-Free Link from APS, which will allow them to post a link to the APS journals website (directly to the article) enabling unlimited free downloads for any user accessing the article via this Toll-Free Link.

## **APPENDIX E**

Ethics Approval of Animal Use



AUP Number: 2008-043-06

PI Name: Sims, Stephen M

AUP Title: Role of cytosolic calcium in the regulation of osteoclasts and bone resorption// Ion Transport and Signalling in Skeletal Cells: P2 Nucleotide Receptor Function in Bone

**Official Notification of AUS Approval:** A MODIFICATION to Animal Use Protocol 2008-043-06 has been approved.

The holder of this Animal Use Protocol is responsible to ensure that all associated safety components (biosafety, radiation safety, general laboratory safety) comply with institutional safety standards and have received all necessary approvals. Please consult directly with your institutional safety officers.

Submitted by: Kinchlea, Will D  
on behalf of the Animal Use Subcommittee

*The University of Western Ontario*  
Animal Use Subcommittee / University Council on Animal Care  
Health Sciences Centre, • London, Ontario • CANADA – N6A 5C1

# Curriculum Vitae

## Matthew W. Grol

### PERSONAL DATA

Date of Birth                      December 2<sup>nd</sup>, 1985  
Citizenship                        Canadian

### EDUCATION

Fall 2007 –                         **Doctor of Philosophy**  
Summer 2013                      Department of Anatomy and Cell Biology  
University of Western Ontario, London, ON  
*Supervisor:* Dr. S. Jeffrey Dixon  
*Thesis Title:* P2X7 nucleotide receptor signaling in osteoblasts

Fall 2003 –                         **Bachelor of Medical Sciences**  
Spring 2007                        Honors Specialization in Biochemistry and Cell Biology  
University of Western Ontario, London, ON  
(*Conferred in June 2007*)

### TEACHING EXPERIENCE

Fall 2011 –                         **Laboratory Coordinator**  
Spring 2012                        Anatomy and Cell Biology 3319: Human Anatomy  
University of Western Ontario, London, ON

Fall 2010 –                         **Laboratory Coordinator**  
Spring 2011                        Anatomy and Cell Biology 3319: Human Anatomy  
University of Western Ontario, London, ON

Fall 2009 –                         **Laboratory Coordinator**  
Spring 2010                        Anatomy and Cell Biology 3319: Human Anatomy  
University of Western Ontario, London, ON

Fall 2008 –                         **Laboratory Demonstrator**  
Spring 2009                        Anatomy and Cell Biology 3319: Human Anatomy  
University of Western Ontario, London, ON

### ACADEMIC SERVICE ACTIVITIES

Fall 2009 –                         **Graduate Student Representative**  
Fall 2012                            Executive Committee of Schulich Council  
University of Western Ontario, London, ON

Fall 2009 –                         ***Ex Officio* Graduate Student Member**  
Fall 2012                            Schulich Graduate Student Council  
University of Western Ontario, London, ON

- November 2011                    **Internal Reviewer, Graduate Student Representative**  
Microbiology and Immunology Graduate Program Review  
University of Western Ontario, London, ON
- September 2010 &  
October 2011                    **Graduate Scholarship Reviewer**  
School of Graduate and Postdoctoral Studies Fall  
Development Series: “Consult the Experts” Sessions  
University of Western Ontario, London, ON

## AWARDS AND SCHOLARSHIPS

- June 2010                         **Dr. Suzanne Bernier Memorial Award in Skeletal Biology**  
University of Western Ontario, London, ON
- Fall 2009 –  
Fall 2012                         **Frederick Banting and Charles Best Canada Graduate Scholarship Doctoral Award** (*Value: \$35,000 each year for 3 years*) – *Accepted*  
Canadian Institutes of Health Research, Ottawa, ON
- Fall 2008 –  
Fall 2009                         **Frederick Banting and Charles Best Canada Graduate Scholarship Masters Award** (*Value: \$17,500*) – *Accepted*  
Canadian Institutes of Health Research, Ottawa, ON
- Fall 2007 –  
Fall 2008                         **Ontario Graduate Scholarship** (*Value: \$15,000*) – *Accepted*  
Ministry of Training, Colleges and Universities, Thunder Bay, ON
- June 2007                         **University of Western Ontario Gold Medal**  
*Description: Awarded for achieving highest academic standing in the Honors Specialization in Biochemistry and Cell Biology degree module of the Bachelor of Medical Sciences program*  
University of Western Ontario, London, ON

## PUBLICATIONS

(Sorted by date submitted)

- To be submitted                    **Grol, M. W.**, Brooks, P. J., Pereverzev, A., Sims, S. M., and Dixon, S. J. Crosstalk between the Wnt/ $\beta$ -catenin pathway and P2X7 nucleotide receptor signaling in osteoblasts. (*In progress*)
- May 2013                         Beaucage, K. L., Xiao, A., **Grol, M. W.**, Holdsworth, D. W., Sims, S. M., Darling, M. R., and Dixon, S. J. (2013) Loss of P2X7 nucleotide receptor function leads to abnormal fat distribution in mice. *Purinergic Signal. (In Revision)*
- January 2013                    Reyes, J. P.\*, **Grol, M. W.\***, Sims, S. M., and Dixon, S. J.

- (2013) Receptor independent effects of 2'(3')-O-(4-benzoylbenzoyl)ATP triethylammonium salt on cytosolic pH. *Purinergic Signal*. (*In Press*) [Epub 2013 May 22; DOI:10.1007/s11302-013-9365-4]  
\* co-first authorship
- October 2012 **Grol, M. W.**, Pereverzev, A., Sims, S. M., and Dixon, S. J. (2013) P2 receptor networks regulate signaling duration over a wide dynamic range of ATP concentrations. *J. Cell Sci.* **126**, 3615-3626
- April 2012 Bridge, K. Pereverzev, A., **Grol, M. W.**, and Dixon, S. J. (2013) Activation of lysophosphatidic acid-1-receptor on osteoblasts induces release of Ca<sup>2+</sup> from intracellular stores and enhances osteogenesis. *J. Cell. Physiol.* (*In revision*)
- March 2012 Milner, J. S., **Grol, M. W.**, Beaucage, K. L., Dixon, S. J., and Holdsworth, D. W. (2012) Finite-element modeling of viscoelastic cells during high-frequency cyclic strain. *J. Funct. Biomater.* **3**, 209-224
- April 2011 **Grol, M. W.**, Zelner, I., and Dixon, S. J. (2012) P2X7-mediated calcium influx triggers a sustained, PI3K-dependent increase in metabolic acid production by osteoblasts. *Am. J. Physiol. Endocrinol. Metab.* **302**, E561-E575
- April 2009 Rockel, J. S., **Grol, M. W.**, Bernier, S. M., and Leask, A. (2009) Cyclic AMP regulates matrix gene expression and metabolism in cultured primary rat chondrocytes. *Matrix Biol.* **28**(6), 354-364
- February 2009 **Grol, M. W.**, Panupinthu, N., Korčok, J., Sims, S. M., and Dixon, S. J. (2009) Expression, signaling and function of P2X7 receptors in bone. *Purinergic Signal.* **5**(2), 205-221  
*Academic Recognition: Leaders in the field noted this publication as being of "outstanding interest" in a recent review – Orriss, I. R., Burnstock, G., and Arnett, T. R. (2010) Purinergic signalling and bone remodeling. Curr. Opin. Pharmacol.* **10**, 322-330

## SELECTED CONFERENCE ABSTRACTS

(FIRST AUTHOR SUBMISSIONS)

- September 2011 **American Society for Bone and Mineral Research 33<sup>rd</sup> Annual Meeting**  
San Diego, CA, USA  
*Title:* Activation of distinct nucleotide receptor subtypes determines the duration of calcium-NFATc1 signaling in osteoblasts over a remarkably wide dynamic range of ATP

concentrations: A novel mechanism for dose-to-duration coupling (Plenary Poster presentation)

*Authors:* **M. W. Grol**, S. Xing, A. Pereverzev, S. M. Sims, S. V. Komarova, and S. J. Dixon

*Role:* Contributed to research, prepared abstract and presented research

June 2011

**Bones and Teeth Gordon Research Conference**

Les Diablerets, Switzerland

*Title:* Persistence of ATP-induced  $\text{Ca}^{2+}$ -NFATc1 signaling in osteoblasts determined by distinct nucleotide receptor subtypes: A novel mechanism for coupling agonist concentration to signal duration (Oral & poster presentations)

*Authors:* **M. W. Grol**, A. Pereverzev, S. M. Sims, and S. J. Dixon

*Role:* Contributed to research, prepared abstract and presented research

June 2010

**CIHR Canadian Student Health Research Forum**

Winnipeg, MB, Canada

*Title:* Live-cell imaging of NFATc1 nuclear translocation induced by activation of P2X7 nucleotide receptors in osteoblasts (Poster presentation)

*Authors:* **M. W. Grol**, H. K. Ma, A. Pereverzev, S. M. Sims, and S. J. Dixon

*Role:* Contributed to research, prepared abstract and presented research

July 2009

**Bones and Teeth Gordon Research Conference**

Biddeford, ME, USA

*Title:* Activation of P2X7 nucleotide receptors induces NFATc1 translocation in osteoblasts: Live-cell imaging reveals the kinetics of NFATc1 nuclear import and export (Poster presentation)

*Authors:* **M. W. Grol**, H. K. Ma, A. Pereverzev, S. M. Sims, and S. J. Dixon

*Role:* Contributed to research, prepared abstract and presented research

June 2008

**14<sup>th</sup> Canadian Connective Tissue Conference**

Montréal, QC, Canada

*Title:* Activation of P2X7 nucleotide receptors increases metabolic acid production by osteoblastic cells (Oral presentation & session chair)

*Authors:* **M. W. Grol**, I. Zelner, and S. J. Dixon

*Role:* Contributed to research, prepared abstract and presented research

**SELECTED CONFERENCE ABSTRACTS***(CO-AUTHOR SUBMISSIONS)*

June 2012

**International Association of Dental Research 83rd  
General Session**

Iguassu Falls, Brazil

*Title:* Crosstalk between Wnt/ $\beta$ -catenin and P2X7 nucleotide receptor signaling in osteoblasts (IADR/Unilever Hatton competition oral and poster presentations)*Authors:* P. J. Brooks, **M. W. Grol**, S. M. Sims, and S. J. Dixon*Role:* Trained and supervised first author, contributed to research, assisted with abstract preparation**OTHER CONFERENCES***(NO ABSTRACT SUBMITTED)*

November 2009

**Bone Health Research Consensus Conference (BHRCC)**

Toronto, ON, Canada

*Description:* Organized by the Institute of Musculoskeletal Health and Arthritis (IMHA) of the Canadian Institutes of Health Research (CIHR), the goal of the BHRCC was to identify important issues, challenges and unmet needs in the area of bone health research and to identify the research questions that should be prioritized in the future*Role:* Contributed to group discussions of the important issues in bone health research and to the identification of prioritized research questions